Characterisation of Leukocytes in Reproductive Tissues Before and After Pregnancy

Rachel Sarah Oldham MPharmacol

Submitted to the College of Medical and Veterinary Life Sciences, University of Glasgow in fulfilment of the requirements for the degree of Doctor of Philosophy

November 2013

Institute of Infection, Immunity and Inflammation
University of Glasgow
120 University Place
Glasgow
G12 8TA

Abstract

Reproduction is a crucial process, required for bringing the next generation into the world. In preparation for pregnancy, and throughout pregnancy itself, reproductive tissues recruit specific populations of immune cells that are thought to contribute in a variety of ways to successful reproduction. Pregnancy culminates in parturition, an inflammatory process characterised by an influx of inflammatory cells into reproductive tissues. Effective healing of reproductive tissues in the post-partum period is vital for continued reproductive success, and it too is thought to involve specific populations of immune cells. For leukocytes to effectively perform their functions in the reproductive system and elsewhere, migration to the right place at the right time is crucial. Key regulators of leukocyte homing are the chemokine family of chemoattractants and their G-protein coupled receptors. The chemokine network is complex and controls migration of leukocytes from the Bone Marrow (BM) into the blood and from the blood into tissues. Chemokines influence leukocyte position within tissues, and orchestrate their departure. Very little is known about the types of leukocytes present within reproductive tissues in the post-partum period, or the chemokines and receptors that could be involved in their migration. Exploring these processes is critical for an understanding of how tissues are repaired in readiness for subsequent pregnancies.

In this thesis I have examined the leukocyte populations in reproductive and peripheral tissues of mice during the post-partum period and compared them to those found in Non-Pregnant (NP) mice. This analysis has encompassed a range of myeloid cell types, and also the complex populations of CD3+ cells that exist in reproductive tissues. I was also interested in how these cells are instructed to enter reproductive tissues, and in particular on the role of CC chemokine Receptor 2 (CCR2), a receptor associated with the recruitment of monocytes and T cells into tissues. My work has clearly identified cells expressing CCR2 both in reproductive tissues and elsewhere, and defined the impact of the genetic deletion of this receptor on leukocyte populations during the post-partum period. These experiments exploited a variety of standard techniques including histology, quantitative Reverse Transcriptase-Polymerase Chain Reaction (qRT-PCR), Enzyme-Linked ImmunoSorbent Assay (ELISA) and Luminex, but they also required the development of challenging multiparameter flow cytometry protocols that allowed the simultaneous analysis, and definitive identification, of several leukocyte populations in various tissues and at specific reproductive time-points.

Chapter 3 describes detailed experiments that focussed on characterising the myeloid cell populations across a variety of tissues in NP, 1 Day Post Partum (DPP) and 7DPP mice. Most strikingly, this revealed a profound accumulation of several myeloid cell populations in reproductive tissues at 1DPP, including inflammatory Ly6C$^{high\ (hi)}$ monocytes and neutrophils. Moreover, many of these myeloid cells expressed active CCR2 and remarkably CCR2 deletion was associated with a dramatic reduction in myeloid cell abundance in the uterine horn one day after birth. Thus, CCR2 appeared to be required for myeloid cell recruitment to the post-partum uterine horn.

Chapters 4 and 5 describe changes in CD3+ cell populations over the post-partum period. Interestingly, the main finding from reproductive tissues was that the large majority of CD3+ cells lacked expression of CD4 and CD8, and were thus termed CD3+ Double-Negative (DN) cells. Three main CD3+ DN cell populations were described. CD3+CD25+NK1.1+TCRβ+ DN cells, likely to be Natural Killer T (NKT) cells, which were mainly found in reproductive tissues and blood. All tissues studied were found to contain CD3+NK1.1-TCRβ+ DN cells, likely to be 'true' DN T cells and CD3+NK1.1-TCRβ-TCRγδ+ DN cells, which were consistent with a γδ T cell phenotype. CD3+ DN cells were also found to increase in number at 1DPP, compared to NP tissues, driven by an increase in DN T cells. In contrast to myeloid cells CCR2 was not required for this change. However, at 1DPP there was a CCR2-dependent increase in the proportion of CD3+ DN cells in the blood.

Finally, in Chapter 6, hormonal influences on leukocyte populations in reproductive and peripheral tissues were considered. This work had two major components: analysing sex differences in myeloid and T cell populations and exploring the effect that lactation has on these cell subsets over the post-partum period. Females were found to have an increased proportion of eosinophils in their blood, whereas males had a higher proportion of monocytes. I also found that female and male reproductive tissues, as well as peripheral tissues, have very similar CD3+ DN cell populations, suggesting that these cells serve roles in reproductive tissues that are not unique to one sex. Finally, CD3+ cell populations in the post-partum period were found to be controlled to some extent by lactation.

Collectively, this work has significantly extended our understanding of leukocytes in various tissues in the post-partum period, and revealed the importance of chemokines in

the regulation of these cells. It has laid the groundwork for future investigations aimed at dissecting the functions of these cells in reproductive tissues in the post-partum period.

Table of Contents

List of Tables and Figures

Chapter 1: Introduction.

Chapter 2: Materials and Methods.

Chapter 3: Myeloid cells in post-partum murine reproductive tissues

Chapter 4: CD3+ cells in murine reproductive tissues before and after pregnancy.

Chapter 5: Chapter 5: Characterisation of CD3+ DN cells in reproductive tissues.

Chapter 6: Hormonal influences on leukocytes in reproductive and peripheral tissues.

Chapter 7: Discussion

Acknowledgements

I would like to thank my supervisors Prof Rob Nibbs and Prof Scott Nelson for their help since I began my PhD. I have learnt so much from working with you both and I have really enjoyed my time doing my project. I would also like to thank the Medical Research Council for funding this work. Thanks particularly to Rob for helping me get my thesis to submission and for encouraging me to overcome the obstacles along the way.

An enormous thank you goes out to everyone who worked in Team Nibbs. Chris, Ross, Mairi, Elinor, Catherine, Laura, Fiona M, Steven and Darren; I learnt an incredible amount from you all and loved working with you. Catherine and Elinor, thanks for being amazing friends and for the many rounds of nachos/coffee/gin. Thanks to Chris for being an all round genius and for "looking after" my bench for me. I would also like to thank everyone else in the GBRC for making work a happy place to be. James, thanks for being a great buddy, even though you only have one topic of conversation.

Thanks to everyone in Reproductive and Maternal Medicine; Dilys, Ann, Fiona M (again), Fiona J, Claire, Joo, Ellie, Jen, Rachel, Salha and Matina. Ellie, I appreciate all the listening to my rants you did and Rachel, your cakes are the best. Thanks to Fiona J for being a lab wiz and constantly lowering the tone. I would also like to thank Diane Vaughn, Joanne Battersby and Tony McDermott for their advice and assistance during my lab work. I really appreciate the effort you went to help me out, especially out of hours!

Rev'd Dr Kevin Francis and Rev'd Stuart MacQuarrie at the University of Glasgow Interfaith Chaplaincy deserve a huge thank you for their continued wise advice and prayers. Lee, Hannah and Mike; thanks for being a gang of friendly faces. I also wish to thank the clergy and congregations of St Bride's (Kelvinside), St Mary's Cathedral (Glasgow), The Church of the Holy Nativity (Newcastle) and St Peter's (Leckhampton).

Thanks to the girls that kept me going; Cathy, Pauline, Margaret, Liz, Elinor B, Jeanette, Melissa, Mechel, Pav, Isabel and especially Kristen and Leslie. You are the two of the most inspiring women I have ever met and I have no idea where I would have ended up without you in my life. Ailsa and George also get a particular mention, you have gone above and beyond and I don't know what I ever did to get such fantastic friends. Sunday

nights just aren’t the same anymore. Thanks to Iain for the regular insults over the last 6 years, long may they continue.
Thanks to all my friends in Cheltenham for not forgetting about me, especially Fay, Jay and Ann-Marie.

The biggest thanks go to my support team in Newcastle; my Gran, Auntie Alison and Auntie Gloria. It has been a wonderful experience to live in such a calm and loving environment and I would not have completed this work without your encouragement. Thank you for putting up with me! I would also like to thank my parents and all of my wider family, I love you all.

I would like to dedicate this work to my brothers Ed and Matt. I love you both more than words can say.

And thanks to Dr John Smith, for inspiring me to do a PhD in the first place.

Author's Declaration

I declare that, except where explicit reference is made to the contribution of others, this thesis is the result of my own work and has not been submitted for any other degree at the University of Glasgow or any other institution.

Signature: ……
Printed name: ……..

Abbreviations

7-AAD	7-AminoActinomycin D
ADAM	A Disintegrin And Metalloproteinase
ANOVA	ANalysis Of VAriance
APC	Antigen Presenting Cell
BM	Bone Marrow
BSA	Bovine Serum Albumin
C	Cervix
CCR	CC chemokine Receptor
CDR	Complementarity Determining Region
CFA	Complete Freund's Adjuvant
CIA	Collagen Induced Arthritis
Comp	Competition
CT	Crossing Threshold value
CX3CR	CX3C chemokine Receptor
CXCR	CXC chemokine Rceptor
D	Diversity region
DARC	Duffy Antigen Receptor for Chemokines
DC	Dendritic Cell
DEPC	Diethylpyrocarbonate
DN	CD8- CD4- / Double Negative
DP	Double Positive
DPP	Days Post-Partum
DS	Detachment Sites
DVR	Digital Video Recorder
EAE	Experimental Autoimmune Encephalitis
EDTA	EthyleneDiamineTetraAcetic acid
ELISA	Enzyme-Linked ImmunoSorbent Assay
FACS	Flow Assisted Cell Sorting
Fig	Figure
fMLP	N-formyl-L-Methionyl-L-Leucyl-Phenylalanine
FMO	Fluorescence Minus One
FPR	Formyl Peptide Receptor
FSC	Forward SCatter

g	grammes
GAPDH	GlycerAldehyde 3-Phosphate DeHydrogenase
GCSF	Granulocyte Colony-Stimulating Factor
GFP	Green Fluorescent Protein
GnRH	Gonadotrophin Releasing Hormone
HBSS	Hank's Balanced Salt Solution
hCG	human Chorionic Gonadotrophin
HEPES	4-(2-HydroxyEthyl)-1-PiperazineEthaneSulfonic acid
hi	high
HRP	HorseRadish Peroxidase
hrs	hours
HLA	Human Leukocyte Antigen
ICM	Inner Cell Mass
IFNγ	InterFeroN γ
iGb3	isoGlobotrihexosylceramide
IL	InterLeukin
iNKT	invariant Natural Killer T
int	intermediate
IQR	InterQuartile Range
J	Joining region
KIR	Killer cell Inhibitory Receptor
KO	Knock Out
LH	Luteinising Hormone
lo	low
LPS	LipoPolySaccharide
LTB_4	LeukoTriene B_4
MBP	Major Basic Protein
MCSF	Macrophage Colony-Stimulating Factor
MHC	Major Histocompatibility Complex
min	minutes
ml	millilitres
MMP	Matrix MetalloProteinase
MOG	Myelin Oligodendrocyte Glycoprotein
MPO	MyeloPerOxidase
MT1-MMP	Membrane Type 1 MMP

NGP	Neutrophil Granule Protein
NK	Natural Killer
NKT	Natural Killer T
NP	Non-Pregnant
dNTPs	Nucleotide TriPhosphates
OVA	OVAlbumin
PALN	Para-Aortic Lymph Nodes
PCR	Polymerase Chain Reaction
PG	Prostate Gland
PGF	Placental Growth Factor
PSGL-1	P-Selectin Glycoprotein Ligand-1
qRT-PCR	quantitative Reverse Transcriptase-Polymerase Chain Reaction
ROS	Reactive Oxygen Species
Rpm	Revolutions per minute
RPMI	Roswell Park Memorial Institute medium
RT	Reverse Transcriptase
S	seconds
S1PR1	Sphingosine-1-Phosphate Receptor 1
SEM	Standard Error of the Mean
SLE	Systemic Lupus Erythromatoses
SP	Single Positive
SSC	Side SCatter
Tc	cytotoxic T cell
TCR	T Cell Receptor
Th	helper T cell
Tg	Transgenic
TLR	Toll-Like Receptor
TMB	3,3',5,5'-TetraMethylBenzidine
TNFα	Tumour Necrosis Factor α
TPA	12-O-TetradecanoylPhorbol-13-Acetate
Treg	T regulatory cell
UH	Uterine Horn
uNK	uterine Natural Killer
V	Variable region
VCAM	Vascular Cellular Adhesion Molecule

VD/Epi	Vas Deferens/EPididymis
VEGF	Vascular Endothelial Growth Factor
VLA	Very Late Antigen
WT	Wild Type
αGalCer	α-GalactosylCeramide

Chapter 1: Introduction

Sexual reproduction is essential for the continuation of mammalian species and requires the success of a myriad of biological processes. Ova and sperm must be produced and matured; the ovum and sperm must meet in the fallopian tube; fertilisation needs to take place; the blastocyst must implant into a receptive uterus; an effective placenta must grow and support the conceptus; and the semi-allogeneic foetus must avoid maternal immune attack during gestation. At the end of all of these hurdles, labour must proceed in a coordinated manner and the mother's reproductive tissues must heal so that the process can begin again.

This project focuses on the leukocytes present in female reproductive tissues during post-partum remodelling, and the influence of chemokines, sex differences, and hormones on these cells. There is surprisingly little data on the post-partum remodelling process. It appears that in humans it is an extended process and that the uterus may never return to its pre-pregnancy state. It begins with restoration of the luminal epithelium, followed by regeneration of the endometrium and closes with repair of the myometrium. To understand this progression, the other major inflammatory events in the reproductive process are discussed during this introduction. Implantation of the blastocyst mimics the extravasation process of leukocyte recruitment, in addition, inflammatory mediators are released to assist in the erosion of maternal tissue and leukocytes such as uterine Natural Killer (uNK) cells are mobilised to the uterus. The last trimester of pregnancy sees an increase in leukocyte infiltration in preparation for labour, which is regarded as a large-scale inflammatory event incorporating leukocyte recruitment, release of tissue modifying enzymes, and changes in tissue composition. Inflammation induced pre-term birth is a major clinical problem and this has led many to postulate that inflammation drives labour, whereas these changes may act to initiate post-partum repair, rather than solely to trigger parturition. My project aims to characterise leukocytes in reproductive tissues and analyse if cell populations differ in the post-partum period from NP animals.

To model the reproductive process in humans, I have studied the reproductive process in mice. Murine female reproductive processes are often used to model those in humans. Dissecting biological pathways using transgenic mice has provided the field with a mine of information. Their easy availability is a distinct advantage to scientific investigation because obtaining primary human tissue can be difficult and recruiting informed subjects can be time consuming. Reproduction in mice will be compared and contrasted with normal human pregnancy. Though my research was conducted to a high ethical standard,

mice could be manipulated in a way that would not be possible if carried out in humans. There are many points of difference between the two species, however it is worth bearing in mind that mice act only as a model of human physiology and it is accepted that they cannot fully represent human biological functions. Animal models probe specific areas or processes, and the relevance of any findings to similar or equivalent processes in humans must be considered alongside limitations. A normal human pregnancy lasts around 40 weeks from the first day of the last menstrual cycle to parturition, whereas in mice pregnancy lasts ~19 days. This could be regarded as a significant difference, however in terms of experimental practicalities, it is a big advantage. Transgenic mice facilitate the dissection of the mechanisms of reproduction, for example the use of a 'Knock Out' (KO) mouse can provide information on the role of the missing gene. Using inbred mice provides another benefit as genetic variation between subjects is eliminated, so underlying biological processes can be examined with more limited subject numbers. Mouse mating and pregnancy follow predictable patterns so tissue can be obtained at specific points during reproduction. Very many similarities between humans and mice have been identified and as long as limitations are borne in mind they can model aspects of human reproduction effectively.

In the introduction to this thesis I will first describe reproductive processes. This will include reproductive anatomy in humans and mice, and a discussion of their differences and similarities. The processes of fertilisation, implantation, placentation, pregnancy, labour and post-partum remodelling will then be broadly discussed. The next section shifts focus and illustrates the development, activation and functions of the immune system, specifically looking at leukocytes and provides a summary of the literature regarding the enigmatic CD3+CD4-CD8- cell population that I examine in my thesis. The role of chemokines in regulating leukocyte migration and localisation, which are key processes in all immune responses, are also discussed. This section closes with further discussion of the chemokine receptor CCR2 on monocytes and T cells. Finally, having discussed reproductive and immune processes separately, I discuss the role of leukocytes in reproductive processes including implantation, mid-late pregnancy, labour and the post-partum period. This section focuses on the changing populations of leukocytes present in reproductive tissues at these times. Finally, the section concludes with a summary of hormonal influences on immune processes, such as lactation in the post-partum period, the effect of sex steroids on chemokines, sex differences in inflammation and the leukocyte composition of the male reproductive tract.

1.1. An overview of reproductive tissues and reproduction.

1.1.1. *Anatomy of female reproductive tract in humans.*

Figure 1.1 illustrates the anatomy of female reproductive tissues. Female humans have two ovaries that sit within the pelvis either side of the uterus. They produce mature ova and release hormones. Production of ova requires oogenesis, the process through which gametes are produced, and is followed by the maturation of the oocyte and ovulation. At birth, a baby girl already has all the germ cells for her lifetime (~2-4 million), although only a tiny fraction of these will ever be released as mature ova. Usually, one oocyte is released as part of each menstrual cycle, before which oocytes develop in follicles within the ovary. Oocytes are nurtured by sex steroids secreted by granulosa cells until one follicle dominates. This causes other follicles to degenerate, preventing release of the oocyte they contain. During ovulation the follicle becomes so large that the surface of the ovary protrudes and ruptures, releasing the oocyte. Ovulation occurs at day 14 of the menstrual cycle and is accompanied by a spike in circulating levels of luteinising hormone (LH), produced by the anterior pituitary in response to Gonadotrophin Releasing Hormone (GnRH) secretion by the hypothalamus. The release of the ovum is assisted by the action of enzymes including proteases such as Matrix MetalloProteinase-1 (MMP-1) and MMP-2 (Hulboy et al., 1997). When an oocyte is released it travels down the Fallopian tube and the remains of the follicle become a body called the corpus luteum. In humans, the role of the corpus luteum is to secrete hormones, primarily progesterone, to sustain a pregnancy until the placenta is established. The production of a small amount of oestrogen also acts to prevent further release of GnRH by the pituitary, thus turning off LH production.

As shown in Figure 1.1, a Fallopian tube is attached to each of the two top corners of the uterus and the other end of the tube opens near to the ovary and has finger-like projections termed fimbria that move in a sweeping motion to guide the oocyte into the Fallopian tube. If successful fertilisation of the ovum occurs, it takes place along the Fallopian tube. The lumen of the Fallopian tube is lined with a ciliated epithelium to aid the movement of the zygote towards to uterus for implantation. Inappropriate implantation in the Fallopian tube results in ectopic pregnancy.

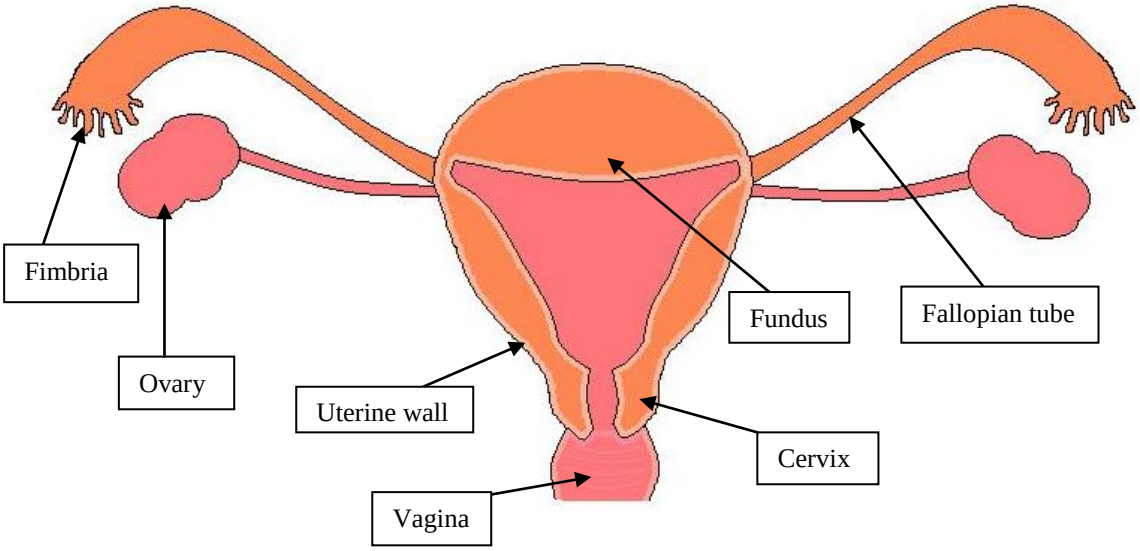

Figure 1.1. Anatomy of female reproductive tissue in humans.

Diagram cut away to show the path of an oocyte from the ovary, through the Fallopian tube and into the uterus. The cervix and vagina separate the uterus from the external environment.

The uterus is a muscular structure that lies between the bladder and the pelvis. An adult nulliparous uterus weighs 30-40grammes (g), whereas a parous uterus weighs around 70-100g. It is anchored in the pelvis by connective tissue ligaments that provide stability. The majority of the wall of the uterus is composed of the myometrium, which consists primarily of smooth muscle cells as well as an extracellular matrix to support the cells, blood vessels, fibroblasts and leukocytes. In the first half of pregnancy myocyte hyperplasia is seen, where increasing numbers of smooth muscle cells are observed. During the second half of pregnancy myocytes undergo hypertrophy and the cells increase in size as the uterus grows during pregnancy (Shynlova et al., 2010). The uterine cavity is lined by the endometrium, a glandular epithelium. In humans, the uterus is subject to a ~28 day menstrual cycle, which incorporates endometrial, endocrine and ovulatory changes. The endometrium is comprised of a functional layer, which is lost during menstruation and a vascular basal layer, which is maintained throughout the cycle. The thickness of the endometrium is controlled by hormone production by the ovary, with endometrial proliferation in response to oestrogen during the first half of the cycle and increased secretory activity by the endometrium in response to progesterone during the second half of the cycle. During the proliferation phase there is rapid growth of the epithelium in order to re-cover the endometrium following menstruation. Once this is achieved the fibroblasts, extracellular matrix and vascular component of the functional layer of the endometrium is

replaced. During the secretory phase, the endometrium is characterised by oedema and the formation of spiral arteries, and decidualisation takes place.

Decidualisation is the process where the fibroblasts of the endometrial stroma differentiate to form large, granular cells with high metabolic activity. The decidua is formed so that implantation can occur. As discussed in section 1.3.2, the leukocyte content changes, inflammatory cytokines are produced and decidual cells provide nourishment for the trophoblasts until they invade far enough to reach the uterine spiral arteries. Trophoblasts digest these glycogen and lipid rich cells, as well as taking in their secretions. If implantation does not occur during the cycle, the corpus luteum is broken down and therefore the source of progresterone is withdrawn and ultimately the decidual layer is shed as menstrual debris on the first 4-5 days of the menstrual cycle. Degradation of the extracellular matrix of the endometrium is likely to be the first step in menstruation, leading to loss of intergrity of endometrial blood vessels and the luminal epithelium. Blood vessels within the endometrium first constrict and then dilate and blood flows first into the stroma and once the epithelium has been degraded, into the uterine lumen. The destruction of the extracellular matrix is achieved through increased activity of MMPs produced by stromal cells and leukocytes such as neutrophils, as they act to aid the intense remodelling of the epithelium and stroma during this time (Hulboy et al., 1997). Menstruation is an inflammatory process and will be discussed in further detail in section 1.3.1.

The main body of the uterus is called the corpus, while the area between the Fallopian tubes is the fundus and the opening of the uterus is called the cervix (Figure 1.1). The cervix is a distinct area composed of firm and dense connective tissue that is around 4cm long and separates the uterus from the vagina. The vagina is a tubular structure covered in a squamous epithelium that connects the cervix with the external surface of the human body, where the vagina opens onto the vulva.

1.1.2. *Anatomy of female reproductive tract in mice.*

As depicted in Figure 1.2, the murine female reproductive system has many distinctions from that seen in humans. However clear parallels also exist. The significance of the differences between the two species will be discussed throughout this section. The murine ovary is fairly similar to that in the human. However, a major difference between humans and mice is that mice release around 10-20 oocytes in each cycle, rather than the usual 1 in humans. Visually, a mouse uterus is quite distinct from that of a human female; two uterine

horns are present, which meet at the cervix (Figure 1.2). A feature of the mouse reproductive process that differs significantly from humans is the fact that mice do not exhibit menstruation, although mouse models have been devised to try to mimic this process and these are discussed in section 1.3.1. Instead, in common with most other mammals, they undergo the oestrous cycle.

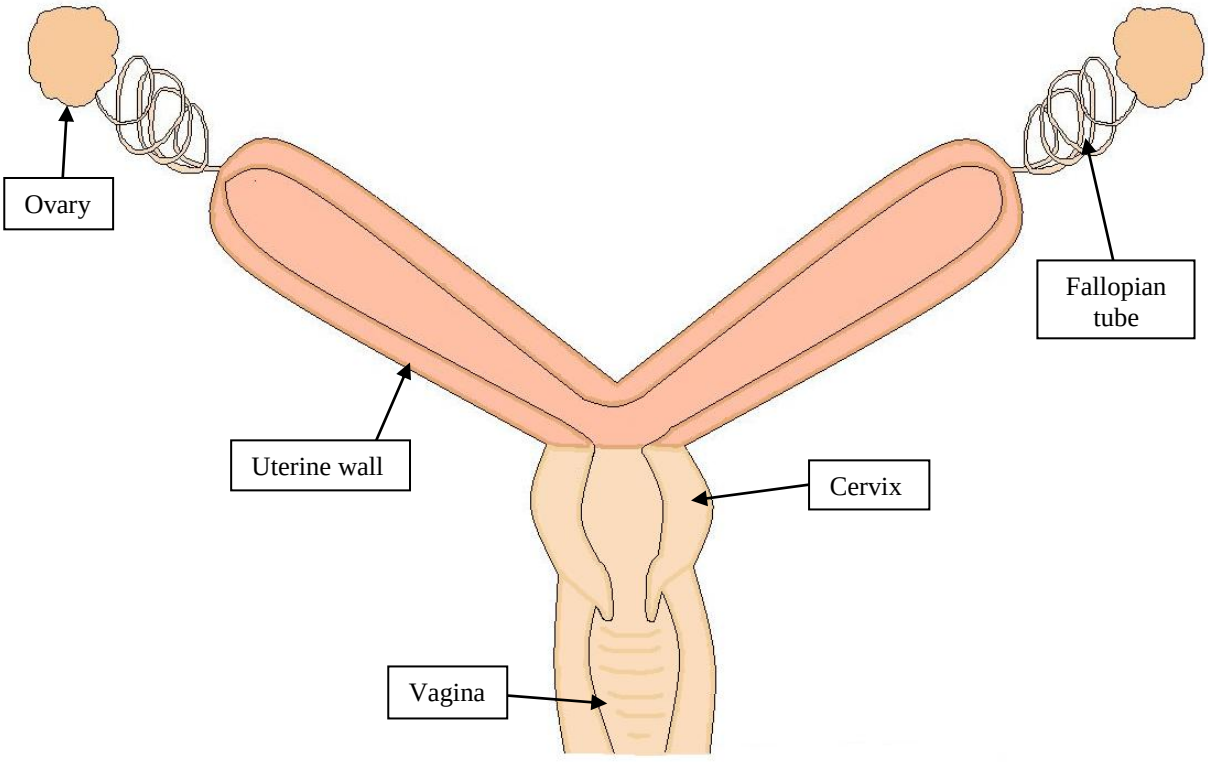

Figure 1.2. Anatomy of the female reproductive tract in mice.

Diagram showing the anatomy of the murine female reproductive system. The oocytes emerge from the ovary and travel down the small, coiled Fallopian tube and then enter the lobes of the uterine horn that sit to the right and left of the abdomen. As with humans, the vagina and cervix form the passage to the outside of the body.

Mice usually ovulate during oestrus but several environmental factors can affect when this phase occurs. The Whitten effect has been observed in mice and describes the process where male pheromones induce and synchronise oestrus in females (Gangrade and Dominic, 1984). This can easily be achieved in the lab by introducing bedding that a male has slept in to a cage containing female mice. The Vandenbergh effect involves the premature induction of oestrus in prepubertal mice stimulated by pheromones of a dominant male mouse. One theory is that contact with male urine, which may contain oestrogens, induces GnRH release by the pituitary in the females and thus, premature ovulation (Guzzo et al., 2012). The mouse oestrous cycle generally lasts 4-5 days and is

usually divided into four stages; proestrus, oestrus, metestrus and diestrus. During proestrus the follicles that will ovulate are identifiable by their size and continue to grow during oestrus. Endometrial thickness increases during proestrus in response to rising estradiol until maximum development is reached during oestrus (Graham, 1966). During metestrus, estradiol decreases and this is mirrored by a decrease in endometrial thickness and vascularity. Progesterone is at its lowest during oestrus, rises during metestrus and peaks during diestrus, when uterine thickness is at its lowest. The behaviour of immune cells in this process will be discussed in section 1.3.1.

1.1.3. *Anatomy of male reproductive tract.*

The other important aspect of sexual reproduction required for fertilisation of the ovum is of course the production and delivery of sperm by the male reproductive organs (Figure 1.3). In contrast with production of oocytes in the female, spermatogenesis does not begin until puberty. Production of sperm begins in the testes, which are housed in the scrotum to keep them 2°C lower than normal body temperature. The reasons for this are not fully understood, but an increase in temperature may induce oxidative stress, impairing spermatogenesis (Shiraishi et al., 2010). Spermatogenesis occurs in the seminiferous tubules, which are tightly coiled inside the testes. Sertoli cells are responsible for contributing to the microenvironment and allowing developing sperm to thrive. Sperm develop in the walls of the tubules and migrate into the fluid-filled lumen. Attached to the outside of the testis is the epididymis, where the tubules exit the testis. Sperm entering the epididymis are not able to fertilise ova, indicating that they mature within this structure (Jones, 1999). This structure ends in the smooth muscle-lined vas deferens, the main duct between the testis and the seminal vesicle. The seminal vesicles are large glands, which add the majority of the seminal fluid and join the vas deferens to create the ejaculatory ducts, which pass through the prostate gland and join the urethra (Figure 1.3). Further nutrients are added to the semen by the prostate gland.

Ejaculation, the process of releasing semen, is controlled by neurons and stimulation results in coordinated contraction of the smooth muscle in the walls of the epididymis, vas deferens, seminal vesicles, ejaculatory ducts and prostate. This results in semen containing around 300 million sperm entering the urethra and through more muscular contractions, being ejected from the end of the erect penis.

The male reproductive anatomy of mice is considered to be similar to that of humans, although in mice spermatogenesis occurs at 8°C below body temperature. Mice are often used as a model for spermatogenesis, and KO mice are often used to tease apart the genes that are important in the production and maturation of sperm (Pitetti et al., 2013, Kajiwara et al., 2012).

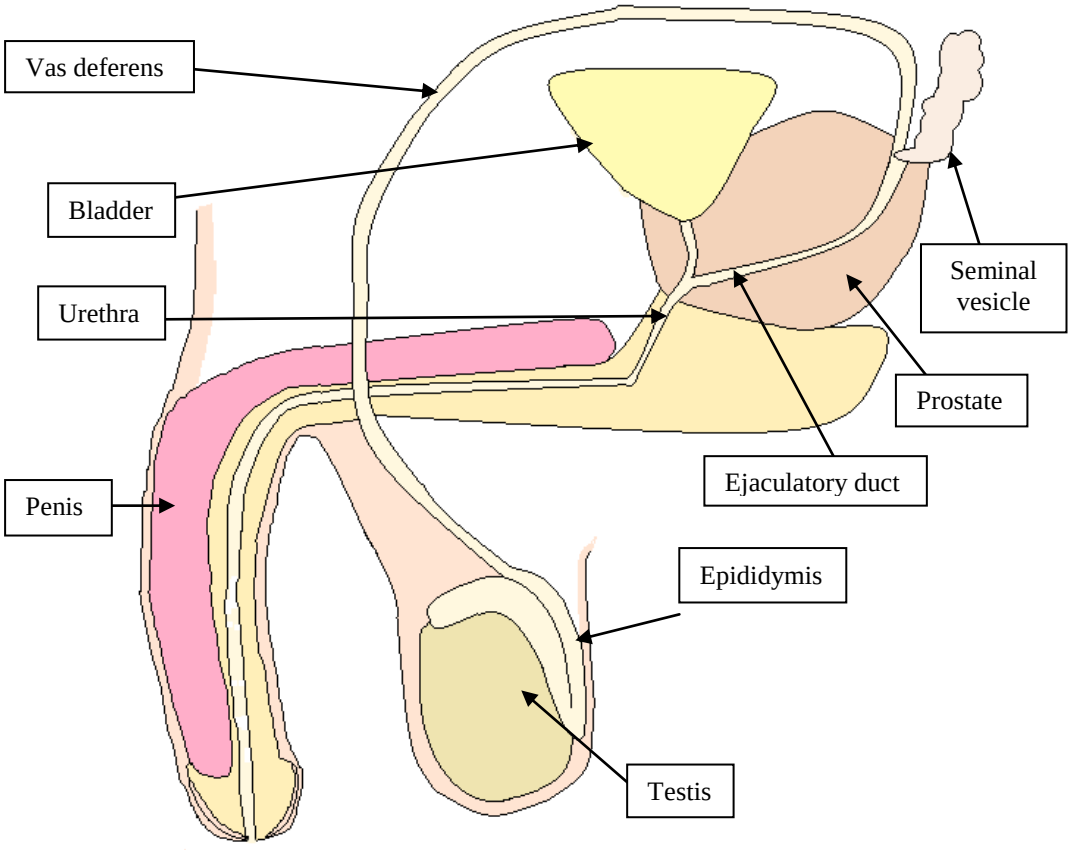

Figure 1.3. Anatomy of male reproductive tissues in males.

Diagram showing a side-on view of the male reproductive tract. Only one testis, epididymis, vas deferens, seminal vesicle and ejaculatory duct are seen, but in the body there is one on each side of the midline. When sperm are released from the testis, they travel up the vas deferens, down through the ejaculatory duct and into the urethra.

1.1.4. *Fertilisation.*

When sperm enter the uterus through the cervix, they make their way to the Fallopian tube. When fertilisation occurs sperm proteins bind to receptors on the zona pellucida. This triggers the acrosome reaction, which releases enzymes to digest the zona pellucida so the sperm can reach the membrane. The first sperm to pass through the entire zona pellucida and fuse with the plasma membrane of the ovum is the fertilising sperm. The DNA from both sperm and ovum is replicated and mitotic divisions begin to occur. The conceptus continues to travel down the Fallopian tube and, in humans, enters the uterus ~5 days

following fertilisation. At this time the zygote is at the blastocyst stage, and is composed of ~100 cells, with an outer trophectoderm and an inner cell mass.

Implantation consists of three phases: apposition, adhesion and invasion. As discussed in section 1.1.1, the endometrium becomes receptive through the process of decidualisation that begins before implantation in the late secretory phase of the menstrual cycle. Implantation completes the process. It has been hypothesised that inflammation is required for implantation and the interplay between implantation and leukocytes will be discussed in section 1.3.2. Briefly, the decidua supports the implantation of the blastocyst through secretion of growth factors, chemokines and cytokines. Decidual leukocytes also act to control trophoblast invasion. Another role of decidual cells is to provide an immunological barrier for the foetus, discussed later in section 1.3.2 (Ramathal et al., 2010).

Only when trophectoderm cells, which constitute the outer layer of the blastocyst, differentiate into trophoblast cells can the blastocyst implant in the endometrium. In humans, implantation occurs around day 21 of the cycle, 7 days after ovulation, and progesterone is maintained by the corpus luteum so the endometrium is receptive. Implantation requires expression of adhesion molecules, cytokines and chemokines. Anti-adhesive mucins such as MUC-1 are often found to be expressed on epithelial surfaces and protect the lining from damage. MUC-1 has been found to be downregulated in many mammalian species in the receptive phase of the cycle (Achache and Revel, 2006), however in humans MUC-1 is present throughout the menstrual cycle (DeLoia et al., 1998). Instead, it may be that MUC-1 is downregulated only in areas appropriate for implantation (Figure 1.4). Blastocyst implantation exhibits some parallels to the way that leukocytes exit the blood. Initially the blastocyst rolls along the surface due to adhesion molecule interactions between the blastocyst and the epithelium. L-selectin is expressed on the trophoblast surface and the carbohydrate ligands that bind this molecule are expressed on the luminal epithelium (Dominguez et al., 2005). Locally expressed chemotactic mediators also play a role in implantation. CCL2, CCL5 and CXCL8 are expressed by the endometrium during implantation, causing an upregualtion in integrins, allowing firm adhesion to the surface of the decidua (Figure 1.4)(Dominguez et al., 2005). Integrins are expressed on both trophoblasts and the luminal epithelium (Achache and Revel, 2006). Osteopontin and fibronectin are expressed by the decidualised endometrium and act as ligands for integrin subunits α3 (CD49c), α5 (CD49e), α6 (CD49f), αV (CD51), β1 (CD29) and β5 expressed by murine blastocysts (Chaen et al., 2012).

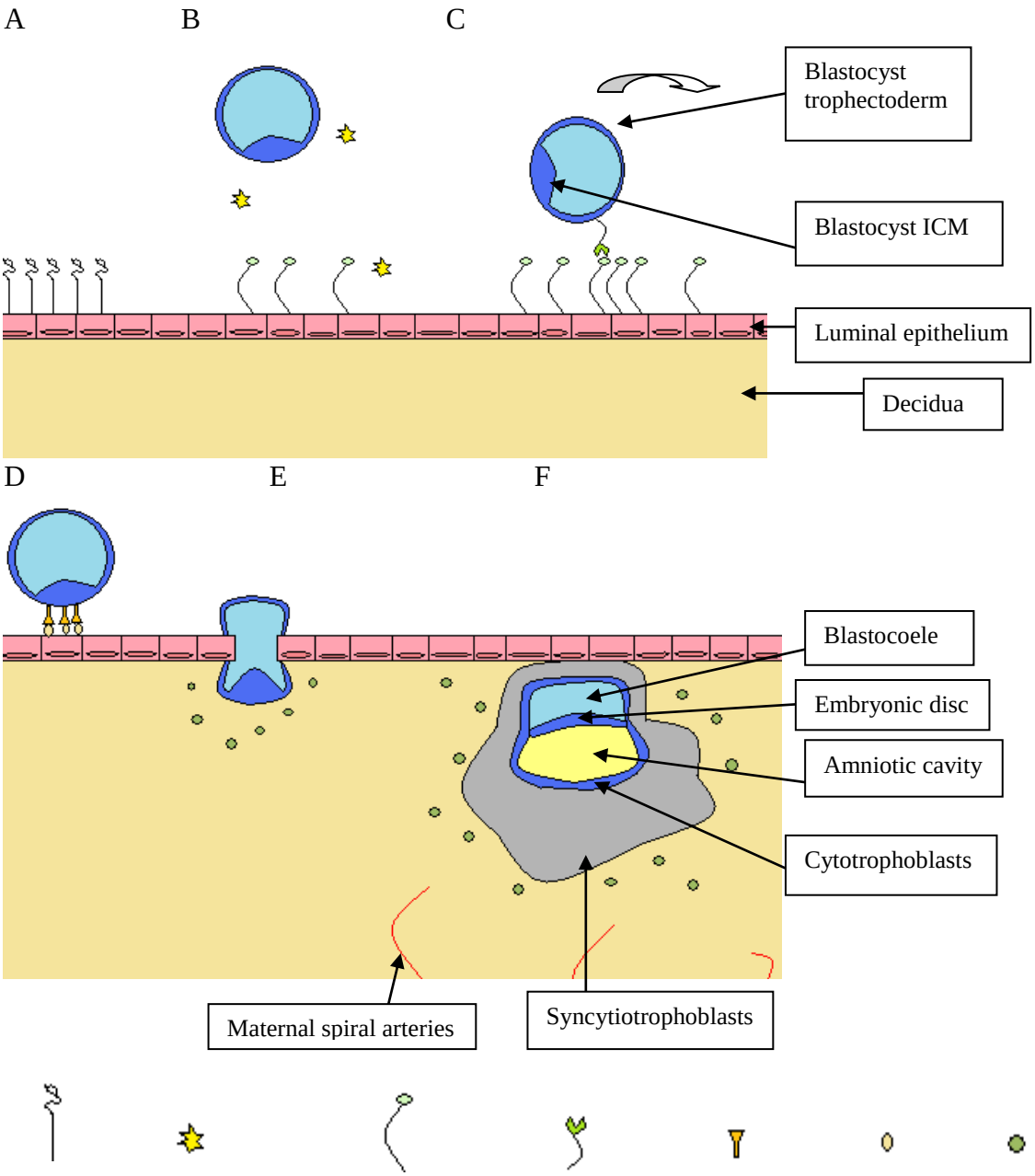

Figure 1.4. Implantation of the blastocyst into the decidua (legend overleaf).

Figure 1.4. Implantation of the blastocyst into the decidua

Illustration of the stages in the implantation of the conceptus. A) Expression of MUC-1 prevents the blastocyst implanting in a suboptimal area. B) Chemokines are thought to attract the blastocyst to the decidua and upregulate integrins on the luminal epithelium. C) The blastocyst forms loose contact with the decidua via L-selectin and rolls along the epithelium. D) Various integrin interactions are then formed, providing firm contact with the epithelium. E) The blastocyst breaches the epithelium and invades the decidual stroma. F) Trophoblasts differentiate forming cytotrophoblasts and syncytiotrophoblasts. They release MMPs, degrading the decidua as they invade towards the spiral arteries.

Implantation in humans results in the Inner Cell Mass (ICM) lying against the epithelium, though this may be as a result of the ICM migrating rather than adhesion on this side of the blastocyst (Dominguez et al., 2005). Contact triggers proliferation of trophoblast cells, which penetrate the endometrium. Invading trophoblasts secrete many types of MMPs, predominantly MMP-9, in order to assist remodelling of the maternal tissues (Hulboy et al., 1997). Decidual cells and leukocytes also contribute MMPs targeting different components of the extracellular matrix in a remodelling process which occurs throughout pregnancy (Anacker et al., 2011). Implantation in mice involves some processes that differ from human blastocyst implantation. Specifically, in mice the blastocyst homes within a crypt formed by the endometrium, which allows it to implant deeper within the decidua. Mouse blastocysts also implant in a different orientation to human blastocysts, with the orientation of the inner cell mass away from the epithelium (Cha et al., 2012). Implantation of the blastocyst provokes decidualisation in mice. Studies in mice have shown that progesterone and oestrogen are required for implantation to occur (Ramathal et al., 2010).

1.1.5. *Placentation.*

The process of placentation is important for the health of the foetus. If trophoblast invasion is insufficient it can result in conditions such as preeclampsia and restricted foetal growth. The blastocyst becomes buried in the endometrium and endometrial cells provide the early nourishment for the embryo, as described in the previous section. Following implantation at around 7 days post-conception, trophoblasts differentiate further into cytotrophoblasts and large multinucleated syncytiotrophoblasts. Cytotrophoblasts can have an invasive phenotype and erode maternal tissue to gain access to spiral arteries in the maternal endometrium. These spiral arteries undergo remodelling themselves in order to produce vessels with a wider lumen and less muscular walls. This may be in order to regulate blood pressure into the placenta. Syncytiotrophoblasts surround the embryo and are the only foetal cells that directly contact maternal cells. These trophoblasts recruit leukocytes, which help to produce an inflammatory environment for placentation to occur and are involved in the process of tolerance to the conceptus. This will be discussed in detail in section 1.3.2. The process of placentation begins, and though the placenta is established by 5 weeks after implantation, maternal blood does not flow into the placenta until the end of the first trimester. The foetal portion of the placenta grows from the trophoblast cells, with the chorionic plate being formed from the syncytiotrophoblasts remaining near the embryo. Chorionic villi develop from trophoblast cells and project into the endometrium, containing large networks of capillaries and surrounded by a pool of

maternal blood. The high surface area and close proximity between the foetal and maternal blood allows for efficient exchange of gases and nutrients.

While the process of placentation is taking place, the amniotic sac forms around the foetus, providing a buffer and protection from external pressure. The foetus floats in the amniotic fluid. As the foetus grows the umbilical cord and placenta become more developed and the amniotic sac grows to fill the uterine lumen. During pregnancy both oestrogen and progesterone continue to rise, stimulating uterine growth and inhibiting uterine contractility (Greenstein and Wood, 2006). Human Chorionic Gonadotrophin (hCG) is another hormone of pregnancy and is produced by syncytiotrophoblast cells during endometrial invasion. This hormone allows the corpus luteum to persist during pregnancy so that it can continue to produce oestrogen and progesterone. In humans the placenta takes over sex steroid production around the second month of pregnancy, and oestrogen and progesterone are synthesised in large quantities. These hormonal changes have an effect on the leukocyte populations in the decidua and circulation: this is discussed further in section 1.3.3.

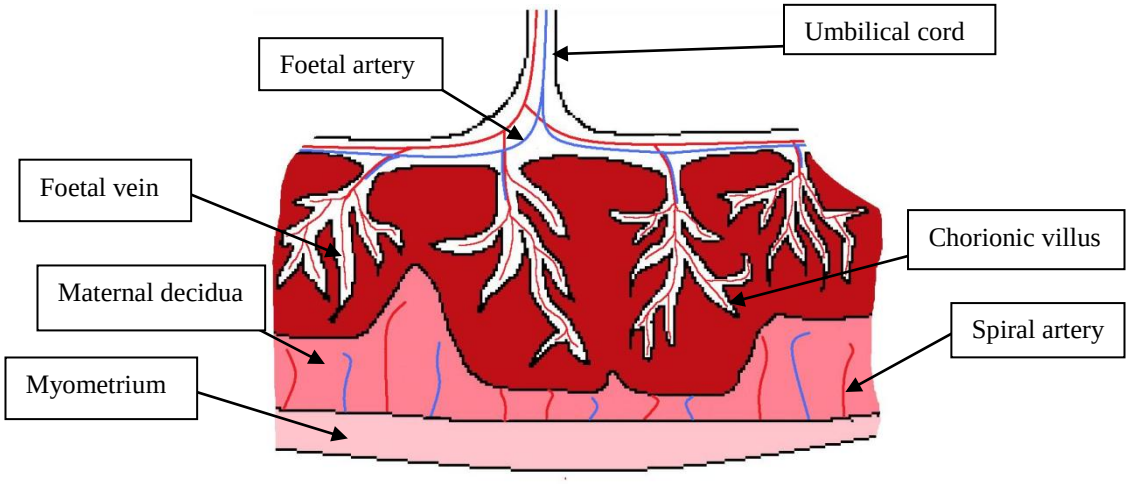

Figure 1.5. Anatomy of an established placenta in humans.

Diagram showing the chorionic villi embedded in the decidua, allowing for a large surface area for nutrient, gas and waste exchange. The foetal artery and foetal vein are connected to the foetus via the umbilical cord. These then form tree-like branches into the chorinic villi that project into maternal tissue and are bathed in maternal blood from the spiral arteries. Oxygenated blood is then carried back to the foetus via the umbilical vein.

Mice have been a valuable model for studying processes such as placentation, however there are important anatomical and physiological differences between the human and mouse placenta (Rossant and Cross, 2001), as demonstrated in Figure 1.5 and Figure 1.6.

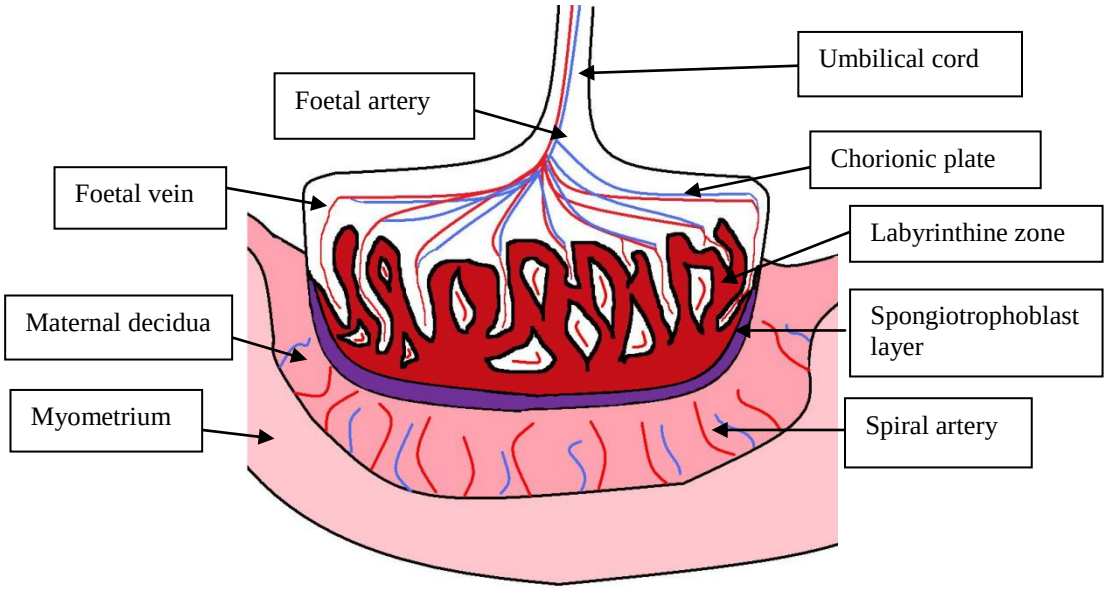

Figure 1.6. Anatomy of an established placenta in mice (legend overleaf).

Figure 1.6. Anatomy of an established placenta in mice.

Diagram to show the labyrinthine zone and other structures present in the established murine placenta. The foetal blood supply enters the placenta via the umbilical cord and reaches the chorionic plate. Projections branch into the decidua, forming a complex of chorionic trophoblasts, blood vessels and stroma. Maternal blood flows from the spiral arteries, through the spongiotrophoblast layer and into the spaces in the labyrinthine zone, allowing for exchange of nutrients and waste. Oxygenated blood is carried back to the foetus via the umbilical vein.

During implantation in the mouse, which occurs at day 4.5 post-conception, the outer layer of the blastocyst, the trophectoderm cells, differentiate to form the extra-embryonic ectoderm and the ectoplacental cone (Rossant and Cross, 2001). After implantation, giant trophoblast cells form around the embryo. These cells show similarities to human cytotrophoblast cells. The chorionic epithelium is then formed from the extra-embryonic ectoderm and foetal blood vessels begin to arise from embryonic tissue (Rossant and Cross, 2001). The trophoblasts branch to form the labyrinthine zone of the placenta, the equivalent of the chorionic villi in human placentas. This zone provides a large surface area that will eventually provide exchange of gases, waste and nutrients. Spongiotrophoblasts then develop between the giant trophoblast cells and the labyrinthine zone and these cells comprise the majority of the junctional zone (Malassine et al., 2003). The maternal blood supply must pass through the spongiotrophoblast layer in order to fill the spaces in the labyrinthine zone to allow foetomaternal exchange (Rossant and Cross, 2001). The placenta is developed by halfway through murine gestation, which typically

lasts between 19-21 days. The mouse placenta does not produce progesterone or oestrogen: instead these hormones are released by the corpus luteum, which persists throughout pregnancy due to the action of mouse placental lactogens (Malassine et al., 2003). A key difference between human and mouse placentation is that trophoblast invasion into the decidua is only superficial in mice whereas in humans trophoblasts invade deeply, reaching the myometrial layer of the uterus (Erlebacher, 2013). In humans blood flow to the placenta is much greater as decidual arterioles have larger lumens than murine decidual arterioles.

1.1.6. *Pregnancy.*

During the last few weeks of pregnancy, smooth muscle cells are reorganised so they can go from the quiescent pregnant state to be able to participate in powerful, coordinated contractions. Oxytocin receptors are expressed in the myometrium in preparation for labour. Coordinated induction of labour is important because parturition before completed foetal development, known as pre-term labour, is a significant clinical problem. As a result, several animal models for the initiation of labour have been considered. Mouse models have pointed to progesterone withdrawal as an endocrine trigger for the initiation of labour, although this is unlikely to be the case in humans as progesterone does not fall until after delivery (Mitchell and Taggart, 2009). It should be noted at this point that labour has been described as an inflammatory process in both pre-term and term birth (Thomson et al., 1999, Osman et al., 2003). Infection is a major cause of pre-term birth, indicating that inflammation may initiate labour. This will be discussed much more fully in section 1.3.4, however a brief discussion of the processes involved in parturition is included here.

1.1.7. *The initiation of labour.*

A major physiological change in the initiation of labour is the softening and ripening of the cervix, allowing this dense structure to dilate sufficiently for birth to occur. This involves enzymatic digestion of collagen, higher hyaluronan content, changes in proteoglycan content and increased tissue hydration. Protein degradation allows for reorganisation of the extracellular matrix for this drastic change in function. MMPs are thought to be the key enzymes involved in this process and different members of this family are able to cleave different components of the extracellular matrix. In many studies, MMPs have been found to be substantially increased in the cervices of women in labour compared to NP women (Hulboy et al., 1997). MMP-8 and MMP-9 concentrations increase in the cervix over the course of cervical dilation in women and this has been linked to the presence of

neutrophils, which release these enzymes from the granules (Winkler et al., 1999). The gene encoding MMP-8 is also increased in expression in the cervix during ripening in mice (Holt et al., 2011). Cervical ripening has been investigated because of its potential role in regulating both term and pre-term birth. The process has been studied in mice where collagen fibre packing in the cervix becomes sparse and more disorganised at term (Holt et al., 2011). Cox-1 and Cox-2 mRNA is increased during cervical ripening. These enzymes produce prostaglandins, which promote inflammatory responses (Holt et al., 2011). Expression of the cytokines InterLeukin (IL)-6, Tumour Necrosis Factor (TNF)α, IL-1α is also elevated during cervical ripening (Holt et al., 2011). Details of how leukocytes are involved in the process of cervical ripening will be discussed in section 1.3.4.

1.1.8. *Post-partum remodelling of the female reproductive tissues.*

Following delivery of the baby and placenta, a woman faces the post-partum recovery period. The trauma to the genital tract may lead to sexual dysfunction or anal or urinary incontinence (Romano et al., 2010). During this time, vaginal lacerations that may have occurred during delivery will also be repaired. The genital tract may never return to a pre-pregnant state but in humans active repair continues until around 6 months post-partum. This is the amount of time taken for the extracellular matrix supporting the genital tract cells to be fully restored (Romano et al., 2010).

Given the significant inflammatory insult of labour, it is remarkable that mice exhibit post-partum oestrus and are able to become pregnant again within 1 day of parturition (Bruce and East, 1956) (Krackow, 1990). However, one study suggests uterine weight remains elevated at 5DPP and the distribution of collagen bundles do not resemble that of nulliparous uteri (Shimizu and Hokano, 1988), showing that the uterine horn has not yet fully remodelled. Another study reported that uterine weight returns to pre-pregnant levels by ~5DPP (Nilsen-Hamilton et al., 2003). The remodelling process following labour is likely to persist during this time. In mice, apoptotic cells are numerous in the stromal and epithelial compartments of the uterus in the first couple of days post-partum but few are seen by 3DPP (Huang et al., 2012). Uterine cells also begin to proliferate to repair the damaged lining: this begins in the stroma within 6hours (hrs) of birth, with increased proliferation in the luminal epithelium in the next few days (Huang et al., 2012). In rats, genes encoding MMP-2 and Membrane Type 1-MMP (MT1-MMP) are more highly expressed at 18hrs and 36hrs post-partum, compared to late pregnancy, but expression tails off at 5DPP (Manase et al., 2006). This is consistent with other observations described in

this section, showing that in rodents, the early post-partum period is the most active in terms of healing. In mice, MPO activity in the cervix is increased considerably from day 15 of pregnancy to 2-4hrs after birth, indicating that this neutrophil derived enzyme is involved in repair following parturition, not cervical ripening before labour (Holt et al., 2011, Timmons and Mahendroo, 2006) These data indicate that repair of the genital tract requires an involvement of neutrophils. MPO is released by neutrophils and generates Reactive Oxygen Species (ROS) during the initial phase of tissue remodelling. The reversal of spiral artery remodelling appears not to be complete by 10DPP, as the radius and thickness of arteries has still not reached a pre-pregnant state (van der Heijden et al., 2009). These data suggest that the inflammatory nature of labour persists into the post-partum period and the secretion of leukocyte-derived mediators may be involved in post-partum remodelling. The presence and role of leukocytes in the post-partum period forms the focus of this study and a discussion on the literature in this area can be found in section 1.3.5.

1.1.9. Summary

This section has outlined some major areas of interest in the reproductive process. Leukocytes and their products are thought to play major roles in the progression through these stages, and this warrants further discussion. In order to fully explain the overlap between the reproductive and immune systems, in the next section I provide a general description of immune processes and the role of leukocytes during inflammation.

1.2. The immune system

The basics of reproductive biology have been introduced, and it is now pertinent to consider another major biological system relevant to parturition: the immune system. As alluded to earlier, labour and subsequent post-partum tissue remodelling are characterised by a strong inflammatory response in reproductive tissues, and this observation is central to the work presented in this thesis. Crosstalk between the immune system and reproductive biology will be considered later: this section will provide a general overview of leukocyte biology.

1.2.1. *Leukocyte development.*

The immune system is comprised of a diverse range of functionally distinct cell types that collectively act as the body's defence mechanism. Leukocytes, also known as white blood cells, are the most important cells of the immune system and are classified according to their ontogeny, surface phenotype and function. In reality, these cell types are plastic and change their function and phenotype in response to various stimuli, however characterising and subsetting these cells can be useful in gaining an understanding of cell function in a snap-shot of time. Leukocytes mature in primary lymphoid organs, circulate in the blood, and interact with other cells, pathogens and other microorganisms, and pathogen products. The presentation of host and foreign antigens in secondary lymphoid organs and other tissues is a key process in the induction of adaptive immune responses and the development of immune memory. Specific leukocyte subsets are recruited from the blood into tissues under homeostatic conditions and these migratory processes play a critical role in immunosurveillance. Tissue damage and/or infection leads to inflammation, which is characterised by the co-ordinated and sequential recruitment of large numbers of blood-borne leukocytes to tackle the infection and repair the damaged tissue. The Bone Marrow (BM) and thymus are primary lymphoid organs, whereas spleen and lymph nodes are secondary lymphoid organs. Most leukocytes are generated in the BM, which contains haematopoietic stem cells that give rise to lymphoid stem cells, platelets, erythrocytes and myeloid cells. Myeloid cells are derived from a granulocyte-monocyte common precursor, and their development is controlled by a variety of cytokines, including Granulocyte Colony-Stimulating Factor (GCSF) and Macrophage Colony-Stimulating Factor (MCSF). Lymphoid stem cells give rise to lymphocytes, including T and B cells. B cells mature in the BM and the spleen, whilst T cell precursors seed the thymus where they undergo selection to create the mature T cell repertoire.

1.2.2. *Granulocytic cells.*

Granulocytes are divided into three main subsets: neutrophils, eosinophils and basophils. All three have granules containing substances important in specific inflammatory responses. The production of neutrophils in the BM is controlled by GCSF and they are released from the BM due to increased activity of the CXC chemokine Receptor 2 (CXCR2) and decreased activity of another chemokine receptor, CXCR4, that holds immature neutrophils in the BM (Martin et al., 2003). Neutrophils in the blood are short-lived, as after executing their tasks in immune defence, they quickly undergo apoptosis. Neutrophils have a half-life of only 6-8hrs and are the first cells to arrive at a site of infection or tissue damage (Summers et al., 2010, Bugl et al., 2012). As circulating neutrophils age they increase their expression of CXCR4 and home back to the BM (Martin et al., 2003). Neutrophils constitute 50-70% of circulating leukocytes in humans and are the largest single leukocyte population (Kindt et al., 2007).

Neutrophils contribute significantly to innate immunity by producing potent immunomodulatory factors such as cytokines and chemokines. Neutrophils are also highly effective phagocytes, and play an important role in immune defense and the repair of damaged tissues by eliminating pathogens and removing host cell debris. Cells that perform this function efficiently are known as professional phagocytes. Neutrophils, along with monocytes, macrophages and Dendritic Cells (DCs) would all be described in this way. In DCs, phagocytosis involves the uptake and digestion of fragments such as cellular debris or damaged cells, and peptide antigens are then processed and presented to naïve helper T (Th) cells via the Class II Major Histocompatibility Complex (MHC) complex to initiate adaptive immune responses (Kindt et al., 2007). Many phagocytes contain granules filled with enzymes such as MPO that generate ROS, which are deadly to both invading and host cells. When damage occurs in the absence of infection, Pattern Recognition Receptors (PRRs) detect damage-associated molecular patterns, such as DNA and intracellular proteins leaking from cells during necrosis. During infection, PRRs recognise pathogen-associated molecular patterns like LipoPolySaccharide (LPS), and initiate an inflammatory cascade involving cell activation, and triggering the release of classic pro-inflammatory cytokines including TNF-α, IL-1β and IL-6, which in turn activate other leukocytes. Activation also causes the release of inducible inflammatory chemokines to attract other cells to the area (Steevels and Meyaard, 2011). Secretion of these factors will also induce changes in nearby endothelial cells, increasing expression of integrin molecules, promoting more immune cells to migrate to the affected area. Excess

inflammation is deleterious to host tissue so the course of these changes must be carefully controlled, neutrophils can cause particularly extensive damage if their activity and longevity are not regulated (Soehnlein and Lindbom, 2010). Antibodies that have bound to a pathogen may have their Fc region detected by an Fc receptor, such as CD16 or CD32. Binding of Fc receptors causes cytoskeletal changes that result in phagocytosis, during which the pathogen is enveloped by the phagocyte and fuses with the lysosome to be degraded. Alternatively, Fc binding may result in Antibody Dependent Cellular Cytotoxicity (ADCC), a function primarily associated with Natural Killer (NK) cells, though macrophages and granulocytes are also capable of this process. During ADCC proteins such as perforin and granzymes, are released triggering apoptosis in the target cell.

Eosinophils egress from the BM in a mature state but do not make up a large proportion of cells in the blood. However during inflammation they are capable of infiltrating peripheral tissues where their lifespan is increased (Rosenberg et al., 2013). Eosinophils are classically associated with allergy and parasitic infections. The main mediators associated with eosinophil migration, activation and survival are the cytokine IL-5 and ligands for the chemokine receptor CCR3, such as CCL11. IL-5 is typically produced by Th2 cells, though other cell types such as NK cells can also be the source of this cytokine (Rosenberg et al., 2013). When activated, eosinophils degranulate, emptying their granule contents into the surrounding environment. Granule proteins such as Major Basic Protein (MBP) can exert anti-parasitic effects and activate other leukocytes such as neutrophils and mast cells (Rosenberg et al., 2013). Eosinophils also exhibit some weak phagocytic activity, though in comparison to other cell types this is not regarded as their main role in immunity. Eosinophils also express MHC class I and MHC class II, as well as costimulatory molecules and have been observed trafficking to secondary lymphoid organs, providing evidence that they are able to modulate T cell responses (MacKenzie et al., 2001). Indeed, antigen processing by eosinophils and presentation to CD4+ T cells has also been demonstrated *in vivo* (MacKenzie et al., 2001). Many of the subtleties of eosinophil function remain unknown and it is likely that a lot of their activities in inflammation are still to be discovered (Rosenberg et al., 2013). The recruitment of eosinophils by chemokines will be discussed in section 1.2.11.

Basophils are rare non-phagocytic granulocytes, representing less than 1% of leukocytes in the blood. They are similar to mast cells, which enter the blood in an undifferentiated state and only mature upon migrating to tissues. Both cell types express the high-affinity IgE

receptor and participate in type I sensitivity reactions, releasing histamine, Th2 cytokines, and leukotrienes (Kadena et al., 1997). Though these cells are of key importance in allergy, they are not investigated in this thesis so will not be discussed further.

1.2.3. *Monocytes and macrophages.*

Monocytes are found in the blood and BM, and differentiate into macrophages upon entry into tissues. Monocytes can also differentiate into DCs and other specialised cell types such as osteoclasts, which are involved in homeostatic and pathogenic bone-destruction, and microglia, which are brain-resident macrophages. Human monocyte subsets are identified by expression of the antigens CD14 and CD16. $CD14^{hi}$CD16- monocytes are primarily involved in inflammation, while CD14+CD16+ monocytes exhibit more homeostatic behaviour. In mice these two subsets are identified by differences in expression of Ly6C and the chemokine receptors CCR2 and CX3C chemokine Receptor (CX3CR1). Experimentally, anti-Ly6C antibodies are used to detect Ly6C. Gr1 antibody is another antibody that is commonly used because it recognises Ly6C, however it also detects Ly6G, the latter being restricted to neutrophils and other granulocytes. In humans and mice, inflammatory monocytes express CCR2, while homeostatic monocytes carry the CX3CR1 chemokine receptor. Human and mouse subsets do show some phenotypic differences, although $CD14^{hi}$CD16- monocytes are considered equivalent to inflammatory $Ly6C^{hi}CCR2^{hi}CX3CR1^{low\ (lo)}$ monocytes and CD14+CD16+ monocytes in humans are thought to share similarities to $CX3CR1^{hi}CCR2^{lo}Ly6C^{lo}$ monocytes in mice (Geissmann et al., 2003).

In mice, monocytes emerge from the BM as $Ly6C^{hi}$ and lose this expression upon maturation in the circulation, giving rise to $Ly6C^{lo}$ monocytes under steady state conditions (Sunderkotter et al., 2004). Monocytes are released from the BM due to the action of CCR2 (Serbina and Pamer, 2006)(described in section 1.2.11). While in the circulation, changes in chemokine receptor expression occur, with CCR2 being reduced and CX3CR1 expression increasing. Monocytes have the ability to differentiate into macrophages and DCs upon entry into tissues. Monocytes contribute to steady state turnover of tissue resident macrophages and DCs as well as generation of cells that contribute to inflammation and pathogen clearance. Strikingly, the two monocyte subsets exhibit disparate homing and functional characteristics (Figure 1.7)(Geissmann et al., 2003), (Sunderkotter et al., 2004). $Ly6C^{hi}CCR2^{hi}CX3CR1^{lo}$ monocytes are preferentially recruited to sites of inflammation (Geissmann et al., 2003) and infection, whereas

$CX3CR1^{hi}CCR2^{lo}Ly6C^{lo}$ monocytes are mostly restricted to blood and non-inflamed tissues. These subsets were first defined in mice using adoptive transfer of monocytes from $CX3CR1^{+/gfp}$ mice in which one CX3CR1 allele had been replaced with Green Fluorescent Protein (GFP). In these mice, cells with expression of CX3CR1, which includes most monocytes, are labelled with GFP and can therefore be tracked (Geissmann et al., 2003). Upon transfer into mice with an inflamed peritoneum, $GFP^{lo}Gr1^{+}$ monocytes (equivalent to $Ly6C^{hi}$ monocytes) quickly migrated to the site of inflammation and differentiated to express CD11c, a marker for DCs (Geissmann et al., 2003). The GFP^{hi}Gr1- subset (equivalent to $Ly6C^{lo}$ monocytes) were found to be longer lived and gave rise to resident CD11c+ DCs in the liver lung and spleen (Geissmann et al., 2003). This subset is characterised by its patrolling behaviour, crawling along the inside of blood vessels under resting conditions (Auffray et al., 2007). The CX3CR1 receptor and the integrin complex CD11a/CD18 were found to be crucial for this homeostatic surveillance movement. Fewer crawling monocytes were observed in CX3CR1 KO mice, compared to the Wild Type (WT), even though the number of Gr1- monocytes was equivalent between the genotypes (Auffray et al., 2007). This suggested that the receptor plays a specific role in monocytes patrolling the endothelium. Antibodies blocking CD11a and CD18 abolished patrolling behaviour, indicating that moving along the vessel wall requires this integrin combination (Auffray et al., 2007). Recent findings indicate that there are populations of both $Ly6C^{lo}$ and $Ly6C^{hi}$ monocytes which reside in the spleen and are mobilised in response to inflammation (Swirski et al., 2009). It is likely that this reservoir of monocytes is of importance in the response to infection and tissue damage, and further investigation is needed to characterise their role.

When monocytes migrate into tissues they can differentiate into macrophages. This transformation includes a large increase in size and the acquisition of new functions such as increased phagocytosis and the ability to secrete an altered repertoire of cytokines and other factors (Kindt et al., 2007). The precise phenotype of the macrophages that develop from the infiltrating monocytes is profoundly influenced by the microenvironment and health status of the tissue. Although development from haematopoietic stem cells has been regarded as the sole pathway for macrophage development, progenitors in the yolk sac have recently been shown to give rise to $F4/80^{bright}$ macrophages, indicating that there are at least two lineages of macrophages (Schulz et al., 2012).

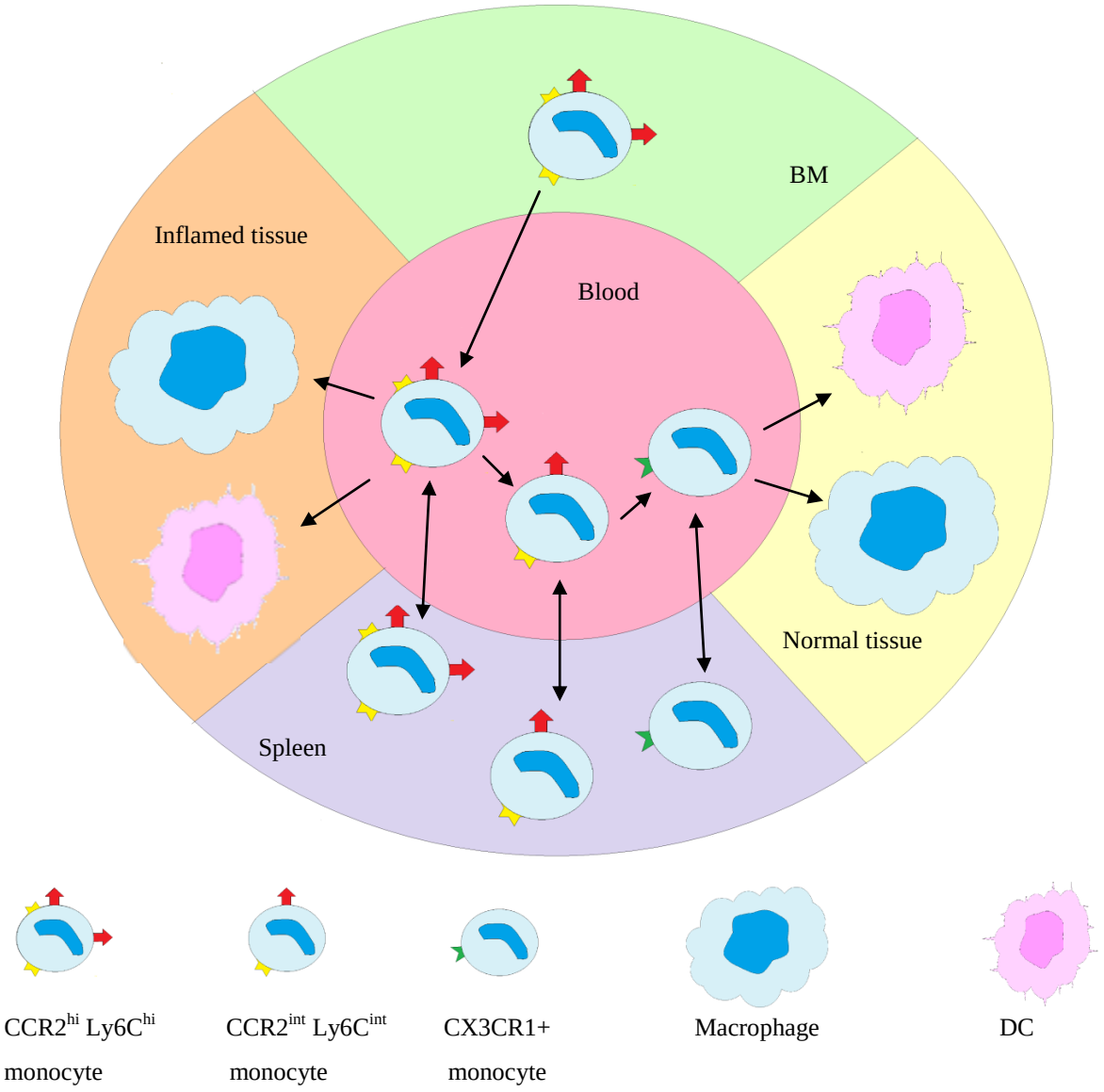

Figure 1.7. Migration and differentiation of monocytes in mice.

Ly6C^{hi} inflammatory monocytes emerge from the BM and either migrate into inflamed tissue and differentiate into inflammatory macrophages and DCs, reside in the spleen or continue to circulate and lose their expression of Ly6C and CCR2. These homeostatic Ly6C^{lo}CX3CR1 monocytes may return to the spleen or patrol blood vessels where they may be recruited to normal tissue.

Macrophages participate in innate and acquired immune responses and their key functions include cytokine production, phagocytosis, antigen processing and presentation. It is now recognised that in some situations macrophages can proliferate within tissues (Murray and Wynn, 2011). Macrophages can be found performing specialised roles in secondary lymphoid organs; macrophages are highly effective as phagocytic cells and clear apoptotic cells and debris, they are often seen as cellular guards due to their relatively long half life

within tissues and their ability to promote inflammation without excess damage to the host (Soehnlein and Lindbom, 2010). Threats to the tissue are detected in a number of ways, including PRRs e.g. Toll-like receptors (TLRs), and Fc receptors, which detect opsonised fragments of pathogens or dying cells. Other signals, such as the phagocytosis of apoptotic neutrophils, stimulate macrophages to resolve inflammation by producing anti-inflammatory cytokines and clearing debris (Soehnlein and Lindbom, 2010). Macrophages also secrete signals that promote repair such as growth factors and lipid mediators called resolvins (Soehnlein and Lindbom, 2010).

Macrophages are often described as being activated in different ways, termed 'classical' and 'alternative', and these different macrophage types have disparate functions. Classically activated macrophages, also referred to as M1 macrophages, are involved in defence against pathogens. Alternatively activated, or M2, macrophages contribute to remodelling. Polarisation of these macrophages is similar to lymphocyte polarisation, with M1 macrophages being generated from monocytes in response to InterFeroN γ (IFNγ) while cytokines such as IL-4 and IL-13 induce M2 production (Mantovani et al., 2013). These macrophages secrete and respond to different kinds of chemokines, notably in humans CCL2 can induce polarisation to M2 macrophages (Roca et al., 2009). In reality, macrophage polarisation is not a simple M1 vs M2 distinction and a whole range of possible phenotypes exist depending on the signals these cells receive from their environment and the requirements of the tissue.

1.2.4. *T Lymphocytes and acquired immunity.*

Lymphocytes are key cellular components of the adaptive immune system. The main lymphocyte types are T cells, B cells and NK cells, however many subsets are included within these broad categories. T cell precursors are generated in the BM and mature in the thymus. B cells are also generated in the BM and begin their maturation here, but then migrate to the spleen where they differentiate into naïve, follicular or marginal zone B cells (Pieper et al., 2013). B cells are central to humoral immunity and crucial for adaptive immunity, and their antigen specific structures are antibodies. Adaptive immunity is reliant on antigen recognition and specificity. Lymphocytes as a whole have an incredibly broad range of antigen receptors. The main feature which distinguishes T cells from other cells is the T Cell Receptor (TCR). The TCR is a heterodimer and most cells express the α and β chains, though 5% of T cells express the γδ combination. Each chain is composed of a Variable (V), Joining (J) and a Constant region. There are also and Diversity (D)

segments, which appear in the β and δ chains. During T cell development in the thymus, functional receptors are produced through a process of gene rearrangement. In α and γ chains the V and J segments are reorganised, whereas in β and δ chains the V, D and J regions are rearranged. The diversity of the receptors is attributed to this process of gene recombination. The α and β chains have three Complementarity Determining Regions (CDRs), which are the most variable sites in the receptor. It was first thought that CDR3 engages the peptide, while CDR1 and CDR2 dock with the MHC, though variations on this have now been reported (Borg et al., 2005).

T lymphocytes are categorised into two principal subsets: CD4+ T cells and CD8+ T cells (Figure 1.8). CD4+ T cells act as Th cells and when activated secrete cytokines that modulate and regulate other components of the immune system. CD8+ T cells are often referred to cytotoxic T cells (Tc) and when activated by their TCR and coreceptors secrete toxic granules to kill the target cell. DCs encounter antigen in the periphery, take it up and process the peptide antigen for presentation to the T cell. DCs then home to secondary lymphoid tissues where they position themselves in T cell areas in order to activate naïve T cells. MHC class I presents peptide to the TCR on CD8+ cytotoxic T cells and whereas MHC class II engages with the TCR on CD4+ helper T cells. A second signal is also required. The second signal may either be stimulatory, such as when CD28 is engaged by B7, alternatively the second signal may be delivered by engagement with CTLA-4, which produces an inhibitory signal. Cytokine help from other CD4+ T cells also stimulates this process. If both of these two signals are received there is rapid clonal expansion, supported by IL-2, producing a population of memory and effector T cells with the same specificity. Activated T cells then differentiate to create different types of effector cell with the same antigen specificity.

When an activated CD8+ T cell counters infected or dysfunctional cells, Tc cells release their granule contents as shown in Figure 1.8. Perforin, granzymes and granulysin act to mediate cell killing. There are two main mechanisms proposed for perforin-mediated granzyme entry to target cells. Perforin molecules may become inserted in the plasma membrane of the target cell, forming pores, allowing granzymes to enter the cell via passive diffusion. Alternatively, after a perforin pore has become embedded in the membrane of the target cell, the membrane may pinch off, forming a vesicle inside the target cell, containing granzymes from the cytotoxic synapse (Susanto et al., 2012). Granzymes then exit the vesicle via perforin, delivering the enzymes to the cytosol.

Granzymes act to induce apoptosis in the target cell via induction of caspases, initially caspase 9, an initiator caspase is activated, which triggers the activity of effector caspases such as caspase 3, 6 and 7 (Susanto et al., 2012). Effector caspases are responsible for cleaving numerous proteins, which cause apoptosis of the target cell.

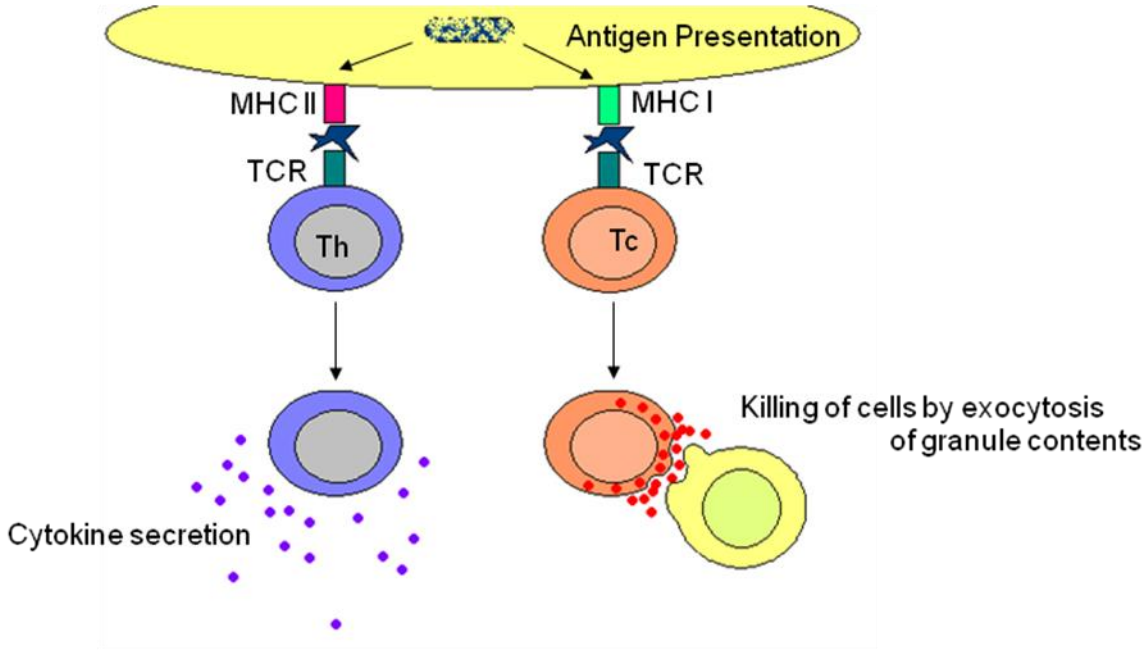

Figure 1.8. T cell activation following interaction with MHC complexes.

Diagram showing simplified effector functions of T cells upon antigen encounter. Professional Antigen Presenting Cells (APCs) present peptide antigens such as fragments of pathogens to the TCR via MHC class II. This interaction activates CD4+ T cells, causing them to polarise into different effector cell types with potential to release cytokines to support the inflammatory response by inducing effector functions in other cells. An infected cell may present foreign antigen to CD8+ T cells via MHC class I, inducing the cytotoxic function of the T cell and causing the exocytosis of cell killing enzymes such as granzymes.

The thymus is the site where most T cells mature and gain CD4 and CD8 co-receptors (Figure 1.9). When αβ T cells develop, progenitors progress through four 'double negative' (DN) cell stages. T cell precursors arrive at the thymus lacking CD4 and CD8 and most T cells emerge from the thymus expressing either one of these receptors. Immature thymocytes do not express TCR/CD3 complexes (Turka et al., 1992), thus the thymus contains triple negative thymocyte subsets (CD3-CD4-CD8-)(Godfrey et al., 1993). This is of note as identification of T cells using CD3 misses out some developing T cell subsets in the thymus. Instead, the DN developmental stages are defined by the expression of the markers CD44 (an adhesion molecule) and CD25 (IL2Rα)(D'Acquisto and Crompton, 2011, Carpenter and Bosselut, 2010, Kindt et al., 2007). DN1 cells are CD44+CD25-, progressing to DN2 where cells are CD44+CD25+, followed by DN3 cells expressing

CD44-CD25+, during the final DN T cell stage cells neither CD44 nor CD25 are expressed. Following the four DN stages, thymocytes become CD4+CD8+ Double Positive (DP) before the positive and negative selection processes ultimately leading to the generation of Single Positive (SP) CD4+ or CD8+ T cells that leave the thymus and circulate in the blood.

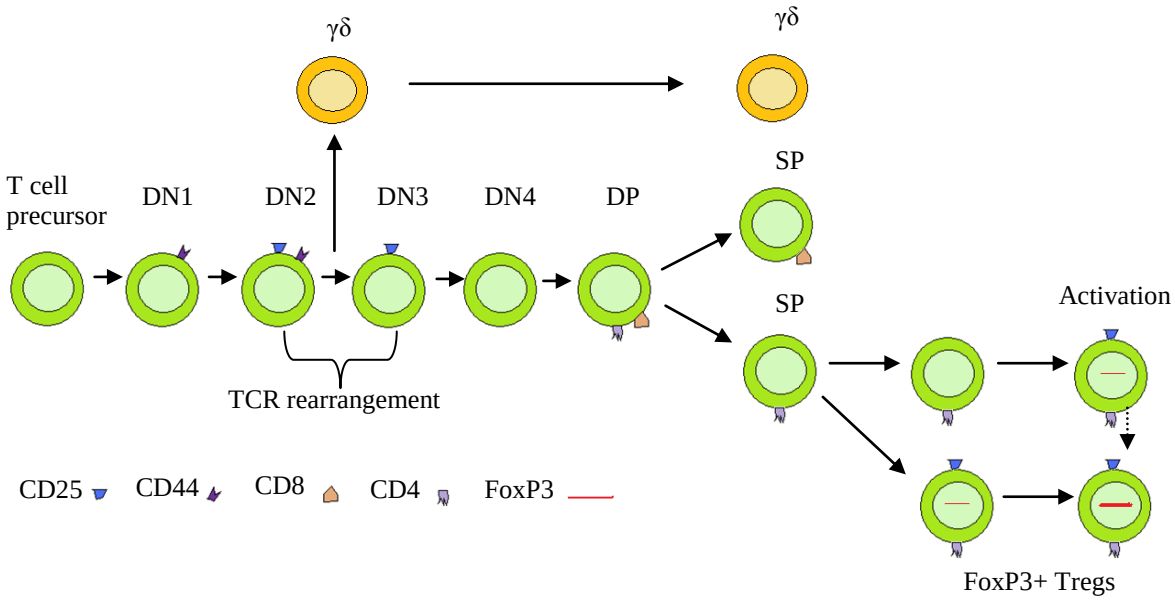

Figure 1.9. Development of T cells in the thymus.

Diagram showing CD44, CD25, CD4, CD8 and FoxP3 distribution during T cell development in the thymus. T cell precursors enter the thymus and enter stage DN1 where cells are CD44+CD25-, DN2 cells express both so are CD44+CD25+. During stages DN2 and DN3 TCR rearrangement occurs, during the process of rearrangement the decision is made about the fate of which TCR subunits will be expressed. Therefore, γδ T cells are generated between DN2 and DN3 and remain unchanged until their release. Continuing αβ T cells progress to DN3 when CD44 expression is downregulated, while CD25 expression is maintained, making DN3 cells CD44-CD25+, whereas DN4 cells lack both receptors. Thymocytes emerge from this stage with neither CD44 or CD25 but gain both CD4 and CD8 coreceptors, making them DP. From this stage either CD4 or CD8 is downregulated, producing SP cells, which migrate from the thymus into the circulation. Regulatory T cells (Tregs) are generated from SP CD4+ T cells entering the circulation. Naïve Tregs have high CD25 expression and low FoxP3 expression, upon activation their FoxP3 expression increases. Activated CD4+ T cells may have some CD25 and FoxP3 expression, making identification of Tregs challenging. Also CD4+ T cells may polarise towards a Treg phenotype. Adapted from (Kindt et al., 2007) and (Sakaguchi et al., 2010).

Between DN2 and DN3 γδ T cells arise as TCR rearrangement begins. In order for mature αβTCR+ CD4+ or CD8+ T cells to be produced cells must undergo positive selection in order that cells that do not respond to self-MHC molecules undergo apoptosis. Then

negative selection eliminates cells that bind self-MHC molecules with high affinity, a process which prevents autoimmune responses (Kindt et al., 2007, D'Acquisto and Crompton, 2011).

T cells carrying TCR-γδ are able to recognise some mycobacterial compounds not detected by αβ T cells (Kabelitz, 2011). Another distinction is that many γδ T cells migrate to the skin, gut, lungs and uterus, compared with naïve αβ T cells, which predominantly home to the lymphoid tissues (Vantourout and Hayday, 2013). Homing of γδ T cells to these sites is likely to be linked with the finding that γδ T cells in murine skin were found to express a single TCR repertoire, as were γδ T cells found in the uterus and vagina (Itohara et al., 1990). It seems that these subsets found at barrier sites are specialised to respond to particular threats posed by those environments. Cells bearing TCR-γδ are also thought to participate earlier in the immune response than αβ T cells (Vantourout and Hayday, 2013). In addition, γδ T cells are thought to be a crucial source of IL-17 during defence against a range of pathogens and against tumours (Sutton et al., 2012).

Our understanding of T cell subsets and their roles has evolved and become more complex over time and our description of cells as fitting into discrete categories is unlikely to reflect the plastic nature of these cells. After activation and clonal expansion, naïve T cells differentiate into a variety of different effector cell types. For many years it was considered that there were only two types of Th cell generated after CD4+ T cell activation, namely Th1 and Th2 types. Th1 cells were regarded as pro-inflammatory and involved in infection by viruses and bacteria, whereas Th2 cells participated in allergy and clearance of parasitic infections. Th1 cells are able to secrete cytokines such as IFNγ, TNFα and IL-12, whereas IL-4, IL-13 and IL-5 are classic Th2 cytokines. This two helper T cell view is far too simplistic and was challenged by the discovery of a number of other cell types, including Th17 cells that secrete IL-17 and IL-23 and have been associated with control of bacterial infections and some autoimmune diseases. The way in which the antigen presenting DC was activated contributes to how the T cell will be polarised. In fact, Th1, Th2 and Th17 cells represent extreme phenotypes and in reality much T cell plasticity exists.

Additional T helper cells that can be generated after naïve CD4+ T cell activation include T Follicular Helper (T_{FH}) cells. These cells express CXCR5, the receptor for the chemokine CXCL13, which allows them to position themselves in CXCL13-rich follicles in secondary lymphoid organs (Fazilleau et al., 2009). Here they interact with activated B

cells presenting antigen in MHC class II, and support these B cells as they enter the germinal centre reaction as described below.

Another cell type which changed the conventional view of T cells was the discovery of regulatory T cells (Sakaguchi et al., 2010). These cells have been shown to suppress inflammation, protect against autoimmunity and will described in section 1.3.2 in their role of promoting tolerance to a semi-allogeneic foetus during pregnancy. Many different kinds of regulatory/suppressor cell have been identified since, such as Th3, Tr1 and CD3+CD4-CD8- cells, but the properties of CD4+CD25+FoxP3+ Tregs have been the most widely studied. The development of CD4+CD25+FoxP3+ Tregs is also displayed in Figure 1.9, naïve Tregs of this kind express FoxP3 and CD25 upon exit from the thymus and activation of these cells leads to a further upregulation of FoxP3. There may also be other developmental pathways such as polarisation of activated CD4+ T cells towards this phenotype. Upon an encounter with an antigen, activation of these cells leads to creation of a tolerogenic cytokine environment, which regulates immune responses. Inadequate Treg responses have been linked to autoimmune diseases, allergy and transplant rejection (Schmetterer et al., 2012). Tregs produce cytokines such as IL-10, TGFβ and IL-35 and downregulate effector T cell responses through molecules such as CTLA-4 (Schmetterer et al., 2012). Tregs can also kill effector T cells via a granzyme/perforin dependent mechanism (Cao et al., 2007) and they may induce apoptosis through Fas/FasL interactions (Strauss et al., 2009). CD25 is the α chain of the IL-2 receptor, and this receptor mediates another mechanism by which Tregs exert their regulatory influences. As CD25 is expressed at such high levels on Tregs the binding of IL-2 to its receptor deprives other cells of a cytokine that is crucial for T cell activation and survival (Pandiyan et al., 2007).

1.2.5. *B cell activation.*

B cells have a key role in the inflammatory response. During maturation in the BM, rearrangement of the genes for both the light and heavy immunoglobulin chains occurs. In the BM self-reactive B cells are selected against to make sure self-tolerance is maintained. On leaving the BM B cells express IgM but the cells are not mature naive B cells until they express IgD and IgM on their cell membrane (Kindt et al., 2007). A subset of B cells found in humans and mice, B1 cells, express IgM and have low expression of IgD. B1 B cells only constitute a small proportion of circulating B cells but are numerous in the pleural and peritoneal cavities (Kindt et al., 2007). The marginal zone is located in the spleen, forming the border between the red and white pulp. The marginal zone contains specialised B cells,

which are partially activated, as well as macrophages and DCs. As blood flows from the marginal sinus marginal zone B cells are exposed to antigens in the blood and they provide a rapid humoral response to any challenges (Muppidi et al., 2011). Marginal zone B cells are $IgM^{hi}CD21+CD1d+$, which distinguishes them from follicular B cells and are positioned in the marginal zone by stimulation of the cannabinoid receptor CB2 (Muppidi et al., 2011) and through the action of CXCR5 and Sphingosine-1-Phosphate Receptor 1 (S1PR1)(Cinamon et al., 2008, Arnon et al., 2013). Marginal zone B cells participate early in the adaptive response and following activation, form short-lived plasma cells, which secrete antibodies.

B cells also reside in follicles in the white pulp, these are known as follicular B cells and have a $IgM^{hi}IgD^{hi}CD23+$ phenotype. When a B cell encounters an antigen, often presented on follicular DCs, then the B cell becomes activated but also internalises and processes the antigen, presenting it in the context of MHC class II. B cells then come into contact with T_{FH} cells that have migrated to the edge of the B cell follicle from the T cell area. These cells engage the B cells via their TCR, CD40L and CD28 interacting with MHC class II, CD40 and B7 on the B cell (Kindt et al., 2007). The T_{FH} cell then secretes cytokines that promote B cell proliferation and together they contribute to the initiation of the germinal centre reaction. Within the germinal centre B cells proliferate, differentiate, develop the ability to produce higher affinity antibodies, and class switch their antibodies. Activated B cells begin in the dark zone of the germinal centre and proliferating B cells (centroblasts) undergo somatic hypermutation in order to create specific, high affinity antibodies, this is essential in producing a specific, efficient immune response. Centroblasts proliferate to produce centrocytes then migrate to the light zone where they stop proliferating and undergo class switching to produce a range of immunoglobulins dependent on the cytokine milieu. Before exiting the light zone the centrocytes mature into either antibody generating plasma cells or long-lived memory cells, preserving the B cell specificity for further encounters with the antigen.

1.2.6. *NK and NKT cells.*

Natural Killer (NK cells) are classified as lymphocytes but unlike B cells and T cells straddle both innate and adaptive immunity. NK cells play a complementary role with Tc cells and though they share many similarities, there are some important distinctions. Tc cells target cells which present antigens via MHC class I. As a result many infected or tumour cells downregulate their MHC class I in order to escape recognition (Topham and

Hewitt, 2009). NK cells target cells that have no MHC class I or express it at low levels, resulting in cell killing and production of large amounts of cytokines such as IFNγ. NK receptors such as NKG2D recognise stress-induced ligands on cells, such as MICA and MICB in humans, and Rae1 and H60 in mice (Raulet, 2003). NKG2D ligands are upregulated on the surface of tumour cells and infected cells, allowing them to be detected by NK cells (Raulet, 2003). In addition, NK cells kill in a perforin/granzyme dependent way, exocytosing their granules to induce apoptosis in target cells. They also target cells through ADCC, recognising opsonised infected cells using the Fc receptor CD16 and release their cytoxic granules, killing the infected cell. $CD56^{dim}$CD16+ NK cells, which form the majority of circulating NK cells are also responsible for secreting cytokines and chemokines when they come into contact with a target cell eg. IFN-γ, TNF-α, CCL2, CCL3, CCL4, CCL5, CXCL8 and CXCL10 (Fauriat et al., 2010). As can be seen from this profile, these cells play a key role in the initiation of inflammation and the secretion of so many chemokines attracts a broad range of cells to the site.

A large population of specialised NK cells are found in the decidua during pregnancy. These cells, called uterine NK (uNK) cells are characterised in humans as $CD56^{bright}$CD16-. NK activity has also been associated with recurrent miscarriage. Patients with high pre-conceptional NK activity experience a much higher rate of miscarriage than those with normal NK activity (Aoki et al., 1995). They initiate spiral artery remodelling and are thought to promote implantation and maintain gestation (Lash et al., 2010). uNK cells and their role in their reproductive process will be discussed further in section 1.3.2.

Natural Killer T (NKT) cells are an NK-related subset which exhibit similar features to T cells, but develop differently to conventional T lymphocytes. Depending on their TCR specificity, some DP thymocytes react to CD1d in the thymus, inducing differentiation into CD4+ or CD4-CD8- DN NKT cells (Gapin et al., 2001). NKT cells express a lipid-specific T cell receptor, which recognises antigens presented by the MHC-like molecule CD1d. NKT cells express a range of markers including the NK marker NK1.1 in mice/CD161 in humans and T cell markers such as the TCR and CD3 (Brennan et al., 2013). There are broadly two categories of NKT cells, type 1 classical invariant NKT (iNKT) cells whose TCRα chain is resistant to gene rearrangement, and type 2 diverse NKT cells whose TCR is variable. Type 2 NKT cells have not been well characterised and their role in health and disease has yet to be determined. The frequency of NKT cells in human blood is highly variable, however there is a large reservoir of NKT cells in the liver (Brennan et al., 2013).

There is an ongoing search for ligands which can be presented to iNKTs; one antigen, α-GalactosylCeramide (αGalCer), derived from a marine sponge, produces a strong biological response when presented by CD1d (Bendelac et al., 2007), however the significance of this is strongly debated as contact with marine sponges by most land mammals is minimal. An alternative explanation is that the sponge sample may have been contaminated, and that αGalCer is in fact a microbial ligand, which humans might come into contact with more readily (Bendelac et al., 2007). Physiological glycolipid ligands have also been sought after and isoGlobotrihexosylceramide **(**iGb3) has been suggested, however it only appears capable of activating iNKT cells in mice, not humans (Sanderson et al., 2013).

Though their TCR is restricted, the ability of iNKT cells to recognise antigens means that they straddle adaptive and innate immunity. CD1d is expressed by many cell types including DCs, macrophages, granulocytes and B cells (Brennan et al., 2013), indicating that iNKT cells may interact with many leukocyte subsets and therefore may have a contributory role in different types of immune responses. If the TCR signal received is weak, iNKT cells can still be activated by pro-inflammatory cytokines, such as IL-12 (Brennan et al., 2013). Upon activation iNKT cells produce large quantities of cytokines, the profile of which depends largely on the phenotype of the cell. Three subtypes of iNKT cells have been proposed but there are probably more to be characterised. The main population of iNKT cells found in the liver and spleen is Th1-like iNKT cells which have been described as NK1.1+, they may be CD4+ or DN and produce IFNγ in response to IL-12 (Watarai et al., 2012, Brennan et al., 2013). In the lungs and intestine, the main subset found is Th2-like iNKTs. These are mainly CD4+ and respond to IL-25, and as their name suggests when activated they rapidly produce Th2 related cytokines such as IL-4, IL-10 and IL-13(Watarai et al., 2012, Brennan et al., 2013). Finally, Th17-like iNKT cells have also been described, these tend to be CD4-, respond to IL-23 and produce IL-17 and IL-22 and have been found in lymph nodes, lungs and skin(Watarai et al., 2012, Brennan et al., 2013).

1.2.7. *CD3+ CD4- CD8- cells: DN T cells and other CD3+ non-T cells.*

Surprisingly, the predominant population of lymphocytes reported to be present in the NP murine female genital tract are CD3+CD4-CD8- T cells, referred to in many studies as double-negative (DN) T cells. Cells within this population have been found to express the αβ T cell receptor and low levels of B220, and the majority are CD25+ (Johansson and

Lycke, 2003). These cells are distributed throughout the genital tract mucosa, in the uterus and cervix. When infected intravaginally with *Chlamydia trachomatis*, these cells were found to decrease as a proportion of total uterine lymphocytes, while the number of SP CD4+ or CD8+ T cells increased in the reproductive tissue (Johansson and Lycke, 2003). This study also found that the CD3+CD4-CD8- population was characterised by an inability to proliferate. It also used DO11.10 TCR-Transgenic (Tg) mice which have a TCR, which is specific for chicken derived OVAlbumin (OVA), expressed by virtually all CD4+ T cells. OVA is then used *in vitro* to test antigen specific stimulation of CD4+ T cells. When mouse uterine lymphocytes were co-cultured with splenocytes and had the effect reducing proliferation when treated with anti-CD3 and OVA, suggesting that uterine lymphocytes have regulatory functions (Johansson and Lycke, 2003). When studied at day 4 of pregnancy, numbers of CD3+B220^{lo} uterine lymphocytes cells remained unchanged compared to NP controls. However, further investigation is required to ascertain if these cells are involved in mediating tolerance during early pregnancy (Johansson and Lycke, 2003).

This population has also been detected in the NP human endometrium, although they appear only to make up between 1.9-4.2% of CD3+ cells (Flynn et al., 2000). Interestingly, these cells were significantly increased as a percentage of CD3+ cells in the late secretory, compared to the late proliferative phase of the menstrual cycle (Flynn et al., 2000). This might suggest that these cells play a role in remodelling during menstruation. Some of these cells were found to be TCRγδ+, but these only made up ~1.7% of CD3+ cells. In human pregnancy, 90% of CD3+ cells in the decidual tissue of pre-term deliveries were CD4-CD8- cells (Gomez-Lopez et al., 2013). In term labouring decidual samples, these DN cells constituted around 30% of the CD3+ cell population but these appeared almost absent in term non-labouring deliveries (Gomez-Lopez et al., 2013). In this study, they identified these cells as memory-like DN T cells. The results are fascinating but difficult to interpret given the range of percentages quoted for uterine CD3+ DN cells in different studies. Does the DN T cell population decrease at term, compared to NP animals or does the DN T cell content of the uterus increase during pregnancy? A related cell population, CD3+CD4-CD8- iNKT cells have also been identified in the peripheral blood and decidua during early human pregnancy (Boyson et al., 2002), it is likely that if DN T cells are defined in the literature simply by CD3+CD4-CD8- that this population will include iNKT cells.

DN T cells have been reported in other circumstances and their study may provide an insight into their role in the reproductive tract. The percentage of CD3+TCRαβ+CD4-CD8- cells in the normal mouse kidney has been reported as 23%, with the liver containing 22%, the spleen with 5% and the blood only 3% (Ascon et al., 2008). The number of these cells in the kidney were found to be significantly decreased 24hrs after ischaemia reperfusion injury, compared to sham operated mice (Ascon et al., 2008). DN T cells have a regulatory phenotype in some circumstances. They appear to be protective against type 1 diabetes in NOD mice (Duncan et al., 2010), inhibit EAE in Lewis rats (Lider et al., 1991) and infusion of syngeneic regulatory CD3+TCRαβ+CD4-CD8- cells into mice permanently induces cardiac xenograft survival (Chen et al., 2003). Adoptive transfer of DN T cells suppresses the *in vivo* proliferation and cytokine production of xenoreactive CD4+ T cells, hinting at a mechanism for prolonged graft survival (Chen et al., 2005). During *Listeria monocytogenes* infection, DN T cells have been shown to express CCL2, suggesting they may play a role in the recruitment of monocytes, monocyte-derived macrophages and other CCR2+ cells during infection (Kadena et al., 1997).

Conversely, DN T cells have been described as being involved in autoimmune processes. Of particular interest, TCR-αβ+ DN T cells are increased in the blood of children with Behcet's disease, an autoimmune disorder where genital ulcers are a defining characteristic (Ling et al., 2007). DN T cells have been found to be doubled from 5% to 10% in the blood of patients with SLE and are major producers of IL-17 in the disease (Crispin et al., 2008). The percentage of TCR-αβ+ DN T cells in the spleen, liver and lymph nodes increases after the onset of autoimmune disease in MRL-lpr/lpr mice (Masuda et al., 1991). The percentage of TCR-αβ+ DN T cells in the blood of patients with autoimmune lymphoproliferative syndrome is increased to 10% and the expression of the marker B220 is increased on these cells (Bleesing et al., 2001). Myasthenia gravis patients also present with significantly more DN T cells in their blood compared with healthy controls (Reinhardt and Melms, 2000).

Diverse origins have been reported for DN T cells. There are different views on whether DN T cells are thymus dependent in their maturation, and thymocytes go through distinct stages of CD4/CD8 negativity during their development (D'Acquisto and Crompton, 2011). Myasthenia gravis patients with thymic lymphofollicular hyperplasia that undergo thymectomy see the elevated DN T cell levels in their blood return to the level of healthy controls, suggesting thymic involvement in DN T cell production (Reinhardt and Melms,

2000). Thymus-independent development of DN T cells has also been described (Johansson and Lycke, 2003, Ford et al., 2006).

There has been some limited characterisation of the surface immunophenotype of DN T cells. CD25, the IL2Rα chain, is reported to be expressed by DN T cells in several papers (Lee et al., 2011a, Fischer et al., 2005, Takeuchi et al., 1992, Lider et al., 1991, Mixter et al., 1999, Utting et al., 2000, Voelkl et al., 2011, Zhang et al., 2000, Duncan et al., 2010), including on DN T cells in the uterine horn (Johansson and Lycke, 2003). Surprisingly, B220, which is predominantly viewed as a B cell marker, has been described on DN T cells (Ascon et al., 2008, Zhang et al., 2006, Bakir et al., 2006, Bleesing et al., 2001, Koyasu, 1994, Mixter et al., 1999), including those in the reproductive tract (Johansson and Lycke, 2003). The MRL/lpr mouse model of Systemic Lupus Erythromatoses (SLE) has a mutation that results in the accumulation of B220+ DN T cells due to the *lpr* mutation in the Fas receptor (Le Gall et al., 2012). B220 may only be expressed on a population of DN T cells because the extent of B220 expression is varied and has not been seen in all cases (Lee et al., 2011a). CXCR5 is also found on DN T cells and these cells migrate in response to CXCL13, the chemokine ligand for this receptor (Ansel et al., 1999, Lee et al., 2005, Lee et al., 2006), although one study only demonstrated very low levels of expression (Huang et al., 2010). Like B220, CXCR5 is typically viewed as a marker of B cells and directs cells to B cell follicles in secondary lymphoid tissues (Carlsen et al., 2002). However, CXCR5 is also expressed on some migratory dermal DCs (Wu and Hwang, 2002) and on T cell subsets that have follicle-homing properties, including T_{FH} cells and follicular regulatory T cells which also express PD-1 (Sage et al., 2012, Slight et al., 2013). The level of CXCR5 expression by DN T cells has been disputed and other chemokine receptors have been described on human DN T cells, including CCR4, CCR5, CCR7, CXCR3, and CXCR4 (Huang et al., 2010). Negative regulators of T cell function have been described on DN T cells. Peripheral DN T cells (TCRαβ+CD3+CD4-CD8-NK1.1-) have been shown to express CTLA-4 and down-regulate co-stimulatory molecules on DCs in a CTLA-4 dependent manner (Gao et al., 2011). However this has been contradicted in other studies, where no CTLA-4 expression was seen (Voelkl et al., 2011, Duncan et al., 2010). Another negative regulator of T cell function is PD-1, a receptor that is responsible for inhibiting T cell signalling and is associated with immune regulation (Lee et al., 2011a, Dinesh et al., 2010). PD-1, similar to CTLA-4 is involved in tolerance and counteracts the co-stimulatory signals of CD28 (Fife and Pauken, 2011). Tregs have been described as expressing PD-L1, a ligand for PD-1 and that this is reported to be

critical for tolerance at the foetomaternal interface (Habicht et al., 2007). DN thymocytes express PD-1 and overexpression of PD-1 results in impaired maturation of these cells in the thymus (Keir et al., 2005).

The CD3+ DN cell population is likely a heterogenous mixture of cell types. In order to identify DN T cells amongst CD3+ DN cells, TCR expression has often been examined. In the literature human DN T cells have been reported to express predominantly TCR-αβ (Levitsky et al., 1991, Masuda et al., 1991, Mixter et al., 1999, Takeuchi et al., 1992, Voelkl et al., 2011, Ascon et al., 2008, Bakir et al., 2006, Fischer et al., 2005, Huang et al., 2010) but TCR-γδ expression has also been found (Huang et al., 2010, Masuda et al., 1991, Bakir et al., 2006, Fischer et al., 2005).

NK1.1 is a marker used to distinguish NK cells and NKT cells in mice (Godfrey et al., 2004). NK cells in the thymus have been demonstrated to be able to develop from thymic DN1 cells (Vargas et al., 2011). NKT cells as with CD3+ DN T cells, can be described as CD3+CD4-CD8-. NKT cells, defined as NK1.1+TCRαβ+ display characteristics of T cells and NK cells and this phenotype describes several subsets (Godfrey et al., 2004). NK1.1 has been recorded on CD3+ DN cells (Levitsky et al., 1991, Ford et al., 2006) but only a low proportion of uterine DN T cells have been reported to express NK1.1 (Johansson and Lycke, 2003).

This disparate collection of markers tell us surprisingly little about DN T cells as a whole as it seems that the precise surface immunophenotype of these cells varies in different situations in different tissues and that CD3+CD4-CD8- describes various populations of cells with different functions.

1.2.8. *Chemokines: key regulators of leukocyte migration.*

In the sections above I have introduced many of the important cellular players of the immune system. In this next section, I discuss the chemotactic cytokines, or chemokines, small (8-10kDa) secreted proteins involved in orchestrating leukocyte migration. Leukocyte homing is of fundamental importance in the immune system because leukocytes must get to the right place at the right time in order to carry out their functions effectively. Moreover, much of the work in the Results chapters of this thesis examines the expression of chemokine receptors, most notably CCR2.

Chemokines are related in terms of their sequence and function and are formally named according to the precise positioning of cysteine residues towards the N-terminus of the mature protein that form disulphide bridges to maintain the structure of the protein. There are four families: C, CC, CXC and CX3C (Figure 1.10).

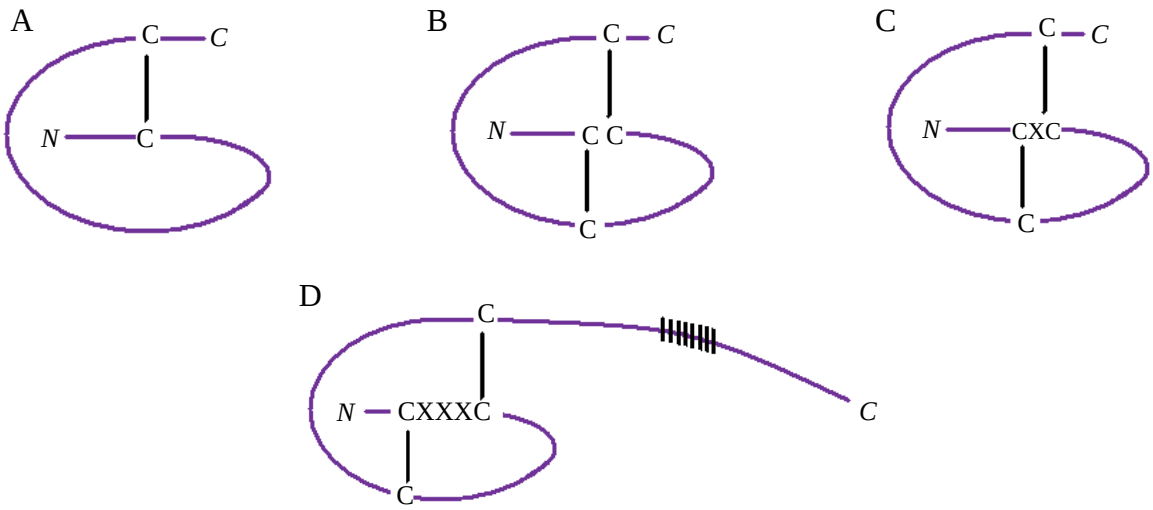

Figure 1.10. Representation of chemokine structural families.

Chemokine families determined by the placement of cysteine residues C, other residues denoted as X. N terminus marked *N* and C terminus marked *C.* A) C chemokine, with only one disulphide bridge. B) CC chemokines, with two disulphide bridges with no other residues between. C) CXC chemokines, one amino acid separates the two cysteines. D) CX3C chemokine, which has a distinctive structure, not only in the amino acids which separate the cysteines in the protein but the long C terminus projects into the cell membrane so the chemokine is tethered. A mucin-like domain is also present. The CXC chemokine CXCL16 is also produced as a tethered protein and has a structure similar to CX3CL1.

The families of chemokine receptors and their ligands are shown in Table 1.1. C chemokines have one disulphide bridge joining a cysteine residue towards the *C* terminus with a cysteine residue towards the *N* terminus. CC chemokines have two disulphide bridges, from cysteine residues side by side, shown in Figure 1.10B. In CXC chemokines these cysteine residues are separated by another amino acid. Finally the single CX3C chemokine CX3CL1 has these bridges separated by three other amino acids. This chemokine is also of interest as its *C* terminal is tethered to cell membranes and includes a mucin-like stalk domain. A similar structure is also seen with CXCL16. The *N* terminal domain, along with other determinants in the body of the chemokine, is seen as an important receptor binding domain for many chemokines (Allen et al., 2007). The *N* terminus has also been shown to be crucial for receptor activation, and the action of enzymes such as MMPs on the *N* terminus have been shown to modify the activity of

certain chemokines (Allen et al., 2007). Several MMPs have been shown to cleave CCL2, CCL8 and CCL13, and MMP-2 has been shown to specifically digest CCL7 (McQuibban et al., 2002). Removing residues from the *N* terminus of CCL2 removes the ability of the chemokine to activate its receptor, but its receptor binding properties are retained, thereby creating an antagonist for CCR2 (McQuibban et al., 2002). Truncated CCL13 also acts as a potent antagonist of CCR2 and CCR3, with an affinity similar to the full-length version but unable to induce chemotaxis like full length CCL13 (McQuibban et al., 2002).

Chemokines play a critical role in directing the migration and positioning of leukocytes during homeostasis, infection and inflammation. Chemokines deliver their signals by binding and activating G protein coupled chemokine receptors. These receptors are usually $G_{\alpha i}$ linked and binding can trigger actin-dependent changes involved in the mechanics of cell movement (Cotton and Claing, 2009). The ability of chemokine receptors to signal is dependent of the presence of the 'DRY domain' in the second intracellular loop of the seven transmembrane receptor. The 'DRY domain' in humans is typically represented in chemokine receptors as the amino acid sequence DRYLAIV (aspartic acid, arginine, tyrosine, leucine, alanine, isoleucine and valine) or subtle variants thereof. Due to the structural similarities within families, some chemokine receptors bind more than one chemokine, although usually only to chemokines within a single subfamily.

Chemokines are often described as being homeostatic and inflammatory, though these distinctions are under constant review as many chemokines classified as homeostatic may have inflammatory functions and *vice versa*. Homeostatic chemokines are constitutively expressed and control leukocyte homing under resting conditions, whereas inflammatory chemokines are produced in response to an inflammatory stimulus or infection. Homeostatic chemokines can identify specific target organs. For example, CCL19 and CCL21 attract CCR7-expressing T cells and DCs to the paracortex of the LN in order to orchestrate T cell priming. CCR9 and its ligand CCL25, is involved in gut-homing, and similarly CCR4 and CCR10 are implicated in migration of leukocytes to skin (Sheridan and Lefrancois, 2011). In contrast, inflammatory chemokines are induced transiently, often to very high levels, and usually in response to infection, tissue damage or innate immune cell activation. These chemokines include CCL2 to CCL13, and CXCL1 to CXCL11 (Graham, 2009).

A

CCR1	CCR2	CCR3	CCR4	CCR5	CCR6	CCR7	CCR8	CCR9	CCR10
CCL3	CCL2	hCCL3L1	CCL17	CCL3	CCL20	CCL19	CCL1	CCL25	CCL27
CCL5	mCCL3	CCL5	CCL22	CCL4		CCL21			CCL28
mCCL6	CCL7	CCL7		CCL5					
CCL7	hCCL8	hCCL8		CCL8					
mCCL9	mCCL12	CCL11		CCL11					
mCCL10	hCCL13	hCCL13		CCL14					
hCCL14	CCL16	hCCL15		CCL16					
hCCL15		CCL16							
CCL16		hCCL24							
hCCL23		hCCL26							
		CCL28							

B

CXCR1	CXCR2	CXCR3-A	CXCR3-B	CXCR4	CXCR5	CXCR6
CXCL6	CXCL1	CXCL9	CXCL4	CXCL12	CXCL13	CXCL16
CXCL7	CXCL2	CXCL10	CXCL9			
hCXCL8	CXCL3	CXCL11	CXCL10			
	CXCL5		CXCL11			
	CXCL6					
	CXCL7					
	hCXCL8					

C

XCR1	CX3CR1	CCX-CKR	CXCR7	D6		DARC	
XCL1	CX3CL1	CCL19	CXCL11	CCL2	CCL11	CCL2	CXCL1
XCL2		CCL21	CXCL12	hCCL3L1	CCL13	CCL7	CXCL5
		CCL25		CCL4	CCL14	CCL8	CXCL6
				CCL5	CCL17	CCL11	CXCL7
				CCL7	CCL22	CCL13	CXCL8
				CCL8		CCL14	CXCL9
						CCL16	CXCL11
						CCL17	CXCL13

Table 1.1 Chemokine receptors and chemokine ligands.

A) CC chemokine receptors and their binding chemokines. B) CXC chemokine receptors and their binding chemokines. C) XCR1, the C chemokine receptor and its ligands; CX3CR1 and its ligand and the decoy receptors CCX-CKR, CXCR7, D6 and Duffy Antigen Receptor for Chemokines (DARC) with their chemokine ligands. Chemokines found only in humans are denoted by the prefix h; chemokines found only in mice are denoted by the prefix. Adapted from (Allen et al., 2007, Comerford and Nibbs, 2005).

Chemokines often require support from GlycosAminoGlycans (GAGs), which immobilise them on the endothelium and other cellular surfaces. On blood vessel endothelial cells, this immobilisation promotes the migration of blood cells into the tissue that the signal originates from (Allen et al., 2007), and prevents chemokines from being washed away in the blood. Interruption of GAG binding impairs leukocyte recruitment to sites of inflammation (Proudfoot et al., 2003). The recruitment of leukocytes to sites of infection and inflammation is a critical aspect of immune defence, tissue repair and remodelling. The migration of cells across the endothelium is a multistep process and has many elements resembling blastocyst implantation, covered in section 1.1.3. (Dominguez et al., 2005). The first step of rolling involves loose contact with selectins, which act to slow the leukocyte. Inflammation upregulates E-selectin and P-selectin on the endothelial surface, and the process of rolling increases the proximity of the cell with the endothelium and may bring it in contact with a chemokine presented on the endothelium. The action of the chemokine on the leukocyte expressing the appropriate receptor may result in a change in the distribution and conformation of integrins on a cell and increase the possibility of the leukocyte forming firm integrin-mediated contact with Ig superfamily Cell Adhesion Molecules (ICAMs) the endothelium. Finally, the leukocyte squeezes between two endothelial cells through, amongst other things, contact between CD31 (PE-CAM-1) on both the leukocyte and the endothelium. Other integrins such as CD11/CD18 bind to JAM-1, a tight junction protein, which ensures that endothelial integrity is maintained (Kindt et al., 2007). Remarkably, leukocytes have even been observed migrating through endothelial cells (Feng et al., 1998).

Neutrophils interact with the endothelium by expressing L-selectin (CD62L) and P-Selectin Glycoprotein Ligand-1 (PSGL-1). When stimulated, neutrophils express the integrins CD11a/CD18 and CD11b/CD18, which form firm contact with ICAM-1 (CD54)(Kindt et al., 2007). The inflamed endothelium also expresses Vascular Cell Adhesion Molecule-1 (VCAM-1, CD106), which binds Very Late Antigen-4 (VLA-4, CD49d/CD29), an integrin found on cells such as monocytes, lymphocytes and eosinophils. Naive T cells express L-selectin (CD62L), CCR7 and CD11a/CD18, which mediate their extravasation through high endothelial venules in lymph nodes (Nijkamp et al., 2011).

1.2.9. *Chemokine receptor regulation.*

The activity of a chemokine receptor on the surface of a cell is controlled in part by a process of desensitisation. The availability of a receptor is carefully controlled in order to regulate the signal. When chemokines bind to receptors, a series of conformational changes occur in the receptor structure allowing phosphorylation of the activated, agonist-bound receptor by G-protein coupled Receptor Kinases (GRKs). The action of GRKs increases the binding affinity for the protein arrestin, which prolongs desensitisation and promotes endocytosis of the chemokine-bound receptor. This involves the plasma membrane of the cell pinching off inside the cell to form a vesicle with the agonist on the inside of the compartment. The receptor can then be cycled back to the surface or the vesicle may fuse with the lysosome and be degraded. The removal of receptors from the cell surface causes desensitisation because there are fewer receptors to respond to the chemokine signal. There are many variables that affect the process of desensitisation by endocytosis, and the same receptor may exhibit different desensitisation profiles depending on the agonist encountered. When studying chemokine receptors, it is important to remember that some receptors constitutively recycle regardless of activation state, some will recycle quickly, whereas binding of some receptors by certain agonists causes more prolonged loss of cell surface receptors.

1.2.10. *Chemokine receptors as scavengers*.

In addition to conventional chemokine receptors that signal into cells when bound by chemokine, there are a group of receptors that appear incapable of signalling. These receptors are characterised by marked alterations in their DRYLAIV motif. Such receptors are described as atypical chemokine receptors and include D6, CCX-CKR, CXCR7 and Duffy Antigen Receptor for Chemokines (DARC). These molecules can act as scavenger receptors (Allen et al., 2007), removing chemokines from the extracellular environment thereby modulating leukocyte migration by controlling chemokine availability. DARC is one of the few chemokine receptors capable of binding chemokines from more than one family and is predominantly expressed on erythrocytes and blood vessel endothelial cells (Graham, 2009, Rot and von Andrian, 2004). It has been proposed that DARC on erythrocytes acts as a chemokine sink during inflammatory conditions and a chemokine reservoir when chemokine levels are falling (Fukuma et al., 2003, Hansell et al., 2011a). In this way it may act to buffer chemokines in the blood to prevent desensitisation chemokine receptors on circulating leukocytes and therefore interfering with appropriate leukocyte extravasation. DARC on endothelial cells has been implicated in the basolateral to apical

transcytosis of chemokines *in vivo* and *in vitro* (Pruenster et al., 2009) for the presentation to leukocytes in the blood. As indicated in Table 1.1C, CCX-CKR binds three homeostatic chemokines, namely CCL19, CCL21 and CCL25, and can act as a scavenger receptor for these molecules (Comerford et al., 2006). This receptor has been detected in spleen and lymph nodes, non-lymphoid tissues such as brain, testis and placenta, and leukocytes such as DCs and T cells (Gosling et al., 2000, Townson and Nibbs, 2002). CCX-CKR appears to promote DC homing to lymph nodes and its over-expression and deletion impairs thymus development, demonstrating that decoy receptors can play key roles in immunology without the capacity to signal (Heinzel et al., 2007, Bunting et al., 2013). CXCR7 appears to have a developmental function and is expressed in the spleen, kidney, testis, ovary and placenta (Sanchez-Martin et al., 2013, Graham, 2009). Lots of variation is seen in the expression data for CXCR7 on peripheral blood cells due to differences in experimental technique (Sanchez-Martin et al., 2013). CXCR7 protein has been noted on activated DCs, memory B cells which differentiate into plasma cells, monocytes, NK cells and basophils in peripheral blood (Infantino et al., 2006). CXCR7 mRNA and protein show that expression of CXCR7 in placental tissue is increased at term, compared to early pregnancy (Tripathi et al., 2009). CXCR7 is also associated with tumours and drives tumour growth in mouse models of breast and lung cancer (Miao et al., 2007). In human disease, immunohistochemistry has shown CXCR7 to be localised on tumour associated vasculature (Miao et al., 2007).

The decoy receptor, D6 binds and internalises a range of CC chemokines and degrades them following internalisation. D6 is expressed in tissues that act as an environmental barrier such as skin, gut, lung and placenta and is thought to protect against exaggerated inflammatory responses at these sites. This ability of D6 to internalise and degrade inflammatory chemokines may also contribute to the resolution of inflammation. D6 has been shown to limit cutaneous inflammation when 12-O-TetradecanoylPhorbol-13-Acetate (TPA) is painted on the skin, due to effective clearance of chemokines by the receptor (Jamieson et al., 2005). When TPA is used as an agent to induce inflammation-driven tumours following an application of the mutagen 7,12-dimethylbenz(*a*)anthracene (DMBA), D6 KO mice develop a higher number of tumours per mouse and a higher percentage of mice exhibit tumours, compared to WT mice (Nibbs et al., 2007). D6 may have a key a role in preventing inflammation mediated foetal loss: pregnant D6 KO females injected with LPS showed a higher rate of abortion than WT females and this effect was abrogated when antibodies blocking CCL3, CCL4, CCL2 and CCL5 were also

administered (Martinez de la Torre et al., 2007). D6 is expressed on the apical face on syncytiotrophoblasts which invade the maternal decidua during implantation and placentation and has been hypothesised to be involved in tolerance to the foetus during pregnancy (Garlanda et al., 2008). Circulating D6-binding chemokines have been shown to be reduced during pregnancy, which may contribute towards a less inflammatory, more tolerogenic environment during pregnancy (Madigan et al., 2010). D6 has also been shown to promote the survival of embryos transferred into allogeneic pseudopregnant hosts, as transfers of D6 KO foetuses resulted in an increased percentage with abnormal development and resorption plaques in allogeneic mice, compared to syngeneic mice (Madigan et al., 2010). Though these four receptors are considered professional scavengers, deletion of signalling chemokine receptors also results in increased circulating chemokine protein, compared to WT animals, showing that signalling chemokine receptors also fulfil this function (Cardona et al., 2008).

1.2.11. *Chemokine receptor expression on leukocytes.*

I have explained some of the basics of chemokine biology, and will now broadly describe the chemokine receptor profiles of different leukocyte subtypes. The chemokine receptors that a cell expresses determine its homing characteristics and this migratory profile is crucial for a leukocyte to deliver its function at appropriate the time and place. As briefly mentioned in section 1.2.3, subtypes of monocytes and macrophages are defined by the chemokine receptors CCR2 and CX3CR1. CCR2 plays a key role in migration of monocytes and other cells such as T cells, NK cells and DCs. Ligands for CCR2 in humans and mice include CCL2, CCL3 (Hansell et al., 2011b), CCL7 (Luster, 1998). There are some differences, CCL12 is a ligand for CCR2 in mice but does not exist in humans and human CCL8 binds human CCR2 but mouse CCL8 does not bind to mouse CCR2, instead acting as a CCR8 ligand (Islam et al., 2011). CCL2, the major ligand for CCR2, attracts monocytes *in vitro* (Carr et al., 1994) and is important for release of these cells from the BM into the circulation (Serbina and Pamer, 2006), and may be involved in infiltration of monocytes to sites of inflammation (Kuziel et al., 1997) and infection (Kurihara et al., 1997). CX3CR1 is also involved in migration of monocytes into tissues under homeostatic conditions. CX3CR1 is required on monocytes patrolling along blood vessels and is required for the rapid invasion of Gr1- monocytes into tissues following damage or infection (Auffray et al., 2007). CX3CL1 is the sole ligand for CX3CR1 and is tethered to cell membranes by a mucin domain, although the chemokine can be cleaved by the enzyme A Disintegrin And Metalloproteinase 17 (ADAM-17)(Tsou et al., 2001). Activation of the

receptor in response to the shed ligand CX3CL1 causes chemotaxis and adhesion of monocytes to cells which present tethered CX3CL1 on their surface (Bazan et al., 1997, Imai et al., 1997, Geissmann et al., 2003). Chemokine receptors are often restricted to particular cell types in order that a chemokine only attracts the cell type required. The chemokine receptors CCR2 and CX3CR1 define two separate monocyte subsets in mice along with the marker Ly6C. Monocytes also emigrate from the BM in response to low circulating levels of TLR4 ligand, and this release is reduced in $CCL2^{-/-}$ and $CCR2^{-/-}$ mice compared with WT animals (Shi et al., 2011).

Neutrophils are another leukocyte subset released from the BM due to the action of chemokines (Bugl et al., 2012). Before neutrophils are released from the BM they express moderate levels of CXCR4. Stromal cells within the BM constitutively produce the CXCR4 ligand CXCL12, and its interaction with CXCR4 on neutrophils promotes their retention in the BM. As neutrophils mature, CXCR4 expression decreases and therefore the CXCL12 signal to the cell is reduced and neutrophils can be released from the BM (Summers et al., 2010, Martin et al., 2003). Neutrophils are often the first inflammatory cells to reach a site of damage and they generate chemokines to attract other inflammatory cells (Nathan, 2006). Neutrophils act as part of the innate immune system and activated neutrophils have respiratory burst and degranulation as their two main weapons for dealing with tissue infection. Neutrophils express CXCR2 and it plays a key role in their recruitment into tissues. Moreover, antagonising this receptor is effective at reducing inflammation-driven tumorigenesis in mice (Jamieson et al., 2012). While neutrophils are circulating in the blood, CXCR2 activity promotes adhesion of neutrophils to the endothelium and lack of CXCR2 prevents neutrophil infiltration into tissues (Smith et al., 2004). Human neutrophils also express CXCR1 (Kimura, 1999), a receptor similar to CXCR2 in that both bind CXCL8 (IL-8) in humans and CXCL6, although CXCR2 also binds CXCL1, 2, 3, 5 and 7.

Other types of receptor also mediate neutrophil chemotaxis such as the high affinity Formyl Peptide Receptor (FPR), which recognises N-formyl-L-Methionyl-L-Leucyl-Phenylalanine (fMLP)(Selvatici et al., 2006). fMLP is thought to derive from bacterial proteins and this exogenous chemoattractant provokes infiltration of neutrophils across this gradient (Selvatici et al., 2006). LeukoTriene B_4 (LTB_4) is an inflammatory mediator which also triggers chemotaxis through BLT1, its receptor (Kim and Luster, 2007). During inflammation, eicosanoids are produced from phospholipids through the action of

phospholipases, this produces arachidonic acid, from which prostaglandins and leukotrienes arise. BLT1 is present on many leukocyte subsets such as granulocytes, monocytes, T cells and B cells, the broad expression of this receptor indicates that the function of this mediator is to attract many subsets of leukocytes to site of inflammation simultaneously (Kim and Luster, 2007). Another proinflammatory mediator C5a, a protein of the complement system, is found in a broad range of inflammatory situations and is a potent chemoattractant for neutrophils and macrophages through the C5aR receptor (Monk et al., 2007). This receptor may also trigger chemotaxis in other myeloid cells and lymphocytes (Monk et al., 2007).

Chemokine receptors on eosinophils have been investigated as potential therapeutic targets in diseases such as asthma. Asthma is characterised by eosinophil accumulation in airway walls and the release of eosinophilic granules can cause tissue damage and exacerbate disease pathology. Typically, eosinophils are described as expressing CCR1 and CCR3 and respond strongly to CCL11 (Hoger et al., 1996). CCR1 expression is more variable than that of CCR3 and its function on eosinophils has not been investigated as fully as CCR3 (Elsner et al., 2005). CCR3 is widely expressed on eosinophils and is a key regulator of eosinophil trafficking into tissues during allergic inflammation, as such it is seen as a potential therapeutic target in diseases such as athsma (Catley et al., 2011).

CCR7 and its ligands CCL21 and CCL19 are associated with homing to secondary lymphoid organs. Naive T cells circulate between the blood, secondary lymphoid organs and lymphatics in order to search for antigen. Both Naive T cells and DCs express CCR7 so these cell types co-localise in the paracortex of lymph nodes, allowing priming of T cells (Moschovakis and Forster, 2012, Bromley et al., 2008). T_{FH} cells downregulate CCR7 and upregulate CXCR5. CXCR5 is activated by the chemokine CXCL13 produced in B cell follicles, and these cells then migrate to lymph node follicles rich in B cells in order to support antibody production. CXCR5 is essential for the homing of naïve B cells to B cell follicles, and plays a role in directing cell migration during the embryonic development of lymph nodes and Peyer's patches. The role of CXCR5 on CD3+ DN cells was discussed in section 1.2.7. Immature DCs express surface CCR1 and CCR5 but these receptors are downregulated following activation with a stimulus such as LPS and CCR7 is then upregulated to promote migration to secondary lymphoid organs (Sallusto et al., 1998). DCs constitutively migrate to draining lymph nodes via afferent lymphatics in order to present antigens to maintain peripheral tolerance but during inflammation DCs rapidly

mobilise to draining lymph nodes, and both processes are CCR7-mediated (Forster et al., 2012). DC presentation of antigen in secondary lymphoid organs is responsible for induction of tolerance and other immune responses and the orchestration of this process by chemokines is key to its success.

After their generation from naïve T cells, effector T cells downregulate CCR7 and upregulate pro-inflammatory chemokine receptors such as CCR5 and CXCR3 to allow them to migrate to inflamed tissues to participate in clearance of pathogenic or damaged cells (Nijkamp et al., 2011). Memory T cells can be divided by their expression of CCR7; effector memory T cells have no expression of CCR7 and are able to circulate through peripheral tissues and rapidly display their effector functions upon contact with an antigen, whereas central memory T cells express CCR7 and traffic through lymphoid organs where they can expand to produce a population of effector cells (Nijkamp et al., 2011). CXCR4 is another receptor involved in the positioning of T cells in secondary lymphoid organs, its ligand CXCL12 is expressed in T cell areas and germinal centres (Bromley et al., 2008). Memory T cells may also carry receptors in order to allow them to home back to the site of their activation. This has been demonstrated in the gut, a mucosal site where T cells constantly come into contact with antigen and a site where tolerance to harmless antigens is crucial. Antigen-specific Treg cells induced by repeated feeding of OVA to mice, in addition to effector T cells induced after oral immunisation, home back to the small intestine using CCR9 and the integrin complex α4β7 (Cassani et al., 2011).

The chemokine receptors expressed by effector T cells depend on the polarisation of the cell. Th1 cells tend to express CCR5, CXCR3 and CXCR6, Th2 cells have a contrasting profile of receptors such as CCR3, CCR4 and CCR8 and CCR6 is associated with Th17 cells (Bromley et al., 2008). A strong role for T cell migration in response to stimulation of CCR5, CXCR3 and CXCR6 has been demonstrated in inflammation, including in synovial fluid of patients with psoriatic and rheumatoid arthritis and samples from inflamed livers (Kim et al., 2001, Cripps et al., 2012). As expected Th2 cells recruited to sites of allergy express CCR3, CCR4 and CCR8 and these receptors have been proposed as targets for drug development in order to reduce the recruitment of Th2 cells to allergic reactions (Lloyd and Rankin, 2003). Chemokine mediated recruitment of T cells is crucial for them to display their effector functions at the site of inflammation. The role of CCR2 on T cells will be more fully discussed in section 1.2.12.

Further complexity is encountered when NK and NKT cells are considered. Different NK cell subsets respond to different chemokines. CXCR6 has been reported to be highly expressed on both NK and NKT cells (Kim et al., 2001, Matloubian et al., 2000, Berahovich et al., 2006). CXCR6 has been reported to be critical for survival and effector function of memory NK cells during viral infection (Paust et al., 2010). In humans CD16+CD56+ NK cells migrate in response to CX3CL1 and CXCL8 *in vitro*, whereas around 10% of CD16- CD56+ NK cells migrate in response to CCL4 (Campbell et al., 2001). In contrast, around 70% of NKT cells mobilised in response to CCL4 and a large population also responded to CCL2 (Campbell et al., 2001). The same study confirmed these findings by identifying the receptors expressed by these subtypes; CD16+CD56+ NK cells expressed high levels of CX3CR1 with CXCR1, CXCR4 and some CXCR2, CD16-CD56+ NK cells expressed high levels of CXCR3 and CXCR4 with varying levels of CCR5 and CCR7, finally NKT cells expressed several receptors with high expression of CCR5 and CXCR4, and varying levels of CCR1, CCR2, CCR6 and CXCR3 expression (Campbell et al., 2001, Krackow, 1990). Interestingly, this study showed that only CD16-CD56+ NK cells and NKT cells expressed CXCR6 (Steevels and Meyaard, 2011). These data were somewhat supported by another study demonstrating expression of CXCR3 and CXCR4 on both CD16+CD56+ and CD16-CD56+ cells, with varying levels of other chemokine receptors including CXCR6 (Berahovich et al., 2006).

This brief discussion of chemokine receptor expression and function on specific leukocyte subsets highlights the complexity of the signals involved in leukocyte migration. Investigation of the chemokine receptor CCR2 forms a key part of this thesis and in the next section, a fuller introduction to the function of this molecule will be given.

1.2.12. *Role of CCR2 on leukocytes during inflammation.*

CCR2, which is regarded as the key receptor involved in monocyte trafficking during inflammation is likely to be of importance in leukocyte trafficking to post-partum reproductive tissues. A few studies are presented in this section to give an insight into the interplay of different cell types that may express this receptor. Various animal models of inflammation have been studied to attempt to tease apart the role of CCR2 on leukocytes but this section will focus specifically on monocytes and T cells. In the Collagen-Induced Arthritis (CIA) model in mice, CCR2 blockade using anti-CCR2 antibodies during the initiation phase provides some protection against disease, whereas blockade during the maintenance phase causes aggravation of arthritis (Bruhl et al., 2004). The opposing

effects were explained by the differing roles on monocytes and T cells, with blockade during initiation affecting the migration of CCR2+ monocytes acting as APCs and blockade during disease maintenance affecting migration of Tregs (Bruhl et al., 2004). On human T cells, CCR2 is often co-expressed with CCR5 on highly differentiated effector memory T cells, which produce a broad range of cytokines and have the ability to migrate in response to several inflammatory chemokines (Zhang et al., 2010). CCR2 signals preferentially on fully differentiated CD4+ T cells in assays of chemotaxis and Ca^{2+} flux (Rabin et al., 1999). The role of CCR2 on mononuclear cells has also been explored in Experimental Autoimmune Encephalitis (EAE), a mouse model of multiple sclerosis. Specific protocols vary, but mice are immunised with an antigen such as Myelin Oligodendrocyte Glycoprotein (MOG) with an adjuvant like Complete Freund's Adjuvant (CFA), and this induces the process of EAE. Some studies have shown that CCR2 KO mice are protected from developing EAE (Fife et al., 2000, Izikson et al., 2000). Whether CCR2 is required on T cells in this model has been a subject for debate. Adoptive transfer techniques have revealed that lack of disease has been shown not to be due to deletion of CCR2 on T cells but due to lack of migration by infiltrating host mononuclear cells. For example, CCR2 KO mice recipients of WT MOG35-55 specific CD4+ T cells are unable to develop EAE, and showed no mononuclear cell infiltrate in their central nervous system (Fife et al., 2000). These data suggest that CCR2 expression is not required on pathogenic T cells but is required for inflammatory cell recruitment to the central nervous system, this is consistent with data showing that CCR2 is required for the presence of monocytes in the circulation (Serbina and Pamer, 2006). Lack of mononuclear cell infiltrate in CCR2 KO mice has been confirmed, however MOG35-55-specific T cell proliferation and IFNγ production are decreased in CCR2 null mice, which might suggest CCR2 deletion does affect T cells (Izikson et al., 2000). These data demonstrate the difficulty in identifying mechanisms for chemokine related processes and also how interdependent leukocyte populations are.

The interplay between CCR2 driven monocyte accumulation and recruitment of T cells has also been studied in models of infection. In a model of intravaginal *Herpes simplex* virus-2 infection, CCR2 KO mice were not able to control primary infection and exhibited an almost complete lack of recruitment of monocytes to the genital mucosa (Iijima et al., 2011). However, CD4 and CD8 T cell numbers were found to be comparable between WT and CCR2 KO mice (Iijima et al., 2011). Lack of CCR2 resulted in reduced accumulation of inflammatory monocyte derived APCs in the genital mucosa, and diminishing

restimulation and cytokine production from CD4+ T cells. These studies demonstrate that CCR2 not only acts on both monocytes and T cells but that monocytes and T cells act interdependently in models of infection and inflammation.

1.2.13. Summary

This section has covered some of the relevant principles of leukocyte biology, including their development, activation, migration and participation in inflammatory responses. A particular focus has been placed on monocytes/macrophages and T cells, as investigation of these populations forms the bulk of my thesis. I also described a subset of CD3+ cells, known frequently in the literature as DN T cells. These cells have been shown to form a large proportion of T cells in the female reproductive tract in NP mice, and in some circumstances, in humans. This poorly defined population of cells is examined extensively in my work. Finally, Chemokines play indispensible roles in constitutive homeostatic leukocyte homing as well as inducible inflammatory migration of all leukocyte populations. This project focuses on the role of CCR2 on leukocytes in the post-partum period, and previous studies have shown that CCR2 is expressed on subsets of T cells as well as monocytes and macrophages.

1.3: The involvement of immune cells in the reproductive process

Some of the topics discussed above have begun to describe the overlap between reproductive and immunological processes in humans and mice. This section will set out the crossover between the sections, beginning with the role of leukocytes during the menstrual cycle, pregnancy and the post-partum period. This will then be extended with a discussion of how lactation may affect leukocytes in the post-partum period and a summary of the influence of sex steroids on CCR2 binding chemokines. Finally, sex differences in inflammation and a summary of leukocytes associated with the reproductive tract will close the section. This section aims to explain the context for my work in the post-partum period and to give an account of leukocyte functions at other inflammatory time-points in the reproductive process.

1.3.1. *Immune cells in human menstruation and the murine oestrous cycle.*

Menstruation is an inflammatory process which requires extensive tissue remodelling (Salamonsen, 1998). As discussed in section 1.1.1, during the first half of the menstrual cycle, known as the proliferative phase, oestrogen is the dominant ovarian hormone and it increases over this time. This stage of the cycle is characterised by regeneration of the endometrium. During this phase few leukocytes are found in the tissue, though some macrophages, mast cells and B cells are present (Thiruchelvam et al., 2013, Salamonsen and Woolley, 1999). Following ovulation, oestrogen declines and progesterone dominates, inducing the secretory phase, when more leukocytes enter the endometrium (Thiruchelvam et al., 2013). One study measuring leukocytes in the human endometrium by flow cytometry, showed a doubling of CD45+ leukocytes as a percentage of total cells, from 38.9% in the late proliferative phase to 79.1% in the late secretory phase (Flynn et al., 2000). This dramatic increase is indicative of the preparation for menstruation, which is considered to be an inflammatory event. Macrophages and uNK cells increase as a percentage of endometrial cells during this stage (Kamat and Isaacson, 1987). In another study, NK cells were found to be increased as a proportion of CD45+ cells and in absolute numbers from the late proliferative to the late secretory phase (Flynn et al., 2000). CD3+ cells as a whole were found to be constant in terms of number throughout the cycle, however CD8+ T cells decreased as a percentage of CD3+ cells from the late proliferative to the late secretory phase and CD3+CD4-CD8- cells were increased over this period (Flynn et al., 2000). CD8+ T cells were dominant in the endometrium, although a large population of CD4+ T cells was also present throughout the cycle. An older study which used chloroacetate esterase to stain granulocytes found that they were rarely present in the

human endometrium in the proliferative phase but were more numerous in the mid-secretory phase and most abundant in the menstrual phase (Poropatich et al., 1987), showing that along with other leukocytes, granulocytes may play a significant role in tissue remodelling.

One of the main ways in which leukocytes contribute to endometrial remodelling is through the production of MMPs. MMP-1, MMP-2, MMP-3, MMP-10 and MMP-11 are all produced by the stroma, but MMP-9 is synthesised by neutrophils and macrophages (Salamonsen and Woolley, 1999), as discussed above, these cells are most numerous in the secretory phase before menstruation. The withdrawal of progesterone in the late secretory phase has been implicated in the increased production of MMPs (Salamonsen et al., 1997), but this is probably one of many factors involved in the release of these proteases. Phagocytosis of endometrial debris and production of pro-inflammatory cytokines are also key functions of leukocytes such as macrophages, which assist endometrial remodelling (Croy et al., 2003).

Though mice do not exhibit menstruation they provide a useful model for examining leukocytes in reproductive tissues. As discussed in section 1.1.4, human endometrial stromal cells differentiate into decidual cells before implantation of the blastocyst, whereas in mice, decidualisation occurs upon blastocyst contact. If implantation does not occur, this specialised tissue must be cleared; in mice, because there is no decidualised tissue to be shed, there is no menstruation. The oestrous cycle is described in section 1.1.2 and the hormonal changes are similar to those in the menstrual cycle. As well as studying the natural cycle present in mice, they have also been used in models of menstruation, where the decidualisation and shedding process is mimicked. The first step in human menstruation is the decline in progesterone and this is recreated in mice. The mouse model was first proposed by Finn and Pope (Finn and Pope, 1984) who demonstrated that mice could be ovariectomised and treated with oestrogen and progesterone, then receive an intrauterine injection of oil to initiate decidualisation. Following this, progesterone is removed, provoking endometrial breakdown modelling human menstruation. This has been refined (Brasted et al., 2003) and used to probe the process of menstruation with greater ease, without the need to acquire human samples. One study found that endometrial leukocytes were increased in number within 12hrs of progesterone withdrawal and appeared to continue to increase until the tissue is so fragmented that they can no longer be supported (Brasted et al., 2003). Macrophages have been identified in areas of endometrial

breakdown (Brasted et al., 2003) and neutrophils may play a key role in endometrial repair as antibody depletion of neutrophils has been shown to result in delayed endometrial repair following withdrawal of progesterone (Kaitu'u-Lino et al., 2007). Similarly, in another study using flow cytometry, uterine granulocyte numbers identified as Gr1+F4/80- cells peaked after 24hrs of progesterone withdrawal and are significantly reduced again at 72hrs after progesterone withdrawal, the time-point when bleeding had stopped. It was also shown that these cells formed the vast majority of CD45+ cells at 24hrs and 72hrs (Menning et al., 2012). In the same study, Gr1-F4/80+ macrophages in the uterus were found to be highest at the time of progesterone withdrawal and declined until 72hrs. These cells formed the second largest CD45+ population following progesterone withdrawal (Menning et al., 2012). CD4+ T cells, CD8+ T cells and CD19+ B cells were slightly increased in number at the time of progesterone withdrawal but did not constitute a large proportion of CD45+ cells in the uterine horn (Menning et al., 2012). Expression of several genes encoding MMPs was increased dramatically following progesterone withdrawal, with expression of MMP-1, MMP-3, MMP-9 and MMP-10 peaking at 24hrs following removal of the progesterone-secreting implant, and MMP-2 and MMP-11 highest at 48hrs. When the natural mouse oestrous cycle was studied, no obvious parallels with the human menstrual cycle were found, presumably as menstruation is a far more destructive process. However, macrophages, lymphocytes and granulocyte are present in the uterine horn of the mouse at all stages of the oestrous cycle but changes in overall numbers do not appear to correlate directly with the changes in oestrogen or progesterone levels (De and Wood, 1990, Wood et al., 2007, Kyaw et al., 1998). Though macrophage numbers do not change, during diestrus macrophages are uniformly distributed in the endometrium and myometrium, whereas during proestrus and oestrus macrophages are concentrated in the subepithelial stroma (De and Wood, 1990, Wood et al., 2007). This may support a role for macrophages in the remodelling of the endometrium as uterine thickness is lost following the oestrous phase, reaching its minimum thickness in diestrus (Wood et al., 2007).

In summary, it appears that during the menstrual cycle, leukocytes are most abundant in the secretory phase of the cycle and immediately before menstruation. This may be in preparation for implantation as well as to drive endometrial breakdown if no pregnancy occurs. The main leukocyte subsets associated with endometrial breakdown are macrophages and neutrophils, and production of MMPs appears to be central to their function during this time.

1.3.2. *Immune cells in implantation and early pregnancy.*

As discussed in section 1.1.3, successful implantation is required for a sustained pregnancy. Trophoblast invasion and development of the placenta require remodelling of the endometrium, and leukocytes play a key role in this process. In preparation for implantation in humans the endometrium undergoes decidualisation and the leukocyte content of the decidua is distinct from that of the NP endometrium with over 70% of leukocytes being uNK cells (Loke et al., 1995). Their phenotype is described as $CD56^{bright}$CD16-CD62L+ and they are at their highest in early pregnancy (Bulmer et al., 2010, Croy et al., 2003). NK activity has also been associated with recurrent miscarriage. Patients with high pre-conceptional NK activity experienced a much higher rate of miscarriage than those with normal NK activity (Aoki et al., 1995). uNK cells initiate spiral artery remodelling and are thought to promote implantation and maintain gestation (Lash et al., 2010). NK cells (CD3-CD56+) decrease in peripheral blood during pregnancy, perhaps suggesting recruitment from the blood to the decidua (Martinez-Garcia et al., 2011). uNK cells might be expected to kill the invading trophoblasts that they contact: however the Killer Inhibitory Receptors (KIRs) on uNK cells recognise the non-conventional Human Leukocyte Antigens (HLAs) trophoblasts express and NK cell cytotoxicity is inhibited. An *in vitro* study showed that when decidual uNK cells were cultured with K-562 cells expressing HLA-G, normally expressed by invasive trophoblasts, cytokine production was suppressed, compared to uNK cells cultured with cells not expressing HLA-G (Rieger et al., 2002). NKG2A, a Killer cell Inhibitory Receptor (KIR) which engages HLA-G is upregulated when uNK cells are cultured with DCs. uNK cells promote trophoblast invasion in a number of ways, including the secretion of pro-angiogenic factors such as Vascular Endothelial Growth Factor (VEGF) and Placental Growth Factor (PGF)(Burke et al., 2010, Hanna et al., 2006). As well as trophoblasts and decidual cells, uNK cells secrete MMPs, and have been found to secrete almost all known MMPs during pregnancy, showing another likely role that these cells play during remodelling (Anacker et al., 2011). Another major function of uNK cells is the modulation of DC responses at the foetomaternal interface. NK cells are able to direct immature DC lysis via signals received through the NKp30 receptor and to a lesser extent through the NKp46 and NKG2D receptors (Ferlazzo et al., 2002). DCs have been described in the decidua but their ability to stimulate T cell responses appears impaired (Laskarin et al., 2007). Also, interaction with non-conventional HLA molecules on trophoblast cells may also act to produce a tolerogenic DC response (Laskarin et al., 2007). DCs secrete cytokines and in turn induce uNK proliferation. Trophoblasts express CD1d, the MHC-like

receptor responsible for antigen presentation to iNKT cells (Boyson et al., 2002). In early pregnancy, compared to peripheral blood, decidual iNKT cells are around 10 fold higher as a proportion of CD3+ cells. Further to this, human decidual iNKT cells have been found to exhibit a Th-1-like phenotype *in vitro* (Boyson et al., 2002).

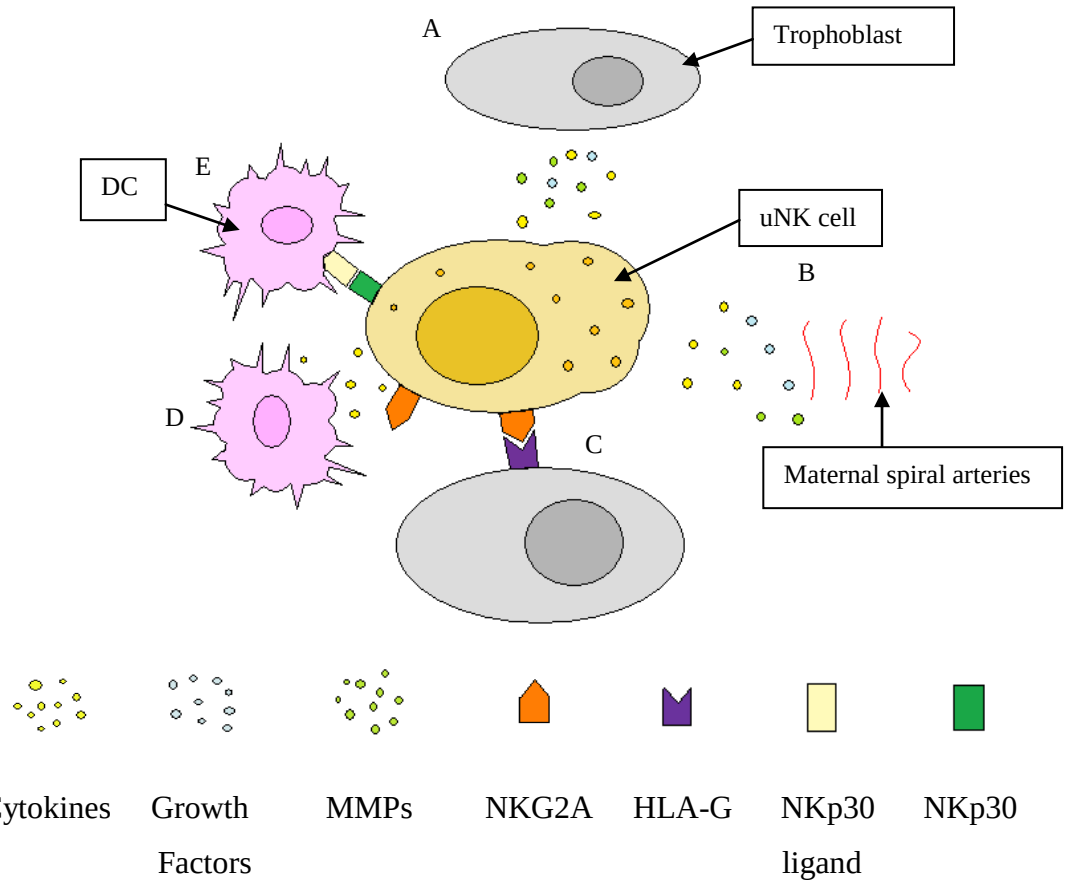

Figure 1.11. uNK interactions during early pregnancy.

(A) uNK cells promote trophoblast invasion through secretion of cytokines, MMPs and growth factors. (B) uNK cells initiate spiral artery remodelling through secretion of cytokines, MMPs and growth factors. (C) Interaction with HLA-G by KIRs such as NKG2A. (D) Cytokine crosstalk between DCs and uNK cells promotes tolerogenic phenotypes in both cell types, for example DCs induce higher NKG2A expression on uNK cells (Laskarin et al., 2007). (E) Potential for immature DC lysis by NK cells, mediated by NKp30.

Macrophages have also been observed at the site of implantation (Kabawat et al., 1985). Although M1 and M2 types represent extreme ends of a continuum of macrophage function, many have associated M2 macrophages with early pregnancy due to their role in supporting angiogenesis and tissue remodelling (Jensen et al., 2012). M2 macrophages are abundant at the foetomaternal interface and secrete immunosuppressive cytokines such as IL-10 and TGF-β, promoting tolerance (Svensson et al., 2011, Nagamatsu and Schust, 2010). M2 macrophages appear to predominate during the first trimester of pregnancy (Cupurdija et al., 2004), although the true phenotype of decidual macrophages has been a

matter of debate. Some reports have shown that maternal decidual macrophages are more diverse, rather than purely being M2 macrophages, indicating that remodelling in early pregnancy requires a range of macrophage subtypes (Svensson et al., 2011, Houser et al., 2011). In humans withdrawal of progesterone with RU486 during early pregnancy causes an influx of CD68+ monocytes into decidual tissue from 12hrs after administration (Critchley et al., 1996). *In vitro* studies have also shown that trophoblast cells induce the migration of monocytes after 48hrs in a two chamber culture system (Fest et al., 2007). This supports the idea that trophoblasts secrete chemotactic factors early in pregnancy to recruit leukocytes that in turn can support the erosion of maternal tissues during implanation.

As the conceptus is semi-allogeneic, maintenance of pregnancy requires evading the maternal immunological defences. This requires a paradoxical approach to immunity, with a balancing act between defence against pathogens and tolerance to the foetus. If infection occurs, pre-term labour could be triggered and if paternal antigens are rejected the pregnancy will be lost. Recurrent pregnancy loss is a devastating clinical condition and women with this condition often have immune abnormalities (Lee et al., 2012). Different subsets of regulatory T cells have been described as being involved in tolerance at the foetomaternal interface and these cells are crucial for the maintenance of pregnancy in the first trimester. Women with recurrent pregnancy loss have been reported to have an increased percentage of Th_{17} cells compared to controls and a decreased percentage of regulatory CD4+FoxP3+ T cells in their circulation (Lee et al., 2011b). This would suggest these women had a less suppressive and more pathogenic response to implantation. Interestingly, contact with seminal fluid induces an expansion of CD4+CD25+ T cells as a percentage of CD4+ T cells in secondary lymphoid organs, compared to mice mated without contact with semen (Robertson et al., 2009, Zenclussen et al., 2010). This indicates an important tolerogenic mechanism provoked by paternal antigens begins even before implantation. A study examining decidual tissues from women found that CD4+CD25^{bright}FoxP3+ cells were localised at the foetomaternal interface and when decidual or peripheral CD45+ cells were stimulated with umbilical cord cells from the foetus, decidual CD4+CD25+ cells reduced their proliferation to a greater extent than peripheral CD4+CD25+ cells (Tilburgs et al., 2008). As described throughout this section, the leukocyte content of the decidua in early pregnancy is distinct from that in peripheral blood. This is also supported by the fact that CD4+ T cells form ~38% of lymphocytes in peripheral blood but in the decidua only ~6% of lymphocytes are CD4+ T cells (Sasaki et

al., 2004). Of these CD4+ T cells, ~22% were of the CD4+CD25+ T cell phenotype in the decidua, whereas in blood ~9% are CD4+CD25+ T cells (Sasaki et al., 2004). These early pregnancy CD4+CD25+ T cells were co-cultured with CD4+CD25- T cells and APCs and stimulated with anti-CD3 antibodies to induce proliferation of CD4+CD25- T cells, and both peripheral and decidual CD4+CD25+ T cells suppressed proliferation in a dose-dependent manner (Sasaki et al., 2004). Another study in humans found that CD4+CD25+ T cells were higher in terms of number in the first trimester decidua than in the blood (Mjosberg et al., 2010). Impressively, in an adoptive transfer model, donor lymphocytes were pooled and the CD25+ cells were depleted and injected into athymic nude mice to produce mice lacking in CD4+CD25+ T cells (Aluvihare et al., 2004). This was found to result in pregnancy failure in mice carrying semi-allogeneic foetuses, but not in those carrying syngeneic pups (Aluvihare et al., 2004). Therapeutic interventions with these cells have also been investigated in mice: the mating combination CBAxDBA/2 is particularly abortion-prone and this high abortion rate has been successfully reduced with an infusion of CD4+CD25+ T cells from BALB/c mated pregnant CBA mice into 0-2 gestational day pregnant mice (Zenclussen et al., 2005).

Implantation and early pregnancy are fascinating from the point of view of paradoxical immunity. The semi-allogeneic conceptus must be tolerated but invading pathogens must be fought off in order to maintain the pregnancy. The early phase of implantation could be seen as pro-inflammatory, as there is a release of MMPs and a recruitment of leukocytes. However, given that the main leukocyte subsets associated with early pregnancy are uNK cells, M2 macrophages and CD4+CD25+ T cells, the picture is clearly more complex than this and a tolerogenic pro-remodelling state is achieved.

1.3.3. *Immune cells in mid-late pregnancy.*

Following the inflammatory implantation phase, there appears to be a quiescent phase during the second trimester where tolerance to the foetus is maintained. It is technically difficult to study this phase in humans so mouse studies have been invaluable in providing an insight into uterine leukocyte populations.

In mice there is conflicting evidence about the macrophage populations in the uterine horn during this phase of pregnancy. It was found that F4/80 expression, a marker expressed on macrophages, was decreased on day 18 of pregnancy, compared with NP controls(Menzies et al., 2012). This is contrary to older reports showing that high numbers of macrophages

are detected using immunohistochemistry in the murine uterine horn, particularly during late pregnancy but numbers appear to be elevated from as early as day 6 onwards (Kyaw et al., 1998, De and Wood, 1991). A three-fold increase in the proportion of macrophages in the uterine horn has been seen on pregnancy day 15 compared with the NP uterine horn (Mackler et al., 1999). In both rats and humans inflammatory monocyte subsets are decreased as a proportion of total monocytes in peripheral blood in the 2^{nd}-3^{rd} trimesters of pregnancy versus NP, however total monocytes remain fairly constant as a proportion of leukocytes throughout pregnancy (Melgert et al., 2012, Luppi et al., 2002a, Fernekorn et al., 2007). Conversely, granulocytes increase as a proportion of leukocytes compared to NP from 2^{nd} trimester onwards (Luppi et al., 2002a, Luppi et al., 2002b, Fernekorn et al., 2007). In mice, the endocytic activity of macrophages has been measured in the uterine horn during pregnancy using an intravenous injection of horseradish peroxidise (Stewart and Mitchell, 1992). Although most endocytic activity was observed by decidual cells nearest to trophoblasts, CD11b+ cells thought to be macrophages also endocytosed horseradish peroxidise in the myometrium (Stewart and Mitchell, 1992). Endocytic activity was increased at gestational day 17, compared to gestational day 13, perhaps indicating that pregnancy moves towards a more inflammatory state during the last trimester (Stewart and Mitchell, 1992). This is supported by the idea that peripheral monocytes become progressively activated in the second half of pregnancy, as they show increased expression of CD11a, CD64 and CD54 (Luppi et al., 2002a). CD11a (LFA-1), an integrin, and its glycoprotein ligand CD54 (ICAM-1) are involved in leukocyte adhesion and migration from blood vessels and CD64 is an Fc receptor.

There are also systemic changes in T cell populations associated with pregnancy. Immunohistochemical analysis of myometrial tissue from pregnant and NP women has also revealed a difference in the T cell subsets present. The density of CD4+ cells is increased in pregnant women compared to NP controls whereas density of CD8+ cells was found not to be significantly different between the two groups (Ivanisevic et al., 2010). Total blood lymphocytes progressively decrease during human pregnancy and have been found to be significantly lower in all three trimesters of pregnancy compared with the blood of NP women (Luppi et al., 2002a, Luppi et al., 2002b). T cells are comprised of specialised subsets that also appear to change in proportion during the reproductive process. In a small study of pregnant women, during the first half of pregnancy CD4+ T cells predominate in the peripheral blood, whereas in the second half of pregnancy CD8+ T cells are the main T cell population (Hoger et al., 1996).

As CD4+CD25+ T cells appear to be so important in the maintenance of the foetus throughout pregnancy, they have been the focus of many studies. In mice, CD4+CD25+ T cells from mid-gestation pregnant mice have been shown to down-regulate CD4+ T cell proliferation in response to paternal antigens, providing more evidence for a regulatory function of these cells during pregnancy (Zhao et al., 2007). The percentage of CD4+CD25+ regulatory T cells increases with gestation in spleen, inguinal lymph nodes, iliac lymph nodes and blood in mice (Aluvihare et al., 2004). This is contrary to reports from humans (Martinez-Garcia et al., 2011, Godfrey et al., 1993) and mice (Zhao et al., 2007) measuring CD4+CD25+ Tregs, showing that these cells decrease in the 2nd and 3rd trimesters in the blood compared to the first. One report suggests that the increase in CD4+CD25+ T cells as a proportion of CD4+ T cells in spleen and non-draining lymph nodes is seen in allogeneically but not syngeneically mated mice (Zhao et al., 2007). The proliferation of these cells in various tissues indicates that this important facet of tolerance is systemic and not an effect local to the uterus. CD4+CD25+ T cells make up a higher percentage of T cells in the blood, spleen and lymph nodes of pregnant mice carrying semi-allogeneic foetuses compared to those with syngeneic pups (Zhao et al., 2007).

During gestation it appears that uterine leukocytes reflect a move towards a more pro-inflammatory state towards the end of pregnancy. Although numbers of uNK cells reduce during pregnancy, CD4+CD25+ T cells continue to be of importance. Though conflicting data exist as to the presence of macrophages, other myeloid cells such as granulocytes increase towards the end of pregnancy and peripheral monocytes appear to become activated to a greater degree, which may indicate a preparation for labour at term.

1.3.4. *Immune cells in labouring females.*

In the uterus during the final phase of pregnancy there is a more inflammatory environment than is seen during mid pregnancy. A study from our group used expression of the gene encoding F4/80 to indicate that macrophages in the uterine horn are significantly increased in labour compared with day 18 of pregnancy in WT mice (Menzies, 2010, Menzies et al., 2012). In humans, CD68+ macrophages increase dramatically in both the upper and lower segments in the myometrium at term during labour compared to before labour (Thomson et al., 1999). This study also showed that in sections of myometrium, neutrophils (identified by neutrophil elastase) increased dramatically in labour, compared with non-labouring term samples (Thomson et al., 1999). Interestingly, when the decidua was studied, no increase in CD45+ cells, CD68+ macrophages or neutrophils was seen in labour (Osman et

al., 2003), compared to non-labouring women, suggesting that the inflammatory influx is restricted to the contracting myometrium. A recent study using flow cytometry found that leukocytes were increased in density in the term decidua regardless of the presence of labour, compared to pre-term samples where infection was not a factor in delivery (Gomez-Lopez et al., 2013). This study found that monocytes, as a proportion of CD45+ cells, increased in the decidua at term compared to pre-term, whereas granulocytes were decreased as a proportion of CD45+ cells at term compared to pre-term, and were further reduced in term labouring samples (Gomez-Lopez et al., 2013).

In humans, CD3+ T cells increase dramatically in the lower segment of the myometrium during labour, compared to before labour (Thomson et al., 1999). In the decidua, results are mixed as in one study, CD3+ T cells remain constant through all three trimesters in the decidua (Williams et al., 2009), whereas in another there does appear to be an increase in decidual CD3+ T cells between the first and third trimesters (Haller et al., 1993). This result is supported by a recent study which found that CD3+ T cells are dramatically higher as a proportion of CD45+ cells in term, compared to deciduas from pre-term women (Gomez-Lopez et al., 2013). Even more strikingly, there is a further increase in CD3+ cells in labouring samples, which revealed that CD3+ T cells constitute over 50% of leukocytes in labour (Gomez-Lopez et al., 2013). This study went on to review the T cell subsets with the CD3+ gate and found that in pre-term decidual samples CD3+CD4-CD8- constituted nearly 90% of CD3+ cells and only a small proportion of CD3+ cells were CD4+ and CD8+. In non-labouring term decidual samples CD4+ T cells dominated, making up nearly 70% of CD3+ cells, ~25% were CD8+ T cells, with the remainder being CD3+CD4-CD8- (Gomez-Lopez et al., 2013). Finally, in term labouring samples ~50% of CD3+ cells are CD4+, with around 20% CD8+ T cells and nearly 30% being CD3+CD4-CD8- (Gomez-Lopez et al., 2013). In this study they found that some CD3+CD4-CD8- cells in the decidua expressed CD45RO and the study proposed that these cells were memory-like DN T cells. Another study in humans found that, as a proportion of CD3+ cells, around 30% were CD3+CD4-CD8- immediately post-partum in the deciduas of women with a completed normal term pregnancy (Tilburgs et al., 2009). Although around 40-50% of these cells were found to express TCR-γδ, many also expressed antigens associated with NK/NKT cells such as CD56, KIRs and CD94, the receptor which recognises HLA-E, indicating many of these cells may be NKT cells (Tilburgs et al., 2009).

In mice, activated T cells (defined as CD3+CD69+) are increased in the decidua in LPS-induced pre-term birth, compared to decidual tissue from normal deliveries (Li et al., 2012). LPS-induced pre-term birth is a mouse model that attempts to mirror some of the aspects of pre-term birth following bacterial infection. The number of T cells in the lymph nodes draining the uterus (the para-aortic lymph nodes (PALN)) is constant during pregnancy in syngeneically mated mice (CBAxCBA), with a small dip in percentage and then a subsequent rise at day 19 of pregnancy. This also seems to be echoed in the skin-draining brachial lymph nodes (Carter et al., 1983). This study also showed a massive increase in B cells in the PALN. Allogeneically mated mice (CBAxC57) showed constant levels of T cells in the PALN until around day 15 when a large fall in percentage was seen, which continued to day 19 of pregnancy. This was a local fall because this was not as exaggerated in the brachial nodes (Carter et al., 1983). This might indicate a systemic response in syngeneically, but not allogeneically, mated mice. This was confirmed in a separate study, showing a similar time-course over pregnancy and finding that in allogeneically mated mice, changes in T cell populations appeared not to be systemic (Newport and Carter, 1983).

When comparing CD56+ NK cells across the three trimesters, several studies have described a fall in decidual uNK cells in the third trimester (Williams et al., 2009, Haller et al., 1993). Though many uNK cells die *in situ*, the remainder appear to be shed with the placenta (Delgado et al., 1996). Activated NK cells identified as DX5+CD69+ are increased in the decidua following LPS-induced pre-term birth in mice, compared to the decidua from a normal delivery (Kaitu'u-Lino et al., 2007). Interestingly, when NKT cells are considered, there seems to be an increase in decidual CD3+CD161+ NKT cells in the third, compared to the first, trimester (Williams et al., 2009). There may be a role for iNKT cells in inflammation induced pre-term birth. When LPS is administered intraperitoneally on gestational day 15, Jα18 KO mice, which lack iNKT cells, were partially protected from pre-term birth, exhibiting a reduced pre-term birth delivery rate and a decreased pup mortality rate (Li et al., 2012). When cultured, Jα18 KO decidual cells showed reduced IFNγ and IL-12 in their supernatant (Li et al., 2012), supporting another study suggesting that decidual iNKT cells can be Th-1 skewed and participate in pregnancy loss (Boyson et al., 2008, Ito et al., 2000).

Cell	Term labour myometrium	Term labour decidua	Inflammation-driven labour decidua
Macrophage 	↑	=	
Neutrophil 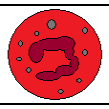	↑	=	
T cell 	↑	↑	↑
NK cell 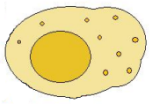		↓	↑

Table 1.2. Leukocytes in the uterus during labour.

It appears that the main site of inflammation in the uterus is the myometrium, which displays increases in macrophages, neutrophils and T cells. Though CD45+ cells increase in the decidua at term, this does not seem to be specific to labour. T cells in the decidua are increased with term and labour, attributed to CD4+ T cells and CD3+CD4-CD8- cells. Decidual uNK cells are shed with normal term labour, however there may be a role for activated NK and NKT cells in inflammation-driven labour.

Several studies have attempted to find the cellular components involved in cervical ripening. In humans, one study showed a large increase in CD68+ macrophages and neutrophil elastase-positive neutrophils in the cervix of labouring women, compared to non-labouring subjects at term (Zenclussen et al., 2005). However, a similar study found no difference in CD11b/CD18+ macrophages or neutrophils identified by the MCA 149 antibody between labouring and non-labouring cervix (Bokstrom et al., 1997). Since this study was completed, more selective markers are now available and newer studies may be more reliable, especially if a technique such as flow cytometry is used.

Mouse studies have reported conflicting results on the proportions of macrophages found in the cervix at term. One study using histology observed an increase in F4/80+ macrophages between day 15 and day 18 (Mackler et al., 1999), however another found that F4/80+ macrophages remained constant between days 15 and 18.75 (Timmons and Mahendroo, 2006). However this has since been confirmed as macrophages were measured by flow cytometry and they remained constant as a percentage of live cells from the cervix between day 15 and day 18.75 of gestation (Timmons et al., 2009). There is also a dramatic increase in expression of *Ym1*, a gene associated with an eosinophil chemoattractant released by alternatively activated macrophages during cervical ripening (Holt et al., 2011).

Neutrophils have often been implicated in cervical ripening. However evidence from mouse models has disputed this (Timmons et al., 2009, Timmons and Mahendroo, 2006). One study using cytospin preparations found that the number of cervical neutrophils between day 15 and day 18.75 of pregnancy remained constant, as did the number of eosinophils (Timmons and Mahendroo, 2006). When the cervix was examined using flow cytometry, neutrophils increase significantly as a percentage of cervical cells 2-4hrs post-partum, compared to day 15 of pregnancy (Timmons et al., 2009). In the same study, monocytes were elevated as a percentage of cervical cells from day 18.75 and remained as such during labour and 2-4hrs post-partum. Eosinophils also peaked during labour, suggesting that there is a large infiltration of these cells before neutrophils reach the cervix (Timmons et al., 2009). Further to this, MPO, the neutrophil-generated enzyme postulated to produce ROS during cervical ripening, was not found to be active in the cervix of pregnant mice (Timmons and Mahendroo, 2006). These data potentially indicate that neutrophils are not required for the process of cervical ripening and that this role may be fulfilled by monocytes, perhaps with some contribution by eosinophils.

One study in mice compared different forms of pre-term birth and found that the percentages of monocytes, macrophages, neutrophils and eosinophils in the cervix were dependent on the method used to induce labour (Holt et al., 2011). When progesterone is withdrawn using the antagonist RU486, monocytes and eosinophils increased significantly in the cervix, whereas in LPS-induced labour neutrophils were the cell type that was increased significantly compared with gestational day 15 (Holt et al., 2011). One model of pre-term labour involves treating NP mice with implants releasing estradiol and progesterone for 17 days to mimic the hormonal conditions of pregnancy. The capsule releasing progesterone is then removed, producing a fall in progesterone similar to that preceding labour in the mouse. Using this model, there was a significant increase in both F4/80+ macrophages and Ly6B(7/4)+ neutrophils in the cervix on days 18 and 19 of treatment in the group which had undergone removal of progesterone (Yellon et al., 2009a). This method has been used by several investigators, and a role for neutrophils in inflammation-driven pre-term birth is supported. After intrauterine LPS administration, histology has shown that Ly6B+ neutrophils are greatly increased in density in the murine cervix (Yellon et al., 2009b). This is supported by a study that found an infiltration of F4/80+ macrophages and Gr1+ neutrophils into the cervix in LPS which induced preterm delivery, but not in normal term delivery (Gonzalez et al., 2011).

Cell	Term labour/ progesterone antagonsim	Inflammation-driven labour
Macrophage 	=/↑	↑/=
Neutrophil 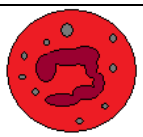	=	↑
Monocyte 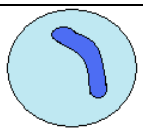	↑	=
Eosinophil 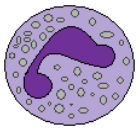	↑	=

Table 1.3. Leukocytes involved in cervical ripening.

The cells involved in cervical ripening are dependent on how labour is initiated. In term labour, neutrophils and macrophages appear to remain constant in the cervix, though macrophages may skew towards an M2 phenotype. It seems that monocytes and eosinophils are the cells that increase in the cervix during term labour and labour induced by progesterone antagonism. Inflammation-induced cervical ripening appears to result in a strong increase in the numbers of neutrophils.

1.3.5. *Immune cells in post-partum females.*

The contribution of macrophages to post-partum tissue remodelling remains a subject for debate. An influx of monocytes and monocyte-derived macrophages into the uterine horn in the post-partum period would suggest a vital role in the remodelling process after birth, but few studies have examined the presence of leukocyte subsets in the uterine horn or cervix at more than one time-point post-partum and those that have lacked the most current methods, such as flow cytometry. A study in mice from 1992 used CD11b/CD18 (Mac-1) to identify macrophages and neutrophils, and suggested that the uterine epithelium is repaired by 4DPP. They found that neither macrophages nor neutrophils were involved in endocytosing debris or repair of the uterus as very few had internalised HorseRadish Peroxidase (HRP), which had been injected intravenously to model the capacity of the cells to take up debris (Stewart and Mitchell, 1992). These findings were contradicted two years later using F4/80, a more selective macrophage marker than CD11b/CD18 (Brandon, 1994). The endometrium and myometrium were found to contain large numbers of F4/80+ cells at post-partum time-points between 1 day and 3 months, with numbers particularly

high at earlier time points (Brandon, 1994). Another histological study in mice normalised F4/80+ macrophages to NP levels and found they were significantly increased in the uterine horn at 1DPP, compared with NP controls. However in the cervix macrophages were decreased compared to immediately post-partum, perhaps suggesting that macrophages are involved in cervical ripening and not repair (Mackler et al., 1999). Another recent study in rats using flow cytometry showed macrophages to be significantly decreased as a percentage of CD45+ cells at 2-6hrs post-partum in the myometrium, compared with gestational day 18 and labour (Shynlova et al., 2012). In the same study, monocytes and neutrophils were found to be significantly increased in proportion at 2-6hrs post-partum compared to gestational days 15 and 18 in the myometrium (Shynlova et al., 2012). Neutrophils have also been found to increase in the cervix from labour to 2-4hrs post-partum (Timmons et al., 2009). However, a different study looking at cell morphology in cervical cytospin preparations found no real change in neutrophils comparing 18.75 of pregnancy to 2-4hrs post-partum. However, at 2-4hrs post-partum, eosinophils were significantly increased in number compared with gestational day 18.75 (Timmons and Mahendroo, 2006). This contradicts another study that reported that Siglec-F+ eosinophils were at their highest in the cervix during labour and appear to decrease at 2-4hrs post-partum (Timmons et al., 2009).

One particular feature of post-partum repair of the uterus is the presence of detachment sites. Detachment sites have been observed in many mammalian species including rabbit (Bull, 1949), dog (Orfanou et al., 2009), hamster (Orsini, 1957), bank vole (Nerquaye-Tetteh and Clarke, 1990) and mouse (Brandon, 1994). The detachment wound appears to correspond with the site of implantation and is where the terminal arteries fed the placenta (Brandon, 1994, Orsini, 1957). The detachment site in the mouse has been described to remain for as long as three months and to not overlap with detachment sites from subsequent pregnancies (Brandon, 1994). However, in the bank vole, old detachment sites have been observed to overlap with fresh sites after multiple pregnancies, suggesting that detachment sites may only prevent implantation in recently used sites on the uterine horn (Nerquaye-Tetteh and Clarke, 1990). Another functional role of detachment sites may be to promote spacing of implanting blastocysts along the length of the uterine horn, as decidualisation seems not to occur in areas with detachment sites, leading to evenly spaced decidualised areas suitable for implantation (Brandon, 1990). In mice, the detachment wound has been described with large numbers of F4/80+ cells at 2DPP and 3DPP and these decline as the detachment wound heals (Brandon, 1994). These wounds become

structures called post-partum nodules by 5DPP, which diminish in size over time but persist until at least 3 months post-partum. Nodules appear to consist primarily of macrophages, and although F4/80 staining decreases over time, these data provided tentative evidence that macrophages may be the primary cell type involved in the repair of the detachment site (Brandon, 1994).

Very little data are available on the behaviour of T cells in the post-partum period, however available data suggest that, as with labour, there seems to be a T cell response in secondary lymphoid organs in the post-partum period. Two studies have found in mice mated syngeneically (CBAxCBA) the percentage of total cells which were T cells increased in both the PALN and brachial lymph nodes during the post-partum period (Carter et al., 1983, Newport and Carter, 1983). In allogeneically mated mice (CBAxC57), T cells remained fairly constant in both the PALN and brachial nodes between around 2-6DPP, perhaps suggesting that T cells are not involved in the resolution of inflammation in the post-partum period in allogeneically mated mice. This might indicate that in allogeneically mated mice, cells such as Tregs achieve a greater degree of systemic tolerance to the foetus. In cows, a decrease in percentage of T cells in peripheral blood mononuclear cells is observed during pregnancy, which is then followed by a subsequent increase in the proportion of T cells in the post-partum period (Kimura, 1999).

It is generally accepted that uNK cells are not a feature of the post-partum uterus (Delgado et al., 1996, Kokubu et al., 2005). Not only are very few uNK cells found in the endometrium and myometrium at 1-9DPP in mice, these cells were not involved in endocytosis as indicated by their inability to internalise previously-injected HRP (Stewart and Mitchell, 1992).

In the post-partum period macrophages appear to be increased in the endometrium and myometrium in the early post-partum period and particularly concentrated in detachment sites. Monocytes and neutrophils are also increased in the early post-partum period in the uterus. In the cervix, early in the post-partum period macrophages seem to be decreased and whereas reports on granulocytes are conflicting. The role of T cells in the post-partum period is not well defined and needs closer study. The difficulty in analysing these studies and others during the reproductive process is the variation in the markers used, and the few time-points that have been examined. This emphasises the need for investigation of

leukocytes in the post-partum period, using up to date techniques, comparing several cell types, and analysing at more than one post-partum time-point.

1.3.6. *The effect of lactation on immune cells in post-partum females.*

In humans prolactin increases during pregnancy, along with estradiol and progesterone (Martinez-Garcia et al., 2011, Hill et al., 1999). Prolactin is also secreted by decidual cells and has been implicated as a factor in implantation (Dunn et al., 2003). Prolactin levels in the blood of mice that retain their litters are significantly higher compared to NP control animals and mice which have had their litters removed. This suggests that lactation produces a hormonal state which is distinct from post-partum mice without pups (Ratkay et al., 2000). In humans, prolactin falls after birth as the placenta, which stimulates the production of prolactin is removed, and only if suckling by the infant occurs, does prolactin subsequently rise due to the release of oxytocin (Hill et al., 1999). Lactation and prolactin are associated with many autoimmune conditions including rheumatoid arthritis and can act to produce a post-partum flare in these conditions (Shelly et al., 2012).

Prolactin is especially important in the development of T cells in the thymus. Prolactin receptor is highly expressed on thymocytes in mice and rats, as well as cells in the BM and spleen (Gagnerault et al., 1993). In the spleen, macrophages express high levels of prolactin receptor (Gagnerault et al., 1993). In the same study, CD4+ T cells and CD8+ T cells in the spleen expressed low levels of prolactin receptor, though prolactin receptor expression by CD4+ T cells and CD8+ T cells in culture increased when cells were stimulated with Con A (Gagnerault et al., 1993). Prolactin induces CD25 expression on DN thymocytes, allowing them to mature further (Carreno et al., 2005). In culture, when young rat thymocytes are treated with prolactin, addition of the hormone negatively regulates the proportion of DN T cells (Carreno et al., 2005). Increasing concentrations of prolactin reduce the proportion of DN T cells, whereas antibodies against prolactin or prolactin receptor increase the proportion of DN thymocytes in culture (Carreno et al., 2005). Interestingly, if CD25 is blocked but prolactin is added, the proportion of DN T cells increases because IL2-induced maturation cannot occur, showing that prolactin is upstream of CD25 (Carreno et al., 2005). Conversely, if prolactin receptor is blocked but IL-2 is added, the DN T cell proportion decreases because the signal to mature is downstream of the block of prolactin receptor (Carreno et al., 2005). IL-2 production by T cells in culture has been shown to be markedly reduced on addition of prolactin (Chavez-Rueda et al., 2005). DN T cells have not been studied directly in lactating and non-

lactating mice in the post-partum period but as many as a third of CD3+ T cells are not described as CD4+ T cells or CD8+ T cells in the spleens of lactating mice in a range of strains (Wei et al., 2011). This may indicate a reservoir of CD3+ DN cells in the spleen during the post-partum period.

1.3.7. *Hormonal control of chemokines.*

This section highlights the effects of hormones and the reproductive process on CCR2 and its ligands, as these molecules form part of my investigations. The role of oestrogen, progesterone and prolactin in the regulation of chemokines may reveal a link between the hormonal environment and leukocyte homing to gestational tissues. In this project various reproductive states are investigated, which will be influenced by the differing hormonal environment. Previous studies into the effects of hormones on chemokines indicate that sex steroids will impact the production of chemokines in both reproductive and peripheral tissues.

CCL2 was not detected in the uteri of ovariectomised mice but was increased in response to treatment with both progesterone and oestrogen (Wood et al., 1999). Circulating CCL3 is increased in post-menopausal women compared to pre-menopausal women, but CCL2 is not significantly changed (Abu-Taha et al., 2009). This finding is extended in mice by using ovariectomy as a model for menopause. Performing ovariectomy increases circulating CCL2 and CCL3 and this can be reversed by treating ovariectomised mice with estradiol (Abu-Taha et al., 2009). CCL2 production by LPS-stimulated macrophages has been shown to be suppressed by estradiol (Frazier-Jessen and Kovacs, 1995, Osman et al., 2003). When splenocytes were taken from oestrogen-treated or placebo-treated animals and stimulated with Con A, the amount of CCL2 protein in the supernatant increased over 3 fold in the oestrogen-treated group compared to the placebo-treated mice, an effect which was further enhanced when IFNγ was also included in the culture (Lengi et al., 2007).

In humans, estradiol peaks just before ovulation, whereas progesterone peaks towards the end of the cycle, its withdrawal triggering menses (Greenstein and Wood, 2006). In the human endometrium, CCL2 is high during the proliferative phase and low during the secretory phase (Jones et al., 1997). In humans CCL7 mRNA is at its highest during the early and mid secretory phases (Jones et al., 2004). As discussed in section 1.3.1., menstruation can be modelled in mice by treating with estradiol and progesterone, provoking decidualisation with an intrauterine injection of oil and removing the

progesterone implant (Menning et al., 2012). CCR2 mRNA increases following progesterone withdrawal, peaking at 48hrs after the implant is removed. Expression of CCL2 and CCL3 both peak at 24hrs post-withdrawal and mRNA levels then drop significantly (Menning et al., 2012).

In pregnancy, estradiol and progesterone increase during the second half of pregnancy and fall after parturition (Greenstein and Wood, 2006). Previous studies have also shown that CCL2 mRNA is present in the uterine horn during pregnancy in the mouse and the presence of this chemokine at day 18 has been confirmed by experiments in our lab (Menzies et al., 2012, Wood et al., 1999, Kyaw et al., 1998). CCL2 was expressed throughout pregnancy with peaks after mating, at implantation, and during the second half of pregnancy (Wood et al., 1999). Results from our lab have shown that the receptor CCR2 and both CCL2 and CCL3 were increased during labour compared to gestational day 18 (Menzies et al., 2012). CCL2 mRNA is higher in the myometrium and gestational membranes of labouring women compared to pregnant quiescent subjects (Esplin et al., 2005). Due to its high expression during labour, CCL2 has been suggested as a target for therapeutic intervention for pre-term labour (Shynlova et al., 2008). It is not surprising that CCL2 is found to be expressed in reproductive tissues at major inflammatory time-points such as implantation, the end of pregnancy, and labour.

Estradiol and progesterone inhibit milk production by suppressing prolactin receptor expression, and although prolactin initially falls after birth, its release is promoted by the suckling reflex and increases during the early post-partum period (Greenstein and Wood, 2006). Regression analysis in mice has shown CCL3, but not CCL2, protein in plasma predicts lactation performance, suggesting a possible interplay between hormones and circulating chemokines in the post-partum period (Wei et al., 2011). In rats, prolactin has been shown to cause regression of the corpus luteum by induction of CCL2 in the corpus luteum, followed by an infiltration of monocytes/macrophages into this body of cells (Bowen et al., 1996).

Levels of CCR2-binding chemokines in the post-partum period are of special interest throughout the project. In mice, CCL3 and CCL2 protein has been found to be increased at 2-6hrs post-partum in murine myometrium, compared with gestational day 15 in normal term birth (Shynlova et al., 2012). A study in rats charts mRNA and protein levels of CCL2 in the myometrium throughout pregnancy, continuing up until 4DPP, with both

measures being at their highest towards labour and dropping off sharply at 1DPP and 4DPP (Shynlova et al., 2008). In mice, CCL2 protein in the cervix measured by ELISA was demonstrated to be significantly increased at 2-4hrs post-partum compared to gestational days 15 and 18.75 (Timmons and Mahendroo, 2006).

In summary, although circulating CCL2 and CCL3 appear to increase following ovariectomy, when mice are treated with oestrogen and progesterone CCL2 is increased, indicating that the effect of these hormones on chemokine production differs in reproductive tissues. This relationship is supported by observations that during the proliferative phase, when oestrogen dominates, CCL2 expression is high in the uterus. A key observation is that CCL2 expression peaks in the uterus during menstruation, implantation, the end of pregnancy, labour and the early post-partum period, linking the major inflammatory events in the uterus with CCL2 induction.

1.3.8. *Sex differences in inflammation.*

As discussed above, hormones can have striking effects on the immune system, and sex differences form another dimension of this issue. Sex differences in immune-driven diseases have been well documented. Gene expression of IFNγ is increased and IL-4 is decreased in the spleens of females, compared with males (De Leon-Nava et al., 2009). In the same study macrophages identified by flow cytometry were also decreased in female spleens, compared with males (De Leon-Nava et al., 2009). In a different study, twice as much IFNγ was produced by female cultured splenocytes, compared to males, and in females plasma estradiol levels were found to correlate with splenocyte IFNγ production (Aloisi et al., 2001). These data suggest that there are sex differences in spleen composition but also in the cytokine milieu. In other compartments, such as the peritoneal cavity, F4/80+ cells, CD3+ cells and CD19+ cells were all increased in numbers in females compared to males (Scotland et al., 2011). Expression of CCR2 and CX3CR1 has been found to be sex-specific in the peritoneal cavity. Resident peritoneal cells displayed increased CCR2 gene expression in females compared to males, however CX3CR1 is more highly expressed in males than females in peritoneal cells (Scotland et al., 2011). Sex differences in populations of T cells have also been observed; pertinent to this project, DN T cells have been found to constitute a significantly higher percentage of CD3+ T cells in male blood compared to females in Rhesus macaques (Qiu et al., 2008). These cellular and molecular differences between males and females may give some insight into why female inflammatory responses are often seen as exaggerated, compared to males.

A wide range of inflammatory diseases display sex differences, including asthma (Melgert et al., 2010, Melgert and Postma, 2009), rheumatoid arthritis (Linos et al., 1980, van Vollenhoven, 2009), SLE (Weckerle and Niewold, 2011, Petri, 2002) and multiple sclerosis (Ramagopalan et al., 2010, Greer and McCombe, 2011), which all show increased prevalence and severity in female patients. Though this sex difference is undoubtedly due to myriad environmental factors, sex steroids have often been the focus of research into this phenomenon.

1.3.9. *Leukocytes in male reproductive tissues.*

Male reproductive tissues have not been examined in detail for their leukocyte content, and they have often been regarded as an immune privileged environment (Witkin et al., 1996). The main APC in the human penile urethral epithelium is the macrophage, and large numbers of CD8+ T cells and CD4+ T cells have also been recorded (Anderson et al., 2011). In the mouse epididymis, macrophages are reported to be the largest APC subset present, and though T cells have been identified, only very few cells of a CD4+ or CD8+ phenotype were found (Nashan et al., 1989). After vasectomy, large increases in macrophages and T cells have been noted in the epididymis (Nashan et al., 1990). Sections stained with haematoxylin and eosin have also been used to confirm that the rat vas deferens contains an increased number of leukocytes following vasectomy, compared with the vas deferens of non-vasectomised rats (Lavers et al., 2006). However, despite these observations, very little data exists on the cellular components of the epididymis and other sections of the male reproductive tract, especially using techniques such as flow cytometry. To my knowledge, no direct comparison of leukocytes in male and female reproductive tissues has been performed, and this is an area that merits further attention.

1.4. *Summary and aims*

Labour is seen as an inflammatory event. However, this inflammation may be generated as a means of repairing the female reproductive tract after parturition. One of the key objectives of my thesis was to analyse the leukocyte populations in reproductive and peripheral tissues in post-partum female mice, and compare this to NP mice. Myeloid cells and T cells were the leukocyte populations of principal interest and hormonal influences were also examined. The preceding Introduction aimed to give a background to these elements of research, and to clearly mark out the need for investigation in these areas of reproductive immunology. In addition, due to the chemokine receptor focus of one of the research labs where I undertook my studies, I was interested in the expression and function of CCR2 during leukocyte migration into reproductive tissues, particularly during the post-partum tissue remodelling period. This was based on the known key role that CCR2 plays in regulating monocyte trafficking but also on interesting anecdotal observations made by technical staff at our animal facility. Their experience was that although CCR2 KO female mice could deliver initial pregnancies satisfactorily, subsequent pregnancies were challenging for these animals and pups were regularly found dead or assistance had to be given to the animals during labour. This led to speculation that CCR2 may play a role in the successful remodelling of female reproductive tissues after the primary pregnancy that might be compromised by CCR2 loss. Effective healing of reproductive tissues following parturition or miscarriage is incredibly important for continued reproductive health, but it is startling that such little work has been completed with a focus on the post-partum cellular infiltrate.

This project aimed to catalogue the leukocytes in reproductive and specific peripheral tissues before and after pregnancy and to characterise their surface phenotype. Throughout this project particular emphasis was placed on the role of CCR2 and its chemokine ligands. Chapter 3 deals specifically with myeloid cells, namely monocytes, macrophages, eosinophils and neutrophils, and examines the role that CCR2 plays on these cells in NP and post-partum females. Technically challenging flow cytometry techniques were developed to allow the successful completion of this study, and these techniques were invaluable for subsequent work. Chapter 4 aimed to characterise the CD3+ cell populations present in reproductive tissues and other organs in NP and post-partum mice, including CD3+CD4+ T cells, CD3+CD8+ T cells and CD3+ DN cells. CCR2 expression was also explored on these cells, and the importance of CCR2 in the trafficking of these cells specifically examined. Chapter 5 aimed to develop the study of CD3+ DN cells, by

defining the cellular constituents of this population using a further panel of discrimatory cell surface markers. This work was restricted to NP and 1DPP females. Chapter 6 aimed to address the role of hormones in regulating these cells, specifically addressing the effect of lactation and sex differences in leukocyte populations.

The major hypotheses for Chapter 3 were:

- There is a large influx of myeloid cells, particularly monocytes/macrophages present at 1DPP in reproductive tissues, compared to NP animals.
- This inflammatory infiltrate is cleared by 7DPP.
- CCR2 plays a key role in the recruitment of these cells.
- Reproductive tissues and peripheral tissues differ in their myeloid cell composition.

The findings in Chapter 3 were built on in Chapter 4, where the following hypotheses were examined:

- CD3+ cells constitute a major leukocyte population in post-partum reproductive tissues.
- CCR2 is active on these cells.
- CCR2 plays a role in the recruitment of these cells.
- Reproductive tissues and peripheral tissues differ in their CD3+ cell composition.

Chapter 5 describes work phenotyping CD3+ DN cells in female reproductive tissues and elsewhere and investigates the following hypotheses:

- CD3+ DN cells are a mixed population of cells that includes a subpopulation of NKT cells.
- The majority of CD3+ DN cells express a TCR on their surface.
- The cellular composition of the CD3+ DN population differs between NP and 1DPP animals.
- There is a distinct population of CD3+ DN cells that dominates in reproductive tissues.

Finally Chapter 6 addresses hypotheses relating to the effect of hormones and sex on these leukocytes, specifically:

- Monocyte populations differ between males and females.

- CD3+ DN cell populations display sex differences in reproductive and peripheral tissues.
- Lactation affects CD3+ cell populations in post-partum mice.

Chapter 2: Materials and Methods

2.1. Mice

C57Bl/6 mice and CCR2 KO mice on a C57Bl/6 background were bred and maintained under specific pathogen free (SPF) conditions in the Central Research Facility, University of Glasgow. CX3CR1$^{gfp/gfp}$ mice on a C57Bl/6 background (a kind gift of Calum Bain) were bred and maintained under SPF conditions at the Veterinary Research Facility, University of Glasgow. Mice were housed in individually ventilated cages, except where indicated, where mice were housed in conventional cages. Apart from ex-breeders, all mice were used between 8-16 weeks of age. Ex-breeders were defined as mice previously designated for breeding with a maximum age of 1 year and were killed a minimum of 3 weeks following their final litter to allow pups to be weaned. C57Bl/6 mice were also purchased from Harlan UK at 7 weeks of age and were housed under SPF conditions at the Central Research Facility. These mice were used between 8-12 weeks of age. All procedures were performed in accordance with the Animals Scientific Procedures Act (1986) and licensed by the United Kingdom Home Office.

2.2. Histology

2.2.1. *Mating of mice for histology.*

WT females (8-16 weeks of age) were set up with males using a timed mating strategy, putting pairs together for between 2-24hrs. Females were checked for pregnancy ~day 15 and if pregnant housed singly. Mice were allowed to give birth, and the day (between hrs of 08.30-16.30) of first observation of the litter was counted as 0DPP.

2.2.2. *Dissection of uterine horn from post-partum and ex-breeders.*

WT ex-breeders and post-partum mothers were killed by exposure to a rising concentration of CO_2 on 1DPP and 7DPP. Uterine horns were dissected out, all fat and connective tissue was removed, and tissue was stored in 10% formalin (Sigma) for at least 24hrs.

2.2.3. *Processing of tissues for histology.*

Tissues were placed in plastic cassettes and processed using a Leica Histokinette (maintained by Jim Reilly, Institute of Infection, Immunity & Inflammation, University of Glasgow) on an overnight programme from neutral buffered formalin (10%, 30mins) through graded alcohols (70%, 1hr; 90%, 1hr; 95%, 1hr; 100%, 1hr; 100%, 2hrs; 100% 2.5hrs) to xylene (3 buckets; 1hr, 1hr, 1.5hrs) to molten paraffin wax (2 buckets; 4hrs, 5hrs).

2.2.4. *Embedding tissues in paraffin.*

Embedding was performed on a Tissue Tek embedding centre (maintained by Jim Reilly, Institute of Infection, Immunity & Inflammation, University of Glasgow). Molten wax was poured into moulds and uterine horn samples were orientated to provide a transverse section of the uterine wall on cutting. Wax hardens around the plastic cassettes and makes up the finished block, allowing blocks to be easily cut.

2.2.5. *Cutting sections and mounting slides.*

Sections 5μm thick were cut using a microtome, floated onto water at 40°C to smooth out creases and a glass slide placed underneath so the paraffin section adhered to the slide as the section was lifted out of the water. Slides were then allowed to dry out. Sections were cut and mounted by Jim Reilly (Institute of Infection, Immunity & Inflammation, University of Glasgow).

2.2.6. *Staining of uterine horn sections.*

Slides were heated in an oven at 60°C for 35mins. Sections were de-dewaxed and taken to tap water using the following method: Xylene (3mins x2), ethanol (100%, 3mins x2; 90%, 3mins x2; 70%, 3mins x2) then running tap water (3mins x2). Firstly slides were stained with Harris haematoxylin for 2mins then washed with running water for 3mins. Background was reduced by dipping twice in 1% acid/alcohol, a quick rinse in running tap water followed by 30seconds (s) in Scott's tap water substitute and a final rinse in running water. Slides were then stained with 1% eosin for 2mins and excess stain was washed off with running tap water. Sections were then dehydrated with ethanol (70%, 30s; 90%, 1min; 100%, 3mins x2) and xylene (3mins x2). A coverslip was then mounted over the tissue from xylene with DPX mountant. Staining of uterine horn sections was carried out by Jim Reilly (Institute of Infection, Immunity & Inflammation, University of Glasgow).

2.3. qRT-PCR

2.3.1. *Dissection of detachment sites from ex-breeders*

WT, CCR2 KO, and CX3CR1$^{gfp/gfp}$ female ex-breeder mice were killed by exposure to a rising concentration of CO_2 and the uterine horn and cervix were dissected out and all fat and connective tissue was removed. The uterine horn was then opened using spring bow scissors and tissue cut either side of the detachment sites. Detachment sites were compared to the rest of the tissue, which contained no detachment sites, and cervix. Tissues were kept in RNA later (Qiagen) overnight, snap frozen in liquid nitrogen and stored at -80°.

2.3.2. *Mating of mice for qRT-PCR analysis.*

Mice were mated as in 2.2.1. Mice were allowed to give birth to their litter and first observation of the litter was counted as 0DPP. Non-lactating mice were either mice that had cannibalised their pups by 1DPP or had had their pups removed by 1DPP.

2.3.3. *Dissection of reproductive tissues for qRT-PCR analysis.*

Mothers were killed by exposure to a rising concentration of CO_2 on 1DPP, 4DPP and 7DPP. Uterine horn and cervix were dissected out and all fat and connective tissue was removed. Tissues were kept in RNA later (Qiagen) overnight, snap frozen in liquid nitrogen and stored at -80°C. The uterine horn tissue varied in size over the time course studied so the tissue was cut into sections to allow more efficient processing, for analysis the mean of all the sections was taken per mouse (NP; 3 sections, 1DPP; 4 sections, 4DPP; 2 sections, 7DPP; 1 section). NP samples were produced and processed by Fiona Menzies and Abdul Khan (Obstetrics and Gynaecology, University of Glasgow) and re-analysed for this project.

2.3.4. *Isolation of mRNA.*

Uterine horn, detachment sites and cervix samples were taken for qRT-PCR analysis of leukocyte markers (Table 2.1 in blue), selected chemokines (Table 2.1 in green) and their receptors (Table 2.1 in yellow) and of the endogenous control GlycerAldehyde 3-Phosphate DeHydrogenase (GAPDH, Table 2.1 in orange). RNA was extracted in a laboratory fume hood using the following method. First, samples were homogenised in 1millilitre (ml) Trizol (Invitrogen) using a sterile plastic homogeniser tip (Camlab) and incubated for 5mins at room temperature to allow dissociation of nucleoprotein complexes. Next, each sample received 0.2ml chloroform and was shaken vigorously for 15s and incubated at room temperature for a further 3mins. Samples were then centrifuged at 13000 revolutions per minute (rpm) for 15mins at 4°C. The aqueous phase was removed using a pastette, added to 0.5ml isopropanol (VWR) to precipitate the RNA, and incubated at room temperature for 10mins. The samples were centrifuged for 10mins at 13000rpm at 4°C. The isopropanol was then decanted to leave a white pellet which was washed with 1ml of 75% ethanol. Samples were then stored at -80°C.

2.3.5. *Solubilisation of mRNA.*

Samples were centrifuged at 10000rpm for 5mins at 4°C and the ethanol wash was gently poured off and the pellet left to air dry. Water treated with DiEthylPyroCarbonate (DEPC) to inactivate RNases was added to each sample (15-30μl) depending on the size of the

pellet. Samples were then vortexed, quickly spun down and incubated at 65°C for 5mins on a heating block. This step was repeated and RNA was then kept on ice and quantified using a Nanodrop by placing 1µl of the sample on the platform and recording the concentration and checking for acceptable purity using 260nm/280nm ratio where 100% purity was 2.00.

2.3.6. *DNase treatment of mRNA.*

RNA was DNase treated with a DNA Free Kit (Ambion). RNA was combined with 10X DNase buffer, DNase I and an appropriate amount of DEPC treated water to a total volume of 25µl. Samples were then incubated at 37°C for 30mins in the OMN-E thermocycler. DNase Inactivation Reagent was then added to each tube, which was mixed and incubated for 2mins at room temperature. Tubes were then centrifuged at 13000rpm for 1min to pellet the DNase Inactivation Reagent and the supernatant transferred to a new tube. Samples were then stored at -80°C.

2.3.7. *Synthesis of cDNA from mRNA*

Synthesis of cDNA was achieved using a high capacity cDNA reverse transcription kit (ABI) with superasin (Ambion). Appropriate amounts of 10X Reverse Transcriptase (RT) Buffer, 25X deoxyNucleotideTriPhosphates (dNTPs), 10X Random Primers, Multiscribe reverse transcriptase, Superasin and Nuclease free water were mixed with DNase-treated RNA. A 'no Reverse Transcriptase' (no RT) control was also produced. Tubes were then briefly centrifuged and incubated for 10mins at 25°C, 120mins at 37°C and 5s at 85°C on a Polymerase Chain Reaction (PCR) express machine. Following this, cDNA was stored at -20°C.

2.3.8. *Quantitative PCR*

Taqman 96 well plates were set up with 10.25µl DEPC treated water, 12.5µl taqman 2X Master Mix (containing polymerase, primers and an internal reference dye, ABI), 1.25µl 20X target probe (ABI) and 1µl cDNA. Samples were run in duplicate and results expressed relative to expression of GAPDH from samples diluted 1/10 in DEPC treated water. Plate controls were used to ensure consistency between plates. Delta CT (threshold cycle) values were calculated by CT_{target}-$CT_{GAPDH,}$ finally results were expressed as $100x2^{\Delta CT}$ in order to express the difference in cycles to cross the threshold as a percentage.

2.4. Flow cytometry: 7 colours

2.4.1. *Mating of mice for flow cytometric analysis*

WT and CCR2 KO female mice were taken either as NP or set up with C57BL/6 WT males using a timed mating strategy. Mice were bred in-house and housed in individually ventilated cages. To improve the success rate of the timed matings, the amount of time mice were paired for was increased to between 2-4 days. To improve the accuracy of time of birth, given increased pairing time, a camera system was optimised.

2.4.2. *Set up of camera system to monitor labour*

When pregnancy was verified, mice were transferred to a filter top cage (Figure 2.1A) containing Vetbed fleece bedding (Henry Schein Animal Health), minimal nesting material consisting of autoclaved white paper and a red shelter (VetTech) (Figure 2.1B). Two C160IR (RF Concepts) cameras with night vision settings were set up to film the nesting material, where mice gave birth (Figure 2.1C). Footage was recorded on an Avermedia SEB5116H Digital Video Recorder (DVR, RF Concepts) and was able to be viewed remotely. The day (between the hours of 00.00-23.59) of first observation of a litter was taken to be 0DPP. Post-partum mice were taken at either 1DPP or 7DPP and were killed by exposure to a rising concentration of CO_2. Non-lactating mice were either mice sacrificed at 7DPP that had cannibalised their pups by 1DPP or had had their pups removed by 1DPP.

2.4.3. *Dissection of mice for flow cytometric analysis.*

Blood was withdrawn by cardiac puncture with a syringe flushed with EthyleneDiamineTetraAcetic acid, (EDTA, Sigma) and a combination of the spleen, PALN, femurs, thymus, uterine horn and cervix were dissected out. Care was taken to remove fat and connective tissue. In males, vas deferens/epididymis, prostate gland and penis were removed as well as blood, spleen and PALN.

2.4.4. *Optimisation of digestion protocol for reproductive tissues.*

Uterine horn, regardless of total number of detachment sites, and cervix were minced with scissors and.digested with shaking for 30mins at 37°C. Uterine horn and cervix received 7ml and 3ml respectively of either: (1) Hank's Balanced Salt Solution (HBSS)/Ca^{2+}/Mg^{2+} (Sigma) containing 0.028 Wunsch units (WU)/ml Liberase Blendzyme 3 (Roche) and 30 μg/ml DNase I (Roche) (2) HBSS/Ca^{2+}/Mg^{2+}, with 200 U/ml hyaluronidase (Sigma), 1 mg/ml collagenase type IV (Seromed), 0.2 mg/ml DNase I (2500 KunitzU/mg; Sigma) and 1 mg/ml Bovine Serum Albumin (BSA)/fractionV (Sigma) or for 30 minutes (mins) at

37°C with shaking. Digested tissues were then mashed using the plunger of a 2ml syringe to pass the cells through a cell strainer to obtain a single cell suspension in complete Roswell Park Memorial Institute medium (RPMI, Invitrogen) containing penicillin (100ug/ml, Invitrogen) and streptomycin (100µg/ml, Invitrogen), L-glutamine (2mM, Invitrogen) and heat inactivated foetal calf serum (10%, Invitrogen).

2.4.5. ***Digestion of reproductive tissues for flow cytometry.***

Uterine horn, cervix, penis, vas deferens/epididymis and prostate gland were minced with scissors in order to facilitate breakdown of the tissue and digested. Uterine horn and cervix received 7ml and 3ml respectively of HBSS/Ca^{2+}/Mg^{2+} containing 0.026 WU/ml Liberase Blendzyme medium thermolysin (Roche) and 50 µg/ml DNase I (Roche) for 40 mins at 37°C with shaking. Each uterine horn was treated identically, regardless of the size of tissue or the number of detachment sites. Tissues were then mashed using the plunger of a 2ml syringe to pass the cells through a cell strainer to obtain a single cell suspension in complete RPMI containing penicillin (100u/ml) and streptomycin (100µg/ml), L-glutamine (2mM) and heat inactivated foetal calf serum (10%). Cells were then centrifuged a 400xg for 5 mins at 4°C and resuspended in complete RPMI.

2.4.6. ***Preparation of thymus for flow cytometry.***

The thymus was minced with scissors and digested with 1mg/ml Collagenase D (Roche) in HBSS (Sigma) at 37°C with shaking for 45min. This preparation was then mashed through a cell strainer using the plunger of a 2ml syringe to obtain a single cell suspension in complete RPMI, washed twice and resuspended in complete RPMI.

2.4.7. ***Preparation of other tissues for flow cytometry.***

Femurs were cut at each end and flushed out with 1ml complete RPMI using a syringe. Spleens and PALN were minced with scissors. Spleen, PALN and BM samples were mashed using the plunger of a 2ml syringe to pass the cells through a cell strainer to obtain a single cell suspension in complete RPMI. Cells were then centrifuged at 400xg for 5min at 4°C. For spleen only, the pellet was disrupted and cells were treated with red blood cell lysis buffer (Sigma) for 1 minute. All samples were then washed twice with complete RPMI at 400xg for 5 mins at 4°C.

2.4.8. *Preparation of blood for flow cytometry.*

Blood cells were incubated 1:9 with 0.8% NH_4Cl with 0.1mM EDTA (Stem Cell Tech) on ice for 10 mins to lyse red blood cells and washed twice with complete RPMI.

2.4.9. *Chemokine uptake assay.*

Cells were counted using a haemacytometer, pipetted into polypropylene 96-well plates at 10^6 cells per well and then incubated with fluorescent chemokine (Almac Sciences, human CCL2-AF647) at a final concentration of 25nM in complete RPMI containing 4-(2-HydroxyEthyl)-1-PiperazineEthaneSulfonic acid (HEPES, 20mM) at 37°C for 65mins.

2.4.10. *Competition assay.*

As for 2.4.9 except where indicated, uterine and spleen cell suspensions were split; all receiving fluorescent CCL2-AF647 (Almac Sciences, 1/200 dilution, 25nM) and half receiving unlabelled murine CCL2 (Peprotech, 250nM) or unlabelled murine CCL22 (Peprotech, 250nM). In figures, competition is denoted by the abbreviation 'comp'.

2.4.11. *Staining for flow cytometry.*

Cells were washed and pre-treated with Fc-block (BD, CD16/32 mAb; 1/100 dilution) in Fluorescence Assisted Cell Sorting (FACS) buffer [PBS (Gibco) containing EDTA (Sigma), fetal calf serum, NaH_3 (Sigma)] for 15mins at 4°C and then washed with FACS buffer. Cells were stained for 15 mins at 4°C with antibodies (Tables 2.2-2.7) and washed twice with FACS buffer. Finally, cells were treated with 7-AminoActinomycin D (BD, 7-AAD, Viaprobe) for 10 mins to identify dead cells and passed through nitex into a FACS tube before being analysed.

2.4.12. *Preparation of beads for compensation.*

Anti-mouse Ig κ/negative control CompBeads (BD) were vortexed and one drop of each was added to 100µl FACS buffer in a FACS tube. Antibodies were diluted to their appropriate concentration and 20µl were added to the beads and incubated for 15-30mins at 4°C. FACS buffer (2ml) was then added and beads centrifuged at 400xg for 5min at 4°C. The FACS buffer was then removed, the beads vortexed and 400µl fresh FACS buffer added.

2.4.13. *Data acquisition.*

Data was acquired on a MACS Quant flow cytometer, the cell suspensions were analysed for their fluorescence, size and granularity. The fluorophores coupled to the antibodies which stain the cells are excited by the lasers in the machine and emit fluorescence at specific wavelengths which is measured by the cytometer. The combinations of fluorescence picked up by the channels allow the experimenter to discover the possible identity of the cell type as illustrated in Figure 2.2A.

Figure 2.2B shows how Forward SCatter (FSC) and Side SCatter (SSC) are measured by the flow cytometer. FSC is proportional to cell size. The detector in the cytometer is placed to collect light diffracted in the forward direction. SSC is a measure of cell granularity. The detector is placed at approx 90° and measures reflected light when there is a change in refractive index.

Fluorescence minus one (FMO) controls were used to define non-specific background staining, and cells were gated to eliminate this. This process is illustrated in Figure 2.2C. FMO controls contained all of the antibodies in a particular stain except the one being studied, this provided a background control that took into account the fluorescence spilling over from other channels. Fluorescence spillover is minimised using a process called compensation.

For example fluorophore A emits light which crosses over with the light emitted by fluorophore B, therefore light from fluorophore B spills over into the channel for fluorophore A and light from fluorophore A spills over into the channel for fluorophore B. This crossover has to be compensated for using single colours. So each fluorophore would be tested in every channel and the spillover subtracted from the channels other than its own.

The machine was compensated using beads stained with the same antibodies as the cell samples. For compensation, first stained beads were run and compensation was altered for each channel. This protocol was optimised to provide staining, high cell retrieval, and a high proportion of cell viability. Voltages for FSC and SSC were kept the same for every experiment, as changing the voltages would result in altered profiles making consistent gating more difficult. Then 7-AAD stained cells were run in the place of stained beads and the compensation changed when appropriate.

After all of the controls were run and compensation adjusted test samples were run. In order to display the number of cells retrieved from reproductive tissues, for these samples all of the stained cells were run through the machine. For peripheral tissues where accurate counts were more easily obtained, representative aliquots were run and total cell numbers calculated from this.

2.4.14. *Data analysis.*

All cells were gated sequentially for live cells first with a physical gate, then for 7-AAD negative cells, then for CD45+ cells to identify leukocytes. Results were analysed using FlowJo 7.5 software.

2.5. Luminex

2.5.1. *Sample preparation.*

Mice were mated as in 2.2.1 or 2.4.1. Mice were killed and blood was taken as in 2.4.3. Blood was centrifuged at 1500xg for 10 mins and plasma was removed and stored at -80°C until use. Luminex was performed in order to quantify CCL2 and CCL3 in mouse plasma, unfortunately due to kit availability two different kits were used to assay the samples: A base kit with CCL2 and CCL3 beads (Life Technologies) and a Milliplex xMAP kit (Millipore). Samples were run in duplicate or triplicate. Each group was split across both plates to reduce error in the quantification between the two plates, the results from each group were analysed by t-test. With each group the results were found to be consistent across both methods and quantification equally reliable.

2.5.2. *xMAP CCL2 + CCL3 quantification.*

All reagents were allowed to warm to room temperature before use. The filter plate was pre-wet by pipetting 200µl of wash buffer into each well, then sealed and incubated at room temperature for 10mins on a plate shaker. The wash buffer was then removed by vacuum manifold and the excess was blotted from the bottom of the plate. Standards and Controls (25µl) were then added and Assay Buffer was added to sample wells. Serum matrix (25µl) was also added to wells and 25µl of sample (diluted 1:1 with Assay Buffer) in the appropriate wells. Beads were sonicated and vortexed and 25µl were added to each well. The plate was then sealed and covered with an opaque plate cover and incubated for 2hrs at room temperature after which, fluid was removed by vacuum manifold. The plate was washed twice with 200µl and wash buffer removed by vacuum, with excess blotted

from the bottom. Detection Antibodies (25µl) were added to each well, the plate was then sealed, covered with an opaque plate cover and incubated on a plate shaker for 1hr at room temperature. Streptavidin-Phycoerythrin (25µl) was then added to each well containing detection antibodies. The plate was then sealed again, covered with an opaque plate cover and incubated at room temperature on a plate shaker for 30mins. All contents were then gently removed by vacuum. The plate was washed again twice with 200µl of Wash Buffer by vacuum filtration, with excess blotted from the bottom of the plate. Sheath fluid (150µl) was then added to wells and beads were resuspended on a plate shaker for 5mins. The plate was then read using a Luminex 200 machine.

2.5.3. *Life technologies CCL2 + CCL3 quantification.*

All reagents were allowed to warm to room temperature before use. The filter plate wells were pre-wet by adding 200µl of Working Wash Solution to each well. The plate was then incubated for 15-30s at room temperature. Liquid was then aspirated from the plate using the vacuum manifold, with excess being removed from the bottom by blotting with clean paper towels. Beads were vortexed then sonicated and 25µl of diluted beads were added to each well. Beads were then washed by adding 200µl of Working Wash Solution to the wells and allowed to soak for 15-30s. The filter plate was then placed on the vacuum manifold to aspirate the liquid. The bottom of the plate was blotted to remove the excess liquid and the wash step repeated. Incubation Buffer (50µl) was then added to each well. Standard dilutions (100µl) were added to wells designated for the standard curve. Assay Diluent (50µl) was then added to each of the sample wells, followed by 50µl of sample. The plate was then covered with an aluminium wrapped plate cover and incubated for 2hrs at room temperature on an orbital shaker to keep beads suspended during incubation. The liquid was then removed by vacuum manifold and excess blotted away. Working Wash Solution (200µl) was then added to the wells and the beads allowed to soak for 15-30s before being aspirated by vacuum manifold. This wash step was repeated and the bottom of the plate blotted thoroughly. Biotinylated Detector Antibody (100µl) was added to each well and incubated for 1hr at room temperature on an orbital shaker to keep beads suspended. After incubation liquid was aspirated, washed twice and the filter plate blotted. Streptavidin-RPE (100µl) was added to each well and the plate incubated for 30mins at room temperature on an orbital shaker to keep beads suspended throughout incubation. Liquid was then removed by vacuum manifold and blotted with paper towels. Working Wash Solution (200µl) was added to the wells, the beads allowed to soak for 15-30s, aspirated by vacuum manifold and the bottom of the plate blotted, beads were washed

three times in total. Working Wash Solution (100µl) was added to each well and the plate placed on an orbital shaker for 2-3mins. The plate was then read using a Luminex 200 machine. Chris Hansell assisted in running some of the samples (Institute of Infection, Immunity & Inflammation, University of Glasgow).

2.6. ELISA

2.6.1. *Quantification of prolactin.*

All reagents and samples were brought to room temperature. Samples were run in duplicate. Each standard (100µl) and diluted sample (100µl) was added to the appropriate wells. The plate was covered and incubated for 2.5hrs at room temperature with gentle shaking. After incubation the liquid was removed. Wash Solution (300µl) was added to each well and then discarded. This wash step was repeated 3 times and after the last wash the plate wash inverted and blotted with clean paper towels. Biotinylated Antibody (100µl) was added for each well and incubated for 1hr at room temperature with gentle shaking. The solution was then removed and the plate was washed 4 times with Wash Solution (300µl), inverted and blotted. Streptavidin solution (100µl) was added to the plate and incubated for 45mins at room temperature with gentle shaking. Following incubation the liquid was discarded, and the plate was washed 4 times with 300µl Wash Solution, inverted and blotted. Tetramethylbenzidine (TMB) One Step Substrate Reagent (100µl) was then added to each well and incubated for 30mins at room temperature in the dark with shaking. Finally 50µl Stop Solution was added to the wells. The plate was read immediately at 450nm on a Magellan Sunrise plate reader. Data was analysed using Magellan 6 software with the calibration curve provided by the protein standards.

2.7. Flow cytometry: four colours

2.7.1. *Dissection.*

Mice were killed as in section 2.4.3 and blood and spleen removed.

2.7.2. *Preparation of tissues for flow cytometry.*

The spleens was minced with scissors and digested with 1mg/ml Collagenase D (Roche) in HBSS at 37°C with shaking for 45min. They were then mashed using the plunger of a 2ml syringe to pass the cells through a cell strainer to obtain a single cell suspension in complete RPMI. Splenocytes were then centrifuged at 400xg for 5min at 4°C. The pellet

was disrupted and cells were treated with red blood cell lysis buffer for 1 minute, then washed twice with complete RPMI. Blood was prepared as in section 2.4.8.

2.7.3. *Chemokine uptake assay.*

Cells were counted using a haemocytometer and pipetted into polypropylene 96-well plates at 10^6 cells per well and then incubated with fluorescent chemokine (Almac Sciences, CCL2-AF647 1/200 dilution) in complete RPMI containing HEPES (20mM) at 37°C for 100mins.

2.7.4. *Staining for flow cytometry.*

Cells were stained as in section 2.4.11. with the antibodies listed in Table 2.8. Isotype controls were used to define non-specific background staining, and cells were gated to eliminate this. Finally, cells were treated with 7-AAD (BD) for 10 mins to identify dead cells during the subsequent analysis and passed through nitex before being analysed using a FACS Calibur flow cytometer. A protocol was optimised to provide good staining, high cell retrieval, and a high proportion of cell viability. Results were analysed using FlowJo 7.5 software.

2.8. Statistical analysis

2.8.1. *Programs.*

All statistical analysis was performed using GraphPad Prism 5. Outliers were excluded where appropriate using a Grubbs' test, with the equation:

$$G = \frac{(\text{outlier} - \text{mean})}{\text{standard deviation}}$$

If G is larger than the critical value based on the n number for significance at the level of p=0.05, then the outlier may be rejected. Outliers could also be rejected due to procedural errors in collecting the data or included depending on the distribution of the data. Critical values for n numbers up to 20 are found in Table 2.9.

Without outlier exclusion the variability of some samples made the entire data set impossible to analyse. Where the standard deviation of the group is large, outliers are unlikely to be detected, which means that the rest of the samples in the group must be fairly close together. With a small sample size excluding data points was not ideal,

however the judgement was made that the extreme nature of some data points was detracting from the analysis of the rest of the values. Figure 2.3 illustrates some examples of outlier exclusion.

2.8.2. *Data presentation.*

Where possible, normality was checked using the D'Agostino and Pearson omnibus normality test. For normally distributed data mean±Standard Error of the Mean (SEM) was the appropriate form of data expression (Figure 2.4A), whereas median + interquartile range (IQR) was used for skewed data (Figure 2.4B). In some cases data points were shown without descriptive error bars when this did not detract from data interpretation (Figure 2.4C).

2.8.3. *Comparing 2 groups.*

If the data passed the normality test and no pairing was seen, an unpaired Student's t-test was used to analyse the data (Figure 2.5A). If the data were normal but the variances were significantly different, a Welch's correction was used to account for this on the appropriate data sets (Figure 2.5B). If the data passed the normality test and pairing was seen, a paired Student's t-test was needed (Figure 2.5C).

2.8.4. *Comparing 3 or more groups.*

For statistical analysis on one level of normally distributed data with equal variances with no repeated measures normal data were analysed by one way ANalysis Of VAriance (ANOVA) with a Tukey post-hoc test, if a significant difference was detected (Figure 2.6A). To test non-normally distributed data or data with unequal variances with no repeated measures a Kruskall-Wallis test was used with a Dunn's post-hoc test if a p value of <0.05 was found (Figure 2.6B). Finally, for non-normally distributed data with repeated measures a Friedman test was utilised (Figure 2.6C). The exception came in chapter 6 (Figure 6.8), comparing reproductive tissues between sexes as matching was present between the tissues within each sex (uterus and cervix had matching, as did penis, vas deferens/epididymis and prostate) but these tissues were considered independent so comparison of all tissues between the sexes could be made.

2.8.5. *Comparing groups on more than one variable.*

To compare groups on more than one level a Two-way ANOVA was employed (Figure 2.7).

Table 2.1. *List of probes used for qRT-PCR*

Gene name	Gene Symbol	Applied Biosciences no.	NCBI sequence
GAPDH	*Gapdh*	4352932E	NM_008084.2
F4/80	*Emr1*	Mm00802529_m1	NM_010130.4
Major Basic Protein	*Prg2*	Mm00435905_m1	NM_008920.4
Neutrophil granule protein	*Ngp*	Mm01250218_m1	NM_008694.2
CD3 antigen	*Cd3*	Mm00438095_m1	NM_009850.2
CD19 antigen	*Cd19*	Mm00515420_m1	NM_009844.2
Forkhead box P3	*FoxP3*	Mm00475162_m1	NM_001199347.1 NM_001199348.1 NM_054039.2
CX3CL1	*Cx3cl1*	Mm00436454_m1	NM_009142.3
CCL2	*Ccl2*	Mm00441242_m1	NM_011333.2
CCL3	*Ccl3*	Mm99999057_m1	NM_011337.2
CCL7	*Ccl7*	Mm00443113_m1	NM_013654.3
CCL12	*Ccl12*	Mm01617100_m1	NM_011331.2
CX3CR1	*Cx3cr1*	Mm00438354_m1	NM_009987.3
CCR2	*Ccr2*	Mm00438270_m1	NM_009915.2

A

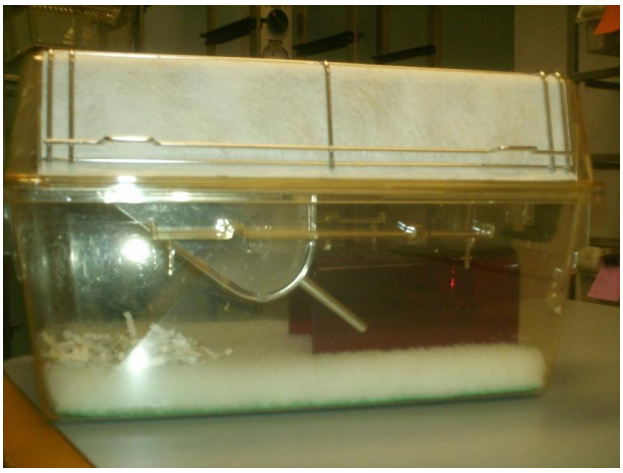

B

C

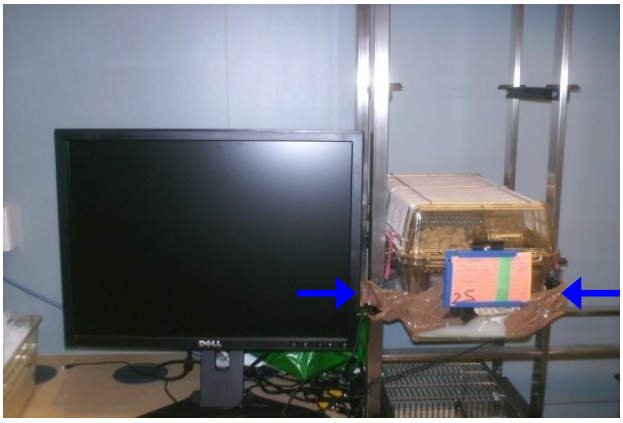

Figure 2.1. *Camera set up for accuracy in timing parturition*.

A) Filter top cage pictured from the side before addition of cameras. B) Cage from above showing minimal nesting material and red shelter. C) Cage with cameras attached to film nesting area (blue arrows indicate camera placement).

Table 2.2. *Antibodies used for detection of myeloid cells by flow cytometry*.

Target	Fluorophore	Supplier	Dilution
CD11b	V450	BD	1/200
Ly6C	FITC	BD	1/200
CD115	PE	eBiosciences	1/150
F4/80	PE-Cy7	eBiosciences	1/200
CD45	APC-Cy7	Biolegend	1/200

Table 2.3. *Antibodies used for detection of CD3+ cells by flow cytometry*.

Target	Fluorophore	Supplier	Dilution
CD3	VioBlue	BD	1/150
CD25	FITC	BD	1/150
CD8	PE	eBiosciences	1/200
CD4	PE-Cy7	eBiosciences	1/200
CD45	APC-Cy7	Biolegend	1/200

Table 2.4. *Antibodies used for detection of CD3+ DN cells and NK cells by flow cytometry*.

Target	Fluorophore	Supplier	Dilution
CD3	VioBlue	BD	1/150
CD25	FITC	BD	1/150
CD8	PE	eBiosciences	1/200
CD4	PE	eBiosciences	1/200
NK1.1	PE-Cy7	BD	1/200
CD45	APC-Cy7	Biolegend	1/200

Table 2.5. *Antibodies used for characterisation of thymocytes by flow cytometry*.

Target	Fluorophore	Supplier	Dilution
CD44	V450	BD	1/200
CD25	FITC	FITC	1/150
CD8	PE	eBiosciences	1/200
CD4	PE-Cy7	eBiosciences	1/200
CD45	APC-Cy7	Biolegend	1/200

Table 2.6. *Antibodies used for characterisation of CD3+ DN cells.*

Target	Fluorophore	Supplier	Dilution
CD3	VioBlue	BD	1/150
CD25	FITC	BD	1/150
TCR-β	FITC	BD	1/200
CXCR5	FITC	BD	1/150
CTLA-4	PE	eBiosciences	1/150
CD8	PE/PE-Cy7	eBiosciences	1/200
CD4	PE/PE-Cy7	eBiosciences	1/200
NK1.1	PE-Cy7	BD	1/200
B220	AF647	eBiosciences	1/200
TCR-γδ	APC	eBiosciences	1/200
PD-1	APC	eBiosciences	1/100
CD45	APC-Cy7	Biolegend	1/200

Table 2.7. *Antibodies used for detection of markers on CD3+DN cells by flow cytometry.*

Target	Fluorophore	Supplier	Dilution
CD3	VioBlue	BD	1/150
TCR-β	FITC	BD	1/200
CD8	PE	eBiosciences	1/200
CD4	PE	eBiosciences	1/200
NK1.1	PE-Cy7	BD	1/200
TCR-γδ	APC	eBiosciences	1/200
CD45	APC-Cy7	Biolegend	1/200

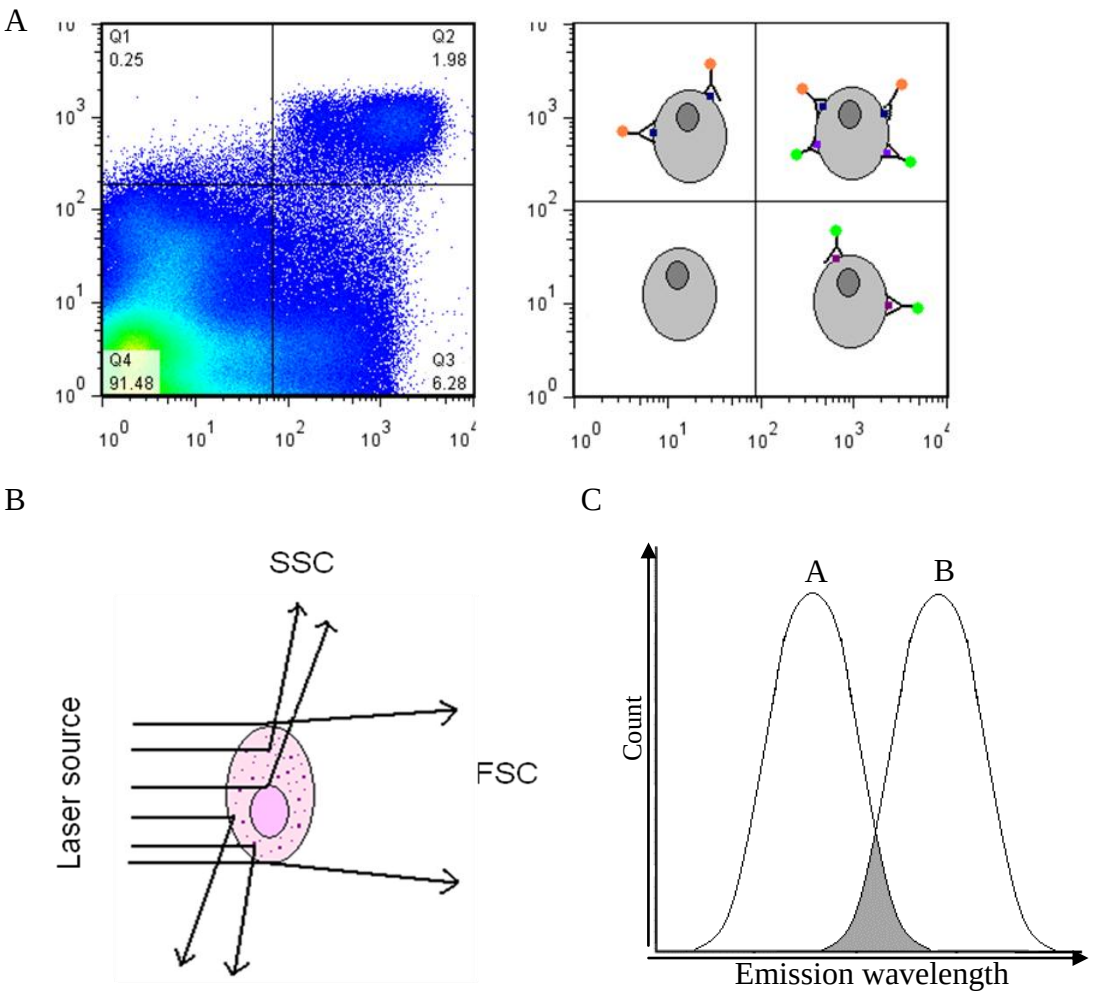

Figure 2.2. *Setting up parameters for flow cytometry.*

A) Gating of cell populations using fluorescent antibodies. B) Determination of cell size and granularity using FSC and SSC. Diffraction of the laser allows measurement of FSC and refraction detects cell granules. C) Histogram to highlight how compensation removes spillover fluorescence from antibody signal.

Table 2.8. *Antibodies used to detect myeloid cells using four-colour flow cytometry*.

Target	Fluorophore	Supplier	Dilution
Ly6C	FITC	BD	1/200
CD11b	PE	BD	1/200
Isotype IgM	FITC	BD	1/200
Isotype IgG2b	PE	BD	1/200

Table 2.9. Critical values for n numbers up to 20 with significance of p=0.05.

N number	Critcal value of G
3	1.15
4	1.48
5	1.71
6	1.89
7	2.02
8	2.13
9	2.21
10	2.29
11	2.34
12	2.41
13	2.46
14	2.51
15	2.55
16	2.59
17	2.62
18	2.65
19	2.68
20	2.71

A

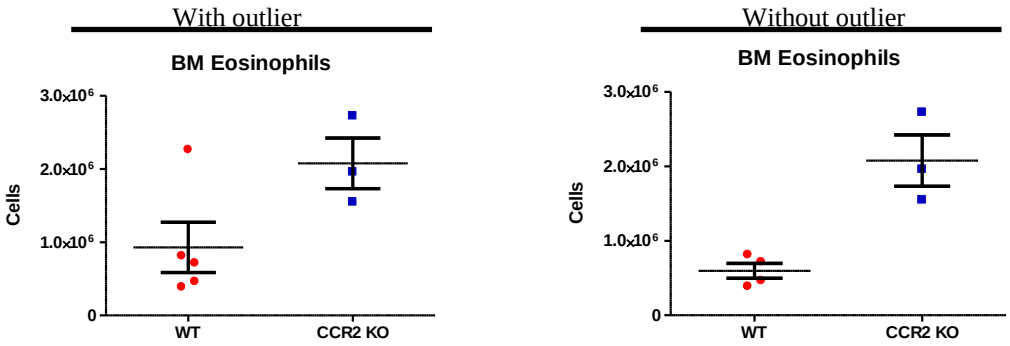

B

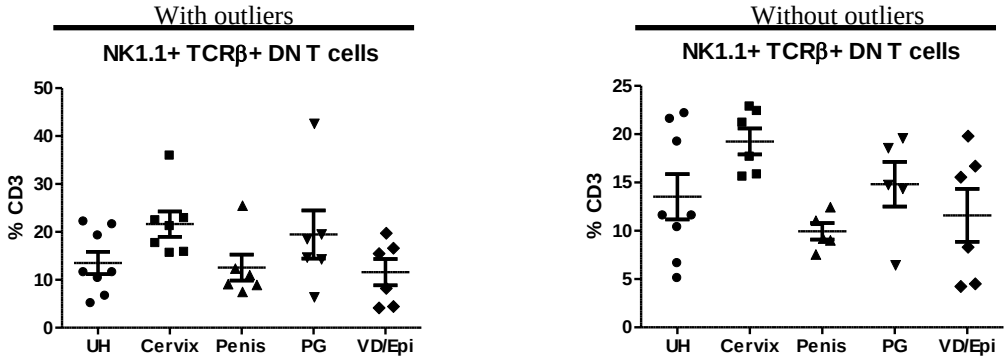

C

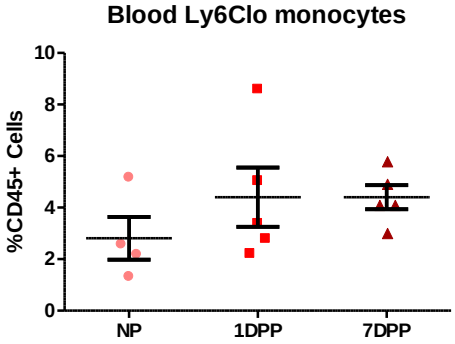

Figure 2.3. *Outliers were excluded using the Grubb's test*.

A) A set of data from Figure 3.21 with and without a detected outlier. B) A set of data from Figure 6.8 with and without 3 detected outliers. C) Graph showing an example where no outliers were detected from Figure 3.9.

A

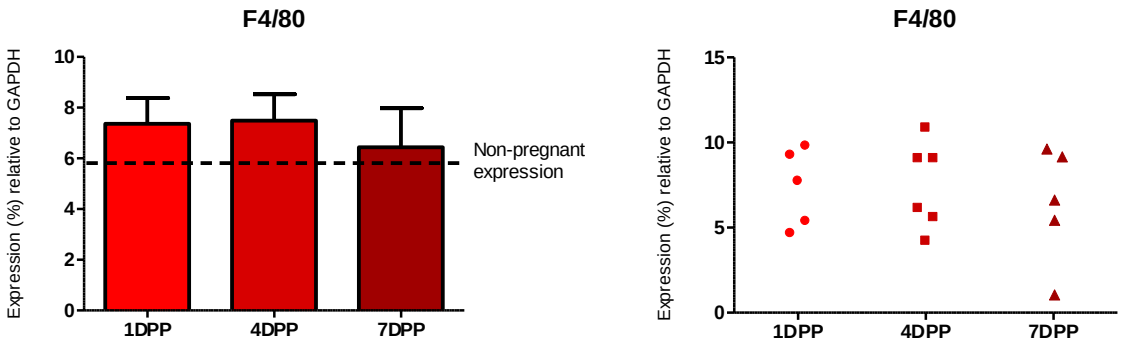

B

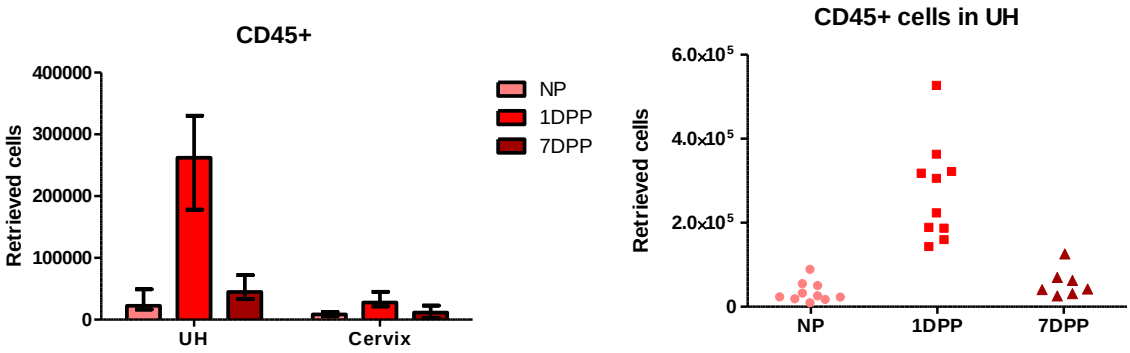

C

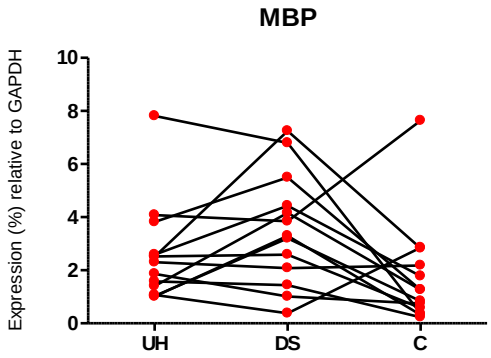

Figure 2.4. *Examples of data presentation*.

A) An example graph from Figure 3.4 showing mean±SEM (left) and the data points alone (right). B) An example graph from Figure 3.7 showing median + IQR (left) and the data points alone (right). C) An example graph from Figure 3.2 showing linked data points alone.

A

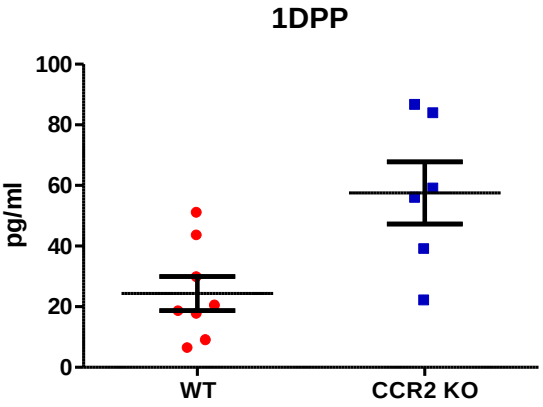

t test	
Table Analyzed	1DPP
Column A	WT
vs	vs
Column B	CCR2 KO
Unpaired t test	
P value	0.0102
P value summary	*
Are means signif. different? (P < 0.05)	Yes
One- or two-tailed P value?	Two-tailed
t, df	t=3.044 df=12
How big is the difference?	
Mean ± SEM of column A	24.35 ± 5.603 N=8
Mean ± SEM of column B	57.54 ± 10.22 N=6
Difference between means	-33.19 ± 10.91
95% confidence interval	-56.95 to -9.429
R square	0.4357
F test to compare variances	
F,DFn, Dfd	2.496, 5, 7
P value	0.2648
P value summary	ns
Are variances significantly different?	No

B

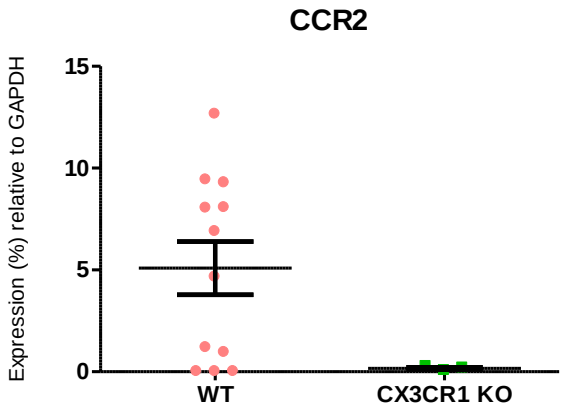

t test	
Table Analyzed	CCR2
Column A	WT
vs	vs
Column B	CX3CR1 KO
Unpaired t test with Welch's correction	
P value	0.0031
P value summary	**
Are means signif. different? (P < 0.05)	Yes
One- or two-tailed P value?	Two-tailed
Welch-corrected t, df	t=3.776 df=11
How big is the difference?	
Mean ± SEM of column A	5.089 ± 1.303 N=12
Mean ± SEM of column B	0.1632 ± 0.05951 N=3
Difference between means	4.926 ± 1.305
95% confidence interval	2.054 to 7.797
R square	0.5645
F test to compare variances	
F,DFn, Dfd	1918, 11, 2
P value	0.0010
P value summary	**
Are variances significantly different?	Yes

C

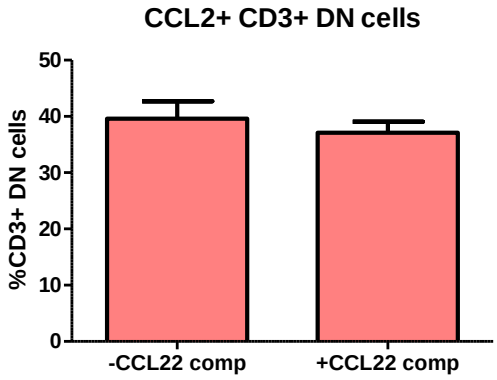

t test	
Table Analyzed	CCL22 comp
Column A	-CCL22 comp
vs	vs
Column B	+CCL22 comp
Paired t test	
P value	0.1250
P value summary	ns
Are means signif. different? (P < 0.05)	No
One- or two-tailed P value?	Two-tailed
t, df	t=2.113 df=3
Number of pairs	4
How big is the difference?	
Mean of differences	2.520
95% confidence interval	-1.275 to 6.315
R square	0.5981
How effective was the pairing?	
Correlation coefficient (r)	0.9790
P Value (one tailed)	0.0105
P value summary	*
Was the pairing significantly effective?	Yes

Figure 2.5. *Different techniques for comparing two groups.*

A) An unpaired Student's t-test, as used in Figure 3.22 B) An unpaired Student's t-test with Welch's correction for unequal variances, as used in Figure 3.1. C) A paired Student's t-test, as used in Figure 4.13.

A

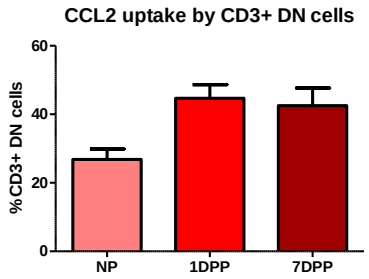

1way ANOVA					
1	Table Analyzed	Blood			
2					
3	One-way analysis of variance				
4	P value	0.0212			
5	P value summary	*			
6	Are means signif. different? (P < 0.05)	Yes			
7	Number of groups	3			
8	F	4.755			
9	R square	0.3336			
10					
11	Bartlett's test for equal variances				
12	Bartlett's statistic (corrected)	1.691			
13	P value	0.4294			
14	P value summary	ns			
15	Do the variances differ signif. (P < 0.05)	No			
16					
17	ANOVA Table	SS	df	MS	
18	Treatment (between columns)	1263	2	631.5	
19	Residual (within columns)	2523	19	132.8	
20	Total	3787	21		
21					
22	Tukey's Multiple Comparison Test	Mean Diff.	q	Significant? P < 0.05?	Summary	95% CI of diff
23	NP vs 1DPP	-17.84	4.153	Yes	*	-33.27 to -2.403
24	NP vs 7DPP	-15.67	3.457	No	ns	-31.96 to 0.6181
25	1DPP vs 7DPP	2.163	0.5268	No	ns	-12.59 to 16.92

B

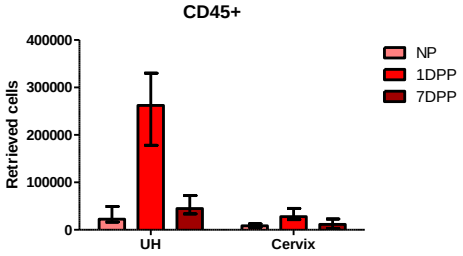

1way ANOVA				
1	Table Analyzed	UH		
2				
3	Kruskal-Wallis test			
4	P value	< 0.0001		
5	Exact or approximate P value?	Gaussian Approximation		
6	P value summary	***		
7	Do the medians vary signif. (P < 0.05)	Yes		
8	Number of groups	3		
9	Kruskal-Wallis statistic	19.76		
10				
11	Dunn's Multiple Comparison Test	Difference in rank sum	Significant? P < 0.05?	Summary
12	NP vs 1DPP	-15.50	Yes	***
13	NP vs 7DPP	-4.857	No	ns
14	1DPP vs 7DPP	10.64	Yes	*

C

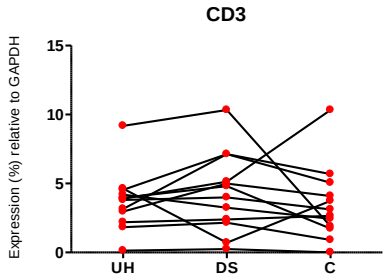

1way ANOVA				
1	Table Analyzed	CD3		
2				
3	Friedman test			
4	P value	0.0458		
5	Exact or approximate P value?	Gaussian Approximation		
6	P value summary	*		
7	Are means signif. different? (P < 0.05)	Yes		
8	Number of groups	3		
9	Friedman statistic	6.167		
10				
11	Dunn's Multiple Comparison Test	Difference in rank sum	Significant? P < 0.05?	Summary
12	UH vs DS	-10.00	No	ns
13	UH vs C	1.000	No	ns
14	DS vs C	11.00	No	ns

Figure 2.6. *Statistical tests used for 3 or more groups.*

A) An example of a one-way ANOVA with a Tukey post-hoc test as in Figure 4.4. B) An example of a Kruskall-Wallis test with a Dunn's post-hoc test as in Figure 3.7. C) An example of a Friedman repeated measures test with a Dunn's post-hoc test as in Figure 3.1.

A

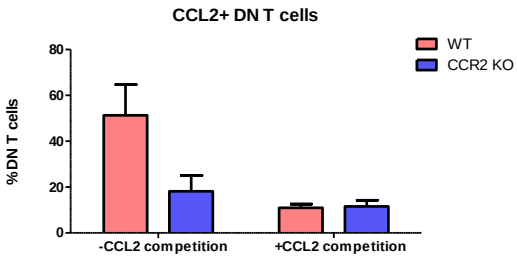

2way ANOVA
Tabular results

1	Table Analyzed	Competition			
2					
3	Two-way RM ANOVA	Matching by cols			
4					
5	Source of Variation	% of total variation	P value		
6	Interaction	18.79	0.0423		
7	CCL2 competition	36.32	0.0131		
8	Strain	17.44	0.0979		
9	Subjects (matching)	21.1300	0.2977		
10					
11	Source of Variation	P value summary	Significant?		
12	Interaction	*	Yes		
13	CCL2 competition	*	Yes		
14	Strain	ns	No		
15	Subjects (matching)	ns	No		
16					
17	Source of Variation	Df	Sum-of-squares	Mean square	F
18	Interaction	1	975.2	975.2	7.343
19	CCL2 competition	1	1885	1885	14.19
20	Strain	1	905.2	905.2	4.127
21	Subjects (matching)	5	1097	219.3	1.652
22	Residual	5	664.1	132.8	
23					
24	Number of missing values	0			

Figure 2.7. *An example of a two-way ANOVA.*

An example of a two-way ANOVA with matching as seen in Figure 4.13.

Chapter 3: Myeloid cells in post-partum murine reproductive tissues

Introduction

The leukocyte composition of reproductive tissues in the post-partum period remains largely unknown. As discussed in section 1.3.5 of the Introduction, some data exist suggesting that macrophages and other myeloid cell types may be responsible for remodelling reproductive tissues after birth (Brandon, 1994, Timmons and Mahendroo, 2006, Mackler et al., 2000, Mackler et al., 1999, Stewart and Mitchell, 1992). Brandon (1994) suggests that macrophages are present throughtout the uterine tissue during the post-partum period, but are found in high numbers in the detachment wound. It has also been suggested that though macrophages (identified by Mac-1/CD11b) are present, they are not responsible for scavenging debris (Stewart and Mitchell, 1992). Macrophages appear to be increased in the 1DPP uterine horn in both the endometrium and myometrium, compared to NP animals (Mackler et al., 1999, Mackler et al., 2000), which when taken together with the idea that macrophages decline during the post-partum period (Brandon, 1994), suggests that the early post-partum period may be the time when macrophages are most abundant. There is much that could be done to improve on these data, for example using markers other than CD11b and F4/80, investigating several post-partum time-points and different methods such as flow cytometry. Focussing on the post-partum period and not labour might reveal more about the resolution of inflammation after parturition. Initial investigations examined the uteri of ex-breeders, but then a timed mating strategy was set up and techniques such as qRT-PCR and flow cytometry were used to profile the cells in reproductive and peripheral tissues in the early post-partum period (1DPP-7DPP). Due to the focus of the literature on monocytes and macrophages in tissue remodelling, these cells were the principal focus of study in this chapter, but other myeloid cells were also investigated. As discussed in chapter 1, in the absence of inflammation, $Ly6C^{lo}$ $CX3CR1^{hi}$ monocytes patrol the blood vessels and have been shown to exhibit CX3CR1 dependent recruitment to non-inflamed tissues (Geissmann et al., 2003, Gordon and Taylor, 2005, Sunderkotter et al., 2004), whilst during inflammation $Ly6C^{hi}$ monocytes migrate to the inflamed tissue using CCR2 and become resident macrophages involved in the resolution of inflammation (Gordon and Taylor, 2005, Geissmann et al., 2003, Sunderkotter et al., 2004). Therefore CCR2 was of considerable interest and could be the key to understanding monocyte migration to healing reproductive tissue, and the development of macrophages therein. Thus, the hypothesis that CCR2 regulates the recruitment of monocytes and macrophages into post-partum reproductive tissues was tested. The expression of chemokines that bind this receptor was examined in the post-partum uterine horn, and CCR2 expression on leukocytes in reproductive tissues and elsewhere was explored. In

addition, the impact of CCR2 deletion on leukocyte abundance in post-partum reproductive tissues was examined by comparing CCR2 KO mice to WT counterparts.

Results

3.1. *Expression of the gene encoding the macrophage marker F4/80 in detachment sites is not affected by deletion of chemokine receptors that drive monocyte migration.*

The leukocyte components participating in post-partum remodelling have been a subject of debate. Detachment sites that develop in the post-partum uterus at the site of placental attachment have been reported to be likely sites of remodelling and have displayed accumulations of macrophages (Brandon, 1994). These detachment sites form in a line along the tissue, as seen in the photograph of a 7DPP uterine horn (Figure 3.1A). Since CCR2 and CX3CR1 control monocyte recruitment to tissue, the presence of detachment sites, and the macrophages they contain, might be compromised in mice lacking these chemokine receptors. Female ex-breeders lacking these receptors, and WT counterparts, were available. These animals had been used to maintain colonies at our animal facility so I initially undertook a speculative experiment to explore if these chemokine receptors affected detachment sites. From gross examination, it was clear that deletion of CCR2 had no effect on the size or number of detachment sites following a single pregnancy (Figure 3.1B), showing that CCR2 was not required for the formation of these structures. This was also the case in CX3CR1$^{gfp/gfp}$ mice (data not shown). These mice have had both copies of CX3CR1 replaced with GFP, although this reporter gene was not used in this study. The detachment sites in both strains expressed equivalent amounts of the macrophage marker F4/80, suggesting that deletion of neither receptor affected macrophage accumulation in these structures. Surprisingly, expression of CCR2 was significantly different between WT and CX3CR1$^{gfp/gfp}$ mice (Figure 3.1E), suggesting that CXCR1$^{gfp/gfp}$ mice may have had a deficit in CCR2-expressing cells in the detachment sites of these mice. However, due to developments in other areas of the work, this observation was not pursued further.

3.2. *No specific enrichment in expression of genes encoding leukocyte markers in detachment sites.*

Next, to attempt to address the question of which leukocyte subsets were present in detachment sites, the expression of genes encoding leukocyte markers was measured in different areas of the reproductive tract of WT female ex-breeders. To do this effectively, ex-breeders that had had multiple litters were chosen as the source of the tissues because by the end of their reproductive life they would have accumulated many detachment sites and so sufficient quantities of RNA could be extracted. Gene expression in these samples was compared to cervix, and to uterine horn tissue that had detachment sites removed. The markers chosen were F4/80 (expressed predominantly by monocytes and macrophages),

CD19 (B cells), CD3 (T cells), FoxP3 (Tregs), Major Basic Protein (MBP, eosinophils) and Neutrophil Granule Protein (NGP, neutrophils).

F4/80, CD19, CD3, FoxP3 and NGP had been used regularly in-house before and in the literature to identify specific leukocyte subsets (eBioscience). A postdoctoral scientist in the group (Fiona Menzies) had previously validated GAPDH as an appropriate endogenous control for murine reproductive tissues by (F Menzies, personal communication). The three distinct tissue samples did display an overall significant difference in CD3 ($p=0.046$, Figure 3.2C) and NGP ($p=0.044$, Figure 3.2F) but all post-tests were not significant. Gene expression of F4/80 (Figure 3.2A), CD19 ($p=0.063$, Figure 3.2B), FoxP3 (Figure 3.2D) and MBP ($p=0.058$, Figure 3.2E) was not significantly different between groups. Thus, expression of these markers was not enhanced in detachment sites suggesting that these structures were not enriched for leukocyte subsets expressing these genes.

3.3. *Alteration of the structure of the uterine horn in the post-partum period.*

These initial investigations into detachment sites were disappointing. Ex-breeder tissue had been used due to its availability and the presumed remodelling present in the tissue, particularly around detachment sites. However, these ex-breeders were a heterogeneous population as they varied in age, number of litters, and time between litters. Thus, attention turned to reproductive tissues shortly after delivery of the first litter when they are likely to be undergoing more dynamic and extensive remodelling. First, uterine horn tissue from aged ex-breeders was analysed alongside uterine horn tissue from 1DPP and 7DPP mice following their first pregnancy to attempt to reveal any differences in the architecture of the uterine horn over this time period. Sections of tissue were stained with haematoxylin and eosin, and examined by light microscopy. Tissue harvested at 1DPP had a more stretched appearance than at 7DPP. At 1DPP the architecture of the uterine horn was clearly different from later time points with the myometrium and endometrium being less well defined (Figure 3.3A). The structure of both the myometrium and the endometrium appeared to be more defined at 7DPP (Figure 3.3B), compared to 1DPP (Figure 3.3A). This is consistent with the tissue changes that take place with decidualisation, where cells increase in size and the water content of the tissue increases. Uterine tissue from ex-breeder mice at the end of their reproductive life appeared far more cellular than 1DPP, and more closely resembled 7DPP tissue (Figure 3.3C). These images added some weight to the idea that substantial changes occur in uterine tissue between 1DPP and 7DPP.

3.4. *The expression of genes encoding CCR2-binding chemokines varies in the uterine horn over the post-partum period.*

RNA was extracted from uterine tissue 1, 4 and 7 days after delivery of the pups and used to examine expression of chemokines and markers of myeloid cells. Any changes in chemokine expression in the uterine horn in the post-partum period could potentially drive leukocyte recruitment. Expression of the genes encoding CCR2-binding chemokines (CCL2, CCL3, CCL7 and CCL12) was explored in the uterine horn. A NP level was added for reference obtained from a study from our group (Menzies et al., 2012) and this was verified using plate controls. Representative samples from that study were run alongside current samples in order to show that the results were comparable between plates. Though not previously thought of as a CCR2-binding chemokine, work in our group had demonstrated that CCL3 blocks CCL2 internalisation mediated by CCR2, suggesting that it is a CCR2 ligand (Hansell et al., 2011b). CCL8 was not included in this analysis. Human CCL8 binds human CCR2, but mouse CCL8 binds mouse CCR8 and not mouse CCR2 (Islam et al., 2011).

Interestingly, CCL2, CCL7 and CCL12 were highest at 1DPP, whereas CCL3 was highest at 4DPP (Figure 3.4). CCL2 expression in the uterine horn was substantially increased at 1DPP, compared with 4DPP and 7DPP (Figure 3.4A). CCL3 expression was significantly increased at 4DPP compared with 7DPP (Figure 3.4B). CCL7 expression was at its peak at 1DPP, at a roughly NP level before dropping at 4DPP and 7DPP (Figure 3.4C). CCL12 expression in the uterine horn was also at its highest at 1DPP compared to 4DPP and 7DPP (Figure 3.4D). These data convincingly showed that there were considerable changes in the expression of CCR2-binding chemokines in the post-partum period in the uterine horn consistent with a role in mediating leukocyte recruitment, particularly at 1DPP.

3.5. *Expression of selected genes encoding myeloid cell markers during the post-partum period.*

Next, the project explored whether qRT-PCR could be used to gauge leukocyte recruitment to the uterus in the post-partum period. However, expression of genes encoding monocyte and macrophage markers did not change significantly over the post-partum period (F4/80 Figure 3.5A, CX3CR1 Figure 3.5B). Although CCR2 expression did not change over the post-partum period (Figure 3.5C) it did appear to be elevated compared to NP expression. Other myeloid cell markers were also tested. MBP expression had increased significantly at 4DPP and 7DPP compared to 1DPP (Figure 3.5D), while NGP, a marker for neutrophils

did not vary over the post-partum period (Figure 3.5E). These results suggested relatively minor changes in leukocyte recruitment during the post-partum period. However, the qRT-PCR approach may not provide an accurate picture of changes in leukocyte abundance in the uterus. Thus, flow cytometry was explored as a more accurate, detailed and quantitative way of analysing and phenotyping leukocytes in the uterine horn and cervix.

3.6. *Optimising digestion techniques for liberating leukocytes from the uterine horn*.

Flow cytometry is a highly accurate method of simultaneously measuring multiple cell surface markers using fluorescently conjugated antibodies. Co-expression of cell surface markers helps provide definitive identification of a variety of cell types, and cells can be analysed according to their size, known as Forward SCatter (FSC), and their granularity, known as Side SCatter (SSC). A dead cell exclusion dye 7-AminoActinomycin D (7-AAD or Viaprobe) is included so that dead cells can be gated out of the subsequent analysis as these cells often bind non-specifically to antibodies. One of the challenges facing any attempt to perform flow cytometry of solid tissues, is the generation of a single cell suspension using tissue digestion that liberates cells without causing too much cell death or cleaving epitopes recognised by the antibodies (Abuzakouk et al., 1996). Two digest methods were tested. Digest 1 was adapted from (Collins et al., 2009), where it had been used to successfully liberate DCs from uterine tissue. It contained Liberase Blendzyme 3 and DNase I. Digest 2, adapted from Kammerer et al (Kammerer et al., 2003), had been used to isolate DCs from the decidua and contained hyaluronidase, collagenase type IV, and DNase I and buffer containing BSA/fraction V. Further details are provided in the Materials and Methods section.

Several pilot experiments were carried out: Figure 3.6 shows a typical test. A simple stain using fluorescently labelled antibodies against Ly6C and CD11b was used to identify myeloid cells. Cells were gated as shown (Figure 3.6A). Gates were drawn using spleen as a template due to its clear staining. Staining was not always consistent between tissues: as splenocytes stained the most clearly they were used to set gates. This meant that gates could be drawn reproducibly between subjects and that gating was identical for all tissues. Gates for each antibody used were drawn using fluorescent minus one (FMO) controls, which contained all of the fluorescent antibodies and 7-AAD except the channel being gated in order to provide a negative control for that marker to gate out background fluorescence. Although more cells were retrieved from the uterine tissue treated with digest 2, a higher number of Ly6C+/CD11b+ cells were consistently identified from uterine tissue

treated with digest 1, making it a more effective digest at liberating myeloid cells of potential interest (Figure 3.6B-C). Although digest 2 appeared more effective for cervix, higher quality uterine horn results were pursued as this formed the main focus of the project.

3.7. *Experimental design for the flow cytometric analysis of myeloid cells (CD45+CD11b+) cells in post-partum and NP mice.*

The sections above aimed to find a method to accurately analyse myeloid cell abundance in the uterine horn in the early post-partum period. qRT-PCR was used to analyse expression of chemokines and myeloid cell markers between 1DPP-7DPP, and although this was useful for assessing chemokine expression, it was seen as far inferior to flow cytometry in analysing the presence of specific leukocyte subsets. A digestion protocol was devised in order to analyse leukocytes by flow cytometry from the uterine horn and the cervix. Although digest 1 was chosen as the method to take forward, it had to be adapted because the type of Liberase originally used was not available. Instead of Liberase Blendzyme 3, an equivalent product was used, namely Liberase Blendzyme TM. One observation from these early experiments was that spleen had a much more defined pattern of antibody staining which was distinct from that seen in the uterine horn and cervix, indicating that different cell types were present or perhaps that tissue digestion and disruption had some effect on the cells that were liberated. With no other method of tissue dissociation available, this potential confounding factor had to be accepted. Spleen staining was used to define gates in these and future experiments because too few cells were retrieved from reproductive tissues to allow for staining controls and because placing gates on more robustly defined populations reduced the variability in this practice between experiments. Nonetheless, despite the technical difficulties associated with preparing solid tissues for analysis by flow cytometry, it was felt that the application of this technique to the analysis of cells in reproductive tissues was a major advance and was subsequently used to provide detailed insights into the specific cell types present during the post-partum period.

Thus, armed with an optimised digestion protocol using DNase I and Liberase Blendzyme TM, I sought to analyse myeloid cells in the uterine horn and cervix in NP mice, and at 1DPP and 7DPP. Monocytes and macrophages were an important cellular focus of the work, so antibodies against Ly6C, F4/80 and CD115 were included along with anti-CD45 and anti-CD11b in the cell staining cocktail. Peripheral tissues were also examined in order to determine both local and systemic responses during the post-partum period. There

was also the opportunity to examine expression of CCR2 by flow cytometry, which was of particular interest. In our lab it had been discovered that it was difficult to reliably detect CCR2 using available anti-CCR2 antibodies, and an alternative method using fluorescently conjugated CCL2-AF647 had been developed. Internalisation of this chemokine by leukocytes gives an indication of their expression of CCR2, which can be verified by using cells from CCR2 KO mice as controls. Thus, to investigate CCR2 activity in the monocyte and macrophage populations in reproductive and peripheral tissues, single cell suspensions of these tissues were incubated with CCL2-AF647 before being labelled with fluorescently labelled antibodies. Cells were then assessed by flow cytometry. NP, 1DPP and 7DPP samples from WT mice were analysed in the first instance, and the data then compared to that generated from similar experiments performed on cohorts of CCR2 KO mice. Below the findings of this study are presented, first broadly focussing on myeloid cells (CD45+CD11b+), then specifically on monocytes and macrophages, and finally the results relating to other CD11b+ myeloid cells are presented.

3.8. *Large increase in myeloid cells in the uterine horn at 1DPP.*

To facilitate the analysis of myeloid cells (CD45+CD11b+) in reproductive tissues, gates were first drawn using spleen samples to remove small cell fragments and cells on the extremes of each of the physical characteristics (Figure 3.7A). Dead cells were then excluded as 7-AAD+ and then CD45+ cells gated to identify the leukocytes in the preparation (Figure 3.7A). Subsequent gates were drawn from these CD45+ cells to identify specific leukocyte cell types. Reproductive tissue samples were analysed using these same gates. Using this approach, the first clear difference was that at 1DPP at least 11-fold more CD45+ cells were retrieved from the uterine horn compared with a NP uterine horn (Figure 3.7B). There was also a significant increase in the number of leukocytes retrieved from the cervix at 1DPP (Figure 3.7B). The number of CD45+ cells significantly decreased at 7DPP compared with 1DPP in both uterine horn and cervix (Figure 3.7B). From this CD45+ population a gate was drawn to identify CD11b+ myeloid cells (Figure 3.7A). Most of the CD45+ cells in the uterine horn and cervix in NP, 1DPP and 7DPP expressed CD11b (Figure 3.7C). In the uterine horn 9-fold more CD11b+ cells were retrieved at 1DPP than from NP mice and at 7DPP this was back down to approximately NP levels. No significant change in CD11b+ cell number was seen in the cervix between the time points studied.

The striking increase in cells retrieved from the uterine horn, and to a lesser extent the cervix, at 1DPP is most likely linked to a certain degree to an increase in the overall size of the tissue. Although some of this increase may be due to local leukocyte proliferation, many of these cells have presumably been recruited from the blood at some point over the course of pregnancy up to 1DPP, and these cells are lost as the uterine horn contracts to 7DPP. The constituents of the myeloid compartment in the uterine horn and cervix changed between NP, 1DPP and 7DPP. The data relating to a specific cell type are presented as the total number of cells retrieved, but also as a percentage of the entire CD45+ population because this gives an indication of whether that cell type becomes over- or under-represented in the myeloid compartment of reproductive tissues during the post-partum period. Lymphoid tissues and blood were also examined in a similar way to compare local and systemic changes during the post-partum period.

3.9. *Monocytes and macrophages are abundant at 1DPP in the uterine horn.*

Following selection for cells expressing CD45 and CD11b, SSC was plotted against anti-Ly6C staining. An inverted L shape gate was drawn for monocytes and macrophages to select Ly6C+SSC$^{lo\text{-}intermediate\ (int)}$ cells (Figure 3.8). This gate was designed using the spleen sample to capture most of the cells that could be described as monocytes or macrophages and avoided cells that were too granular to be monocyte/macrophages, especially Ly6C^{int}SSC^{int} cells that were likely to be neutrophils (see below). All the cells in this inverted L-shaped gate expressed F4/80, which is found on monocytes, and which is more highly expressed by tissue macrophages. Staining of blood was used to set the gate for macrophages. Macrophages are absent from blood, so applying this gate to reproductive tissues would identify those cells that are F4/80^{hi}. Thus, for this study, resident macrophages were defined as CD45+CD11b+SSC$^{lo\text{-}int}$F4/80^{hi}. Ly6C^{lo} monocytes were CD45+CD11b+SSC$^{lo\text{-}int}$F4/80^{lo}Ly6C^{lo} and Ly6C^{hi} monocytes defined as CD45+CD11b+SSC$^{lo\text{-}int}$F4/80^{lo}Ly6C^{hi}. Representative images for these gates in uterine horn tissue are included in Figure 3.8A. Although discrete populations are not apparent in the Ly6C/SSC plot of uterine horn, the majority of cells in the inverted L-shaped gate expressed F4/80, consistent with a monocyte/macrophage identity. Clearly these cells only represented a small proportion of CD11b+ cells in the uterine horn, and the same was true in the cervix.

Mirroring the increase in CD11b+ cells in 1DPP uterine horn, substantially greater numbers of Ly6C^{lo} monocytes, Ly6C^{hi} monocytes and macrophages were retrieved from

1DPP uterine horn than from NP or 7DPP samples (Figure 3.9, right). Interestingly, when presented as a percentage of CD45+ cells, only Ly6C^{lo} monocytes showed evidence of being specifically enriched in the myeloid cell compartment of 1DPP uterine horn compared to NP animals, although there was a marked reduction in the representation of all three cell types in the CD45+ population by 7DPP when compared to 1DPP (Figure 3.9, left). In the cervix, although significantly more Ly6C^{hi} monocytes were retrieved from 1DPP tissue compared with 7DPP, no other statistically significant differences were seen.

Monocytes and macrophages were also enumerated in lymphoid tissues (spleen, BM, PALN) and blood taken at the same time as the uterine horn and cervix. This enabled investigation into whether the striking increase in these cells in the 1DPP uterine horn was mirrored by changes in their abundance elsewhere in the mouse (i.e. were these local or systemic changes?) or whether it led to their depletion from other tissues. The staining profiles of spleen, blood, BM, PALN gated for resident macrophages, Ly6C^{lo} monocytes, Ly6C^{hi} monocytes (Figure 3.9A, gates [2], [3] and [4] respectively) differ slightly: gates were drawn as in Figure 3.8 to ensure consistency between tissues. In short, very few differences were found in these tissues between samples from NP, 1DPP or 7DPP mice (Figure 3.9), although there was an increase in the number of Ly6C^{lo} monocytes in the BM at 1DPP compared to NP, and an increase in the percentage of BM CD45+ cells classified as Ly6C^{hi} monocytes at 1DPP vs NP. Thus, despite the substantial increase in monocytes and macrophages in the 1DPP uterine horn, no major changes in these cells were seen elsewhere in mice at this time.

Collectively, these results clearly demonstrate that monocytes and macrophages are abundant in the uterine wall at 1DPP, far exceeding the numbers found in NP uterine horn, and that these cells have gone from the uterine horn by 6 days later (7DPP). This appears to have minimal impact on these populations of cells elsewhere in the mouse. In addition, the data suggest that Ly6C^{lo} monocytes are increased as a proportion of leukocytes present in 1DPP uterine horn.

3.10. *CCL2-AF647 uptake is at its lowest at 7DPP in reproductive tissues*.

Ligands for CCR2 are good candidates for directing the migration of monocytes into reproductive tissues in the post-partum period, and these cells have the potential to generate tissue macrophages. To do this, CCR2 needs to be expressed on the migrating cells. To investigate CCR2 expression in monocyte and macrophage populations in

reproductive and peripheral tissues, single cell suspensions of these tissues had been incubated with CCL2-AF647 before being labelled with fluorescently labelled antibodies. Thus, I was able to explore whether these cells showed any evidence of CCR2 expression. Figure 3.10A shows typical fluorescence histograms for monocytes and macrophages in the spleen and uterine horn. Compared to splenocytes that were incubated in the absence of CCL2-AF647, Ly6C^{hi} monocytes and resident macrophages in spleen and uterine horn showed high levels of CCL2-AF647 uptake, indicative of expression of CCL2 receptors (Figure 3.10A). In contrast, Ly6C^{lo} monocytes displayed relatively little fluorescence.

CCL2-AF647 uptake by monocytes and macrophages was analysed in a range of tissues from NP, 1DPP and 7DPP mice (Figure 3.10C-D). A subset of Ly6C^{lo} monocytes internalised CCL2-AF647 in the post-partum period in all samples, but, compared with NP animals, at 1DPP and 7DPP fewer uterine horn Ly6C^{lo} monocytes were CCL2-AF647+, and total fluorescence was lower in these cells at these time points (Figure 3.10B). In the cervix, fluorescence of Ly6C^{lo} monocytes was also reduced at 7DPP compared with NP mice (Figure 3.10B, right). In contrast, essentially all Ly6C^{hi} monocytes were CCL2-AF647+ in spleen, blood and BM. In uterine horn and cervix, the large majority of Ly6C^{hi} monocytes were also CCL2-AF647+. However, the proportion that were CCL2-AF647+ was significantly reduced at 7DPP, compared with NP animals (Figure 3.10C, left), and in the uterine horn, the total CCL2-AF647 fluorescence of Ly6C^{hi} monocytes was reduced at 1DPP and 7DPP, compared with NP uterine horn (Figure 3.10C, right). A large proportion of resident macrophages internalised CCL2-AF647+ and this increased in the cervix at 1DPP, compared with NP and 7DPP animals (Figure 3.10D, left). In the uterine horn, although the proportion of macrophages that were CCL2-AF647+ was unchanged between groups, the total fluorescence in these cells was lower at both post-partum time points than NP animals (Figure 3.10D, right). However, it was notable that cells in the macrophage gate consistently contained cells that had the CCL2-AF647 uptake profile of Ly6C^{hi} monocytes so it is possible that the resident macrophage gate was contaminated with a fraction of Ly6C^{hi} monocytes, although the inclusion of additional markers would be required to verify this.

These data suggest expression of CCR2 by monocytes present in reproductive tissues and elsewhere. This is not unexpected, but it is possible that CCL2-AF647 is internalised into these cells by the scavenger receptor D6, which also binds CCL2, or by mechanisms that do not involve chemokine receptors. This could be examined by including unlabelled

chemokines, such as CCL22, to specifically compete away any D6-mediated CCL2-AF647 uptake activity (Hansell et al., 2011b). Alternatively, CCR2 KO animals could be used as a control to confirm that CCL2-AF647 uptake by WT cells was CCR2 dependent. Data relating to this are shown in section 3.11.

3.11. *CCR2 deletion dramatically reduces CCL2-AF647 internalisation in monocyte and macrophage populations in the reproductive tract and peripheral tissues at 1DPP.*

Determining CCR2 dependence was key to understanding the significance of CCL2-AF647 internalisation. Thus, data from WT mice 1DPP from Figure 3.10 were compared to data generated from 1DPP CCR2 KO mice in order to determine how CCR2 affected CCL2-AF647 internalisation by these cells in reproductive tissues. As with the WT animals, the post-partum animals examined had just completed their first pregnancy. Ly6C^{lo} monocytes, internalised a fairly low amount of CCL2-AF647 in WT mice at 1DPP, but still exhibited a considerable reduction in proportion and fluorescence of CCL2-AF647+ Ly6C^{lo} monocytes in CCR2 KO uterine horn and cervix (Figure 3.11A-B). In the absence of CCR2, and in both the uterine horn and the cervix, Ly6C^{hi} monocytes showed an even more dramatic reduction in the percentage of cells that were classified as CCL2-AF647+ and in the extent of CCL2-AF647 uptake (Figure 3.11C). Similarly, significant reductions were seen in the CCL2-AF647+ fraction of resident macrophages, in both reproductive tissues (Figure 3.11D, left). A similar analysis was also undertaken on 1DPP peripheral tissues from WT and CCR2 KO mice, which clearly demonstrated that CCL2-AF647 uptake by Ly6C^{lo} monocytes, Ly6C^{hi} monocytes, and macrophages was largely dependent on CCR2 (Figure 3.12). These data firmly support the idea that monocytes and macrophages in post-partum reproductive tissues and elsewhere express CCR2, and that this CCR2 is capable of binding CCL2.

3.12. *Increases in the proportions and numbers of granulocytes in reproductive tissues over the post-partum period.*

Similar analyses to those performed above were then undertaken on other CD11b+ cell populations in the reproductive tissues, lymphoid tissues and blood from NP, 1DPP and 7DPP animals. The swell in numbers of myeloid cells in the uterine horn, and the elevated expression of the eosinophil marker MBP during the post-partum period (Figure 3.5, Figure 3.7), suggested that the size of granulocyte populations could vary between NP, 1DPP and 7DPP. Although the antibody panel used in the flow cytometry had been primarily designed to identify monocytes and macrophages, it also allowed eosinophils to

be identified as CD45+CD11b+Ly6C^{lo}SSC^{hi}CD115- cells (Rose et al., 2012) and neutrophils as those cells with a CD45+CD11b+Ly6C^{int}SSC^{int}CD115- phenotype (Ribeiro-Gomes et al., 2012) (Figure 3.13A-B). Lack of CD115 expression by these cells allowed monocyte contamination to be reduced (Rose et al., 2012). If more flow cytometry channels had been available, then more specific markers for these subsets could have been included, although it was considered that the cell populations defined above would primarily contain eosinophils and neutrophils. However, the presence of small populations of other contaminating cells cannot be excluded.

Eosinophils and neutrophils were far more abundant than monocytes and macrophages in the uterus and cervix at all time points (Figure 3.13C-D). The number of eosinophils and neutrophils retrieved from the uterine horn increased significantly in the uterine horn at 1DPP compared with the other groups, and, although the proportion of CD45+ cells defined as eosinophils was not different between the three groups, neutrophils represented a far greater fraction of the CD45+ population at 1DPP compared to NP or 7DPP (Figure 3.13C-D). There were also fewer total neutrophils retrieved from the cervix at 7DPP, compared with 1DPP (Figure 3.13D, right), and eosinophils comprised a greater fraction of the CD45+ population in the cervix at 7DPP compared with NP.

Data from spleen, blood, BM and PALN were also analysed using the same gates (Figure 3.14) with cell definitions remaining constant in each tissue. Eosinophils were far less abundant in these tissues than in the uterus and cervix. Compared to NP and 1DPP, a significantly higher proportion of CD45+ cells in the spleen at 7DPP were classified as eosinophils, which was also mirrored by the absolute numbers (Figure 3.14C). Eosinophils were significantly higher at 7DPP, compared with NP in the PALN (Figure 3.14C). The level of neutrophils in the spleen and PALN remained constant in terms of proportion and numbers over the post-partum period (Figure 3.14D), although a greater proportion of CD45+ BM cells were neutrophils at 1DPP compared to NP.

Thus, eosinophils and neutrophils are abundant in the uterine wall at 1DPP, far exceeding the numbers found in NP uterine horn. These cells have disappeared from the uterine horn by 6 days later (7DPP). Eosinophil numbers also increase in the spleen during the post-partum period. In addition, the data show that neutrophils represent a greater proportion of the leukocytes present in 1DPP uterine horn compared to NP and 7DPP.

3.13. *Low level CCR2-dependent internalisation of CCL2-AF647 by some granulocyte populations*.

Granulocytes were also tested for their ability to internalise CCL2-AF647. Although eosinophils and neutrophils are generally not thought to express CCR2, it has been seen in some inflammatory or other specific situations (Borchers et al., 2002, Hartl et al., 2008, Johnston et al., 1999, Reichel et al., 2006, Souto et al., 2011, Yang et al., 2012). In the spleen, eosinophils showed some CCL2-AF647 uptake whereas this activity in neutrophils was almost superimposable on the negative control. However, in the uterine horn neutrophils and eosinophils had similar fluorescence profiles with clear evidence that these cells could internalise CCL2-AF647 (Figure 3.15A). Very few differences in granulocyte CCL2-AF647 internalisation were found over the post-partum period, although the proportion of CCL2-AF647+ eosinophils in the cervix was significantly lower at 7DPP compared with NP and 1DPP cervix (Figure 3.15B, left). The CCR2 dependence of CCL2-AF647 uptake was analysed at 1DPP by comparing WT data from Figure 3.15 with CCR2 KO data. In the absence of CCR2, fewer neutrophils in reproductive tissues were capable of internalising CCL2-AF647, and fewer cervical eosinophils were classified as CCL2-AF647+ (Figure 3.16B), indicating that subsets of these cells expressed CCR2 in WT reproductive tissues.

The CCR2 dependence of CCL2-AF647 uptake by granulocytes in lymphoid tissues and blood was also analysed at 1DPP by comparing WT data from Figure 3.15 with CCR2 KO data. The data were extremely variable between individual mice, and choosing an image representative of all the individuals was difficult. Moreover, and particularly for eosinophils, it was difficult to make a judgement about whether uptake was CCR2 dependent in peripheral tissues and perhaps the analysis of higher numbers of mice is required before a firm conclusion could be drawn. Nonetheless, in the WT BM a significantly higher percentage of eosinophils were CCL2-AF647+ in WT mice compared with CCR2 KOs (Figure 3.17A-B), suggesting that a small population of eosinophils express CCR2 in WT animals. In addition, greater numbers of neutrophils in the PALN of WT mice appeared to internalise CCL2-AF647 than those neutrophils present in the PALN of CCR2 KO mice (Figure 3.17A and C).

3.12. *CCR2 deficient mice have far fewer myeloid cells in their uteri than WT mice at 1DPP.*

The data so far demonstrate that: (i) the expression of CCR2-binding chemokines peaks at 1DPP in the uterine horn; (ii) eosinophils and neutrophils are abundant in the 1DPP uterine horn, and a subset of these cells appear to express CCR2; and (iii) there is a large increase in CCR2-expressing monocyte/macrophage cells in the 1DPP uterine horn. These observations led naturally to the question of whether CCR2 was required for these cells to be present in the uterus and cervix. Thus, NP, 1DPP and 7DPP uterine horn and cervix from CCR2 KO mice were investigated and the proportion of CD45+ cells defined as monocytes, macrophages, eosinophils and neutrophils was calculated, along with the total number of each cell type retrieved. These data were then compared to the results generated from WT mice that have been presented above.

The first striking observation was that far fewer CD45+ cells were retrieved from the uterine horn of 1DPP CCR2 KO mice compared with WT counterparts. This was less apparent in NP uterine samples and was not seen with 7DPP uterine horn, or the cervix at any time-point. Individual myeloid subsets were then compared in detail in these tissues.

3.12.1. *Monocytes and macrophages.*

In NP uterine horn, there were no significant differences in the number of $Ly6C^{lo}$ monocytes, $Ly6C^{hi}$ monocytes, or macrophages retrieved between strains, although these cells represented a greater proportion of the CD45+ cells (Figure 3.18). At 1DPP, all these cell types were retrieved in far greater numbers from WT mice compared to CCR2 KO, but only $Ly6C^{hi}$ monocytes represented a greater proportion of the CD45+ cells present at this time. No effect of CCR2 deletion was seen at 7DPP, and there was no significant impact of CCR2 deletion on $Ly6C^{lo}$ monocytes or macrophages in the cervix. However, $Ly6C^{hi}$ monocytes were more common in the NP cervix of WT mice than CCR2 KOs, both in terms of the number retrieved and the proportion of CD45+ cells that they represented (Figure 3.18D). Moreover, compared with CCR2 KO, greater numbers of $Ly6C^{hi}$ monocytes were retrieved from WT cervix 1DPP (Figure 3.18D, right) but this was only of borderline significant when they were examined as a proportion of CD45+ cells ($p=0.052$, Figure 3.18D, left). The number of macrophages in the cervix also appeared to be reduced in CCR2 KO mice, but this failed to achieve statistical significance.

Peripheral blood and lymphoid tissues had also been harvested from 1DPP CCR2 KO mice and these samples were analysed for the various myeloid subsets that had been investigated in the reproductive tissues. WT 1DPP data from Figure 3.9 were compared to the 1DPP CCR2 KO data to determine how CCR2 affected the abundance of these cells in peripheral tissues. As expected (Serbina and Pamer, 2006), Ly6C^{hi} monocytes were reduced in the spleen and blood of CCR2 KO mice (Figure 3.19). The proportion of CD45+ leukocytes in the spleen that were Ly6C^{hi} monocytes was over three times in WT mice than in those lacking CCR2, and, even more dramatically, in WT mice the total number of Ly6C^{hi} monocytes in the spleen at 1DPP was over 6 times that of the CCR2 KO mice (Figure 3.19B). In the blood of WT mice, the frequency of Ly6C^{hi} monocytes amongst CD45+ cells was over seven fold higher than that seen in CCR2 KOs (Figure 3.19B). Notably, however, from my data it seems that these cells were not retained in the BM of CCR2 KO mice where they are reported to get stalled in these animals (Serbina and Pamer, 2006). In addition to these changes in Ly6C^{hi} monocytes, the WT spleen contained nearly four times the number of Ly6C^{lo} monocytes as spleens from CCR2 KO mice (Figure 3.19A). Results for resident macrophages were variable due to the fact that relatively few were found using the method employed, although the number of resident macrophages was higher in the WT spleen, compared with the CCR2 KO (Figure 3.19C, right).

3.12.2. *Eosinophils and neutrophils.*

The proportion of CD45+ cells in the uterine horn identified as eosinophils or neutrophils was similar between WT and CCR2 KO (Figure 3.20A, left). However, at 1DPP, greater numbers of eosinophils and neutrophils were retrieved from WT uteri than from equivalent samples of CCR2 KO tissue (Figure 3.20A, right), and more neutrophils could be isolated from the WT cervix at this time compared to CCR2 KO.

CCR2 deficiency had no impact on eosinophil or neutrophil abundance in spleen, blood or PALN. However, CCR2 deficiency was associated with an increased number of eosinophils in the BM (Figure 3.21A). The proportion of neutrophils also increased in CCR2 KO BM, compared with WT (Figure 3.21B). This was surprising, and indicated that CCR2 activity might negatively regulate populations of granulocytes in the BM. Previous studies that have reported that Ly6C^{hi} monocytes are retained in CCR2 KO BM (Serbina and Pamer, 2006), did not show data for other BM cell types and it is possible that the impact of CCR2 deficiency on eosinophils is specific to animals at 1DPP.

Thus, CCR2 deficiency was associated with substantial and systemic changes in the distribution and abundance of monocytes, macrophages and other myeloid cells in NP mice and during the post-partum period.

3.13. *Plasma CCL2 levels are higher in CCR2 KO than WT mice.*

During the preparation of blood for flow cytometry, plasma had been isolated and stored. Previous reports have shown a role for CCR2 in scavenging CCL2 (Volpe et al., 2012) and CCR2 KOs have been shown to exhibit higher levels of CCL2 in plasma (Cardona et al., 2008). Thus, Luminex technology was used to measure chemokine protein in plasma harvested from NP mice, and from mice 1, 4 or 7 days post-partum (Figures 3.22 and 3.23). CCL2 and CCL3 were investigated because (i) uterine expression of the genes encoding these chemokines was higher during the post-partum period than in house measurements of NP samples (Figure 3.4), and (ii) they were compatible to be measured at the same time with the kits available. In the NP mice, and consistent with the previous reports (Cardona et al., 2008), CCR2 KO mice had roughly double the amount of CCL2 protein in their plasma, compared to WT mice (Figure 3.22A). A significant difference was also seen at 1DPP (Figure 3.22B) and at 4DPP (Figure 3.22C), showing this phenotype was still seen during the early post-partum period. At 7DPP however there was no difference between the WT and CCR2 KO levels of CCL2 in plasma (Figure 3.22D). In contrast to CCL2, systemic CCL3 levels were not significantly different between WT and CCR2 KO mice at any of the time points (Figure 3.23A-D). Levels of the chemokine also appeared not to fluctuate in the plasma over the post-partum period in contrast to what was seen for mRNA gene expression in the uterine horn (Figure 3.4).

3.14. Summary

In this chapter I have described my investigations of myeloid cell populations in reproductive and peripheral tissues using techniques such as qRT-PCR and flow cytometry. The main hypotheses were that monocyte and macrophage subsets would be recruited to post-partum reproductive tissue and that this infiltration would be reliant on CCR2. The main findings of this chapter were:

- Myeloid cells are abundant at 1DPP and there is a clear increase in cells retrieved from the uterine horn at this time. The retrieved number of cells falls to NP levels at 7DPP. Enlarged populations of monocytes and neutrophils are responsible for the increase in myeloid cells in this tissue at 1DPP.

- Secondary lymphoid tissues and blood did not display many changes between NP, 1DPP and 7DPP populations of myeloid cells, except Ly6C^{hi} monocytes and neutrophils, which were increased in BM at 1DPP compared to NP mice.
- At 1DPP, all myeloid cell populations studied contained at least some cells that expressed CCR2 in either uterine horn or cervix. In peripheral tissues monocytes and macrophages isolated at 1DPP expressed CCR2, but CCR2 expression by granulocytes at this time-point was influenced by the tissue studied. As expected, Ly6C^{hi} inflammatory monocytes demonstrated the strongest CCR2 activity, compared to the other myeloid subsets, in all tissues studied. At 1DPP, far fewer myeloid cells were retrieved from the uterine horn of CCR2 KO mice, compared to WT controls. Ly6C^{hi} monocytes were particularly strongly affected by CCR2 deletion. There was also an absence of Ly6C^{hi} monocytes in the blood and spleen of CCR2 KO mice, whereas granulocytes were increased in the BM when CCR2 was deleted.
- In NP mice and in the early post-partum period, CCL2 was increased in the plasma of CCR2 KO mice, compared to WT mice. However, at 7DPP circulating CCL2 was equivalent between WT and CCR2 KOs. No CCR2 dependent difference was seen in levels of circulating CCL3.

These data support the idea of an inflammatory infiltrate containing myeloid cells in the uterine horn in the early post-partum period and highlight the role of CCR2 in this process. These observations are discussed in greater depth in the Discussion in Chapter 7. Chapter 4 continues this work by describing T cell populations in reproductive and peripheral tissues in the post-partum period and further tests CCR2 activity on these cells.

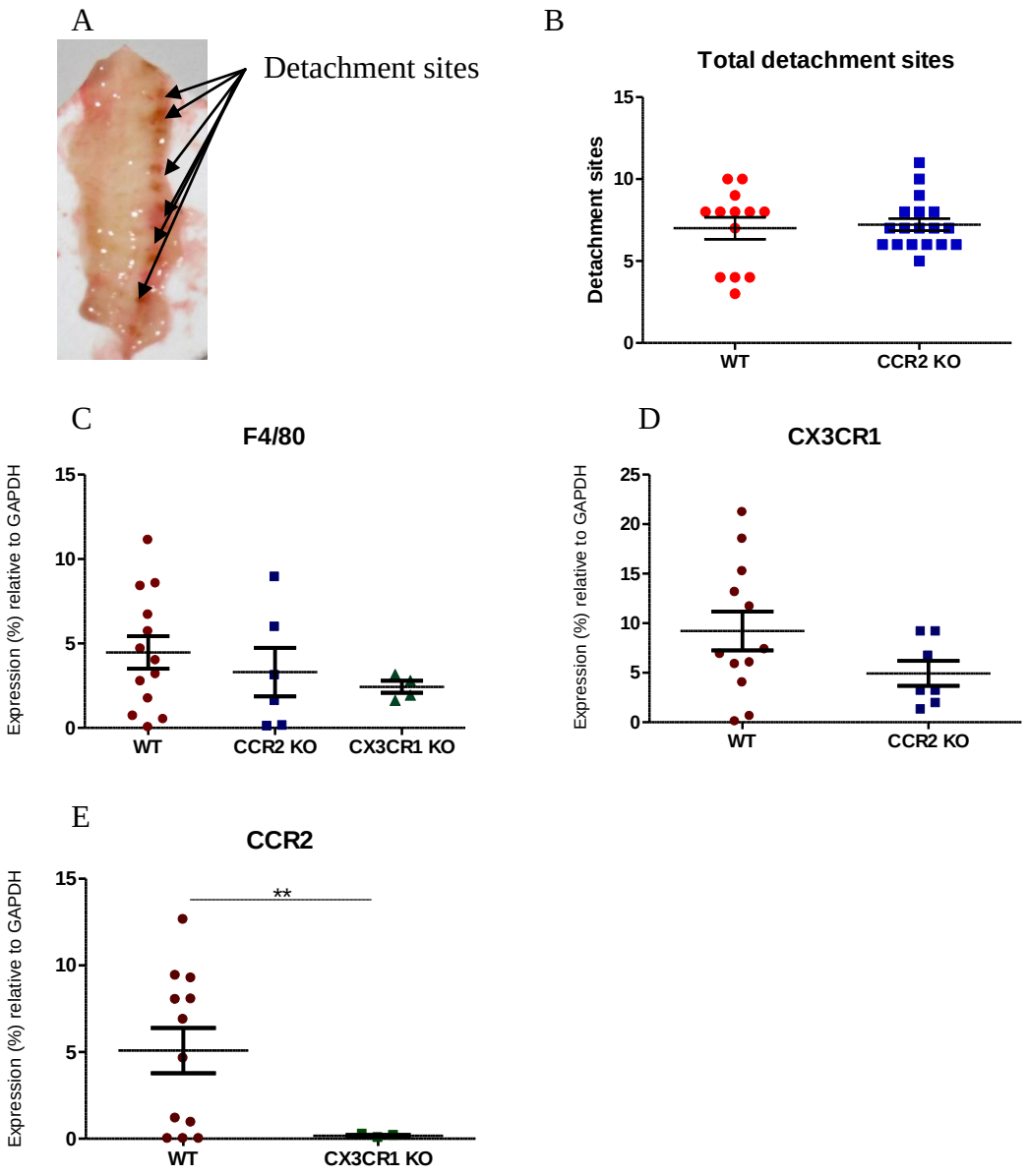

Figure 3.1. *Expression of the gene encoding the macrophage marker F4/80 in detachment sites is not affected by deletion of chemokine receptors that drive monocyte migration.* Investigation into expression of monocyte and macrophage markers in WT, CCR2 KO and CX3CR1 detachment sites in the Uterine Horn (UH) of ex-breeder mice. Expression was calculated as $100x2^{\Delta CT}$ where $\Delta CT=CT^{target}-CT^{GAPDH}$ to establish target expression as a percentage of expression of the endogenous control. (A) Representative photograph of UH demonstrating detachment sites lining up in the tissue. (B) Number of detachment sites on the tissue per mouse following one pregnancy in WT (n=13) and CCR2 KO (n=18) females. (C)-(E) Expression of markers in detachment sites of WT (n=12-13), CCR2 (n=6-7) and CX3CR1 (n=4); F4/80 (C), CX3CR1 (D) and CCR2 (E). Data were presented as mean ± SEM. Statistical analysis was carried out by unpaired Student's t-test or one-way ANOVA as appropriate, **p<0.01.

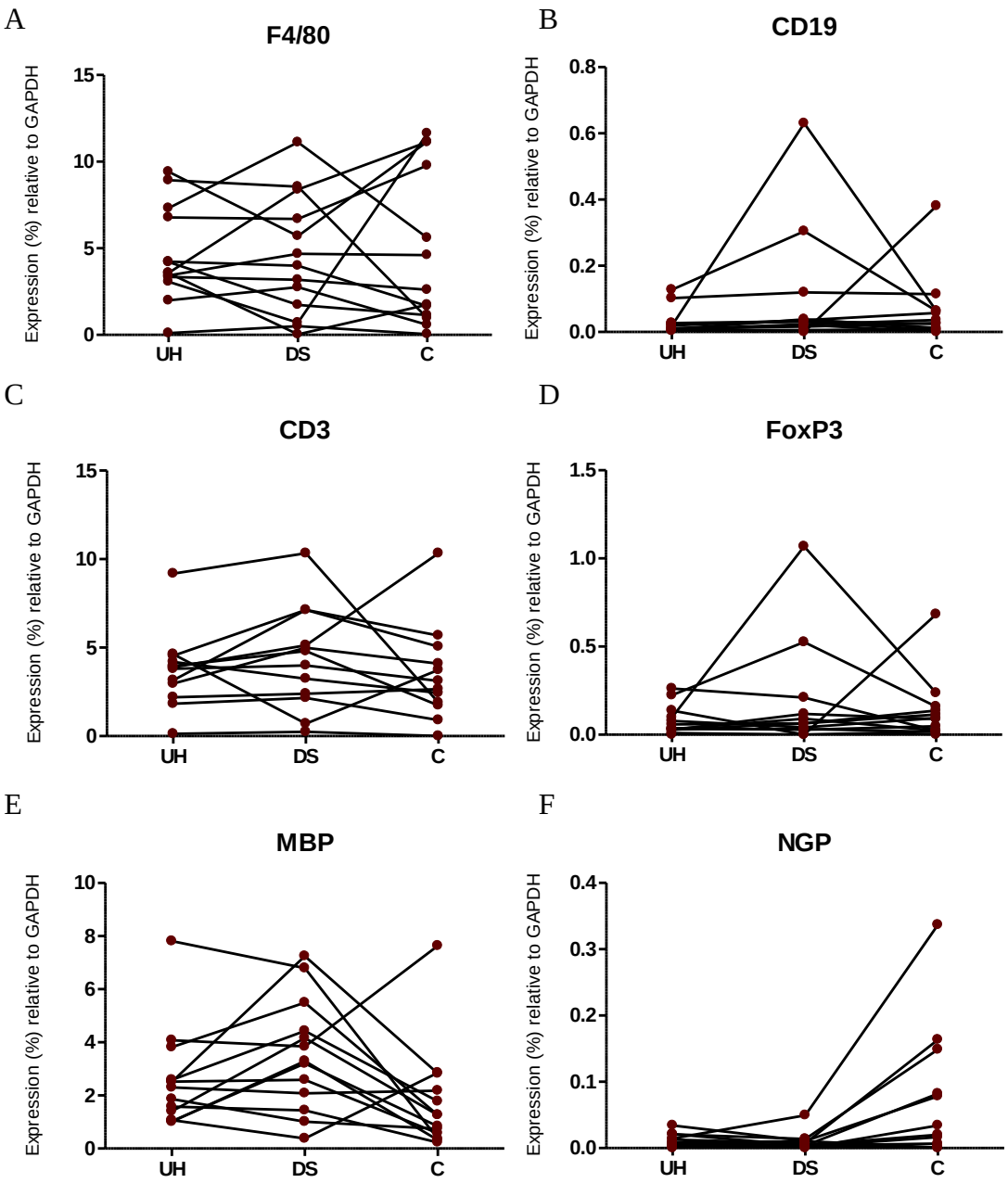

Figure 3.2. *No specific enrichment in expression of genes encoding cell markers in detachment sites.*

Uterine horn tissue without detachment sites (UH), uterine horn tissue with detachment sites (DS) and Cervix (C) and were compared for gene expression of cells markers in ex-breeders (n=12-13). Expression was calculated as $100x2^{\Delta CT}$ where $\Delta CT=CT^{target}-CT^{GAPDH}$ to establish target expression as a percentage of expression of the endogenous control. Gene expression relative to GAPDH of: (A) F4/80 (B) CD19 (C) CD3 (D) FoxP3 (E) MBP (F) NGP. Each set of linked points represents expression from one individual. Statistical analysis was carried out by a Friedman test with repeated measures, with a Dunn's post-hoc test, not significant.

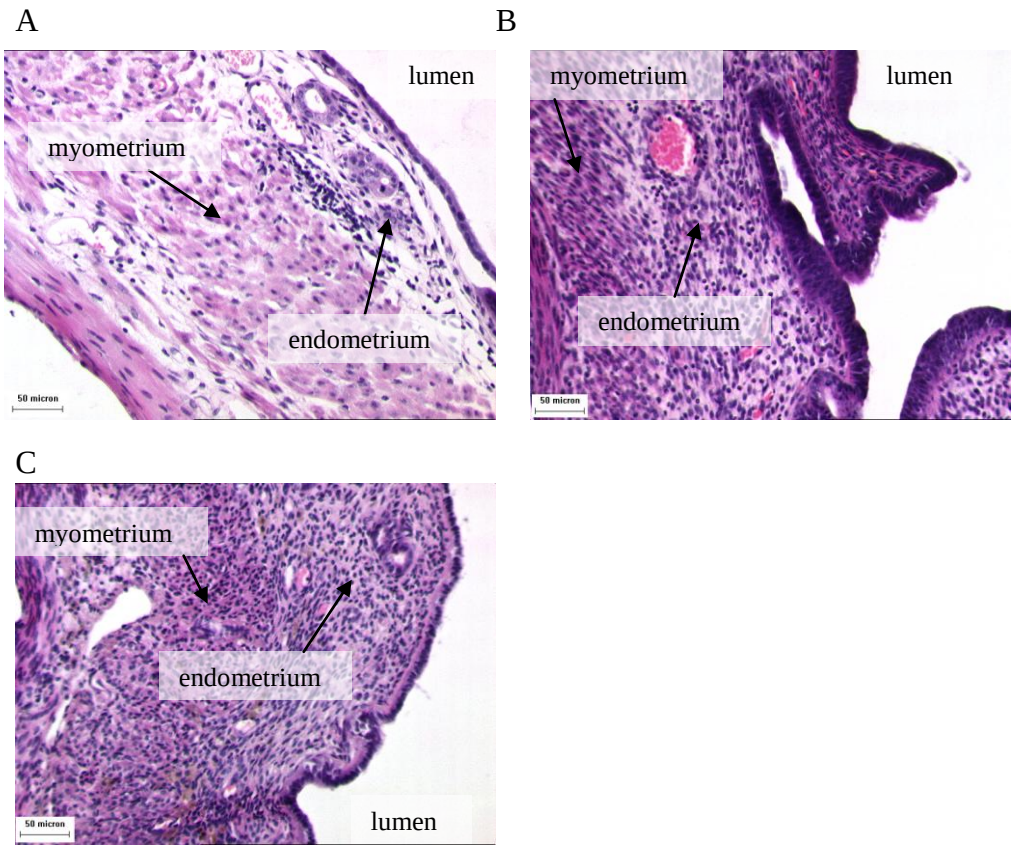

Figure 3.3. *Alteration of the structure of the uterine horn in the post-partum period*. Uterine horn tissue was removed from WT females at 1DPP (A), 7DPP (C) and from ex-breeders (D). Tissue was fixed, processed and embedded before being cut and stained with haematoxylin and eosin by Jim Reilly (Institute of Infection, Immunity & Inflammation, University of Glasgow). The myometrium and endometrium can be clearly identified in all stages of the post-partum period.

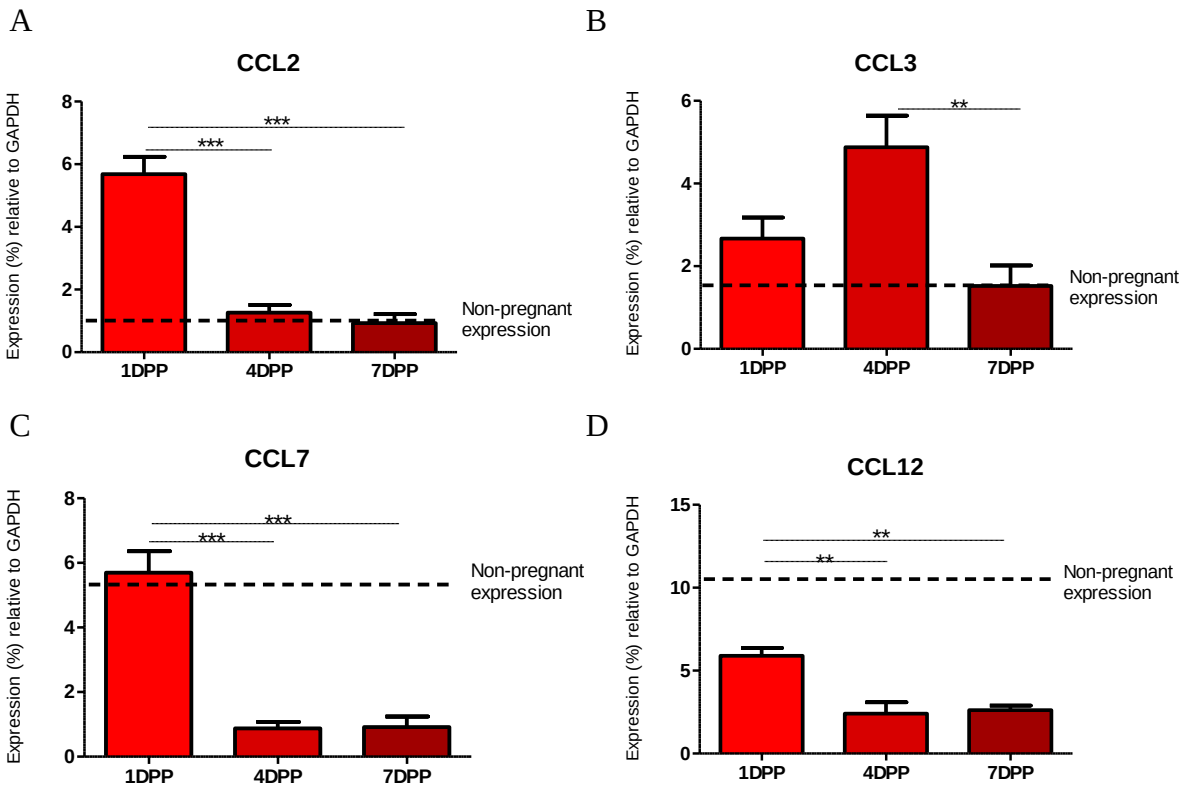

Figure 3.4. *CCR2-binding chemokine gene expression varies in the uterine horn over the post-partum period*.

Gene expression of CCR2 binding chemokines in the UH of mice at 1DPP (n=5), 4DPP (n=6) and 7DPP (n=5) after their first pregnancy. Expression was calculated as $100x2^{\Delta CT}$ where $\Delta CT=CT^{target}-CT^{GAPDH}$ to establish target expression as a percentage of expression of the endogenous control. (A) CCL2 (B) CCL3 (C) CCL7 (D) CCL12. Results are presented as mean±SEM. Statistical analysis was carried out by one-way ANOVA with a Tukey post-test, **p<0.01, ***p<0.001. NP samples were produced and processed by Fiona Menzies and Abdul Khan (Obstetrics and Gynaecology, University of Glasgow) and re-analysed for this project.

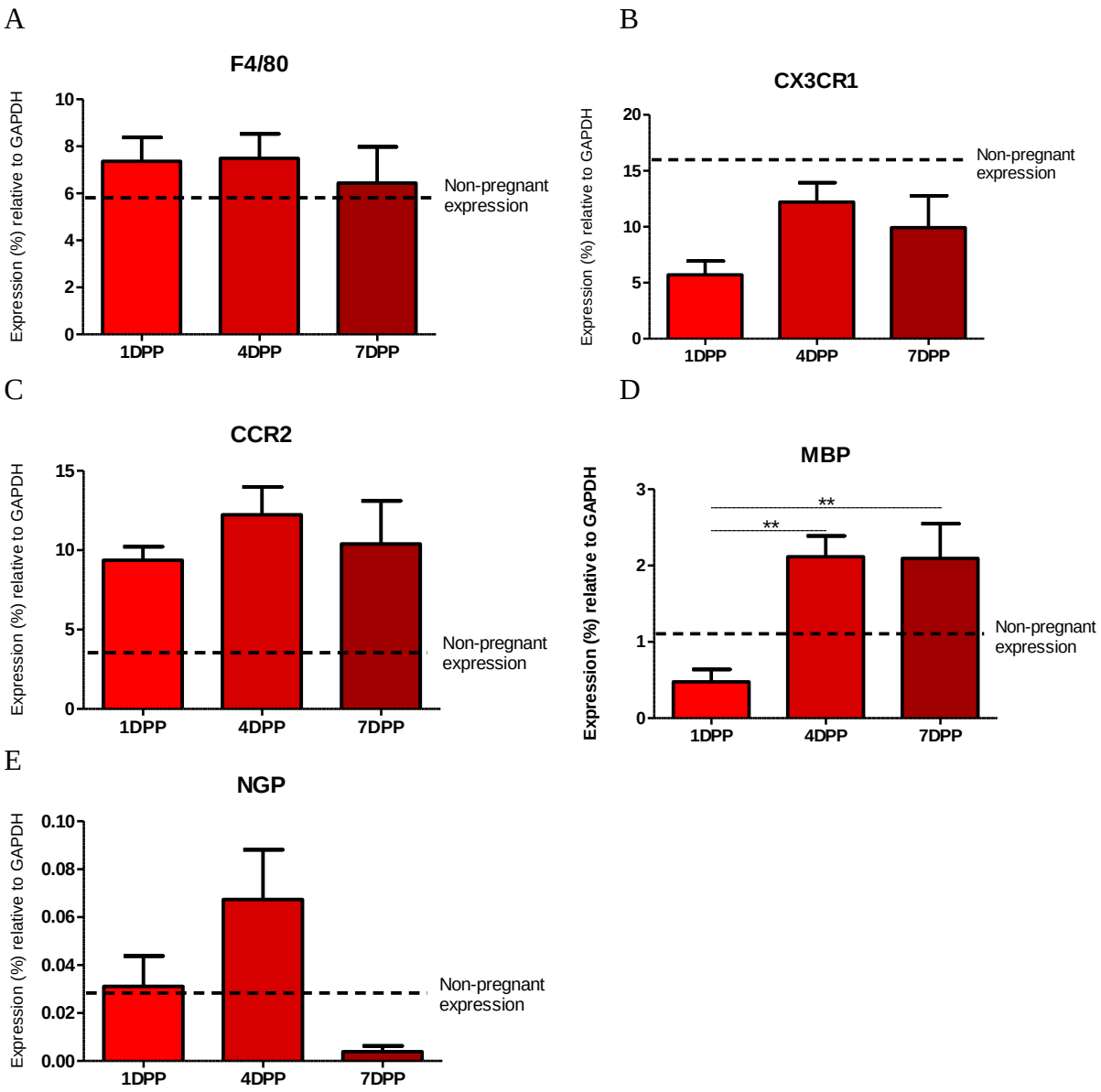

Figure 3.5. E*xpression of genes encoding monocyte and macrophage markers does not vary over the post-partum period.*

mRNA expression of myeloid cell markers in the UH of mice in at 1DPP (n=5), 4DPP (n=6) and 7DPP (n=5) after their first pregnancy. Expression was calculated as $100x2^{\Delta CT}$ where $\Delta CT=CT^{target}-CT^{GAPDH}$ to establish target expression as a percentage of expression of the endogenous control. Gene expression relative to GAPDH: (A) F4/80 (B) CX3CR1 (C) CCR2 (D) MBP (E) NGP. Data presented as mean±SEM. Statistical analysis was carried out by one-way ANOVA with a Tukey post-test, **p<0.01. NP samples were produced and processed by Fiona Menzies and Abdul Khan (Obstetrics and Gynaecology, University of Glasgow) and re-analysed for this project.

Figure 3.6. *Optimising digestion techniques for liberating Ly6C+CD11b+ cells from the uterine horn*.

Two digests were tested for their ability to liberate Ly6C+CD11b+ cells from the NP UH. Digest 1; Liberase + DNase 1. Digest 2; hyluronidase + collagenase + DNase 1. A) Gating strategy for all tissues shown for splenocytes. Physical gate removes cells at the extremes (top; unstained cells, bottom; stained cells), 7-AAD negative live cells (top; unstained cells, bottom, stained cells), Ly6C+/CD11b+ quadrant is a simple gate for monocyte-like cells (top; FMO controls). Gates placed on spleen cells were used for all tissues. B) Ly6C/CD11b staining for spleen and digested UH and cervix for both protocols. C) Table showing numbers of cells from the UH that were retrieved, gated as live and stained Ly6C+/CD11b+ in the two digest conditions.

A

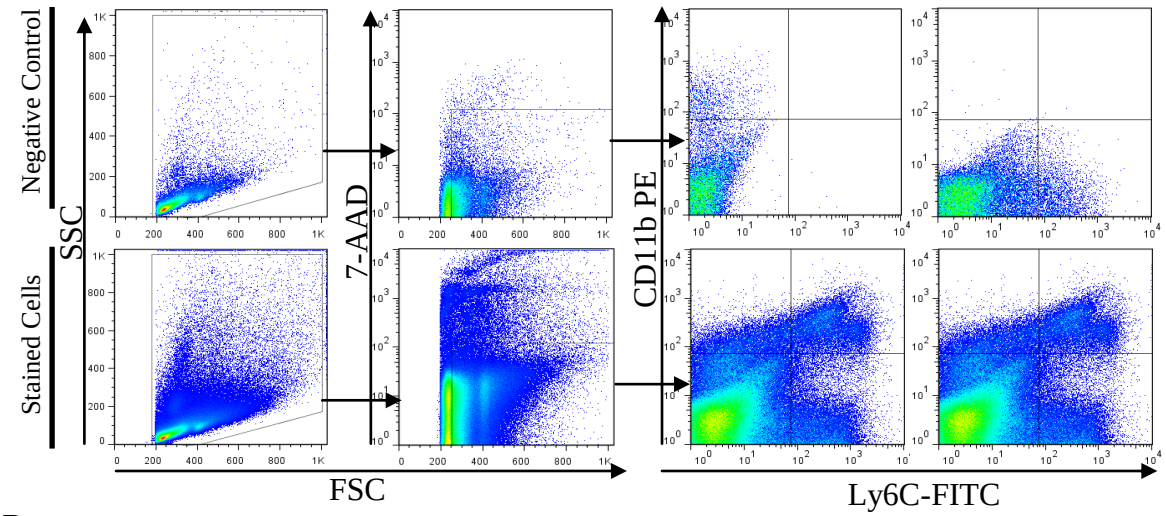

B

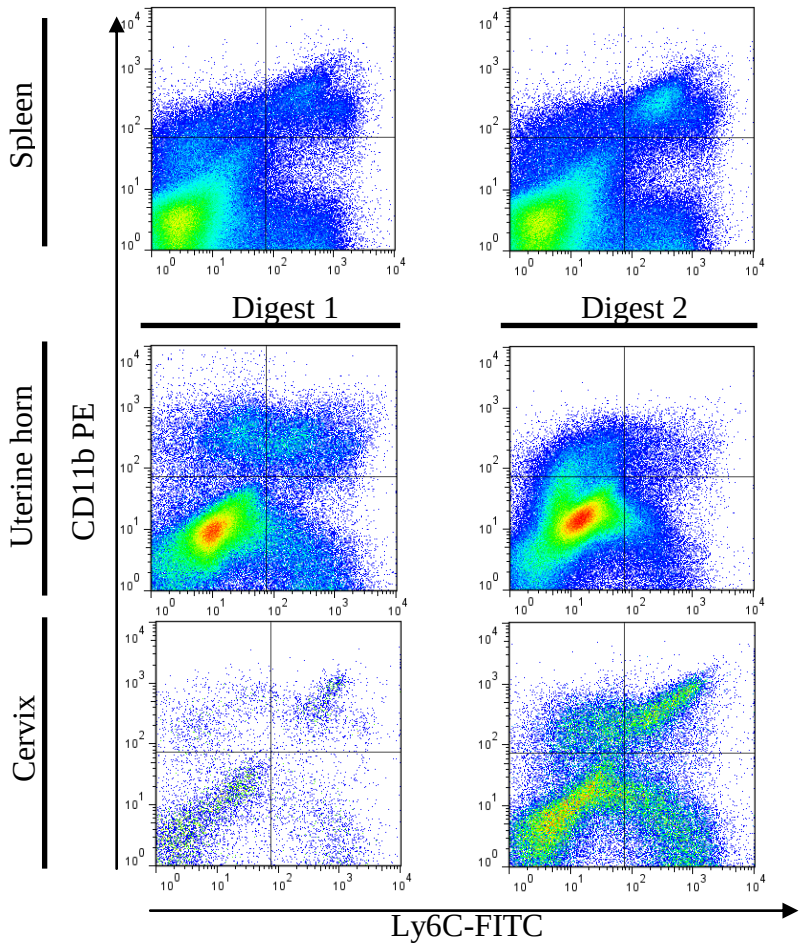

C

	Total cells retrieved	Live	Ly6C+ CD11b+
Digest 1	257580	162857	12292
Digest 2	509700	251939	4888

Figure 3.6. *Optimising digestion techniques for liberating Ly6C+CD11b+ cells from the uterine horn (legend opposite).*

Figure 3.7. *Large increase in myeloid cells in the uterine horn at 1DPP*.

Total leukocytes or myeloid cells in reproductive tissues in the post-partum period, measured by flow cytometry. (A) Representative plots of the gating strategy for detection of CD45+CD11b+ myeloid cells by flow cytometry. Physical and live gates drawn as in Figure (fig) 3.5, CD45 and CD11b gates drawn from staining in the spleen. Ly6C aided CD11b gating by separating CD11b+ cell populations. (B) Left; CD45+ cells retrieved from the UH and cervix of NP, 1DPP 7DPP mice (n=7-12), expressed as median and IQR. Analysed by Kruskall-Wallis test with a Dunn's post-hoc test to compare all groups *$p<0.05$, **$p<0.01$, ***$p<0.001$. Right; representative plots showing CD45+ gate for 1DPP UH and cervix. (C) Left; CD45+CD11b+ cells retrieved from the UH and cervix of NP, 1DPP and 7DPP mice (n=4-5), expressed as mean±SEM. Analysed by one-way ANOVA with a Tukey post-hoc test ***$p<0.001$. Right; representative plots showing CD45+CD11b+ gate from the 1DPP UH and cervix.

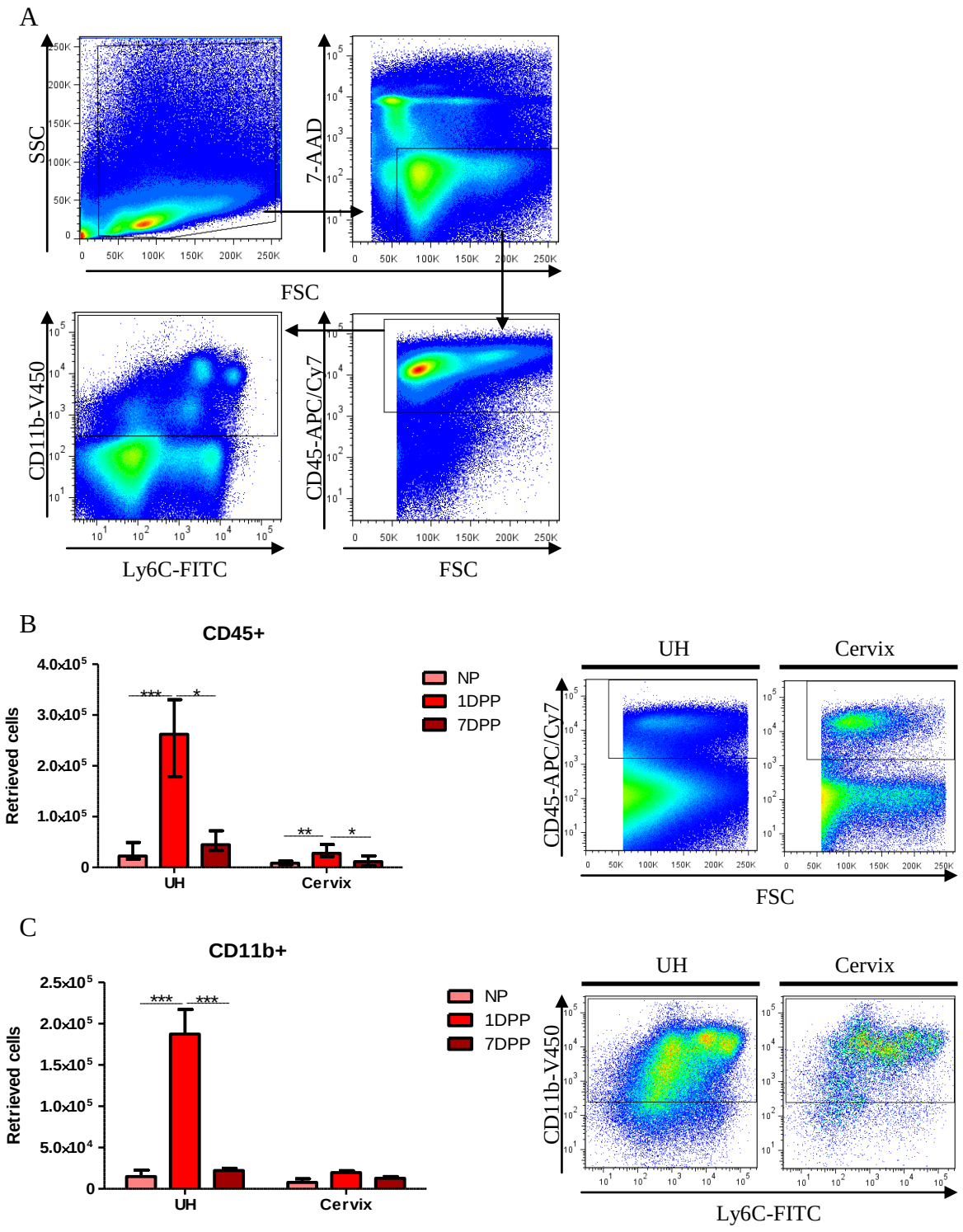

Figure 3.7. *Large increase in myeloid cells in the uterine horn at 1DPP (legend opposite).*

Figure 3.8. *Ly6C^{lo} and Ly6C^{hi} monocytes are abundant at 1DPP in the uterine horn.*
Measurement of monocyte and macrophage subsets in reproductive tissues using flow cytometry in NP females and at 1DPP and 7DPP during the post-partum period (n=3-5). Cells pregated as CD45+CD11b+. (A) Representative images of gating strategy in spleen, blood and UH at 1DPP for isolation of resident macrophages, Ly6C^{lo} monocytes and Ly6C^{hi} monocytes. From the Ly6C/SSC plot an inverted L gate is drawn to capture Ly6C+SSC$^{lo\text{-}int}$ cells, these cells were then split based on F4/80; [1] was defined as monocytes, F4/80^{hi} cells were defined as resident monocytes [2]. Gate [1] was then split by expression of Ly6C in the spleen, separating two clear populations, Ly6C^{lo} monocytes [3] and Ly6C^{hi} monocytes [4]. (B) Ly6C^{lo} monocytes as a percentage of CD45+ cells (left) and total Ly6C^{lo} monocytes retrieved (right). (C) Ly6C^{hi} monocytes as a percentage of CD45+ cells (left) and total Ly6C^{hi} monocytes retrieved (right). (E) Resident macrophages as a percentage of CD45+ cells (left) and total resident macrophages retrieved (right). Data presented as mean±SEM. Statistical analysis was carried out by one-way ANOVA with a Tukey post-test, *$p<0.05$, **$p<0.01$.

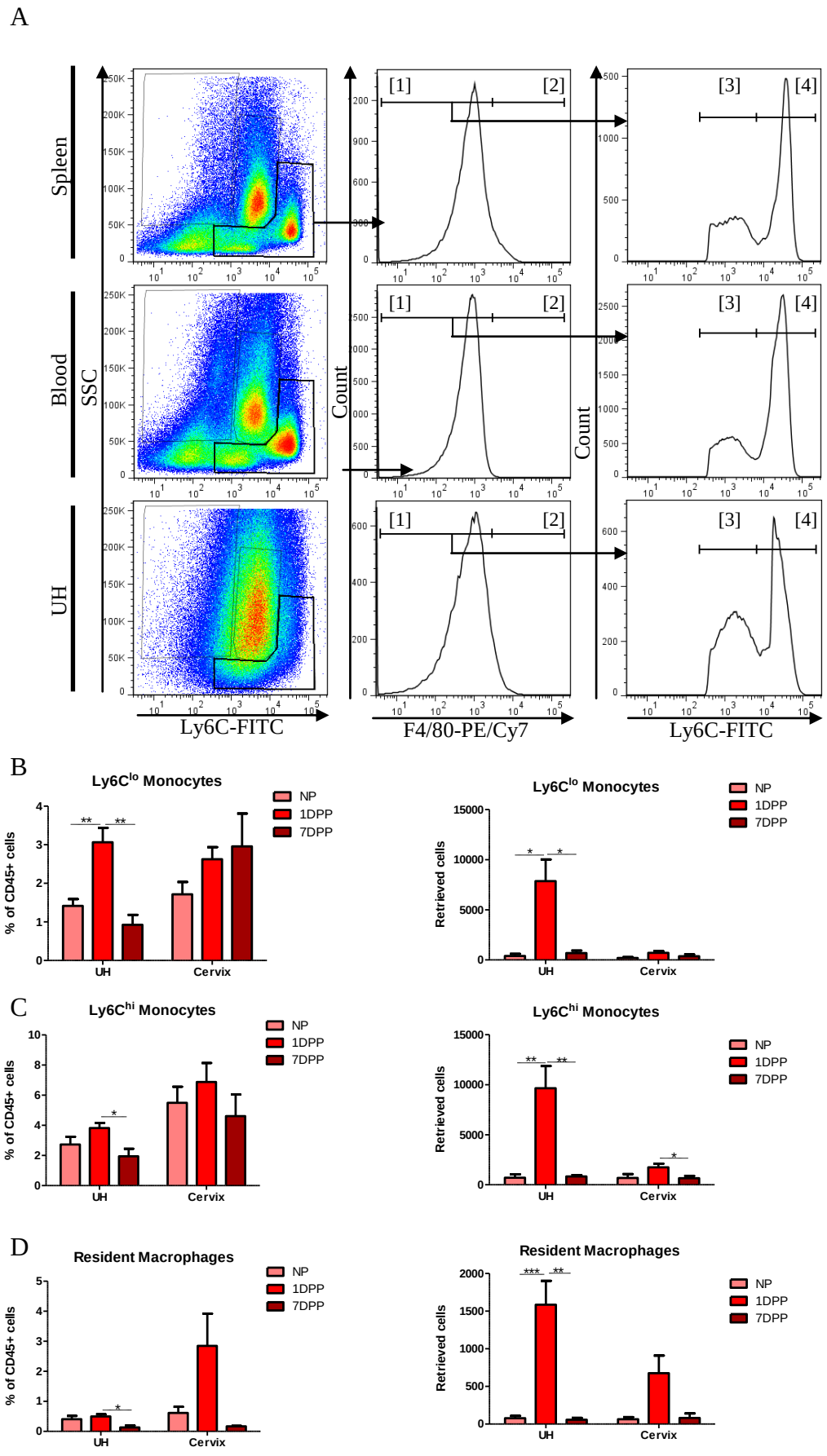

Figure 3.8. *Ly6C^{lo} and Ly6C^{hi} monocytes are abundant at 1DPP in the uterine horn (legend opposite).*

Figure 3.9. *Monocyte and macrophage subsets remained largely unchanged in the post-partum period in peripheral tissues*.

Measurement of monocyte and macrophage subsets in spleen, blood, BM and PALN in the post-partum period using flow cytometry (n=4-5). (A) Representative gating as in fig 3.8. Absolute numbers were calculated by taking a live cell count and multiplying the proportion of the population as a total of live cells. (B) $Ly6C^{lo}$ monocytes as a percentage of CD45+ cells (left) and absolute numbers of $Ly6C^{lo}$ monocytes (right). (D) $Ly6C^{hi}$ monocytes as a percentage of CD45+ cells (left) and absolute numbers of $Ly6C^{hi}$ monocytes (right). (E) Resident macrophages as a percentage of CD45+ cells (left) and absolute numbers of resident macrophages (right). Data were presented as mean±SEM. Statistical analysis was carried out by one-way ANOVA with a Tukey post-test, *$p<0.05$.

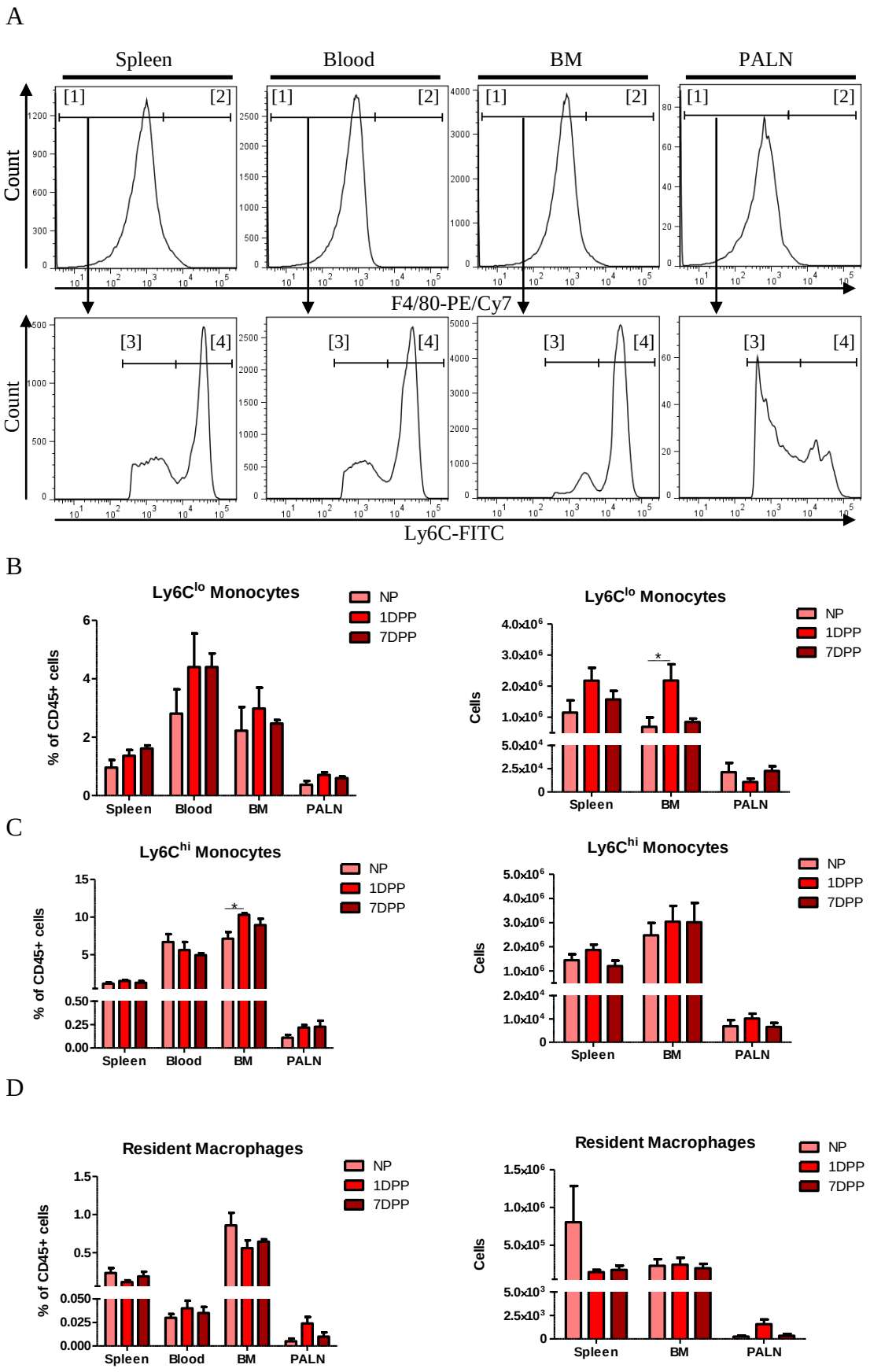

Figure 3.9. *Monocyte and macrophage subsets remained largely unchanged in the post-partum period in peripheral tissues (legend opposite).*

Figure 3.10. *CCL2-AF647 uptake is at its lowest at 7DPP in reproductive tissues.*
Uptake of fluorescent CCL2 was measured by flow cytometry in spleen (n=4-5), UH (n=3-5), cervix (n=3-5), blood (n=4-5), BM (n=4-5), PALN (n=4-5) and in NP, 1DPP and 7DPP mice. Cells were incubated with CCL2-AF647 for 65mins. Gates are drawn as in fig 3.8. (A) Typical histogram of fluorescent CCL2 uptake of monocyte and macrophage populations in the spleen, with the FMO (no CCL2) control for the total CD11b population shown in red. (B) Left; Proportion of $Ly6C^{lo}$ monocytes internalising CCL2. Right; geoMFI of CCL2+ $Ly6C^{lo}$ monocytes. (C) Left; Proportion of $Ly6C^{hi}$ monocytes internalising. Right; geoMFI of CCL2+ $Ly6C^{hi}$ monocytes. (D) Left; Proportion of resident macrophages internalising. Right; geoMFI of CCL2+ resident macrophages. Data were presented as mean±SEM. Statistical analysis was carried out by one-way ANOVA with a Tukey post-test, *$p<0.05$ **$p<0.01$.

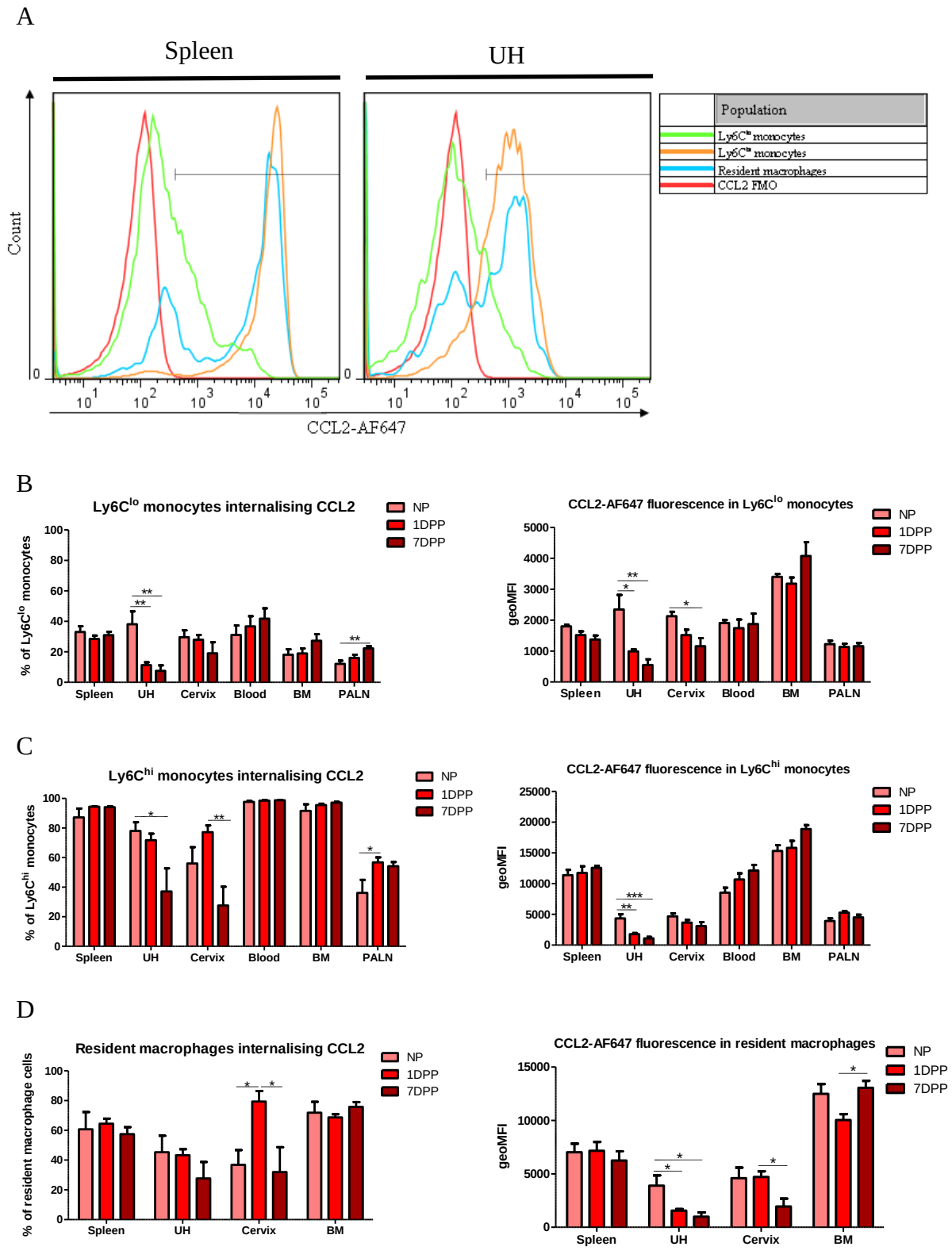

Figure 3.10. *CCL2-AF647 uptake is at its lowest at 7DPP in reproductive tissues (legend opposite).*

Figure 3.11. *CCR2 deletion dramatically reduces CCL2 internalisation in monocyte and macrophage populations in the reproductive tract at 1DPP*.

Uptake of fluorescent CCL2 was measured by flow cytometry in UH (n=3-5) and cervix (n=3-5) at 1DPP in WT and CCR2 KO mice. Cells were incubated with CCL2-AF647 for 65mins. Gates are drawn as in fig 3.8. (A) Typical histogram of fluorescent CCL2 uptake of $Ly6C^{lo}$ monocyte (left), $Ly6C^{hi}$ monocyte (centre) and resident macrophage (right) populations in the UH. A representative WT profile is shown in blue and a representative CCR2 KO profile is shown in orange. The FMO (no CCL2) control for the total CD11b population for the spleen is shown in red as a negative control. (B) Left; Proportion of $Ly6C^{lo}$ monocytes internalising CCL2. Right; Geometric mean fluorescence intensity (geoMFI) of CCL2+ $Ly6C^{lo}$ monocytes. (C) Left; Proportion of $Ly6C^{hi}$ monocytes internalising. Right; geoMFI of CCL2+ $Ly6C^{hi}$ monocytes. (D) Left; Proportion of resident macrophages internalising CCL2. Right; geoMFI of CCL2+ $Ly6C^{hi}$ resident macrophages. Data are presented as mean±SEM. Statistical analysis was carried out by unpaired Student's t-test with a Welch's correction for unequal variances when appropriate *$p<0.05$ **$p<0.01$ ***$p<0.001$.

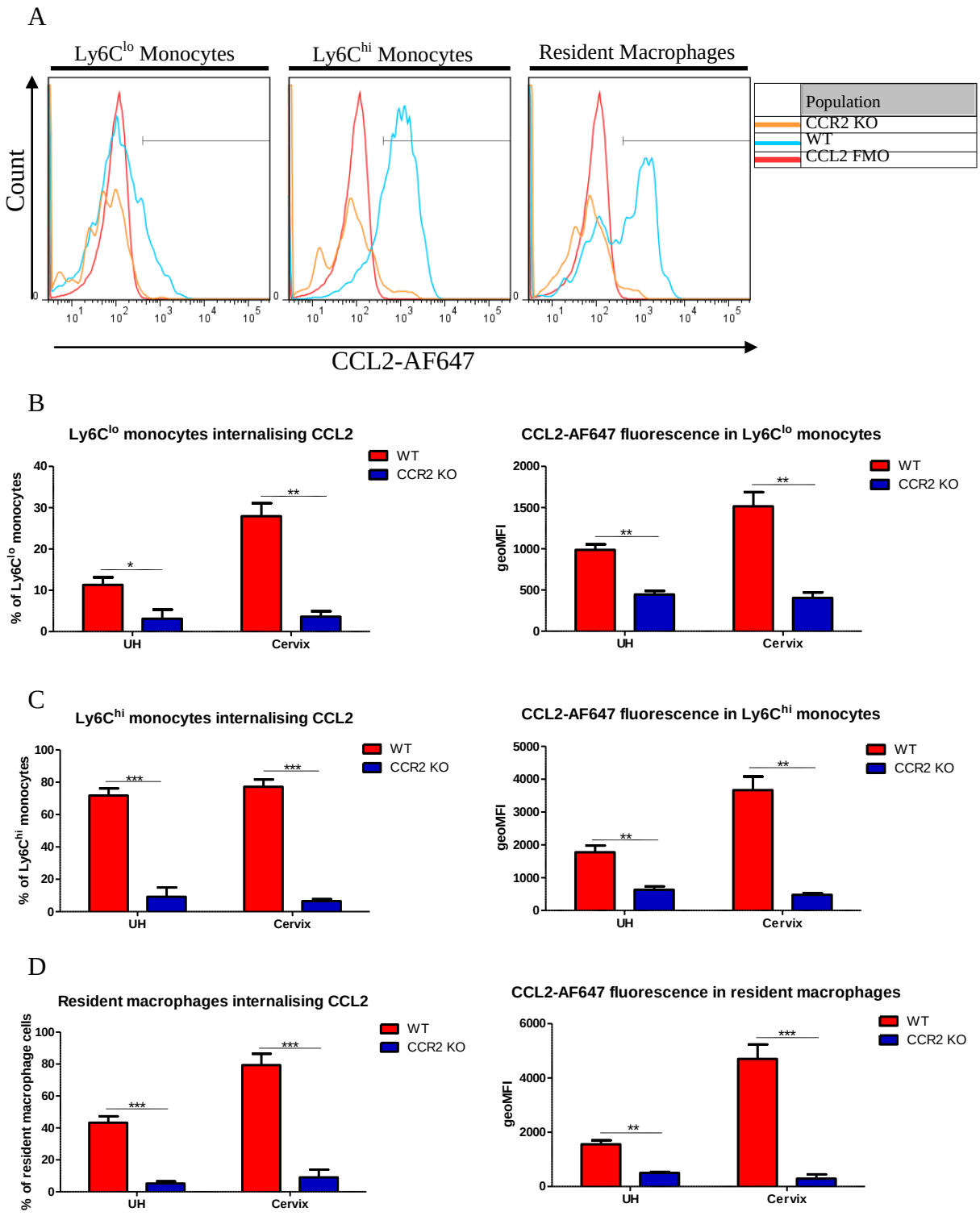

Figure 3.11. *CCR2 deletion dramatically reduces CCL2 internalisation in monocyte and macrophage populations in the reproductive tract at 1DPP.*

Figure 3.12. *CCR2 dependent CCL2-AF647 internalisation by monocytes and macrophages in peripheral tissues at 1DPP*.

Uptake of fluorescent CCL2 was measured by flow cytometry in spleen (n=3-5), blood (n=3-5), BM (n=3-5) and PALN (n=3-5) at 1DPP. Cells were incubated with CCL2-AF647 for 65mins. Gates are drawn as in fig 3.9. (A) Typical histogram of fluorescent CCL2 uptake of $Ly6C^{lo}$ monocyte (top) and $Ly6C^{hi}$ monocyte (middle) and resident macrophage (bottom) populations. A representative WT profile is shown in blue and a representative CCR2 KO profile is shown in orange. The FMO control for the total CD11b population for the spleen is shown in red as a negative control. Resident macrophage populations were negligible in blood and PALN. (B) Left; Proportion of $Ly6C^{lo}$ monocytes internalising CCL2. Right; Geometric mean fluorescence intensity (geoMFI) of CCL2+ $Ly6C^{lo}$ monocytes. (C) Left; Proportion of $Ly6C^{hi}$ monocytes internalising CCL2. Right; geoMFI of CCL2+ $Ly6C^{hi}$ monocytes. (D) Left; Proportion of resident macrophages internalising CCL2. Right; geoMFI of CCL2+ resident macrophages. Data are presented as mean±SEM. Statistical analysis was carried out by unpaired Student's t-test with a Welch's correction for unequal variances when appropriate *$p<0.05$ **$p<0.01$ ***$p<0.001$.

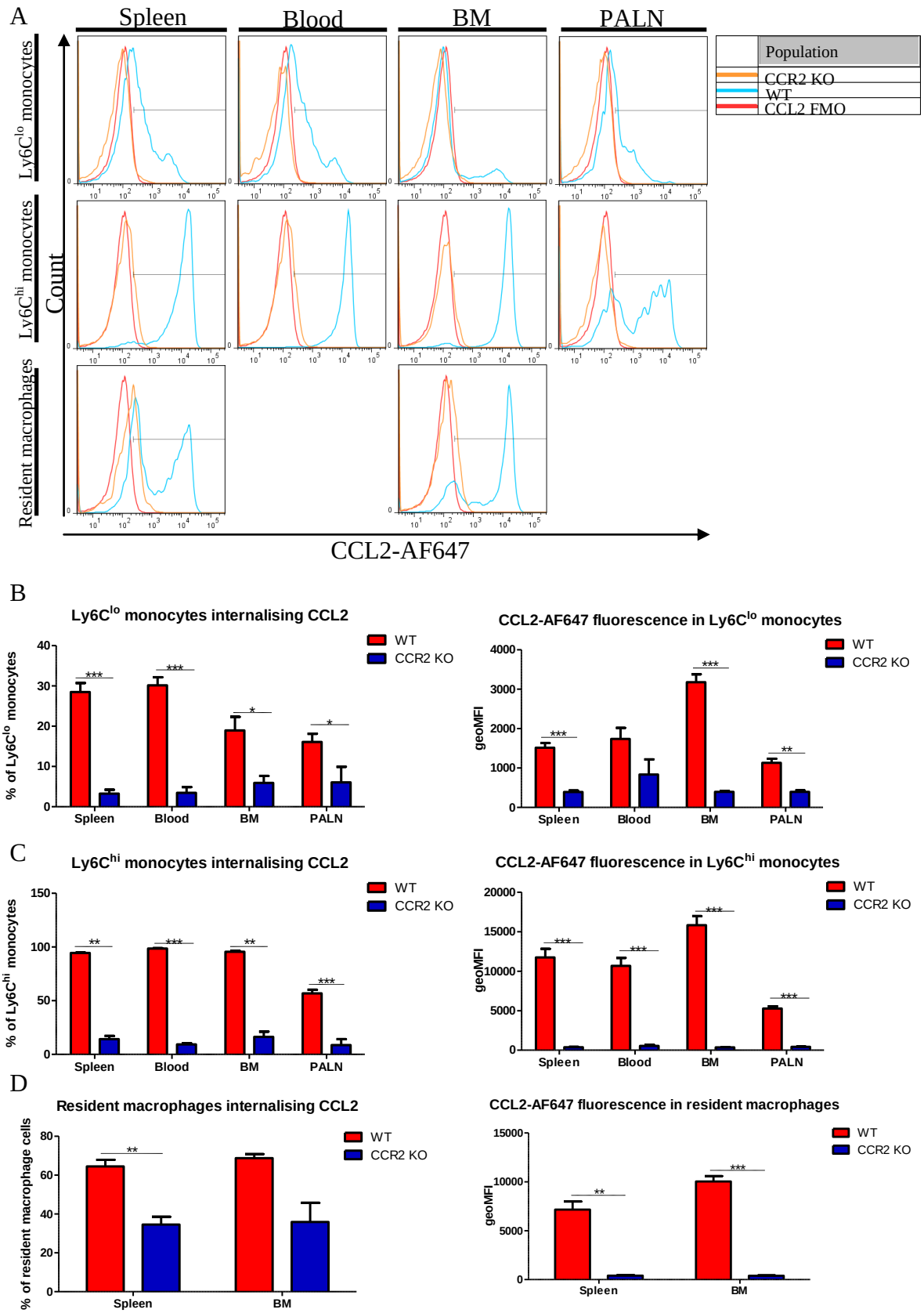

Figure 3.12. *CCR2 dependent CCL2-AF647 internalisation by monocytes and macrophages in peripheral tissues at 1DPP (legend opposite).*

Figure 3.13. *Increases in the proportions of granulocytes in reproductive tissues over the post-partum period.*

Measurement of granulocytes in reproductive tissues using flow cytometry stained for CD45, CD11b, Ly6C and CD115 in NP, 1DPP and 7DPP mice (n=4-5). (A) Gating strategy based on splenocytes for isolation of eosinophils and neutrophils. Cells gated for CD11b+ were then split by Ly6C/SSC with $Ly6C^{lo}SSC^{hi}$ cells [1] then being gated as CD115- to remove monocytes and macrophages, these cells were defined as eosinophils for this study. $Ly6C^{int}SSC^{int}$ [2] cells were also gated as CD115- and these cells were defined as neutrophils. (B) A representative image of Ly6C/SSC for UH (left) and cervix (right) at 1DPP. (C) Left; Eosinophils as a percentage of CD45+ cells. Right; Eosinophils retrieved. (D) Left; Neutrophils as a percentage of CD45+ cells. Right; Neutrophils retrieved. Data presented as mean±SEM. Statistical analysis was carried out by one-way ANOVA with a Tukey post-test, *$p<0.05$, **$p<0.01$ ***$p<0.001$.

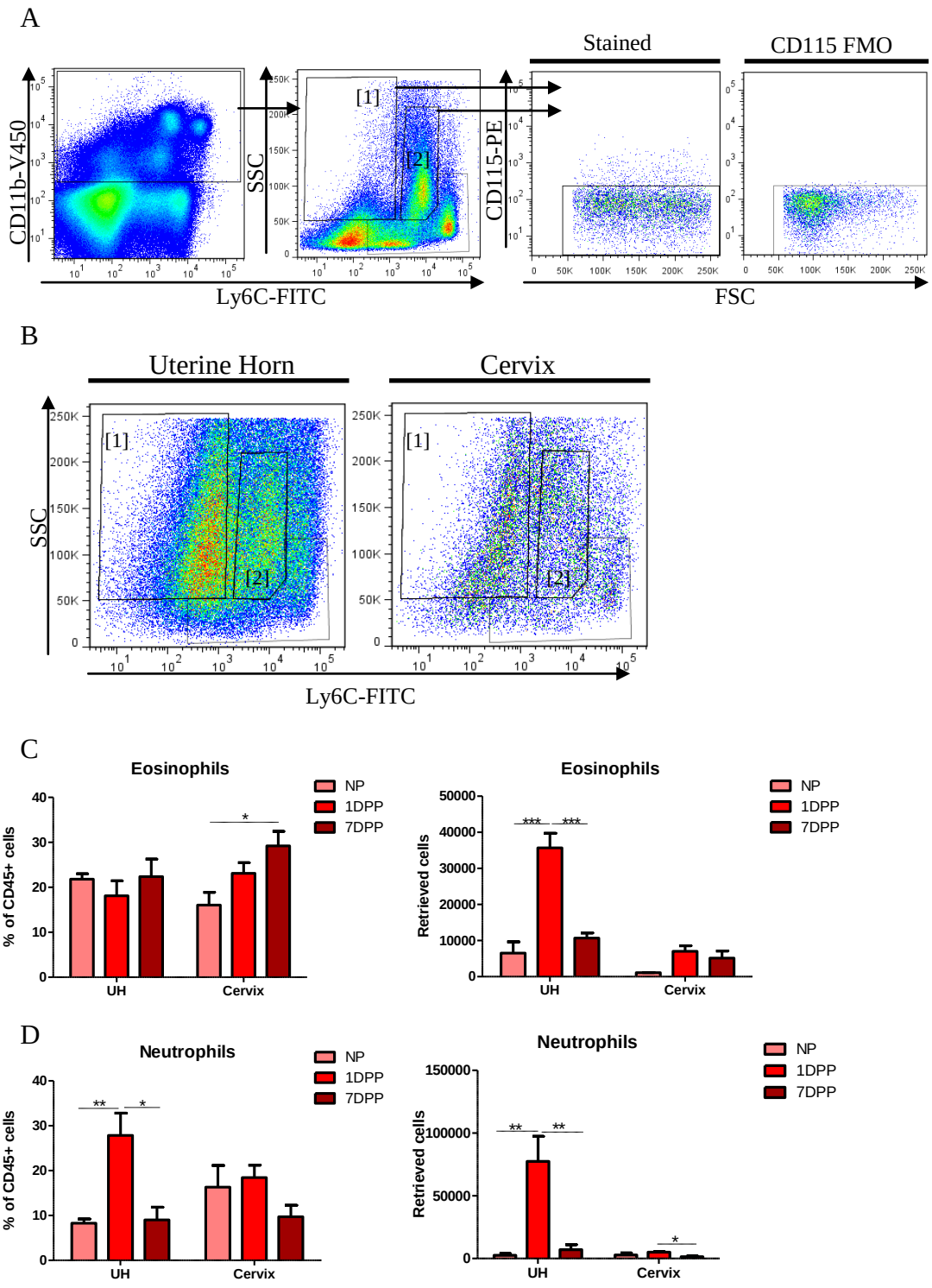

Figure 3.13. *Increases in the proportions of granulocytes in reproductive tissues over the post-partum period (legend opposite).*

Figure 3.14. *Peripheral tissues show changes in proportions of neutrophils and eosinophils in the post-partum period*.

Measurement of eosinophils and neutrophils in spleen, blood, BM and PALN in NP females and at 1DPP and 7DPP (n=3-5). (A) Gating strategy based on splenocytes for isolation of eosinophils and neutrophils as in fig 3.13. CD11b+ gate was split by Ly6C/SSC with $Ly6C^{lo}SSC^{hi}$ cells [1] then being gated as CD115- to be defined as eosinophils. $Ly6C^{int}SSC^{int}$ [2] cells were also gated as CD115- and defined as neutrophils. (B) Ly6C/SSC profiles in spleen, blood, BM and PALN. (C) Eosinophils as a proportion of CD45+ cells (left) and absolute numbers of eosinophils (right). Absolute numbers were calculated by taking a live cell count and multiplying the proportion of the population as a total of live cells. (D) Neutrophils as a proportion of CD45+ cells (left) and absolute numbers of neutrophils (right). Data presented as mean±SEM. Statistical analysis was carried out by one-way ANOVA with a Tukey post-test, *$p<0.05$ **$p<0.01$.

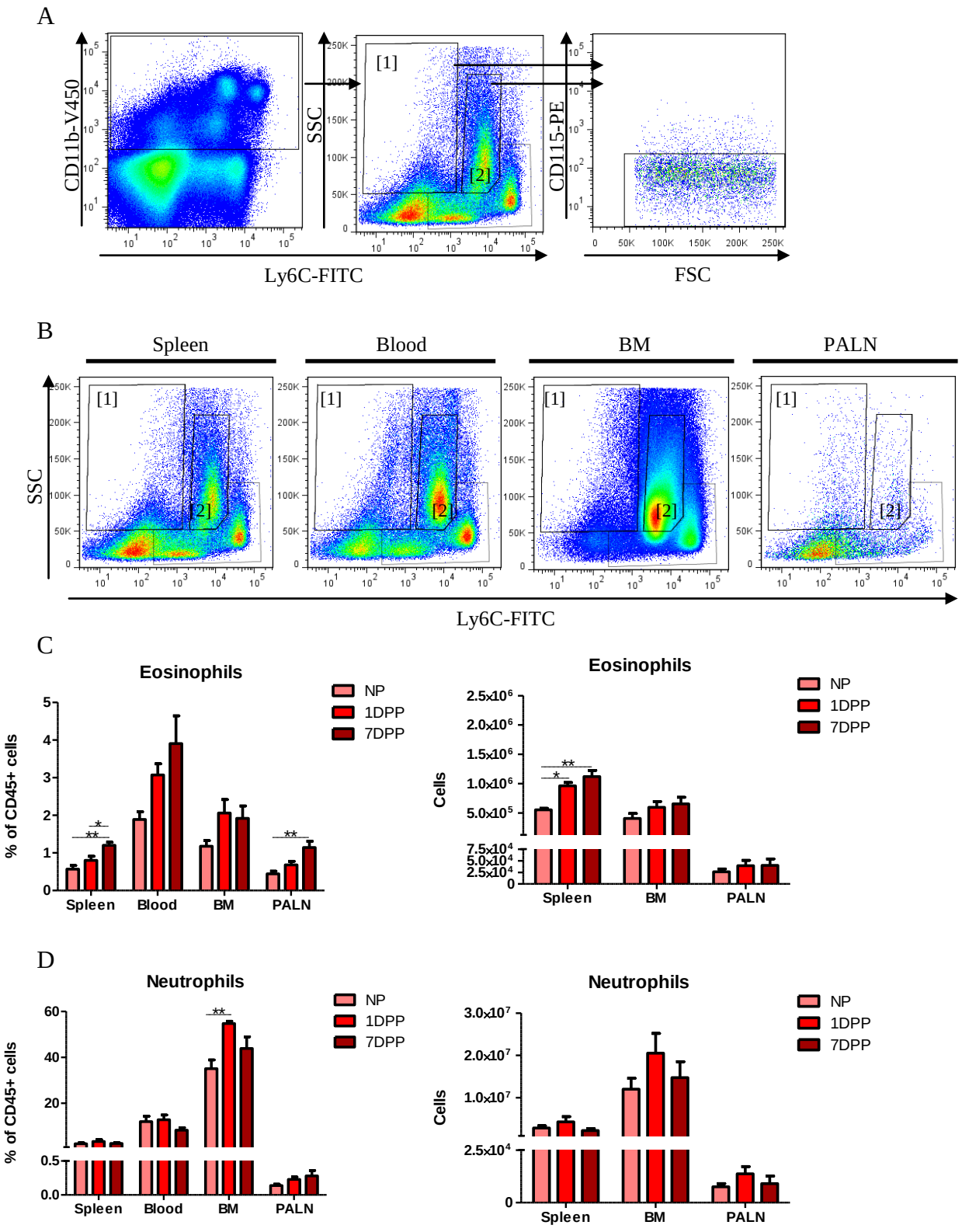

Figure 3.14. *Peripheral tissues show changes in proportions of neutrophils and eosinophils in the post-partum period (legend opposite).*

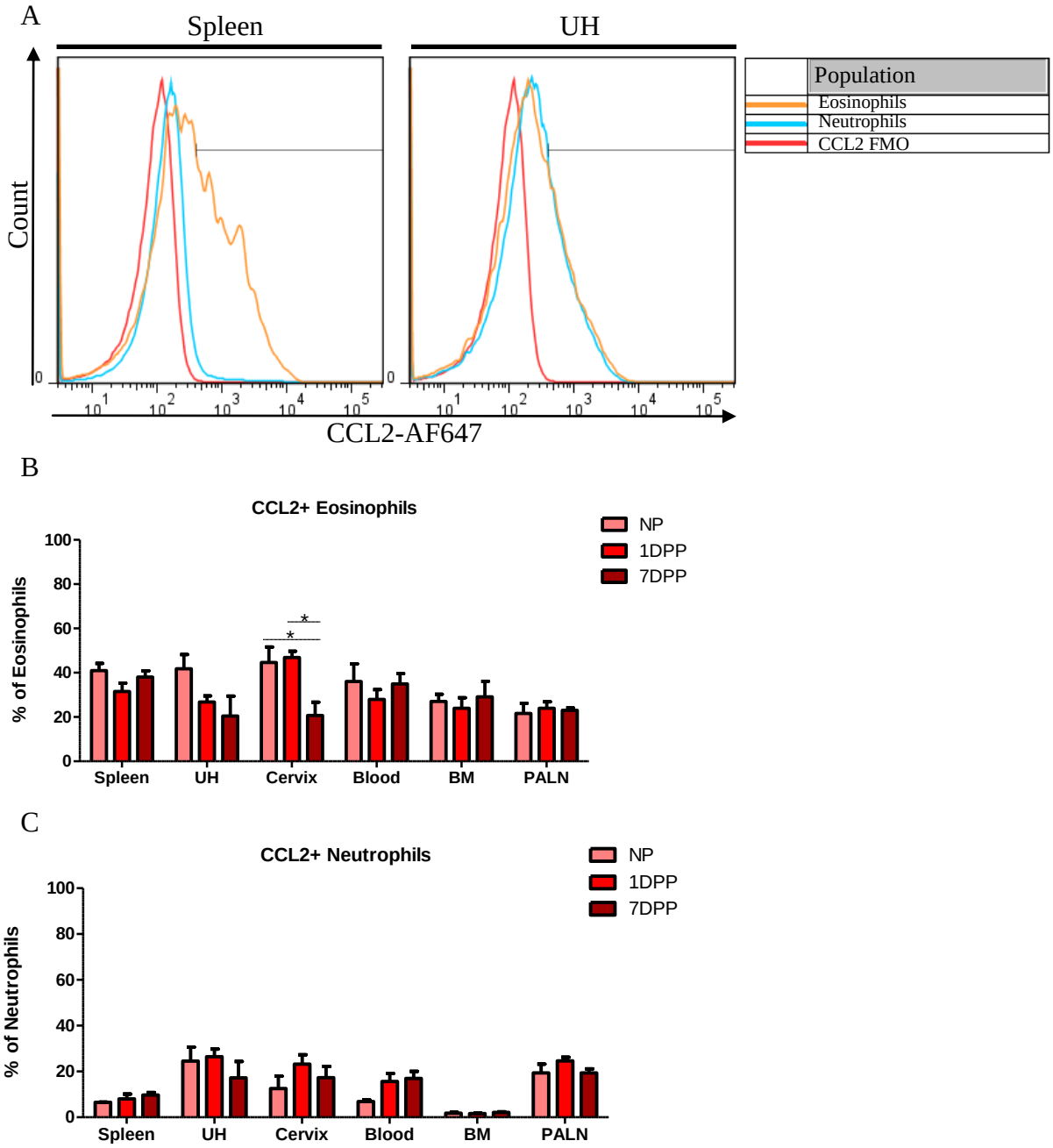

Figure 3.15. *Granulocytes internalise low levels of CCL2-AF647.*

Uptake of fluorescent CCL2-AF647 was measured by flow cytometry in spleen (n=4-5), UH (n=3-5), cervix (n=3-5), blood (n=4-5), BM (n=4-5), PALN (n=4-5) in NP, 1DPP and 7DPP mice. Cells were incubated with CCL2-AF647 for 65mins. Gates are drawn as in fig 3.13. (A) Typical histogram of fluorescent CCL2-AF647 uptake of eosinophil and neutrophil populations in the spleen, with the FMO control for the total CD11b population shown in red. (B) Proportion of eosinophils internalising CCL2-AF647. (C) Proportion of neutrophils internalising CCL2-AF647. Data were presented as mean±SEM. Statistical analysis was carried out by one-way ANOVA with a Tukey post-test, *p<0.05 **p<0.01 ***p<0.001.

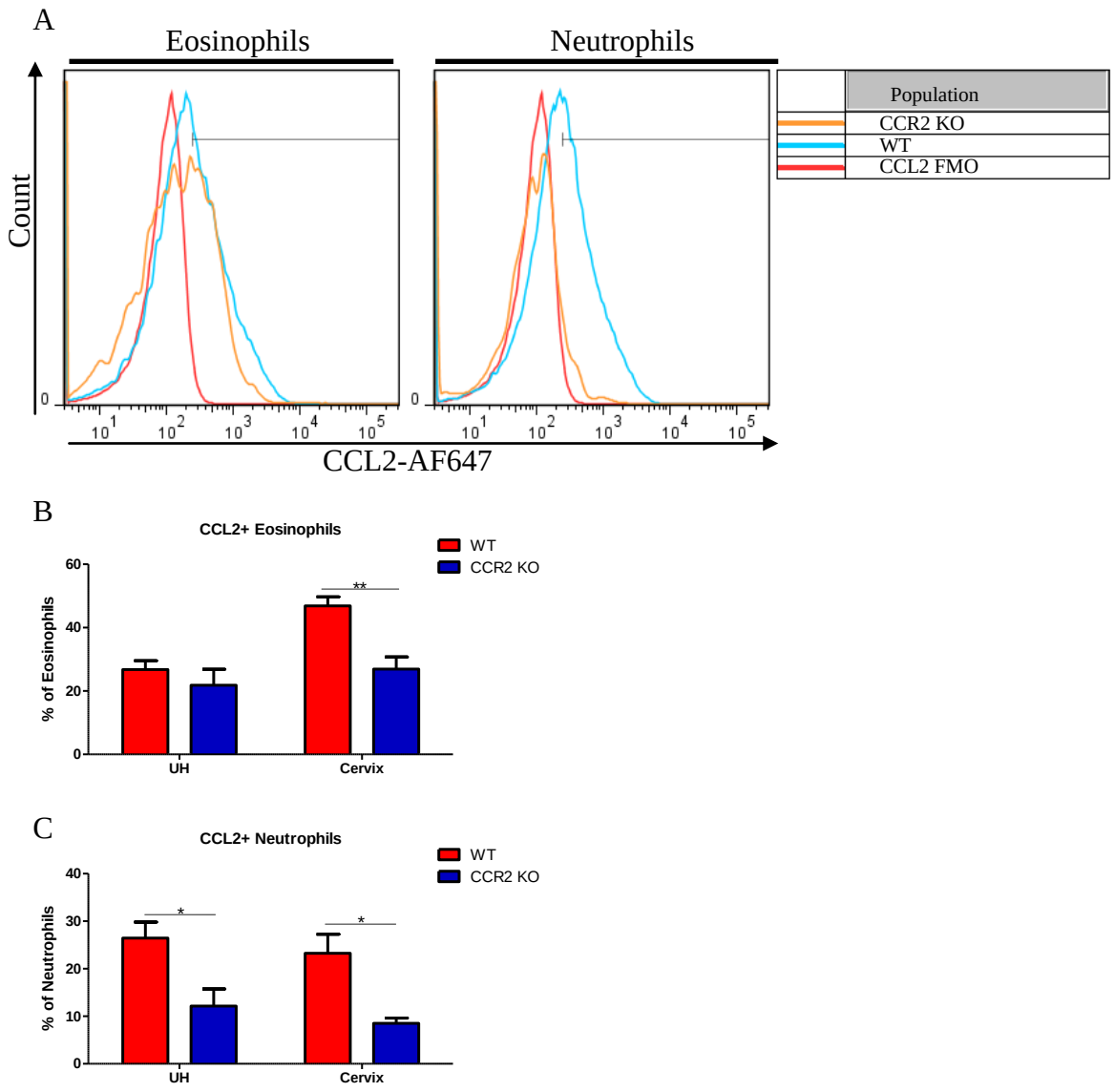

Figure 3.16. *CCR2 deletion reduces CCL2-AF647 internalisation in reproductive tract eosinophils and neutrophils at 1DPP*.

Uptake of fluorescent CCL2 was measured by flow cytometry in UH (n=3-5) and cervix (n=3-5) at 1DPP in eosinophils and neutrophils. Cells were incubated with CCL2-AF647 for 65mins. Gates are drawn as in fig 3.13. (A) Typical histogram of fluorescent CCL2 uptake of eosinophil (left) and neutrophil (right) populations in the 1DPP UH. A representative WT profile is shown in blue and a representative CCR2 KO profile is shown in orange. The FMO control for the total CD11b population for the spleen is shown in red as a negative control. (B) Proportion of eosinophils internalising CCL2 in the UH and cervix at 1DPP in WT and CCR2 KO mice. (C) Proportion of neutrophils internalising CCL2 in the UH and cervix at 1DPP in WT and CCR2 KO mice. Data are presented as mean±SEM. Statistical analysis was carried out by unpaired Student's t-test with a Welch's correction for unequal variances when appropriate *p<0.05 **p<0.01.

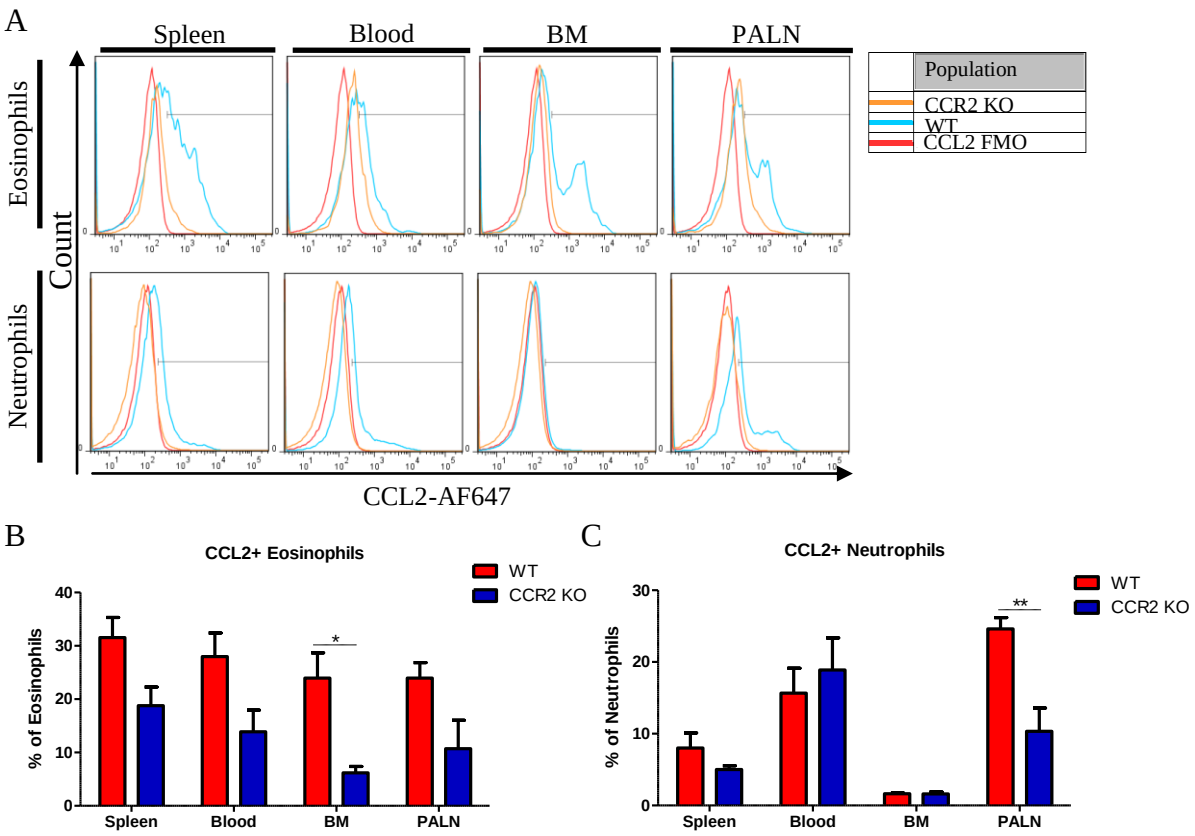

Figure 3.17. *Peripheral tissues tend not to have a reduced proportion of granulocytes internalising CCL2-AF647.*

Uptake of fluorescent CCL2-AF647 was measured by flow cytometry in spleen (n=3-5), blood (n=3-5), BM (n=3-5) and PALN (n=3-5) at 1DPP in WT and CCR2 KO mice. Cells were incubated with CCL2-AF647 for 65mins. Gates were drawn as in fig 3.14. (A) Typical histogram of fluorescent CCL2-AF647 uptake of eosinophil (top) and neutrophil (bottom) populations in the spleen, blood, BM and PALN. A representative WT profile is shown in blue and a representative CCR2 KO profile is shown in orange. The FMO control for the total CD11b population for the spleen is shown in red as a negative control. (B) Proportion of eosinophils internalising CCL2-AF647. (C) Proportion of neutrophils internalising CCL2-AF647 in peripheral tissues at 1DPP. Data presented as mean±SEM. Statistical analysis was carried out by unpaired Student's t-test with a Welch's correction for unequal variances when appropriate *p<0.05 **p<0.01 ***p<0.001.

Figure 3.18. *CCR2 deficient mice have far fewer monocytes and macrophages in their reproductive tissues at 1DPP.*

Measurement of monocytes and macrophages in reproductive tissues in WT and CCR2 KO mice using flow cytometry at NP (n=3-6), 1DPP (n=3-5) and 7DPP (n=3-6) time points. Gates are drawn as in fig 3.8. (A) Left; $Ly6C^{lo}$ monocytes as a proportion of CD45+ cells. Right; Total $Ly6C^{lo}$ monocytes retrieved. (B) Left; $Ly6C^{lo}$ monocytes as a proportion of CD45+ cells. Right; Total $Ly6C^{lo}$ monocytes retrieved. (C) Left; $Ly6C^{hi}$ monocytes as a proportion of CD45+ cells. Right; Total $Ly6C^{hi}$ monocytes retrieved. (D) Left; $Ly6C^{hi}$ monocytes as a proportion of CD45+. Right; Total $Ly6C^{hi}$ monocytes retrieved. (E) Left; Resident macrophages as a proportion of CD45+ cells. Right; Total Resident macrophages retrieved. (F) Left; Resident macrophages as a proportion of CD45+ cells. Right; Total Resident macrophages retrieved. Data were presented as mean±SEM. Statistical analysis was carried out by unpaired Student's t-test with a Welch's correction for unequal variances when appropriate *$p<0.05$ **$p<0.01$ ***$p<0.001$.

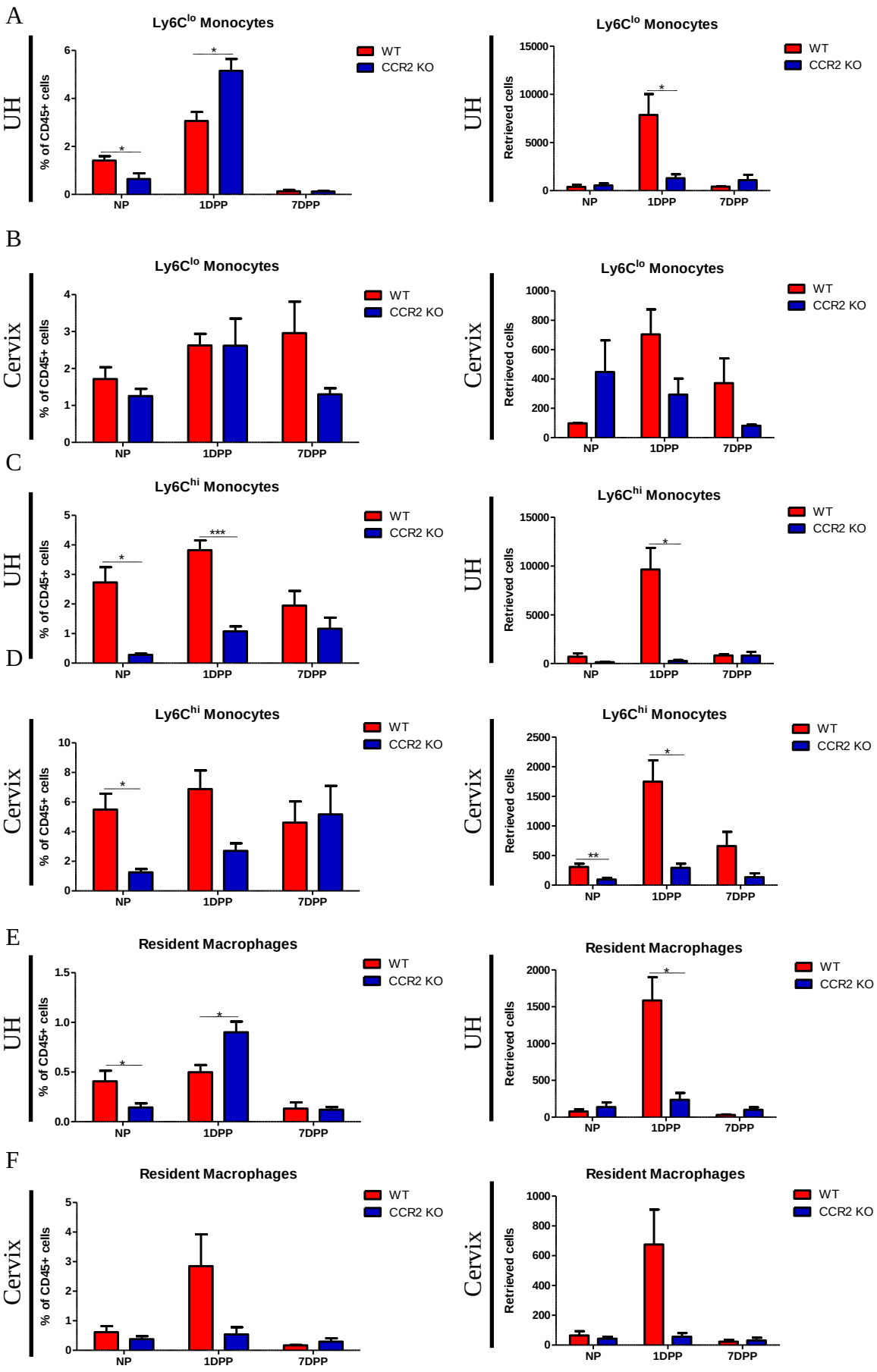

Figure 3.18. *CCR2 deficient mice have far fewer monocytes and macrophages in their reproductive tissues at 1DPP (legend opposite).*

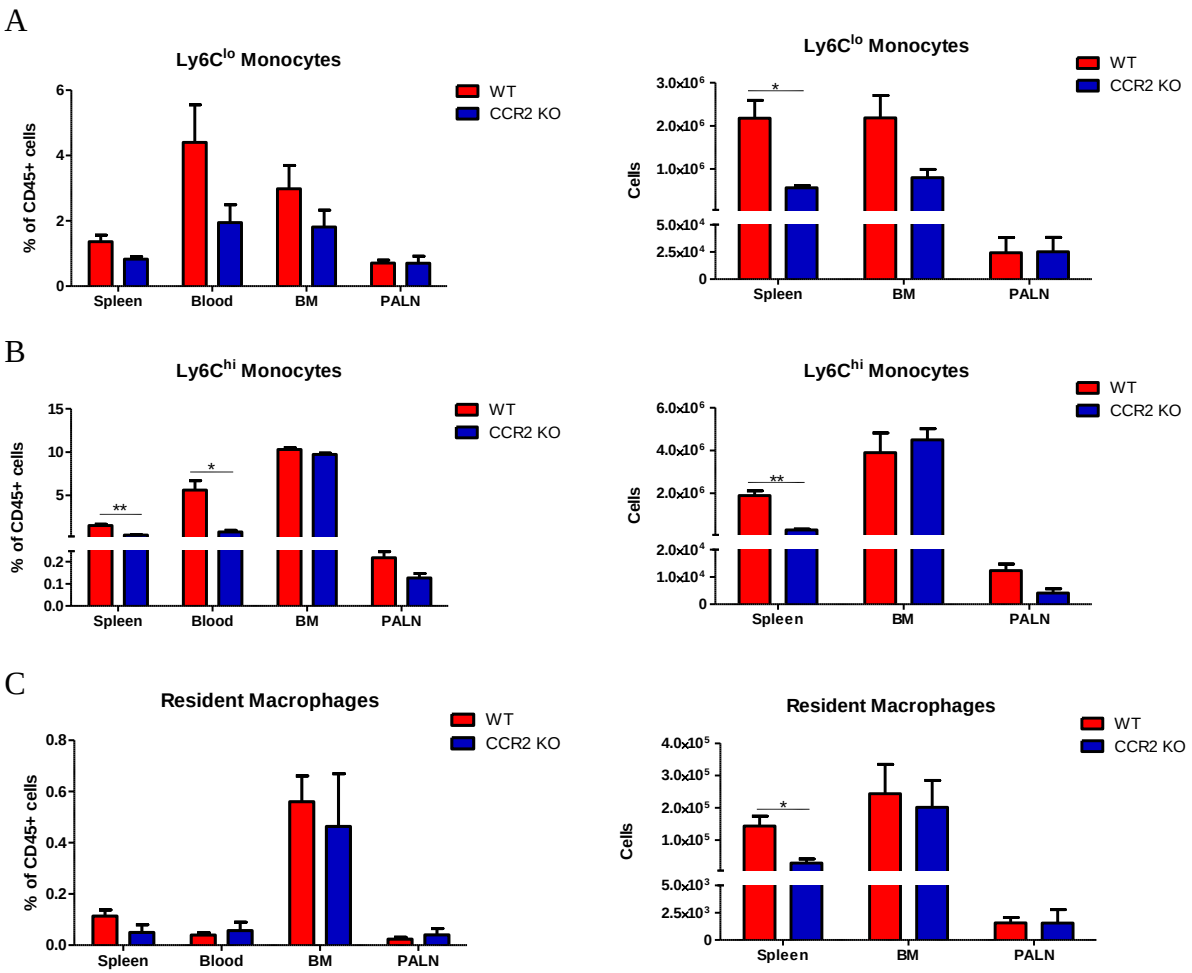

Figure 3.19. *The spleens of CCR2 KO mice contain fewer monocytes and macrophages than WTs at 1DPP*.

Monocytes and macrophages in spleen (n=3-5), blood (n=3-5), BM (n=3-5) and PALN (n=3-5) in WT and CCR2 KO mice at 1DPP measured using flow cytometry. Gates are drawn as in fig 3.9. (A) Left; Ly6C^{lo} monocytes as a proportion of CD45+ cells. Right; Absolute cell numbers of Ly6C^{lo} monocytes. Absolute numbers are calculated by taking a live cell count and multiplying the proportion of the population as a total of live cells. (B) Left; Ly6C^{hi} monocytes as a proportion of CD45+ cells. Right; Absolute cell numbers of Ly6C^{hi} monocytes. (C) Left; Resident macrophages as a proportion of CD45+ cells. Right; Absolute cell numbers of resident macrophages. Data are presented as mean±SEM. Statistical analysis was carried out by unpaired Student's t-test with a Welch's correction for unequal variances when appropriate *$p<0.05$ **$p<0.01$.

Figure 3.20. *CCR2 deletion reduces the number of granulocytes in reproductive tissues at 1DPP.*

Measurement of granulocytes in reproductive tissues in WT and CCR2 KO mice using flow cytometry at NP (n=4-6), 1DPP (n=3-5) and 7DPP (n=3-4) time points. Gates are drawn as in fig 3.13. (A) Left; Eosinophils in UH as a proportion of CD45+ cells in the post-partum period. Right; Total eosinophils retrieved from the UH in the post-partum period. (B) Left; Eosinophils in cervix as a proportion of CD45+ cells in the post-partum period. Right; Total eosinophils retrieved from the cervix in the post-partum period. (C) Left; Neutrophils in UH as a proportion of CD45+ cells in the post-partum period. Right; Total neutrophils retrieved from the UH in the post-partum period. (D) Left; Neutrophils in cervix as a proportion of CD45+ cells in the post-partum period. Right; Total neutrophils retrieved from the cervix in the post-partum period. Data are presented as mean±SEM. Statistical analysis was carried out by unpaired Student's t-test with a Welch's correction for unequal variances where appropriate *$p<0.05$ ***$p<0.001$.

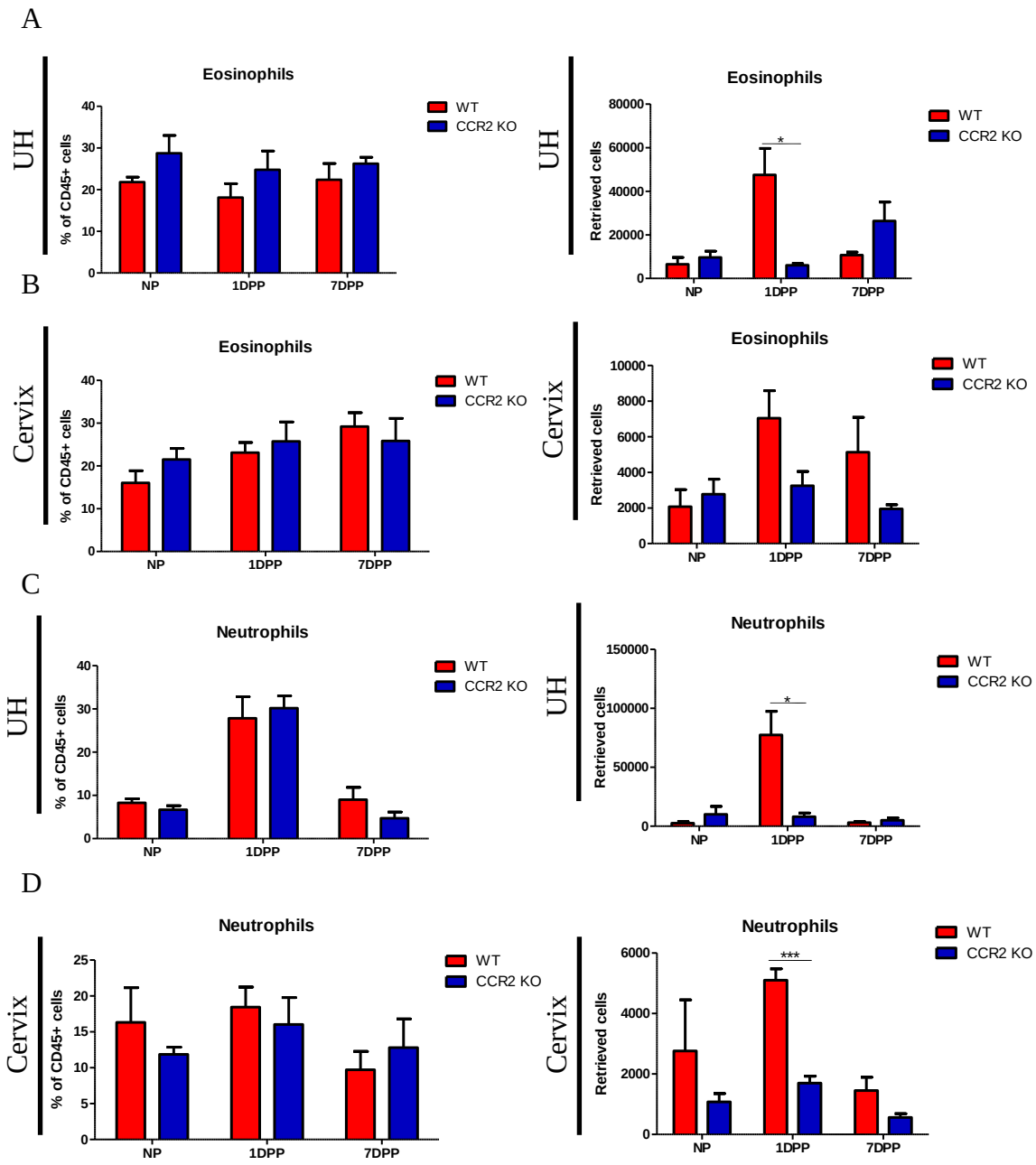

Figure 3.20. *CCR2 deletion reduces the number of granulocytes in reproductive tissues at 1DPP (legend opposite).*

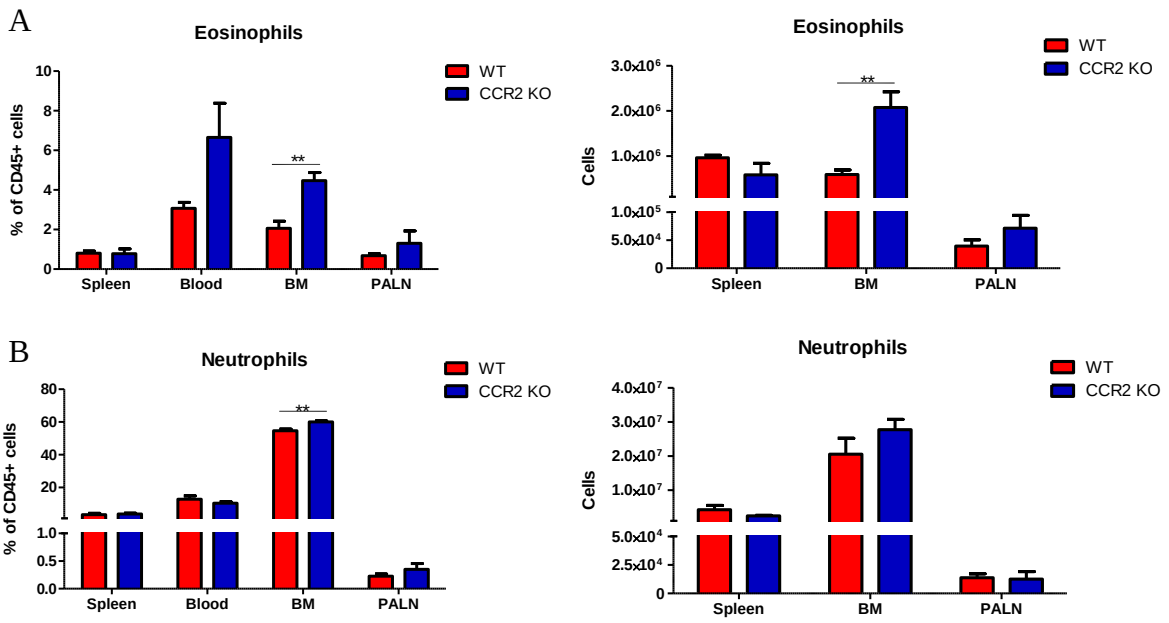

Figure 3.21. *Numbers and proportion of eosinophils in CCR2 KOs are double that of WTs in BM at 1DPP.*

Granulocytes in spleen (n=3-5), blood (n=3-5), BM (n=3-5) and PALN (n=3-5) in WT and CCR2 KO mice at 1DPP measured using flow cytometry. Gates are drawn as in fig 3.14. (A) Left; Eosinophils as a proportion of CD45+ cells in spleen, blood, BM and PALN. Right; Absolute cell numbers of eosinophils from spleen, BM and PALN. Absolute numbers were calculated by taking a live cell count and multiplying the proportion of the population as a total of live cells. (B) Neutrophils as a proportion of CD45+ cells in spleen, blood, BM and PALN. Right; Absolute cell numbers of neutrophils from spleen, BM and PALN. Data are presented as mean±SEM. Statistical analysis was carried out by unpaired Student's t-test with a Welch's correction for unequal variances when appropriate **p<0.01.

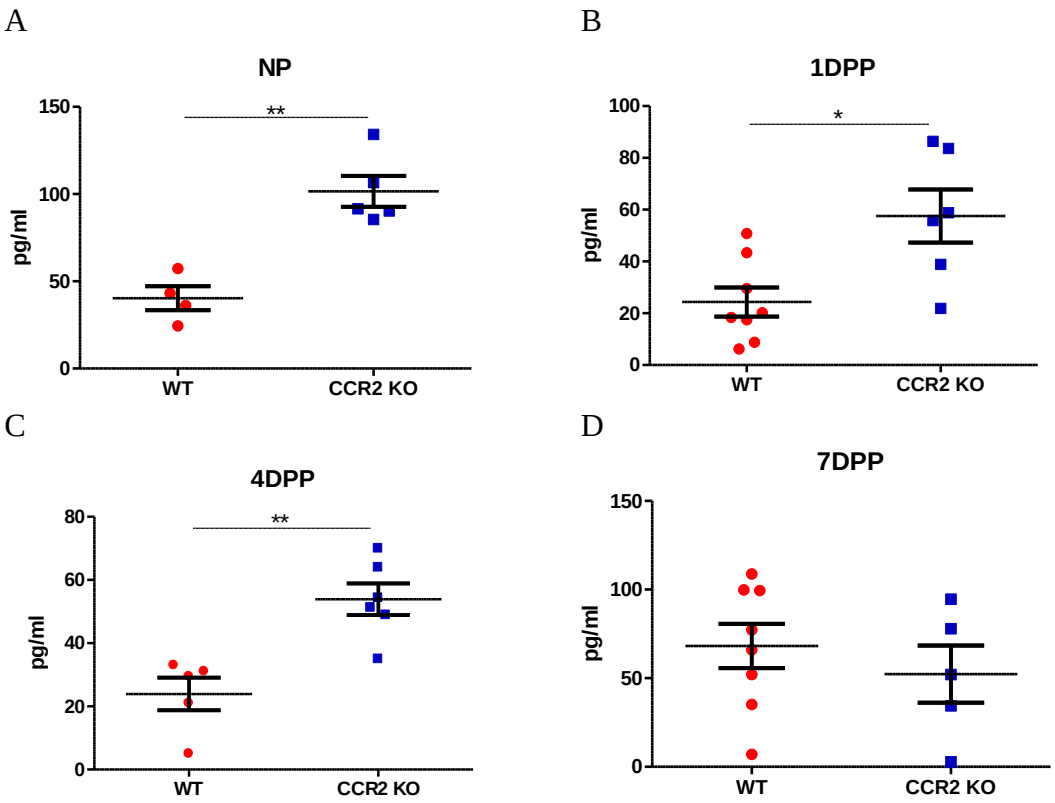

Figure 3.22. *CCL2 levels are higher in CCR2 KO than WT plasma in the early post-partum period*.

CCL2 measured in the plasma of WT (n=4-8) and CCR2 KO (p=5-6) mice in the post-partum period following their first litter. (A) CCL2 in NP mice in WT and CCR2 KO plasma. (B) CCL2 at 1DPP in WT and CCR2 KO plasma. (C) CCL2 at 4DPP in WT and CCR2 KO plasma. (D) CCL2 at 7DPP in WT and CCR2 KO plasma. Data are presented as mean±SEM. Statistical analysis was carried out by unpaired Student's t-test, *$p<0.05$, **$p<0.01$. Assistance in testing the samples was given by Chris Hansell (Institute of Infection, Immunity & Inflammation, University of Glasgow).

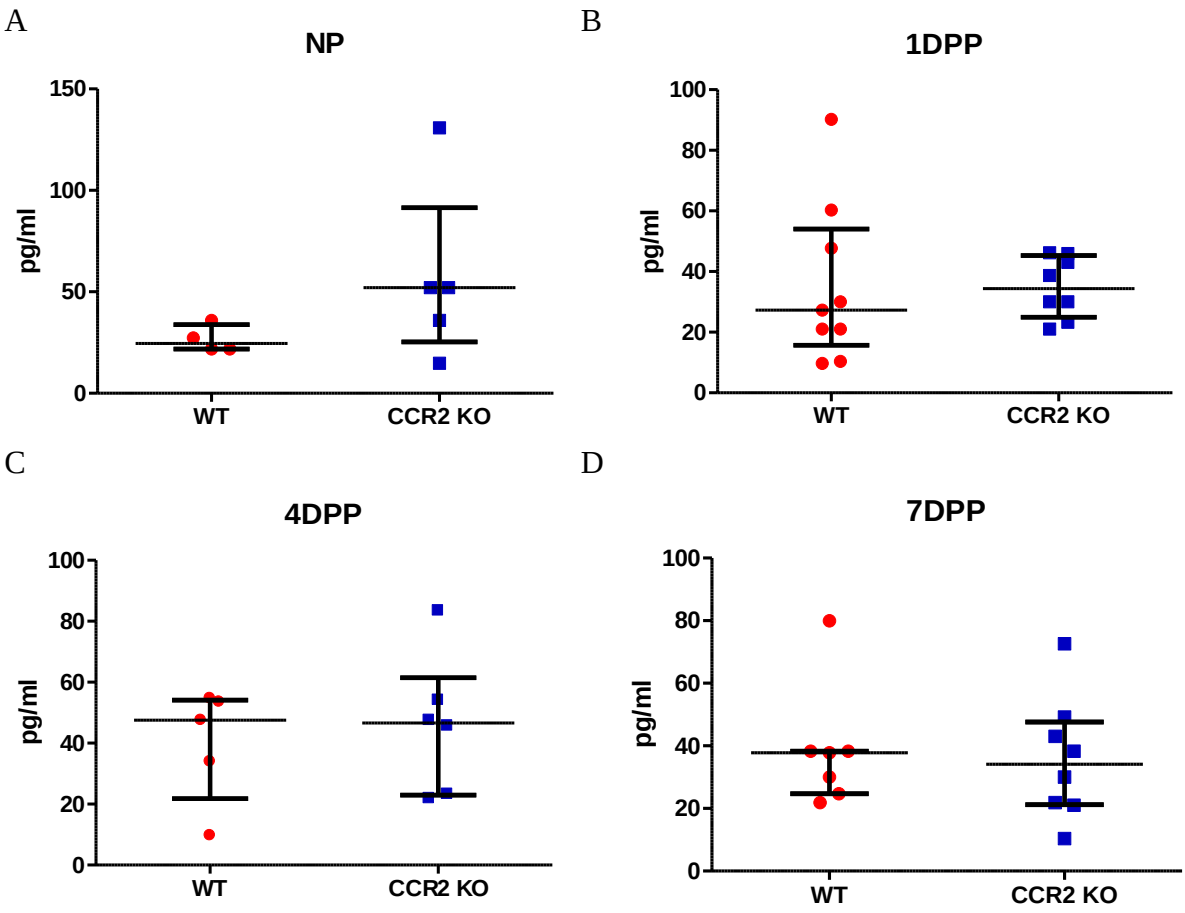

Figure 3.23. *No difference is seen in levels of CCL3 in the plasma of CCR2 KO and WT mice*.

CCL3 measured in the plasma of WT (n=4-9) and CCR2 KO (n=5-8) mice in the post-partum period following their first litter. (A) CCL3 in NP mice in WT and CCR2 KO plasma. (B) CCL3 at 1DPP in WT and CCR2 KO plasma. (C) (D) CCL3 at 7DPP in WT and CCR2 KO plasma. Data are presented as median and IQR are shown. Statistical analysis was carried out by Mann-Whitney U test, not significant. Assistance in testing the samples was given by Chris Hansell (Institute of Infection, Immunity & Inflammation, University of Glasgow).

Chapter 4: CD3+ cells in murine reproductive tissues before and after pregnancy

Introduction

After profiling myeloid cell subsets in post-partum reproductive tissues, examining CD3+ cell subsets was a natural progression because T cells, the principal CD3+ cell type, and myeloid cells closely interplay during inflammation and one subset can readily affect the behaviour of the other. The role of T cells during the post-partum period has received minimal attention, but population changes have been observed in both reproductive (Hoger et al., 1996, Kallikourdis et al., 2007, Kallikourdis and Betz, 2007, Ivanisevic et al., 2010) and peripheral tissues (Carter et al., 1983, Newport and Carter, 1983) during the reproductive process, giving cause to believe that T cells are sensitive to changes in reproductive status. Interestingly, human T cells have exhibited chemotaxis to CCL2 (Carr et al., 1994). Furthermore, expression of CCR2 has been found on subsets of CD4+ T cells in mice and humans (Bruhl et al., 2004, Connor et al., 2004, Rabin et al., 1999) and CD8+ T cells (Nansen et al., 2000, Terwey et al., 2005) in humans[11,12]. The effects of CCR2 deletion during models of inflammation have been investigated, and many of these studies have attempted to tease apart these effects on cells such as monocytes and T cells. This has been attempted in EAE (Fife et al., 2000, Izikson et al., 2000) and CIA (Bruhl et al., 2004) and during *Herpes simplex* infection (Iijima et al., 2011) but not in a model of post-partum inflammation. Having already analysed which myeloid cells were present in reproductive and peripheral tissues, demonstrated CCR2 expression by these cells, and explored the impact of CCR2 deletion, investigating CD8+ and CD4+ T cell populations was a priority in order to glean the wider leukocyte context of these changes. The main questions were: (i) Are increases in myeloid cells in post-partum reproductive tissues specific to these cells, or are CD3+ cell populations also increased? (ii) Is CCR2 active on CD3+ cell populations during this period? and (iii) Does CCR2 deficiency alter CD3+ cell distribution and abundance post-partum? T cell populations contain many subsets and investigating which subsets predominate during the post-partum period was another key research question.

In the work described in this chapter CD3+ cells were examined in reproductive and peripheral tissues to give an idea of both local and systemic changes in these cells during the post-partum period. The results showed that a high proportion of CD3+ cells in reproductive tissues were CD3+ 'double-negative' (DN) cells i.e. lacked expression of CD8 and CD4, and so this subset of cells was examined in depth. CD4+CD25+ T cells were also assessed in the same way to investigate whether counting the CD4+ T cell population as a whole masked effects on this subset. The CD4+CD25+ T cell population contains a high proportion of regulatory T cells. At the same time the CCL2/CCR2 axis in

CD3+ cells was explored in an effort to identify if any potential changes in leukocyte distribution could be potentially driven by this chemokine/receptor interaction. CCR2 KO and WT females were examined to see if there were any direct or indirect effects of deletion of CCR2 on CD3+ cells in these sites. This also included an analysis on post-partum CD3+ DN cells and CD4+CD25+ T cells.

Results

4.1. *Large increase in CD3 transcripts and CD3+ cells in the uterine horn during the post-partum period.*

First, two common T cell markers were chosen, CD3 and FoxP3, and their expression was examined by qRT-PCR in RNA samples prepared from the post-partum uterine horn. CD3 is a surface protein that associates with the TCR and is well established as a pan T cell marker (Kindt et al., 2007). CD3 was found to increase significantly over the post-partum period, with gene expression being increased at 4DPP and 7DPP compared with 1DPP (Figure 4.1A). FoxP3 is a transcription factor expressed by a major population of regulatory T cells (Sakaguchi et al., 2010). No significant differences were observed for expression of FoxP3 over the post-partum period (Figure 4.1B). However, as discussed in the previous chapter, there are distinct limitations to using gene expression analysis as an indicator for the presence of cells in the tissue being studied. Thus, to investigate cell markers on individual cells more accurately, flow cytometry was used.

A gating strategy was used to identify CD45+CD3+ cells. These cells would commonly be described as T cells, as CD3 is a pan T cell marker, but other cell types can express CD3. Therefore in this report CD3+ cells are only described as T cells when the presence of another T cell marker was confirmed. CD3 expression was defined using splenic samples in which all antibodies were included, except for anti-CD3 (CD3 FMO, Figure 4.1C). Splenocytes stained more cleanly and provided the basis for gating strategies across all tissues studied.

CD3+ cells constituted between approximately 25-30% of CD45+ in the uterine horn and cervix across all time-points studied (Figure 4.1D, left). The picture for the number of retrieved cells was quite different, with a large increase in the number of cells retrieved from the uterine horn at 1DPP compared to NP and 7DPP, though no statistically significant changes were seen in the cervix (Figure 4.1D). These results are consistent with those in the previous chapter in that far greater numbers of leukocytes were retrieved from 1DPP tissue. However, the proportion of these cells that are CD3+ is unchanged between the time points studied.

Interpretation of results from Chapter 3 and Chapter 4 side by side should be done cautiously because the results were obtained from different individuals during different experiments. Firstly, experimental variation was high, and secondly, T cells can express

CD11b in some circumstances and it was not possible to definitively rule these out from the analysis in Chapter 3.

PALN CD3+ cells were reduced at 1DPP, compared to NP animals (Figure 4.1E). The numbers of CD3+ cells retrieved from the spleen was higher at 1DPP, compared to NP and 7DPP, although CD3+ cells did not increase as a proportion of CD45+ cells, perhaps indicating that there was an overall increase in the cellularity of the spleen at this time-point (Figure 4.1E). In Chapter 3, other than eosinophils, no significant increases in myeloid cell types were observed in the spleen at 1DPP, compared to NP mice.

4.2. *The majority of CD3+ cells in the reproductive tract lack expression of CD4 and CD8.*

CD3+ cells express other markers that identify different subtypes with distinct functions. CD4 and CD8 are co-receptors and are represented on different subsets. CD8 is generally found on Tc cells and CD4 is generally found on Th cells, and both types of cells have been found to vary in abundance in reproductive and peripheral tissues during the reproductive process (Carter et al., 1983, Newport and Carter, 1983, Hoger et al., 1996, Ivanisevic et al., 2010). Therefore, these cells were profiled using flow cytometry in the uterine horn and cervix.

Gating for CD4+ and CD8+ cells within the CD3+ population was based on the clear separation of these populations in the spleen (Figure 4.2A). Strikingly, in contrast to the spleen, reproductive tissues gated for CD45 and CD3 positivity contained a majority of cells that were CD4-CD8- (i.e. 'double negative' (DN); Figure 4.2A). CD8+ T cells displayed a wide spread as a percentage of CD3+ cells, particularly in NP and 7DPP mice and no significant differences were observed in either reproductive tissue (Figure 4.2B, left). CD8+ T cells tended towards increasing as a number of retrieved cells in the uterine horn but this was not significant ($p=0.067$). There was no difference seen in CD4+ T cells in the proportion or numbers in either tissue over the post-partum period or in NP females (Figure 4.2C).

Though CD3+ DN cells have been reported in reproductive tissues before (Johansson and Lycke, 2003, Fidel et al., 1996, Flynn et al., 2000, Dambaeva et al., 2009), my work demonstrates how dominant this population is in these tissues. In uterine horn and cervix, CD3+ DN cells on average comprised between ~60-85% of CD3+ cells between NP, 1DPP

and 7DPP (Figure 4.2D, left). In terms of cells retrieved from the tissues, 1DPP uterine horn had over 9 times as many CD3+ DN cells as were found in NP uterine horn (Figure 4.2D, right). CD3+ DN cells in the cervix were over 5 times more numerous at 1DPP compared with NP females (Figure 4.2D, right). Thus, compared to CD4+ and CD8+ T cells, there appeared to be specific recruitment of CD3+ DN cells into the uterine horn and cervix at 1DPP.

Within the CD4+ T cell population, CD4+CD25+ T cells were also explored. These cells contain a population described as playing a role in a variety of reproductive situations, including participating in mediating tolerance to the foetus in mice (Mold et al., 2008, Kallikourdis and Betz, 2007, Aluvihare et al., 2004, Kallikourdis et al., 2007). They also have been described as being reduced in human ectopic reproductive tissues (Basta et al., 2010) and fluctuating during the murine oestrous cycle (Kallikourdis and Betz, 2007). They are regarded as having regulatory or suppressive functions and have often been termed Tregs (Sakaguchi et al., 2010, Peterson, 2012). CD25 was included in the T cell stain in order to allow for discrimination of these cells from the CD4+ T cell population as a whole.

When looking at retrieved cells, in the uterine horn there was a large increase in CD4+CD25+ T cells at 1DPP, compared with NP females and 7DPP mice (Figure 4.2E, right). In the cervix there was also an increase in CD4+CD25+ T cells at 1DPP, compared to NP cervix (Figure 4.2E, right). Though numbers were low, this increase in CD4+CD25+ T cells in 1DPP reproductive tissues, which paralleled changes in CD3+ DN cell abundance, could indicate a shift in T cell function to more regulatory CD3+ cell phenotypes in the early post-partum period.

4.3. *An increased proportion of CD3+ cells in the blood were DN at 1DPP.*

Although reproductive tissues appeared not to display any change in CD4+ or CD8+ T cells subsets in the post-partum period (Figure 4.2), there have been reports of systemic lymphocyte subset changes during pregnancy and the post-partum period in mice and humans (Carter et al., 1983, Newport and Carter, 1983, Hoger et al., 1996). CD8+ T cells, CD4+ T cells, CD3+ DN cells and CD4+CD25+ T cells were therefore identified and quantified in spleen, blood and PALN in NP, 1DPP and 7DPP animals (Figure 4.3).

No changes in CD3+ cell subsets were observed for PALN. Spleen displayed a general increase in CD3+ cell subsets, with CD8+, CD4+, CD3+ DN and CD4+CD25+ subsets all increased in number at 1DPP (Figure 4.3). One curious observation was the population of CD8+CD4+ (DP) cells in spleen and PALN. Though this only comprised a small population and CD3+ DP cells have been described previously (Ortolani et al., 1993, Parel and Chizzolini, 2004), the possibility that they may have been doublets was noted. Doublets are two cells associating together that the flow cytometer recognises as one 'event', so the markers of both cells appear to be expressed by only one cell.

Blood displayed no change in the percentage of CD3+ cells that were CD8+ or CD4+CD25+ across the time points studied (Figure 4.3C, Figure 4.3F, left). Strikingly however, there was a lower proportion of CD4+ T cells amongst blood CD3+ cells at 1DPP compared to NP (Figure 4.3D, left), and a concomitant increase in CD3+ DN cells (Figure 4.3E, left). Representative dot plots from the blood of NP and 1DPP females are shown in Figure 4.3B. By 7DPP, CD4+ T cells had returned to NP levels, but CD3+ DN cells were still elevated in the blood. Thus, there were clearly a greater number of CD3+ DN cells in the blood at 1DPP, compared with NP, and this appeared to be retained up to 7DPP.

4.4. *CCR2-mediated internalisation of CCL2-AF647 by CD3+ DN cells and CD4+CD25+ T cells in blood during the post-partum period*.

As with the myeloid cells in the previous chapter, CCL2-AF647 internalisation by CD3+ cells was measured to determine whether there was any CCR2 on these cells that could be potentially facilitating cell migration into reproductive tissues from the blood. When lymphoid tissues and blood were examined, representative histograms showed that only minimal amounts of fluorescent chemokine were internalised by CD8+ T cells and CD4+ T cells, although uptake by CD3+ DN cells and CD4+ CD25+ T cells was much more marked (Figure 4.4A). Cells of all types showed a marginally higher percentage of CCL2-AF647+ CD3+ cells in the blood than in lymphoid tissues. No differences in proportion of CCL2-AF647+ CD8+ T cells and CCL2-AF647+ CD4+ T cells over the post-partum period were seen in blood or either of the other tissues (Figure 4.4B-C). However, the proportion of CCL2-AF647+ CD3+ DN cells was ~45% at 1DPP, while in NP females it was only ~27% (Figure 4.4D, left). The lymphoid tissues showed no fluctuation in the proportion of CD3+ DN cells that were CCL2-AF647+ (Figure 4.4D), and the number of CCL2-AF647+ CD4+CD25+ cells was unchanged in all tissues between the groups

(Figure 4.4E). Since a greater proportion of blood CD3+ cells were DN at 1DPP, and a higher percentage of these cells were capable of internalising CCL2-AF647+, the actual number of CCL2-AF647+ CD3+ DN cells in the blood was presumably far greater at 1DPP than NP (Figure 4.3).

To determine whether CCL2-AF647+ uptake was mediated by CCR2, 1DPP WT and CCR2 KO samples were compared (Figure 4.5). No CCR2 dependent CCL2-AF647 uptake was observed in CD8+ T cells (Figure 4.5B). Uptake by blood CD4+ T cells required this receptor (Figure 4.5C), and it was responsible for CCL2-AF647 uptake by CD4+ CD25+ T cells at 1DPP, most notably in blood (Figure 4.5E). CCR2 deficiency also reduced CCL2-AF647+ uptake by CD3+ DN cells in blood and PALN, but not spleen (Figure 4.5D). Thus, at 1DPP, CCR2 appears to be expressed by small subsets of CD4+ and CD4+CD25+ T cells, and most notably by CD3+ DN cells, particularly those circulating in the blood. In the case of CD3+ DN cells, this could be linked to the large increase in CD3+ DN cells in reproductive tissues 1DPP.

4.5. *CCR2 is not detectably expressed by CD3+ cells in reproductive tissues.*

Next, CCR2 expression by CD3+ cells in reproductive tissue was examined (Figure 4.6 & 4.7). CD4+ and CD8+ T cells internalised very little CCL2-AF647, although some could be classified as CCL2-AF647+. The proportion of CD8+ T cells internalising CCL2-AF647 varied between 20-40% over the time-points in the uterine horn and 35-60% in the cervix but no significant change was seen in either tissue over time (Figure 4.6B). Fewer CD4+ T cells appeared to be CCL2-AF647+, between approximately 5-30% in uterine horn and 30-45% in the cervix and there was no significant change between NP, 1DPP and 7DPP (Figure 4.6C). The proportions of CCL2-AF647+ CD3+ DN cells and CCL2-AF647+ CD4+ CD25+ T cells were relatively high, compared with the other cell types but neither changed significantly in the reproductive tissues across the different groups (Figure 4.6D). However, uptake between 1DPP WT and CCR2 KO animals was roughly equivalent for all four cell types in both tissues, as indicated by the representative histograms and graphs shown in Figure 4.7. Thus, the small amount of internalisation seen with WT cells could not convincingly be attributed to CCR2 expression, and may have been mediated by non-specific mechanisms or by a receptor other than CCR2, such as the scavenger receptor D6.

4.6. *CCR2 deficiency has no impact on the abundance of CD3+ cell subsets in reproductive tissues.*

Next, the impact of CCR2 deficiency on CD3+ cell abundance was explored in reproductive tissues and elsewhere. Although CCR2 was not active on CD8+ T cells, CD4+ T cells, CD3+ DN cells and CD4+ CD25+ T cells in reproductive tissues at 1DPP, it was present on some of these subsets in blood and could theoretically have been down-regulated by ligand-driven internalisation upon arrival in the reproductive tissues. Moreover, as seen in the previous chapter, myeloid cells were subject to marked changes in CCR2 KOs at 1DPP and knock on effects disturbing CD3+ cell populations could have occurred. Reproductive tissues from CCR2 KO females were studied and the data presented alongside WT data from Figure 4.2 in order to determine if they displayed a deficit in CD8+ T cells, CD4+ T cells, CD3+ DN cells and CD4+ CD25+ T cells at 1DPP (Figure 4.8). There was quite a lot of variation between individuals, but it was clear that there were no differences between WT and CCR2 KO at 1DPP when any CD3+ cell subset was examined. Thus, in contrast to myeloid cells (Chapter 3), CCR2 deficiency has no effect on CD3+ cell recruitment to post-partum reproductive tissues.

4.7. *Effects of CCR2 deletion on CD3+ cell populations vary depending on reproductive status*.

CD3+ cells were also enumerated in the blood, spleen and PALN of 1DPP CCR2 KO mice and compared to 1DPP WT data from Figure 4.3 (Figure 4.9). Although there were some subtle effects of CCR2 deficiency in spleen and PALN, the most striking result was in the blood where there was a substantial difference in CD3+ DN cells. The proportion of CD3+ cells with a DN phenotype in the blood of WT mice was over 2.5 times that observed in CCR2 KO animals (Figure 4.9C, left). Representative plots in Figure 4.9E illustrate this difference. CD4+ T cells were somewhat more frequent amongst CCR2 KO CD3+ cells, although this failed to achieve statistical significance (Figure 4.9B, left). This surprising difference may not have been post-partum specific, so the experiment was repeated in NP animals (Figure 4.10A-B). BM was included on this occasion, and it was notable that a high proportion of CD3+ cells in this tissue were DN (Figure 4.10A, left). However, in spleen, PALN, BM and blood there were no differences in the percentage or numbers of CD3+ DN cells between WT and CCR2 KO. Unexpectedly, therefore, these data suggest that CCR2 is required for a post-partum switch in the CD3+ population in the blood characterised by an increased frequency of DN cells.

The CD3+ DN cells in the reproductive tissues of NP WT and CCR2 KO mice were also analysed. On this occasion, DN cells constituted a higher percentage of CD3+ cells in NP reproductive tissues (Figure 4.10B, left) than previously seen (Figure 4.2). However, no difference was seen between WT and CCR2 KO animals either for the percentage of DN cells in the CD3+ population or for the number of cells retrieved (Figure 4.10B). This was consistent with findings from comparisons done on 1DPP tissues (Figure 4.8).

4.8. *DN cells in the NP thymus show a subtle change in their developmental stages when CCR2 is deleted.*

This investigation into the effect of CCR2 deficiency on NP lymphoid tissues was also extended to the thymus. Thymocytes were gated differently to other tissues as CD3 does not label all T cells in the thymus (Turka et al., 1992, Godfrey et al., 1993). Instead, as shown in Figure 4.11A, cells were gated by CD45 and separated by CD4 and CD8. This staining was clearly very different to that seen in other tissues studied, with a large DP population, which was not present when CD4/CD8 staining was examined in other tissues such as the spleen (Figure 4.3). When the proportions were examined around 70% of CD45+ cells in both WT and CCR2 KO were DP cells (Figure 4.11B, left). Proportions and numbers of CD8+ cells, CD4+ cells and DN cells in the thymus were similar between WT and CCR2 KO (Figure 4.11B). DN cells were then split by their expression of CD25 and CD44, markers which define the developmental stages of DN cells. CD44+CD25+ DN cells, corresponding to stage DN2, were reduced in CCR2 KOs compared to WTs (Figure 4.11C, left). The reduction in proportion of CD44+CD25+ DN cells in CCR2 KOs may indicate some role for CCR2 in the progression of cells through the developmental stages in the thymus.

4.9. S*ome CCL2-AF647 uptake by CD3+ DN cells in NP peripheral tissues was CCR2 dependent.*

CCL2-AF647 uptake by CD3+ DN cells was also investigated in CCR2 KO and WT NP mice (Figure 4.12). Typical fluorescence profiles for lymphoid tissues and blood are displayed in Figure 4.12A. In NP females, there was a reduction in CCL2-AF647+ CD3+ DN cells in CCR2 KO spleen and PALN, compared to these tissues from WT mice, demonstrating that some of these cells express CCR2 (Figure 4.12B). The percentage of CCL2-AF647+ CD3+ DN cells from BM was not different between WT and CCR2 KO mice (Figure 4.12B). Finally, NP blood exhibited no consistent CCR2 based difference in percentage of CCL2-AF647+ CD3+ DN cells (Figure 4.12B), contrary to the large

difference seen at 1DPP (Figure 4.9). These results indicated that the relationship between CCL2-AF647 uptake and CD3+ DN cells was dynamic and was sensitive to reproductive status.

4.10. *CCL2-AF647 uptake by CD3+ DN cells is CCR2-dependent in NP uterine horn*.

No CCR2-dependent CCL2-AF647 uptake had been seen at 1DPP by CD3+ DN cells in reproductive tissues (Figure 4.7), but in NP females the proportion of WT CD3+ DN cells in the uterine horn that internalised CCL2-AF647 was at least double that seen in CCR2 KO uterine horn indicative of CCR2 expression by some of these cells (Figure 4.13B). However, no CCR2 dependent CCL2-AF647 uptake was seen in the cervix (Figure 4.13B).

The CCR2 dependence of CCL2-AF647 uptake by WT CD3+ DN cells was confirmed by competition experiments in which excess unlabelled CCL2 or CCL22 was included during the incubation step. Unlabelled CCL2 should block uptake mediated by CCR2 and the scavenger receptor D6, while CCL22, which is a ligand for D6 and not CCR2, should only block D6-mediated CCL2-AF647 internalisation (Hansell et al., 2011b). CCL2-AF647 internalisation by WT uterine CD3+ DN cells was unaffected by CCL22 competition (Figure 4.13C-D), but was successfully blocked by an excess of unlabelled CCL2 (Figure 4.13E-F). This confirmed that the majority of CCL2-AF647 uptake by CD3+ DN cells in the NP uterine horn of WT mice was mediated by CCR2.

4.11. Summary

In this chapter the project focussed on T cell subsets in the post-partum period. The broad increase in myeloid cells in the uterine horn in Chapter 3 suggested the T cells may also have been recruited to the tissue as part of a typical inflammatory response to the process of labour. CCR2, shown in Chapter 3 to be active on myeloid cells during the post-partum period, was also investigated on T cells for its activity and whether CCR2 deletion affected T cell populations at 1DPP and in NP mice. Potential regulatory populations were also investigated, namely CD3+ DN cells and CD4+CD25+ T cells.

- In terms of the number of retrieved cells, there was a large increase in CD3+ cells in the uterine horn, driven mainly by the rise in the numbers of CD3+ DN cells and CD4+CD25+ T cells. CD3+ DN cells were found to constitute the overwhelming majority of CD3+ cells in reproductive tissues.

- At 1DPP there was a CCR2-dependent shift from CD4+ T cells towards CD3+ DN cells in the blood, resulting in a large increase in these cells at 1DPP compared to NP animals.
- At 1DPP, subsets of blood borne CD3+ DN cells and CD4+CD25+ T cells displayed CCR2 activity. No CCR2 activity was seen by any T cell subset in reproductive tissues at 1DPP, and CCR2 deletion had no effect on T cell populations in uterine horn or cervix.
- In NP blood, no CCR2 activity was seen on CD3+ DN cells, and no baseline CCR2-related differences were seen in the CD3+ DN cell population.
- When NP uterine horn was examined, there was no effect of CCR2 on the proportion or numbers of CD3+ DN cells. However unlike at 1DPP, CCR2 activity was confirmed on these cells.

These results indicate that CCR2 is responsible for the increase in the proportion of CD3+ DN cells in the blood at 1DPP, and that these cells are the dominant lymphocyte population seen in the uterine horn. Therefore, further characterisation was desirable in order to draw conclusions about their possible function. Chapter 5 describes the use of multicolour flow cytometry to characterise this population in far greater detail based on carefully selected surface markers.

Figure 4.1. *Large increase in CD3 transcripts and CD3+cells in the uterine horn during the post-partum period*.

(A-B) Expression of genes encoding CD3 and FoxP3 in the UH of mice in at 1DPP (n=5), 4DPP (n=6) and 7DPP (n=5) after their first pregnancy. Expression was calculated as $100x2^{\Delta CT}$, where $\Delta CT=CT^{target}-CT^{GAPDH}$ to establish target expression as a percentage of expression of the endogenous control GAPDH. NP mRNA samples were produced and processed by Fiona Menzies and Abdul Khan (Obstetrics and Gynaecology, University of Glasgow) and re-analysed for this project. (C-D) CD3+ cells in reproductive tissues in NP (n=4), 1DPP (n=5), 7DPP (n=5) mice, measured by flow cytometry were also examined. (C) Representative plots of the gating strategy for detection of CD45+CD3+ cells by flow cytometry. After a physical gate to remove cell debris and aggregates (not shown), cells were gated live by 7-AAD-, then as CD45+ for total leukocytes and finally CD3+ cells. Gates were drawn using the CD3 FMO (no CD3) splenocyte control. (D) Reproductive tissues. Left; CD3+ cells as a percentage of retrieved CD45+ cells. Right; Total CD3+ cells retrieved. (E) Peripheral tissues. Left; CD3+ cells as a percentage of retrieved CD45+ cells. Right; Absolute number of CD3+ cells. Results presented as mean±SEM. Statistical analysis was carried out by one-way ANOVA with a Tukey post-test, *$p<0.05$ **$p<0.01$ ***$p<0.001$.

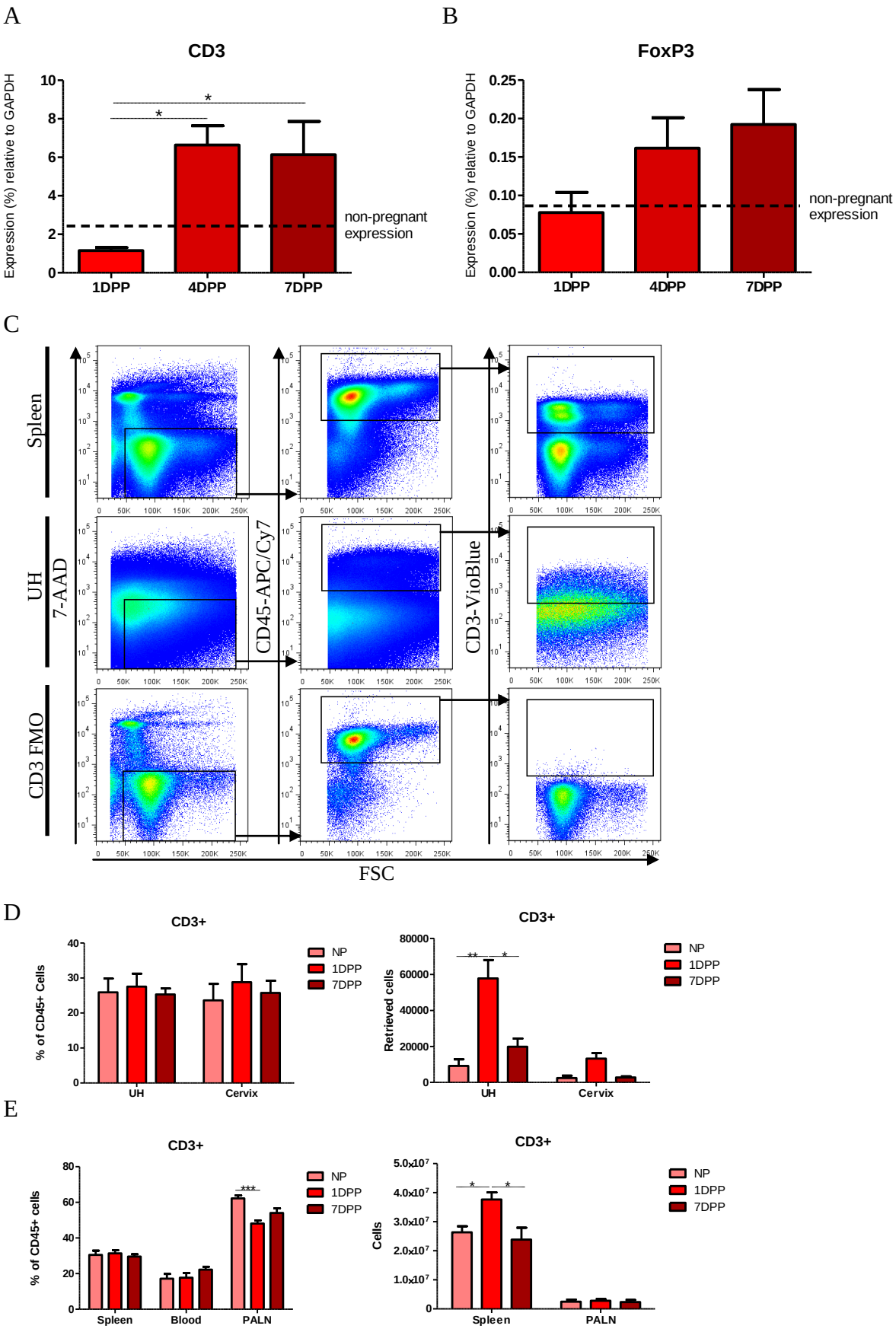

Figure 4.1. *Large increase in CD3 transcripts and CD3+cells in the uterine horn during the post-partum period (legend opposite).*

Figure 4.2. *CD3+ DN cells in the reproductive tract increase dramatically at 1DPP.*
Measurement of CD3+ cells in single cell suspensions of reproductive tissues using flow cytometry stained with antibodies against CD45, CD3, CD4 and CD8 in NP, 1DPP and 7DPP mice (n=3-5). (A) Splenocytes from each individual were stained to construct a gating strategy for identification of [1] CD8+ T cells, [2] CD4+ T cells, [3] CD3+ DN cells and [4] CD4+CD25+ T cells. Representative images of CD4/CD8 staining in spleen and reproductive tissues at 1DPP from one individual are shown. (B) Left; CD8+ T cells as a percentage of CD3+. Right; Total CD8+ T cells retrieved. (C) Left; CD4+ T cells as a percentage of CD3+ cells. Right; Total CD4+ T cells retrieved. (D) Left; CD3+ DN cells as a percentage of CD3+. Right; Total CD3+ DN cells retrieved. (E) Left; CD4+CD25+ T cells as a percentage of CD3+ cells. Right; Total CD4+CD25+ T cells retrieved. Data presented as mean±SEM. Statistical analysis was carried out by one-way ANOVA, with a Tukey post-test *$p<0.05$, **$p<0.01$.

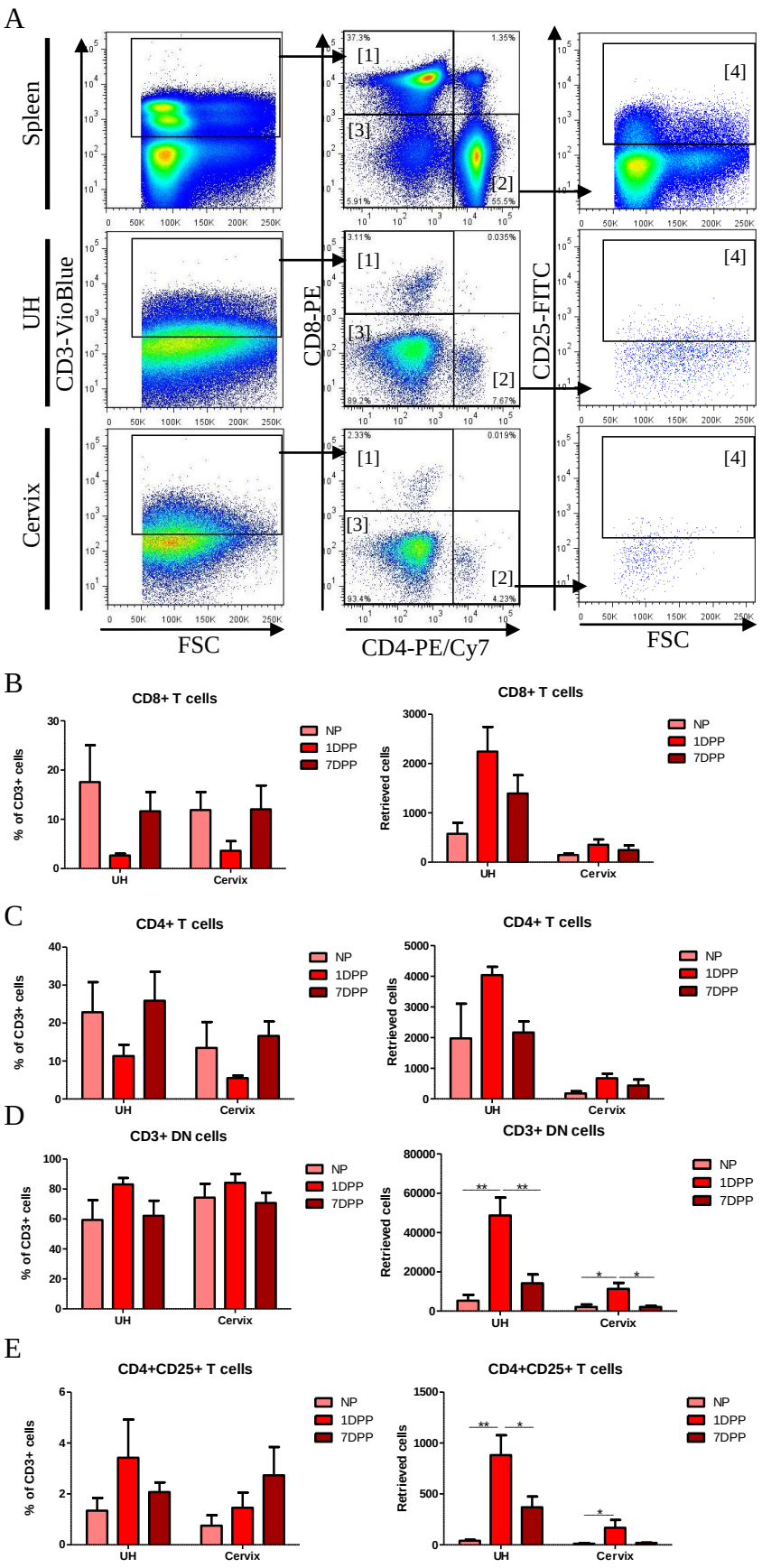

Figure 4.2. *CD3+ DN cells in the reproductive tract increase dramatically at 1DPP (legend opposite).*

Figure 4.3. *An increased proportion of CD3+ cells in the blood are DN at 1DPP*.
CD3+ subsets in the spleen (n=3-9), blood (n=5-9), and PALN (n=4-9) of NP females, at 1DPP and 7DPP by flow cytometry. (A) Gating strategy based on splenocytes as in fig 4.2, [1] CD8+ T cells, [2] CD4+ T cells, [3] CD3+ DN cells and [4] CD4+CD25+ T cells. (B) Plots showing large increase in CD3+ DN cells in blood at 1DPP, gated for CD45 and CD3. (C) Left; CD8+ T cells as a proportion of CD3+ cells. Right; absolute numbers of CD8+ T cells. (D) Left; CD4+ T cells as a proportion of CD3+ cells. KW. Right; absolute numbers of CD4+ T cells. (E) Left; CD3+ DN cells as a percentage of CD3+ cells. KW. Right; Absolute CD3+ DN cell numbers. (F) Left; CD4+ T cells as a proportion of CD3+ cells. KW. Right; absolute numbers of CD4+ T cells. Data presented as mean±SEM. Data were analysed using one-way ANOVA with a Tukey post-test, except where indicated by KW where a Kruskall-Wallis test with a Dunn's post-test due to unequal variances was used *$p<0.05$ **$p<0.01$ ***$p<0.001$.

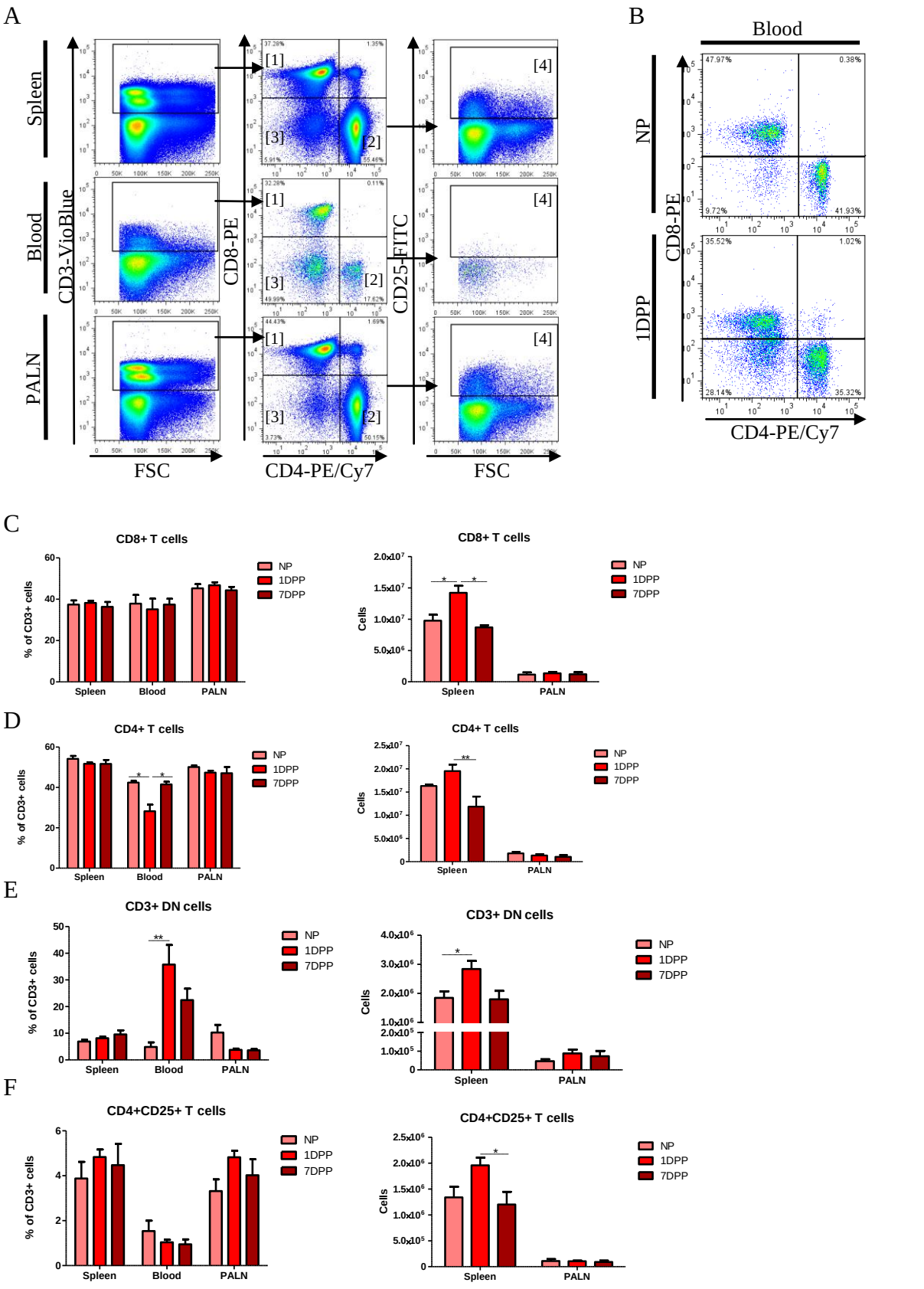

Figure 4.3. *An increased proportion of CD3+ cells in the blood are DN at 1DPP (legend opposite).*

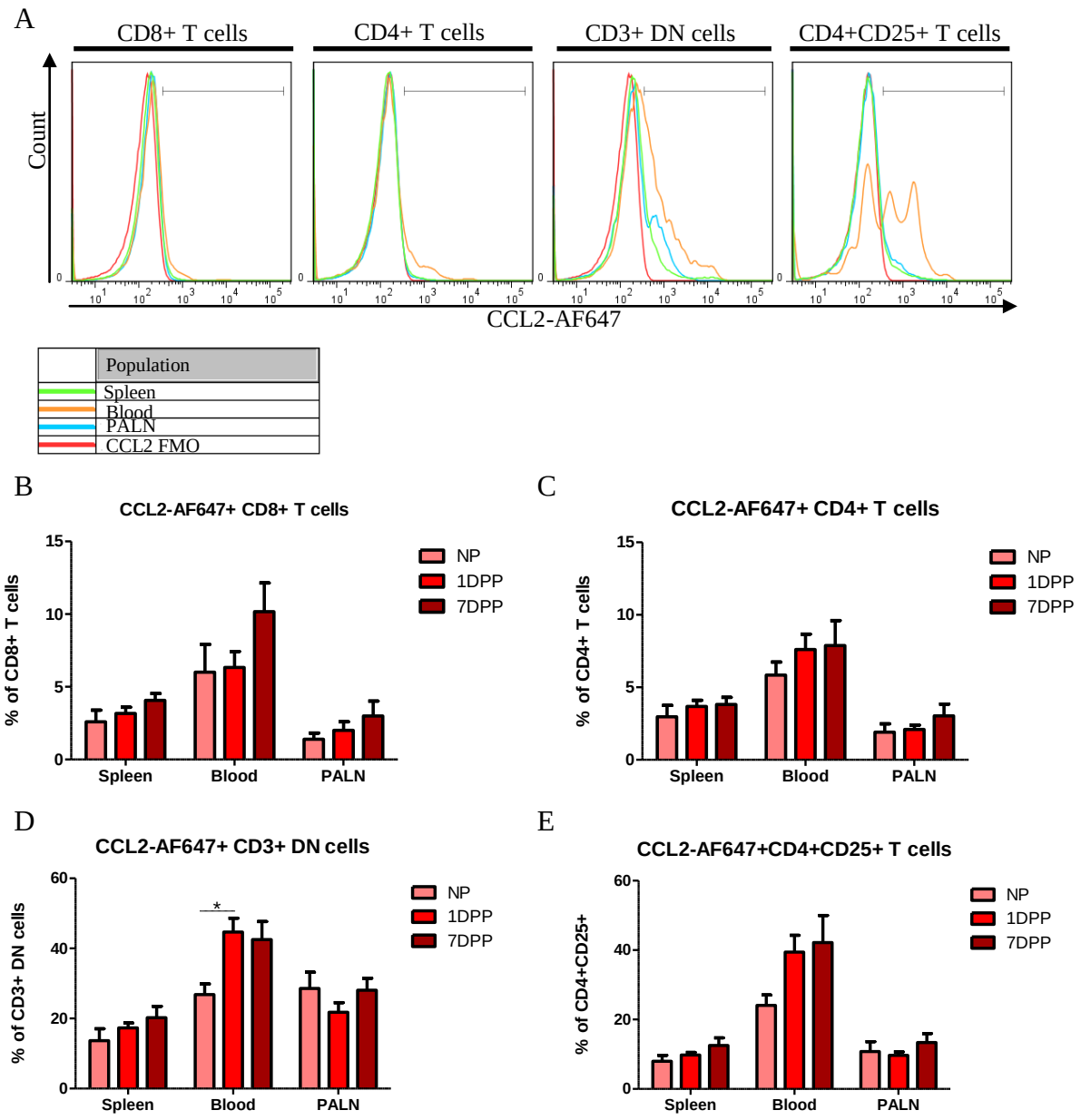

Figure 4.4. *Internalisation of CCL2-AF647 is highest in CD3+ DN cells and CD4+CD25+ T cells in peripheral tissues during the post-partum period.*

Uptake of fluorescent CCL2-AF647 by CD3+ cells measured by flow cytometry in spleen (n=6-9), blood (n=6-9) and PALN (n=6-9) in NP, 1DPP and 7DPP females. Single cell suspensions were incubated with 25nM CCL2-AF647 for 65mins. Gates were drawn as in fig 4.3. (A) Typical histogram of fluorescent CCL2-AF647 uptake of CD3+ cell populations in peripheral tissues at 1DPP, with the FMO control (no CCL2-AF647) shown for CD3+ spleen in red. Proportion of cell type internalising CCL2-AF647 (B) CD8+ T cells (C) CD4+ T cells (D) CD3+ DN cells (E) CD4+CD25+ T cells. Data presented as mean±SEM. Statistical analysis was carried out by one-way ANOVA with a Tukey post-test *$p<0.05$.

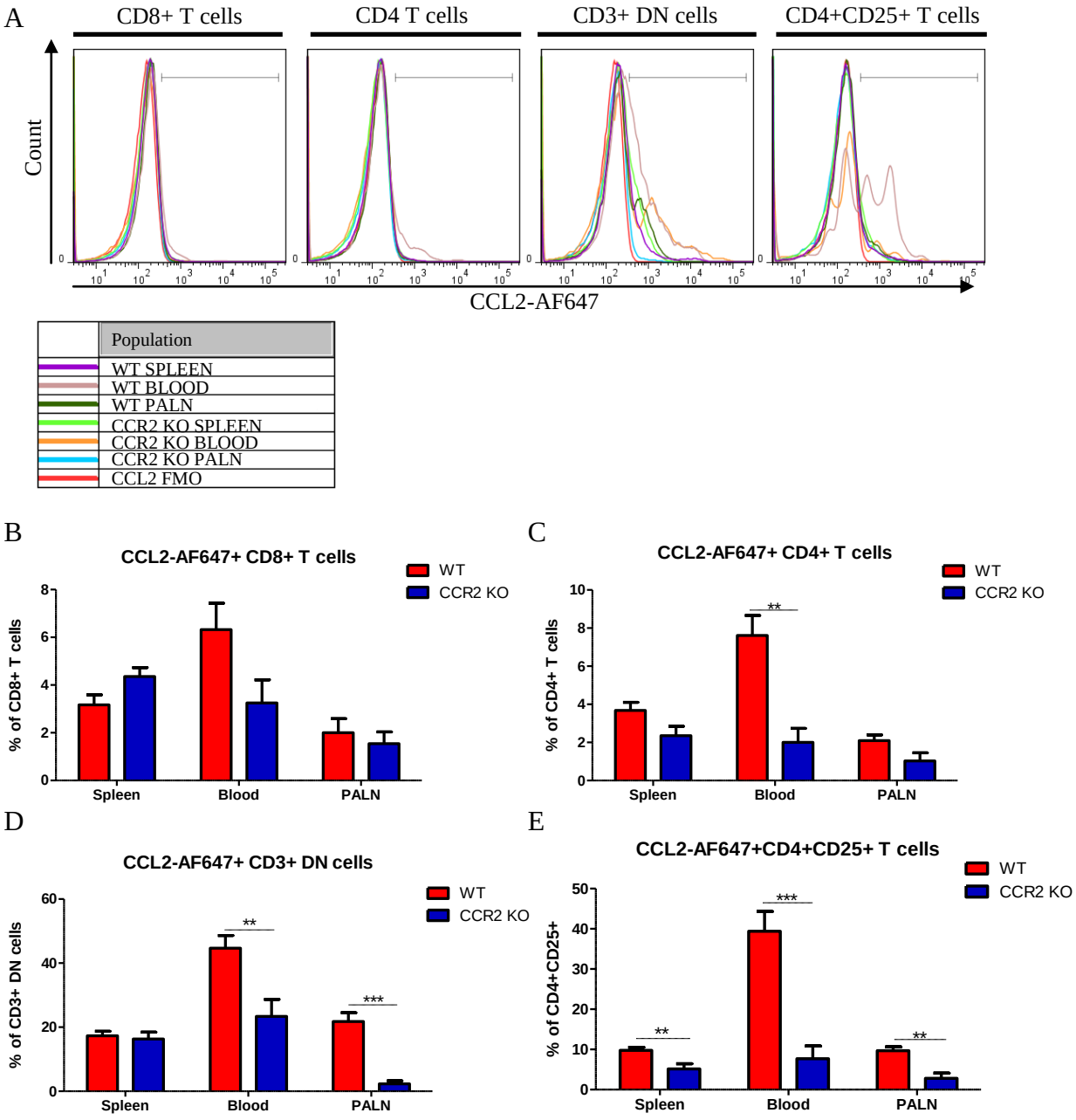

Figure 4.5. *In blood and PALN CCL2-AF647 uptake by CD3+DN cells and CD4+CD25+ T cells is CCR2 dependent at 1DPP.*

Uptake of fluorescent CCL2-AF647 by CD3+ cells was measured by flow cytometry in spleen (n=5-9), blood (n=4-9) and PALN (n=4-9) in 1DPP WT and CCR2 KO females. 1DPP WT data shown in fig 4.4. Single cell suspensions were incubated with 25nM CCL2-AF647 for 65mins. (A) Typical histograms of fluorescent CCL2 uptake by CD3+ cells subsets, with the WT FMO control (no CCL2-AF647) for CD3+ spleen shown in red. Proportion of cell type internalising CCL2-AF647 (B) CD8+ T cells (C) CD4+ T cells (D) CD3+ DN cells (E) CD4+CD25+ T cells. Data presented as mean±SEM. Statistical analysis was carried out by Student's t-test, with a Welch's correction where appropriate *p<0.05 **p<0.01 ***p<0.001.

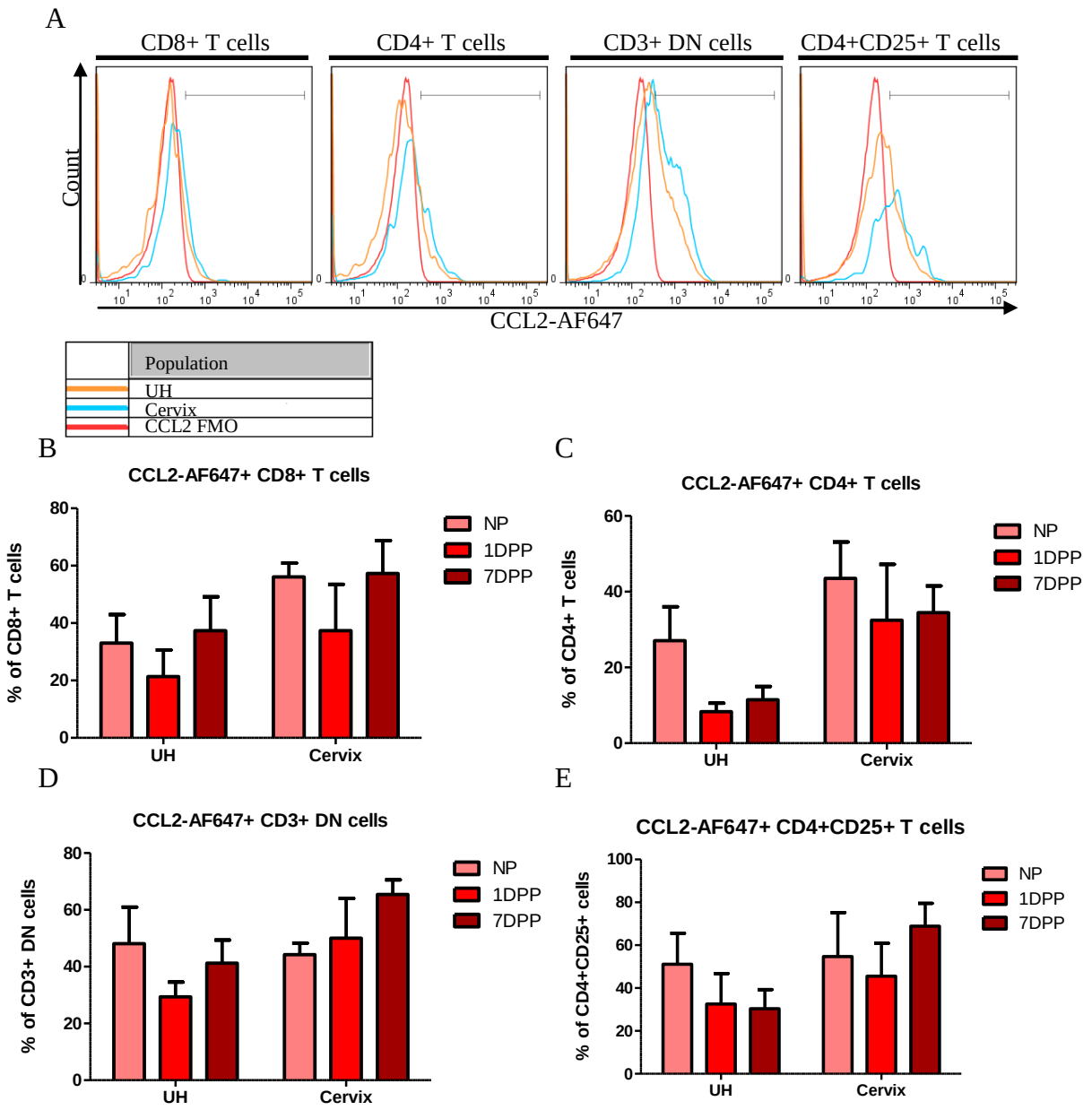

Figure 4.6. *No variation in CCL2-AF647 internalisation in any CD3+ subset studied in reproductive tissues during the post-partum period.*

Uptake of fluorescent CCL2-AF647 by CD3+ cells was measured by flow cytometry in UH (n=3-5), cervix (n=3-5) in NP, 1DPP and 7DPP mice. Single cell suspensions were incubated with 25nM CCL2-AF647 for 65mins. (A) Typical histogram of fluorescent CCL2-AF647 uptake of CD3+ cell populations, with the FMO control (no CCL2-AF647) from CD3+ spleen shown in red. Percentage of cell population internalising CCL2-AF647 (B) CD8+ T cells (C) CD4+ T cells (D) CD3+ DN cells (E) CD4+CD25+ T cells. Data presented as mean±SEM. Statistical analysis was carried out by one-way ANOVA, not significant.

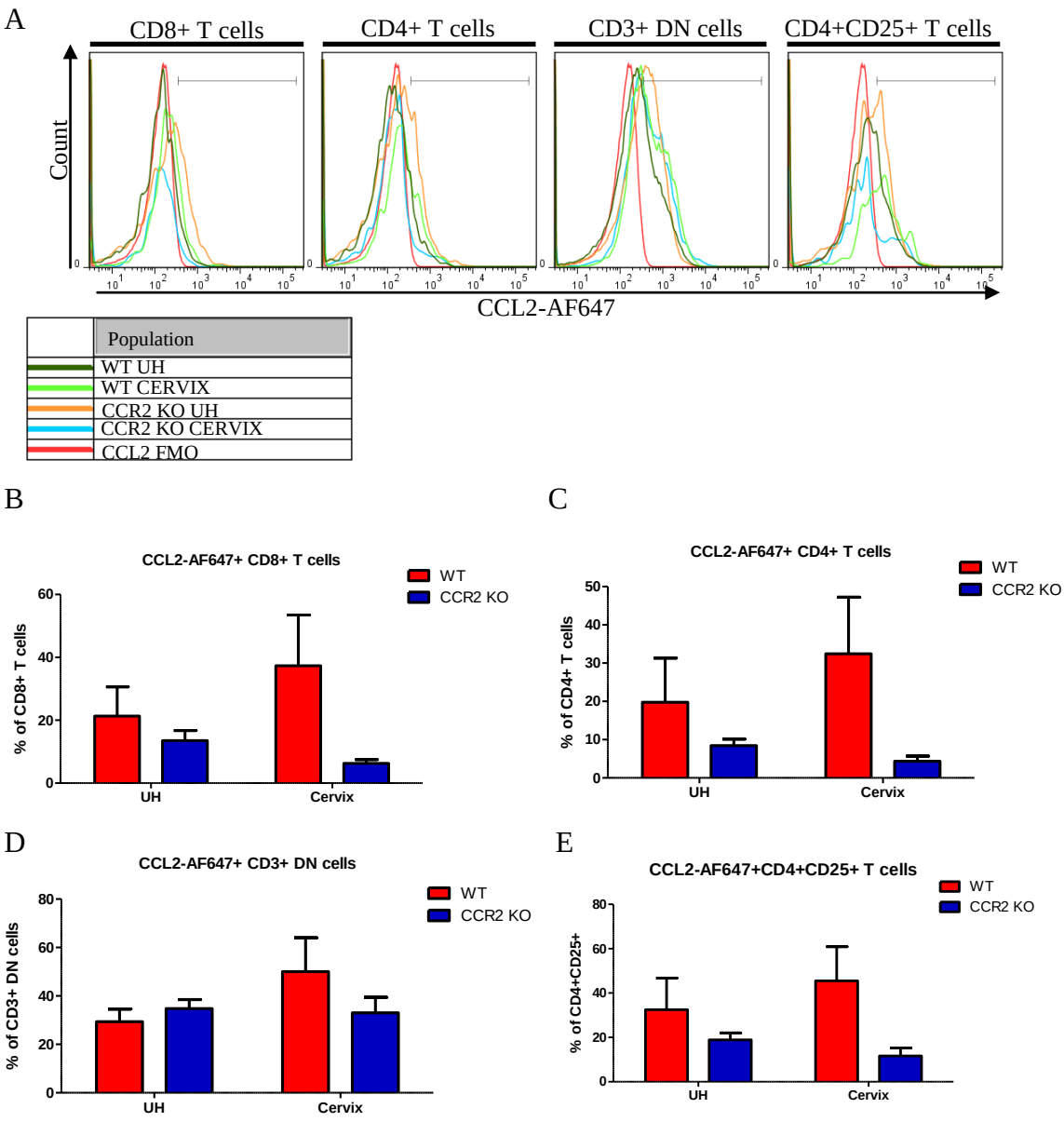

Figure 4.7. *CCL2-AF647 uptake by CD3+ cells in reproductive tissues was not CCR2 dependent at 1DPP*.

Uptake of fluorescent CCL2-AF647 by CD3+ cell subsets measured by flow cytometry in UH (n=4-5) and cervix (n=4-5) in 1DPP WT and CCR2 KO females. 1DPP WT data shown in fig 4.6. (A) Typical histograms of fluorescent CCL2-AF647 uptake by CD3+ cell populations, with the FMO (no CCL2-AF647) control for CD3+ spleen shown in red. Proportion of cell population internalising CCL2-AF647 (B) CD8+ T cells (C) CD4+ T cells (D) CD3+ DN cells (E) CD4+CD25+ T cells. Data presented as mean±SEM. Statistical analysis was carried out by Student's t-test, with a Welch's correction where appropriate, not significant.

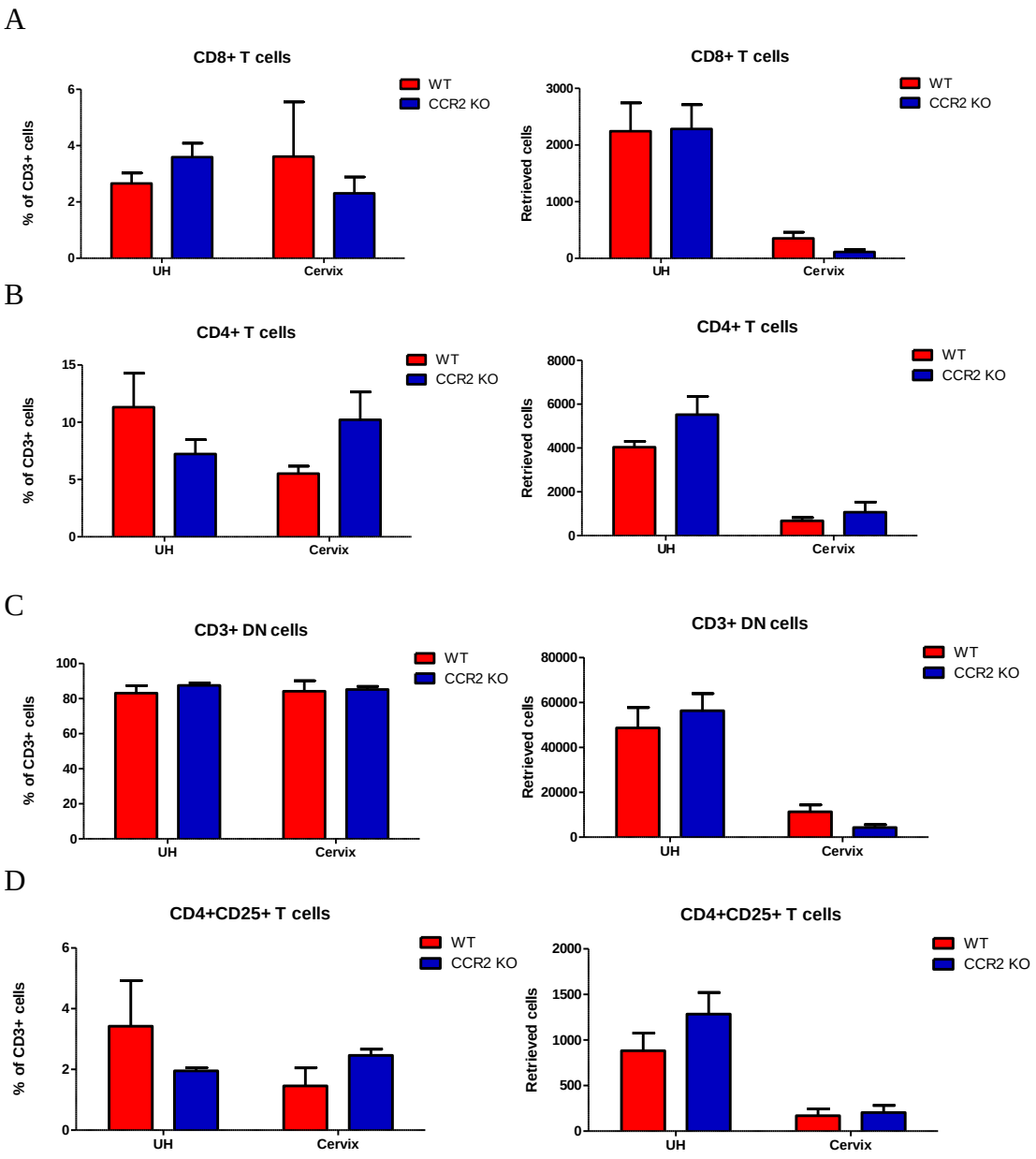

Figure 4.8. *No difference in abundance of CD3+ cell subsets in WT and CCR2 KO reproductive tissues*.

CD3+ cells measured by flow cytometry in UH (n=3-5), cervix (n=3-5) in 1DPP WT and CCR2 KO females. 1DPP WT data from fig 4.2. (A) Left; Proportion of CD8+ T cells. Right; CD8+ T cells retrieved. (C) Left; Proportion of CD4+ T cells. Right; CD4+ T cells retrieved. (D) Left; Proportion of CD3+ DN cells. Right; CD3+ DN cells retrieved. (E) Left; Proportion of CD4+CD25+ T cells. Right; CD4+CD25+ T cells retrieved. Data presented as mean±SEM. Statistical analysis was carried out by Student's t-test, not significant.

Figure 4.9. *The dramatic rise in blood CD3+ DN cells at 1DPP is not seen in CCR2 KOs*. CD3+ cells measured by flow cytometry in spleen (n=4-9), blood (n=4-9) and PALN (n=4-9) in 1DPP WT and CCR2 KO females. 1DPP WT data shown in fig 4.3. (A) Left; Proportion of CD8+ T cells. Right; Numbers of CD8+ T cells. (B) Left; Proportion of CD4+ T cells. Right; Numbers of CD4+ T cells. (C) Left; Proportion of CD3+ DN cells. Right; Numbers of CD3+ DN cells. (D) Left; Proportion of CD4+CD25+ T cells. Right; Numbers of CD4+CD25+ T cells. (E) Comparable plots gated for CD45 and CD3 from blood showing the larger proportion of CD3+ cells that were DN in WT, compared with CCR2 KO at 1DPP. Data presented as mean±SEM. Statistical analysis was carried out by Student's t-test, with Welch's correction where appropriate, *p=0.05.

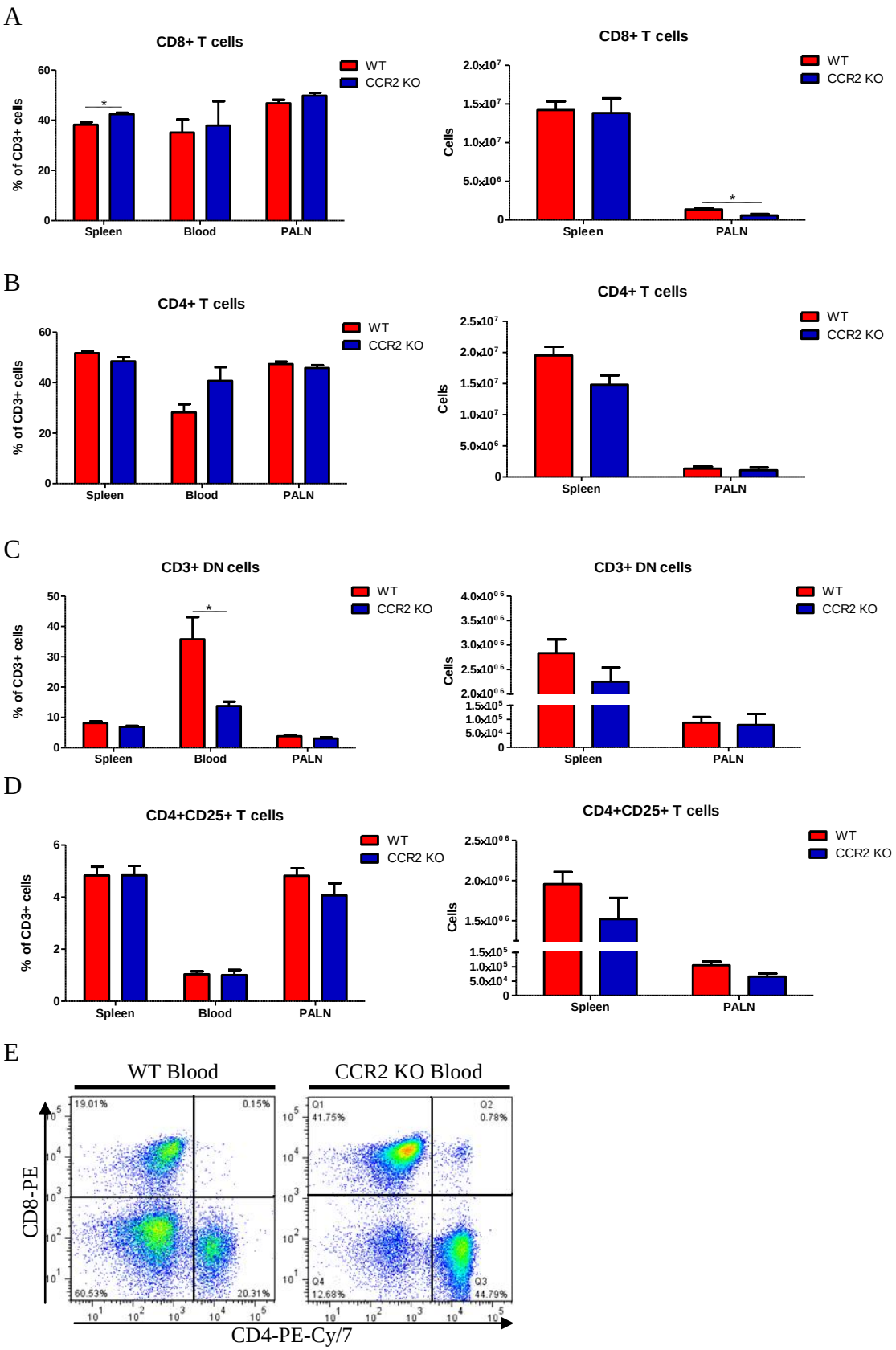

Figure 4.9. *The dramatic rise in blood CD3+ DN cells at 1DPP is not seen in CCR2 KOs (legend opposite).*

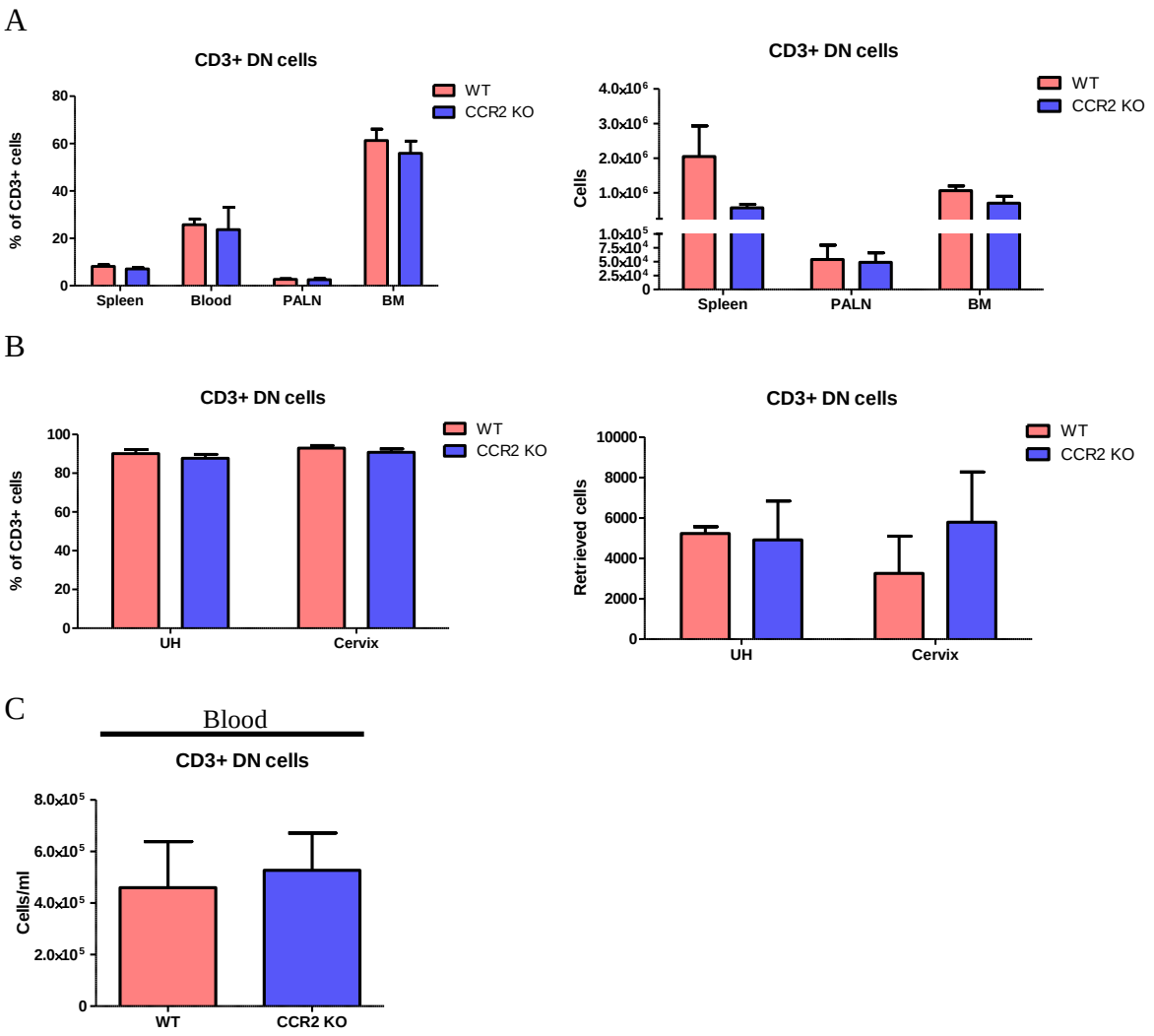

Figure 4.10. *No difference in CD3+ DN cell percentage or numbers between WT and CCR2 KO in NP tissues.*

Measurement of CD3+ DN cells using flow cytometry in spleen (n=4), blood (n=4-6), PALN (n=4), BM (n=4) UH (n=3-4) and cervix (n=3-4) in WT and CCR2 KO NP females. (A) Left; Proportion of CD3+ DN cells. Right; Retrieved CD3+ DN cells. (B) Left; Proportion of CD3+ DN cells. Right; Retrieved CD3+ DN cells. (C) CD3+ DN cells per ml of blood. Statistical analysis carried out by Student's t-test, with Welch's correction where appropriate, not significant.

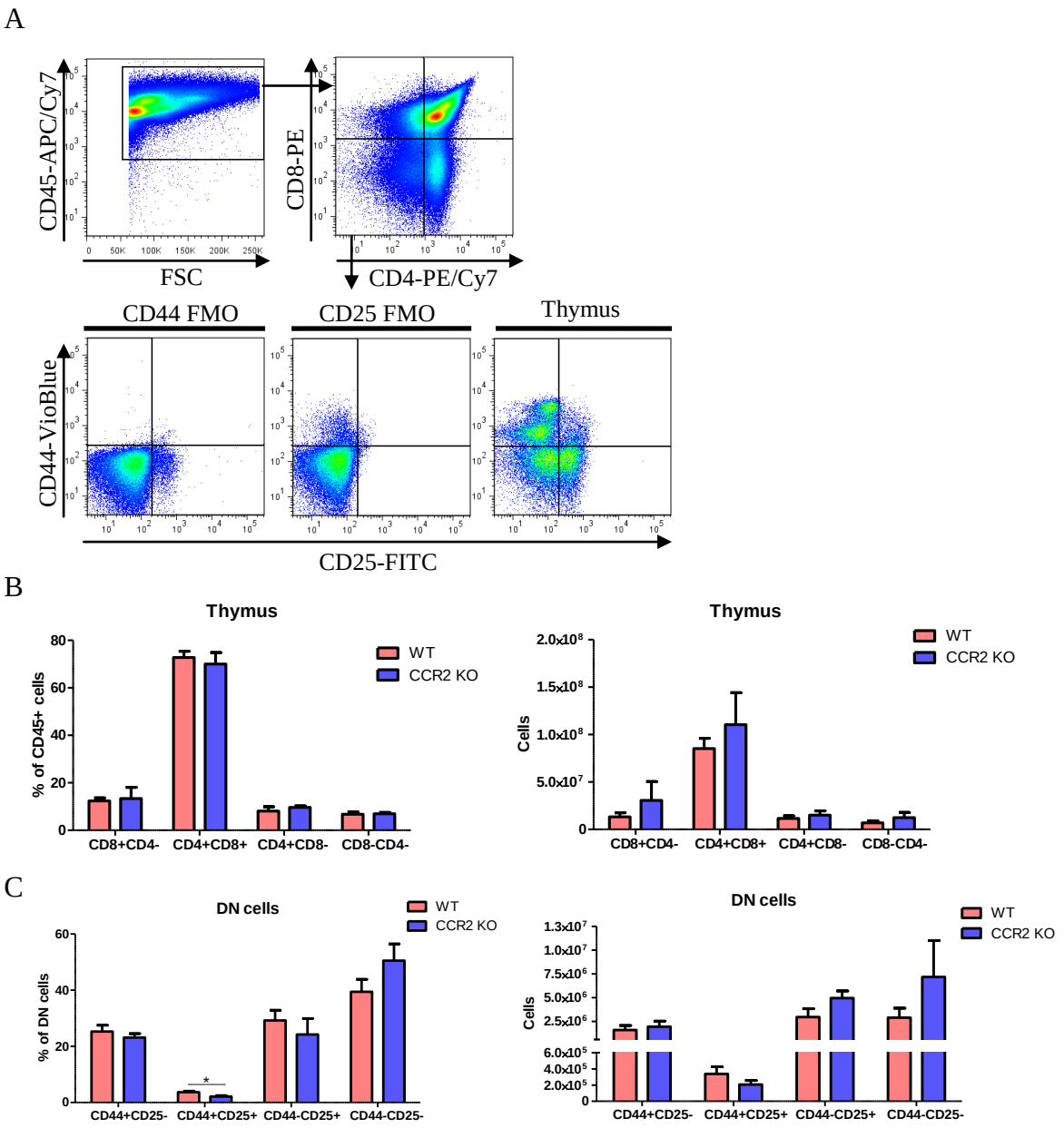

Figure 4.11. *CD44+ CD25+ DN cells make up a lower percentage of DN cells in the thymus of CCR2 KO mice, compared with WTs*.

Measurement of thymocyte subsets, including DN cells, using flow cytometry in the thymuses (n=3-4) from CCR2 KOs and WTs. (A) New gating strategy of CD45+ thymocytes using CD4/CD8 staining and CD44/CD25 expression of DN cells. CD44/CD25 gating drawn up using CD44 and CD25 FMO controls. (B) Left; Percentages of CD45+ cells in each CD4/CD8 quadrant. Right; Numbers of cells in each CD4/CD8 quadrant. (C) Left; Percentages of DN cells in each CD44/CD25 quadrant. Right; Numbers of DN cells in each CD44/CD25 quadrant. Data presented as mean±SEM. Statistical analysis carried out by Student's t-test, with Welch's correction where appropriate *p<0.05.

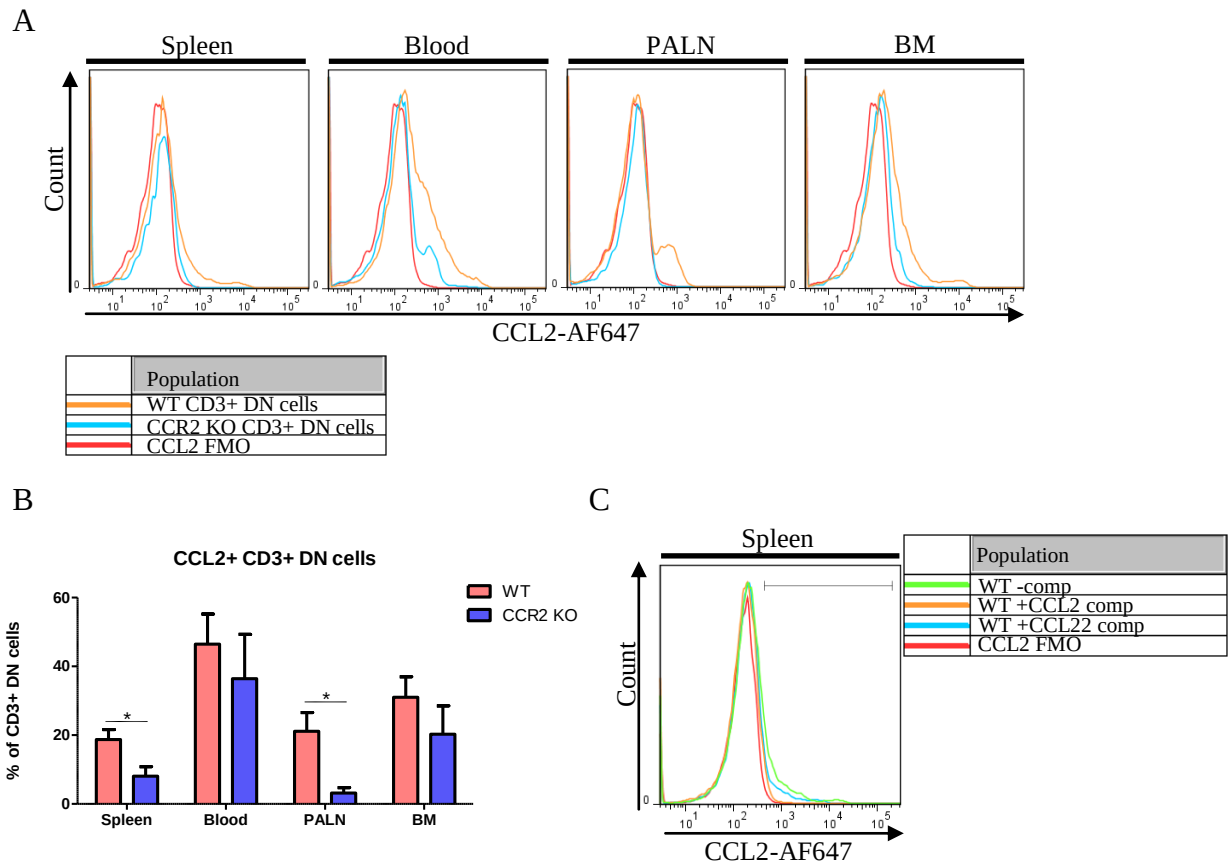

Figure 4.12. *Some CCL2-AF647 uptake by CD3+ DN cells in NP peripheral tissues was CCR2 dependent.*

Measurement of CCL2-AF647 uptake by CD3+ DN cells using flow cytometry in spleen (n=4), blood (n=4-6), PALN (n=4) and BM (n=4) in WT and CCR2 KO NP females. (A) Representative histograms for CCL2-AF647 uptake in peripheral tissues, CCL2-AF647 FMO for CD3+ spleen shown in red. (B) Proportion of CD3+ DN cells internalising CCL2-AF647. (C) Example of fluorescent CCL2-AF647 uptake in spleen with unlabelled chemokine comp. CCL2-AF647 FMO for CD3+ spleen shown in red. Data presented as mean±SEM. Statistical analysis carried out by Student's t-test, with Welch's correction where appropriate *p<0.05.

Figure 4.13. *CCL2-AF647 uptake was CCR2 dependent in NP uterine horn.*

Measurement of CCL2-AF647 uptake by CD3+ DN cells using flow cytometry in UH (n=3-4) and cervix (n=3-4) in WT and CCR2 KO NP females. Including competition of CCL2-AF647 uptake with an excess of unlabelled CCL22 and CCL2 in UH (n=4). CCL2-AF647 FMO for CD3+ spleen shown in red. (A) Gating for identifying CCL2-AF647 uptake based on CCL2-AF647 FMO in the spleen. Representative images for UH and cervix with CCL2-AF647+ gate. (B) Proportion of CD3+ DN cells internalising CCL2-AF647. Data presented as mean±SEM. Statistical analysis carried out by Student's t-test, with Welch's correction where appropriate *$p<0.05$. (C) Representative histograms showing CCL2-AF647 uptake with and without CCL22 comp. (D) Effect of CCL22 comp on the proportion of CD3+ DN cells internalising CCL2-AF647. Data presented as mean±SEM. Statistical analysis carried out by paired Student's t-test, not significant. (E) Representative histograms showing CCL2-AF647 uptake with and without CCL2 comp. (F) Effect of CCL2 comp. Left; Proportion of CD3+ DN cells internalising CCL2-AF647. CCR2 effect $p=0.098$, CCL2 comp effect $p<0.05$, interaction $p<0.05$. Data presented as mean±SEM. Statistical analysis carried out by two-way ANOVA with matching.

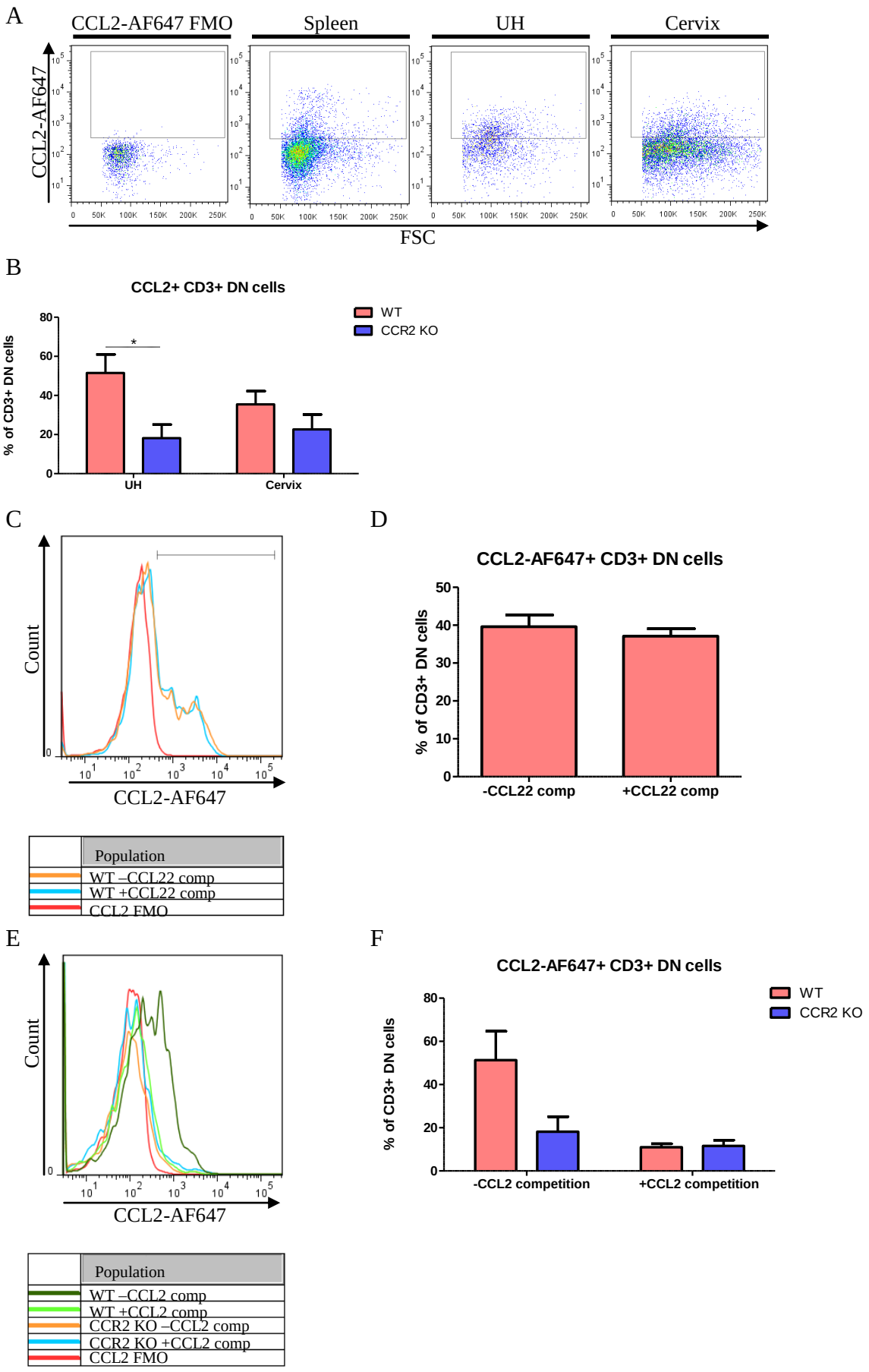

Figure 4.13. *CCL2-AF647 uptake was CCR2 dependent in NP uterine horn (legend opposite).*

Chapter 5: Characterisation of CD3+ DN cells in reproductive tissues

Introduction

The previous chapter showed that most CD3+ cells in the reproductive tissues of mice lack expression of CD4 and CD8. Compared to NP and 7DPP, at 1DPP these CD3+ DN cells were present at much higher numbers in the uterine horn, and their frequency as a proportion of the CD3+ population was higher in the blood. Unexpectedly, this increase in the blood was found to be CCR2-dependent. CCR2 expression was examined on CD3+ DN cells throughout the mice, but expression of no other markers was explored and the precise cellular constituents of this population were undefined. As this population was defined based on CD3 expression, a major hypothesis was that it would contain CD4-CD8- T cells of the type described by Johansson and Lycke (Johansson and Lycke, 2003). In humans, ~30% of CD3+ cells in the decidua during term labour are also CD3+ DN cells, and this study suggested that the majority of these cells were DN T cells (Gomez-Lopez et al., 2013). In addition, some of these cells could be NKT cells, which are known to be CD3+. NKT cells can be separated into different phenotypes based on surface expression of certain markers and the cytokines they produce. Th1-like iNKT cells, Th2-like iNKT cells and Th17-like iNKT cells have all been described, although only Th1-like iNKT cells and Th17-like iNKTcells could be described as CD3+ DN cells, as the Th2-like iNKT cells reportedly express CD4 (Brennan et al., 2013). Th1-like iNKT cells were of particular interest in the context of post-partum inflammation as they have been described in the endometrium during the pregnancy and may contribute to inflammation-induced pre-term birth (Li et al., 2012, Ito et al., 2000, Boyson et al., 2008).

A more in depth characterisation of CD3+ DN cells was therefore a natural progression for the work. Defining cells due to a lack of expression of markers is imprecise and gives very little insight into the nature of the population being studied. Therefore, a search for additional markers to classify the cells in the CD3+ DN cell subset was a high priority. The varied expression of CCR2 in different tissues gave some weight to the idea, supported by the literature, that cells defined as CD3+CD4-CD8- contain several distinct cell types. Flow cytometry allows the profiling of this population, within the limits of channel and antibody availability. One of the main issues to resolve was whether some, or all, of the cells were true T cells, and antibodies against TCRs were therefore included. A panel of antibodies against other markers was also chosen, based on likely candidates discussed in the literature. These markers were tested in a number of tissues and the data are presented in this chapter. Thus, having identified in Chapter 4 that the majority of CD3+ cells in reproductive tissues at all time-points were CD3+ DN cells, I hypothesised that these cells

were a mixed population, likely to contain i) ‘true’ DN T cells, expressing TCR-αβ, ii) NKT cells, expressing NK1.1 and TCR-αβ and iii) TCR-γδ T cells and other CD3+ DN cells. While following this line of investigation I identified three major subsets of cells within the CD3+ DN population, and these cells were further profiled in NP and 1DPP animals. It was also clear from this work that by analysing larger numbers of mice and by using more fluorescent channels it is possible that these subsets could be subdivided further.

Results

5.1. *CD25 and NK1.1 are expressed on subsets of CD3+ DN cells*.

To begin to try to fractionate CD3+ DN cells into more clearly defined subsets, antibodies against NK1.1, a marker of NK and NKT cells, had been included in the NP samples analysed at the end of Chapter 4. NKT cells show characteristics of NK cells and T cells, and express CD3, so they could be present in the CD3+ DN population. Splenocytes stained in the presence or absence of NK1.1 antibodies were used to draw gates to help identify NK1.1+ cells in samples prepared from other tissues (Figure 5.1A). When CD3+ DN cells in reproductive tissues were analysed using these gates, ~30% to ~50% of CD3+ DN cells in the uterine horn and cervix were classified as NK1.1+ in both WT and CCR2 KO mice (Figure 5.1A-B). It was also striking that NK1.1 was expressed at a lower level on splenic NK1.1+ cells than on NK1.1+ cells retrieved from reproductive tissues, although the significance of this observation is not clear. Thus, in NP females, CD3+ DN cells are a mixed population and NK1.1+ was present on a significant proportion of CD3+ DN cells in reproductive tissues. These cells are likely to be NKT cells. NK1.1 expression was also examined on CD3+ DN cells in lymphoid tissues and blood of NP mice analysed at the end of Chapter 4 (Figure 5.1B). The smallest NK1.1+ population of CD3+ DN cells was seen in the PALN and thymus comprising only ~10% of these cells. In the spleen 20-25% of CD3+ DN cells expressed NK1.1 (Figure 5.1B), while in the blood and BM this rose to between 30-60%. No significant differences in the abundance of NK1.1+CD3+ DN cells were seen between WT and CCR2 KO mice.

Another marker ascribed to CD3+ DN cells in the literature is CD25 (Lee et al., 2011a, Fischer et al., 2005, Takeuchi et al., 1992, Lider et al., 1991, Mixter et al., 1999, Utting et al., 2000, Voelkl et al., 2011, Zhang et al., 2000, Duncan et al., 2010), and it has been reported to be expressed by these cells in the uterine horn (Johansson and Lycke, 2003). CD25 is a marker associated with conventional Treg cells and is the IL-2 receptor α chain. Antibodies against CD25 had been included in the samples analysed at the end of Chapter 4, primarily to allow detection of CD4+CD25+ Treg, but I also examined its expression on CD3+ DN cells with a view to separating an NKT-like subtype from a Treg-like subtype.

CD25+CD3+ DN cells were defined based on gates set using FMO staining from the spleen (Figure 5.1C). In WT mice, around half of the CD3+ DN cells in NP uterine horn and cervix were CD25+. CCR2 did not exert any effect on the abundance of either population (Figure 5.1D). CD25 expression was also detectable on a subset of CD3+ DN

cells in spleen, BM and PALN, and particularly in blood, and again CCR2 deficiency had no effect on cell abundance (Figure 5.1D).

5.2. *CD25 is expressed by most NK1.1+CD3+ DN cells in NP reproductive tissues and blood.*

The pattern of CD25 expression and NK1.1 expression suggested some overlap in their expression in reproductive tissues and elsewhere. Thus, a quadrant gate was constructed based on the CD25 and NK1.1 FMO gating used previously. An example of these quadrants is seen in Figure 5.2A. These plots clearly showed that CD3+ DN cells from different tissues varied in their extent of co-expression of NK1.1 and CD25. The top right gate, representing CD25+NK1.1+ CD3+ DN cells, appeared to only have a well-defined population in the uterine horn, cervix and blood (Figure 5.2A). When the data from several individuals were expressed together graphically (Figure 5.2B), it was clear that most NK1.1+ CD3+ DN cells in the uterine horn and cervix were CD25+. In stark contrast, most NK1.1+ CD3+ DN cells in spleen and PALN lacked CD25 expression. A small proportion of NK1.1+ CD3+ DN cells in the BM expressed CD25, and this population was more prominent in the blood. Interestingly, the NK1.1+CD25+ CD3+ DN cell population is phenotypically similar to Th1-like iNKT cells, which exist in an activated state and respond to lipid antigens presented by CD1d (Brennan et al., 2013). My data show that these cells make up a greater proportion of CD3+ DN cells in uterine horn, cervix and blood, than elsewhere in the mouse. However NK1.1+CD25- and NK1.1-CD25+ cells were also present amongst CD3+ DN cells in NP reproductive tissues.

5.3. *CCR2 is expressed primarily by NK1.1-CD25- cells in the CD3+ DN population.*

Some of the CD3+ DN cells in the uterine horn, spleen and PALN of NP mice showed evidence of CCR2 expression (Figures 4.12 and 4.13). When CCL2-AF647 uptake by the four populations defined by expression of CD25 and NK1.1 was analysed, it was clear that the large majority of CCR2-dependent uptake was found amongst CD25-NK1.1- CD3+ DN cells in spleen, blood and uterine horn (Figure 5.3). CCR2-dependent uptake was also found in uterine horn in the small NK1.1+CD25- CD3+ DN cell population, but this was not seen in any other tissue (Figure 5.3A). Perhaps the most striking CCR2-mediated internalisation of CCL2-AF647 was seen from NK1.1-CD25+ CD3+ DN cells in the PALN, where ~70% of WT cells were CCL2+ but <10% of CCR2 KOs had internalised the fluorescent chemokine (Figure 5.3C). These data seem to support the idea that CD3+

DN cells represent a mixed population and that different tissues contain different types of CD3+ DN cells, with different levels of CCR2 activity.

5.4. *Expression of additional markers by CD3+ DN cells.*

The results above indicated that, as expected, CD3+ DN cells in NP mice are a mixed population. According to the literature, several other surface markers can be expressed by CD3+ DN cells. Although limited time and resources prevented them from all being thoroughly tested, experiments were performed on NP female WT mice in order to draw up a panel of markers to be studied further. CD3+ DN cells were identified in reproductive tissues, and staining was compared with staining in the spleen.

B220 has been reported to be a marker of uterine CD3+ DN cells (Johansson and Lycke, 2003). However, just by comparing the images in Figure 5.4A, it was clear that very few CD3+ DN cells in the uterine horn detectably expressed B220, whereas a population of B220+ CD3+ DN cells was clearly observed in the spleen. In order to get an idea of whether a TCR complex was present on CD3+ DN cells in the uterine horn, antibodies recognising TCR-β and the TCR-γδ complex were both tested. TCR-β appeared to be expressed by many CD3+ DN cells in the uterine horn, and a defined population of TCR-β+ CD3+ DN cells was also clearly visible in the spleen (Figure 5.4B). TCR-γδ was present on a distinct population of CD3+ DN cells in the spleen however only a small population of TCR-γδ+ cells could be identified in the uterine horn (Figure 5.4C).

CD3+ DN cells have been described as being CTLA-4+ (Gao et al., 2011) or CTLA-4- (Voelkl et al., 2011, Duncan et al., 2010). However in this experiment CTLA-4 staining of CD3+ DN cells was not convincing in either uterine horn or spleen (Figure 5.4D). PD-1 is associated with CD3+ DN cells in the thymus (Keir et al., 2005) and a small proportion of CD3+ DN cells were PD-1+ in the uterine horn and spleen (Figure 5.4E). The final marker tested was CXCR5, a chemokine receptor associated with recruitment of cells into follicles in secondary lymphoid organs that has been reported to be expressed on DN T cells (Ansel et al., 1999, Lee et al., 2005, Lee et al., 2006). Although very few CD3+ DN cells in the spleen expressed CXCR5, the uterine horn CD3+ DN cells appeared to contain a much higher percentage of cells that showed CXCR5 positivity (Figure 5.4F).

This analysis was then extended to the peripheral tissues studied in earlier experiments. Markers on CD3+ DN cells in peripheral tissues were gated as in Figure 5.5. B220

appeared to produce a clear population in each tissue, except for the thymus (Figure 5.5A). This suggested that in many peripheral tissues the mixed CD3+ DN cell population contained a B220+ CD3+ DN cell population, which was not present in uterine horn (Figure 5.4). A cluster of TCR-β+ and TCR-γδ+ cells was clearly visible in the CD3+ DN cell population in each lymphoid tissue examined (Figure 5.5B-C). Compared to these tissues, a higher proportion of CD3 DN cells in the blood were TCR-β+, and fewer were TCR-γδ+ (Figure 5.5B-C), rather like the uterine horn (Figure 5.4B). Again, CTLA-4 did not stain CD3+ DN cells in any of the tissues studied (Figure 5.5D). This may have been due to a lack of optimisation or reagent failure because no convincing CTLA-4+ cells were identified even outside of the CD3+ DN population (data not shown). As expected there was good staining for PD-1 in the thymus, and some staining was seen on CD3+ DN cells in the spleen, but few PD-1+ cells were observed in the blood, PALN and BM (Figure 5.5E). The last marker in the panel was the chemokine receptor CXCR5. This receptor was present on a substantial proportion of CD3+ DN cells in blood, and, to a lesser extent, those in BM, but very few CXCR5+ CD3+ DN cells were present in the spleen, PALN and thymus (Figure 5.5F).

The percentage of CD3+ DN cells expressing each individual marker were calculated (Figure 5.6). The percentage of CD3+ DN cells expressing NK1.1 and CD25 had also been determined in these experiments, and these data are also presented in Figure 5.6 to attempt to correlate their expression to that of the other markers. As only limited animals were available at this time, the n number for some of the markers was as low as 2, which must be taken into account when assessing these results. However, it was notable that the pattern of markers expressed by CD3+ DN cells was very similar between uterine horn and cervix, suggesting that the populations of CD3+ DN cells were very similar in these two tissues (Figure 5.6A). Cells expressing NK1.1, TCR-β, CD25, or CXCR5 were most prominent in uterine horn and cervix, where few CD3+ DN cells were positive for B220, TCR-γδ, CTLA-4 and PD-1 (Figure 5.6A). Interestingly, a similar pattern was observed amongst CD3+ DN cells in blood (Figure 5.6B), although a somewhat lower percentage expressed CD25 and a higher proportion were B220+. In spleen and PALN, TCR-γδ+ cells were more highly represented, while those expressing NK1.1 or TCR-β were less abundant. In all tissues, the sum of cells expressing TCR-β or TCR-γδ was 80-90%. Since these two markers are unlikely to be co-expressed, it seemed that most CD3+ DN cells carried a TCR. This is investigated further in the section below. As might be expected, CD3+ DN cells in the thymus demonstrated a very different pattern of expression, most strikingly,

strong expression of PD-1 (Figure 5.6B). Clearly, CD3+ DN cells in the thymus were quite distinct from those found in the other organs studied in this project. Having a different surface phenotype did not necessarily rule them out as precursors for cells found elsewhere. These cells might migrate from the thymus and give rise to other types of DN cells.

5.5. *NKT cells are a major CD3+ DN cell population, particularly in reproductive tissues and blood.*

Next, I wanted to identify any markers that might be co-expressed in order to provide a more definitive identification of CD3+ DN cell subsets. Due to only certain channels being free on the flow cytometer and the availability of antibodies in those colours, only selected combinations of markers were successfully tested. Quadrant gates were based on FMO staining as in Figure 5.4 and 5.5. Across all tissues, very few CD3+ DN cells could be classified as TCRβ+TCRγδ+ (Figure 5.7A, left), which was reassuring as these receptors are usually seen as mutually exclusive. Moreover, with the exception of the spleen and PALN, nearly all CD3+ DN cells carried a TCR. When NK1.1 and TCR-β were studied together, it was found that a sizeable proportion of CD3+ DN cells in the uterine horn, cervix and blood could be defined as NK1.1+TCRβ+ (Figure 5.7B, left). These cells were a much smaller proportion of the CD3+ DN cells in the spleen, PALN, BM and thymus (Figure 5.7B left). Co-expression of NK1.1 and TCR-β is consistent with an NKT cell identity. There were also plenty of TCRβ+NK1.1- cells amongst the CD3+ DN population in all tissues examined: these cells can be classified as DN T cells. Expression of NK1.1 and B220, TCR-β and B220, and CXCR5 and PD-1, was largely mutually exclusive in all tissues examined (Figure 5.7 C-E).

5.6. *Summary 1.*

The main findings of these studies were:

- There is a clear delineation in the expression of markers on CD3+ DN cells from different anatomical locations;
- Most CD3+ DN cells express a TCR, irrespective of their location;
- A sizeable proportion of the CD3+ DN cells in the uterine horn, cervix and blood of NP mice are NKT cells defined as CD3+CD4-CD8-NK1.1+TCRβ+CD25+;
- TCRβ+NK1.1- cells are present amongst the CD3+ DN population in the uterine horn, cervix and blood of NP mice;

- Many CD3+ DN cells in the uterine horn, cervix and blood of NP mice express the chemokine receptor CXCR5.

5.7. *The composition of CD3+ DN cells appears to change towards a more TCRβ+ NK1.1- phenotype at 1DPP.*

Having defined cells in the CD3+ DN population more clearly, next I wished to investigate how these populations differed between NP and 1DPP mice. To do this, CD3+ DN cells were to be split into three major subsets based on expression of NK1.1 and TCR-β i.e. NK1.1+TCRβ+ NKT cells, NK1.1-TCRβ+ DN T cells, and NK1.1-TCRβ- cells. NK1.1-TCRβ- cells were also tested for expression of TCR-γδ. First, reproductive tissues were analysed (Figure 5.8). In uterine horn, the smaller populations of NK1.1+TCRβ- CD3+ DN cells and NK1.1-TCRβ- CD3+ DN cells were decreased as a proportion of total CD3+ DN cells at 1DPP compared to NP (Figure 5.8B, left). In the cervix the very low percentage of the NP CD3+ DN population defined as NK1.1+TCRβ- had decreased further at 1DPP (Figure 5.8B, right). In both uterine horn and cervix, TCRβ+NK1.1- CD3+ DN cells dominate, and this population significantly increases in uterine horn in terms of proportion and numbers at 1DPP (Figure 5.8B-C). Compared to Figure 5.7, there are fewer NK1.1+TCRβ+ cells in the CD3+ DN population from the uterine horn and cervix. The differences in these results can be easily explained as the data from Figure 5.8 onwards were generated from different mice to the rest of the chapter and therefore would have been subject to the natural experimental variation, which has been seen throughout this project.

For the rest of the experiments in this chapter the number of cells retrieved was calculated, because cells were divided into aliquots in order to be stained with multiple antibody cocktails. A significant increase was observed in the number of TCRβ-NK1.1- CD3+ DN cells seen in the 1DPP females in the cervix (Figure 5.8C).

To address the question of whether cells increased in number in proportion to the size of the reproductive tissues, the uterine horn and cervix were weighed and the number of cells per g of tissue was calculated. This showed that overall the number of CD3+ DN cells per g did not seem to change between NP and 1DPP uterine horn tissue. No change in the two largest populations was seen in either tissue (Figure 5.8D).

5.8. ***An increase in the proportion of TCRβ+NK1.1- in the CD3+ DN population in 1DPP blood, compared with NP mice.***

CD3+ DN cells in the spleen, blood and PALN were also examined. Spleen CD3+ DN cells had a distinct profile, with TCRβ+NK1.1- cells and particularly TCRβ-NK1.1- cells, dominating the CD3+ DN population in terms of proportion and numbers in NP and 1DPP samples (Figure 5.9A). The percentage and number of cells in the NK1.1+ subgroups were tiny. No differences between NP and 1DPP were observed although the double positive TCRβ+NK1.1+ CD3+ DN cells displayed a change in their percentage of the CD3+ DN population that could be seen as approaching significance (p=0.063, Figure 5.20A, left).

As hinted at before, CD3+ DN cells in the blood were comprised of different ratios of NK1.1/TCRβ cells than spleen or PALN. In fact the composition of CD3+ DN cells in the blood was more similar to the pattern seen in uterine horn and cervix. Though not the main CD3+ DN cell population, NK1.1+TCRβ+ CD3+ DN cells formed a much more visible population in the blood compared with the spleen and PALN, where these cells were barely detectable. Like uterine horn, the blood displayed an increased proportion of TCRβ+NK1.1- CD3+ DN cells in the early post-partum period, compared to NP females (Figure 5.9B, left). The most important result from this figure showed that CD3+ DN cells do not increase per ml in blood. This is crucial and suggests that the change in proportions of CD3+ populations at 1DPP, compared to NP mice is not driven by an increase in CD3+ DN cells. It therefore follows that the differences in populations are due to a CCR2 dependent decrease in CD4+ T cells.

PALN CD3+ DN cells, which only made up a small percentage of CD3+ cells in both NP and 1DPP females were predominantly TCRβ-NK1.1- and these increased in number in 1DPP females (Figure 5.20C, right).

5.9. ***The proportion of TCRβ-NK1.1- CD3+ DN cells expressing TCRγδ increases at 1DPP in the uterine horn.***

TCRβ-NK1.1- CD3+ DN cells were an intriguing population, seen in all tissues studied. These cells were obviously a mixed population and the studies earlier in the chapter attempting marker characterisation suggested strongly that these cells were γδ T cells. Expression of TCR-γδ was studied in the TCRβ-NK1.1- CD3+ DN cells in the NP and 1DPP mice examined in Figures 5.8 and 5.9.

Expression of TCR-γδ was low in reproductive tissues (Figure 5.10), consistent with previous results (Figure 5.6). Interestingly, in the uterine horn, expression of TCR-γδ more than doubled at 1DPP, compared to NP mice (Figure 5.10A, left). Numbers of TCRγδ+TCRβ-NK1.1- CD3+ DN cells in both tissues, tended to increase at 1DPP but this was not significant (Figure 5.10B).

Even at 1DPP it cannot be said that most TCRβ-NK1.1- CD3+ DN cells have a γδ T cell phenotype, so these remain a largely unidentifiable population. However, in the uterine horn at 1DPP there is a shift with γδ T cells constituting more of these cells than is seen in NP females.

5.10. *TCRγδ+TCRβ-NK1.1- CD3+ DN cells are more abundant in spleen at 1DPP, compared with NP mice.*

TCRβ-NK1.1- CD3+ DN cells were also examined in spleen, blood and PALN for their expression of TCR-γδ. Contrary to reproductive tissues, the majority of these cells in the spleen and PALN expressed TCR-γδ, so are likely to be γδ T cells (Figures 5.11A and C). Numbers of TCRγδ+TCRβ-NK1.1- CD3+ DN cells were increased in the spleen at 1DPP (Figure 5.11A) but this was not seen in the other tissues and no significant changes in proportion of TCRγδ+ cells were recorded. Blood TCRβ-NK1.1- CD3+ DN cells expressed lower levels of TCR-γδ (Figure 5.11B), echoing findings for reproductive tissues (Figure 5.10) but no changes were seen between NP and 1DPP individuals. Compared to secondary lymphoid organs, fewer TCRβ-NK1.1- CD3+ DN cells could be classified as γδ T cells.

5.11. *Summary 2.*

CD3+ DN cells in tissues were split into NK1.1+TCRβ- cells, NK1.1+TCRβ+ NKT cells, NK1.1-TCRβ+ DN T cells and NK1.1-TCRβ- cells. The main findings were:

- Almost all NK1.1+ cells were TCRβ+, and this NK1.1+TCRβ+ NKT population constituted around ~20-40% of CD3+ DN cells in uterine horn, cervix and blood.
- NK1.1-TCRβ+ DN T cells were a large population in uterine horn, cervix and blood and these increased as a proportion of CD3+ DN cells in uterine horn and blood at 1DPP, compared to NP mice.
- No increase in the number of CD3+ DN cells per ml of blood was seen at 1DPP, compared to NP blood.

- In spleen and PALN, NK1.1-TCRβ- cells dominated and most of these cells were found to express the alternative TCR, TCR-γδ.
- NK1.1-TCRβ- cells were also seen in uterine horn, cervix and blood although TCRγδ+ cells were not as abundant as they were in secondary lymphoid tissues. Interestingly, in uterine horn, the proportion of cells expressing TCR-γδ was increased at 1DPP, compared to NP individuals.

CD3+ DN cells were successfully segregated into cells that had surface phenotypes consistent with them being NKT cells, DN T cells, and γδ T cells. There was also a small population of CD3+ DN cells that lacked expression of a TCR or NK1.1. The abundance of these cell populations did not appear to change dramatically between NP and 1DPP tissues. These different cell types, and their possible functions in reproductive tissues and elsewhere, are discussed in greater depth in the Discussion section (Chapter 7).

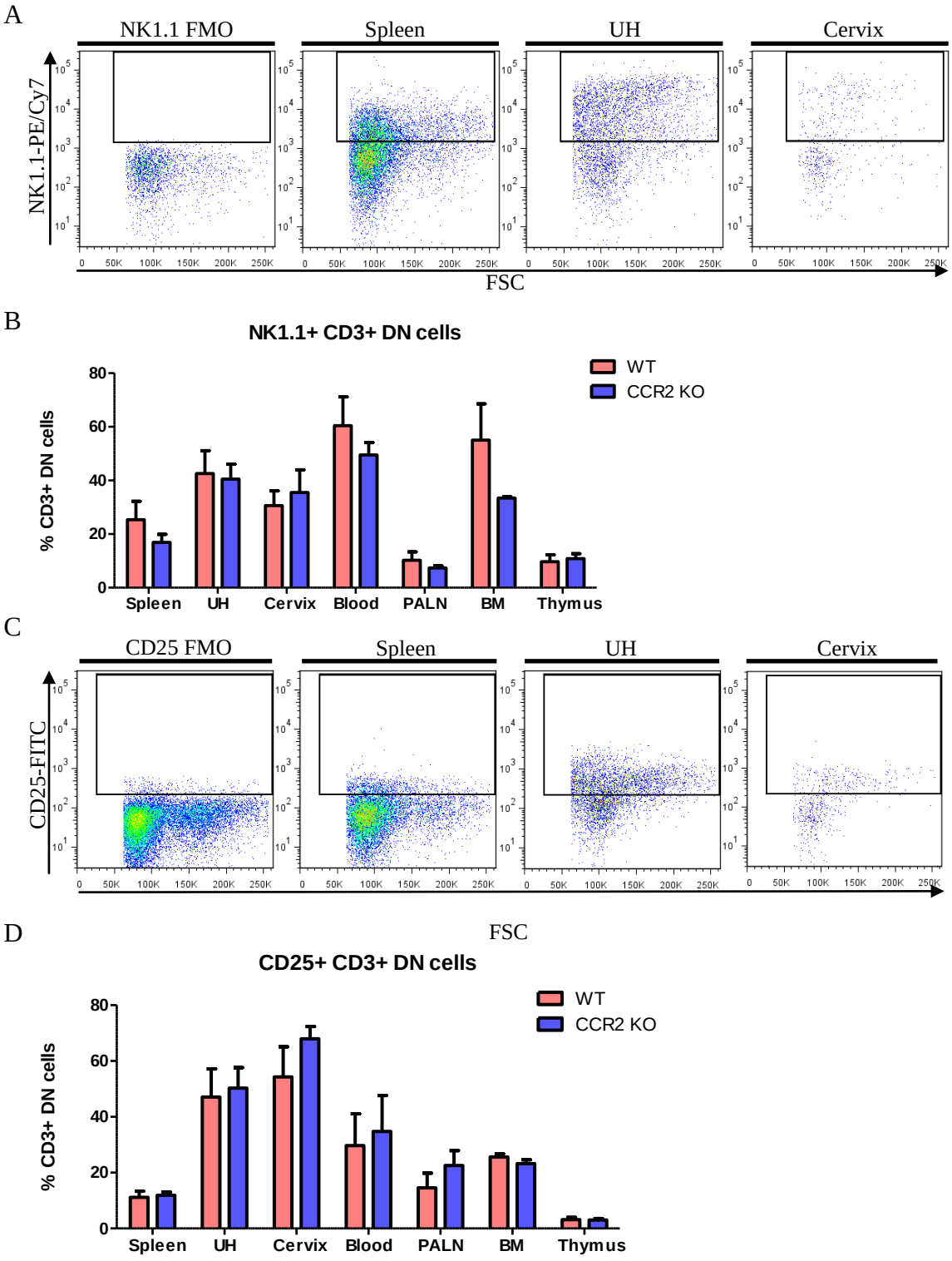

Figure 5.1. *CD25 and NK1.1 are expressed on subsets of CD3+ DN cells.*
Measurement of NK1.1 and CD25 surface expression on CD3+ DN cells and using flow cytometry in WT (n=3) and CCR2 KO (n=4) NP females. (A) Representative gating of NK1.1+ gate based on NK1.1 FMO staining of the spleen. (B) Proportion of CD3+ DN cells expressing NK1.1. (C) Representative gating of CD25+ gate based on CD25+ FMO staining of the spleen. (D) Proportion of CD3+ DN cells expressing CD25. Data presented as mean±SEM. Statistical analysis carried out by Student's t-test, not significant.

A

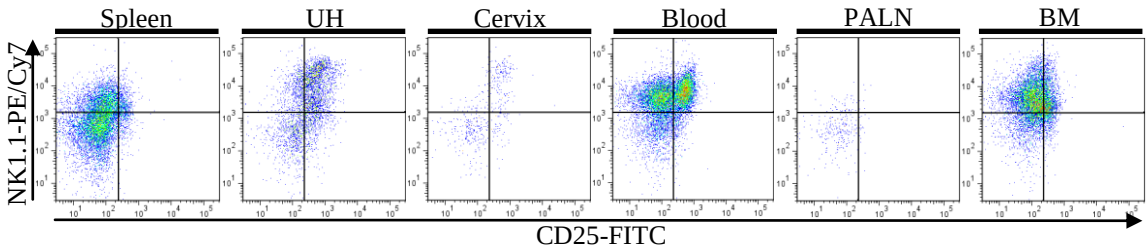

B

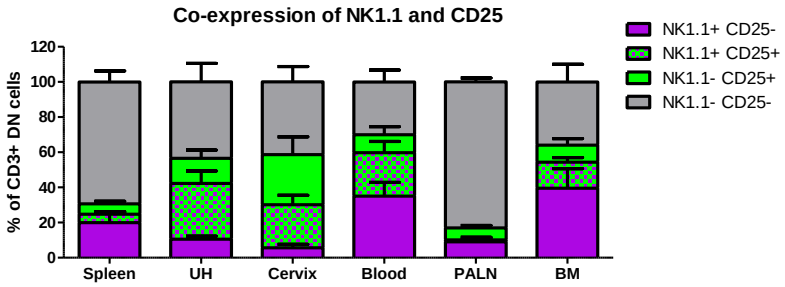

Figure 5.2. *Identification of NK1.1+ CD25+ CD3+ DN cells in NP reproductive tissues and blood.*

Measurement of NK1.1 and CD25 on CD3+ DN cells from NP WT mice using flow cytometry (n=3). NK1.1 and CD25 horizontal and vertical gating based on FMO staining (as shown in fig 5.1). (A) Representative images of quadrant gate for CD25/NK1.1. (B) Proportion of CD3+ DN cells expression CD25 and NK1.1. Results shown as mean±SEM.

Figure 5.3. *CCR2 is expressed primarily by NK1.1-CD25- cells in the CD3+ DN population.*

Measurement of CCL2-AF647 uptake by CD3+ DN cells in NP WT and CCR2 KO females using flow cytometry. Uptake histograms are displayed with WT shown in orange, CCR2 KO in blue, CCL2 FMO for spleen in red. (A) Left; Percentage of NK1.1+CD25- CD3+ DN cells internalising CCL2-AF647. Right; Representative histograms showing CCL2 uptake in NK1.1+CD25- CD3+ DN cells. (B) Left; Percentage of NK1.1+CD25+ CD3+ DN cells internalising CCL2-AF647. Right; Representative histograms showing CCL2 uptake in NK1.1+CD25+ CD3+ DN cells. (C) Left; Percentage of NK1.1-CD25+ CD3+ DN cells internalising CCL2-AF647. Right; Representative histograms showing CCL2 uptake in NK1.1-CD25+ CD3+ DN cells. (D) Left; Percentage of NK1.1-CD25- CD3+ DN cells internalising CCL2-AF647. Right; Representative histograms showing CCL2 uptake in NK1.1-CD25- CD3+ DN cells. Data presented as mean±SEM. Statistical analysis carried out by Student's t-test, with Welch's correction where appropriate *$p<0.05$.

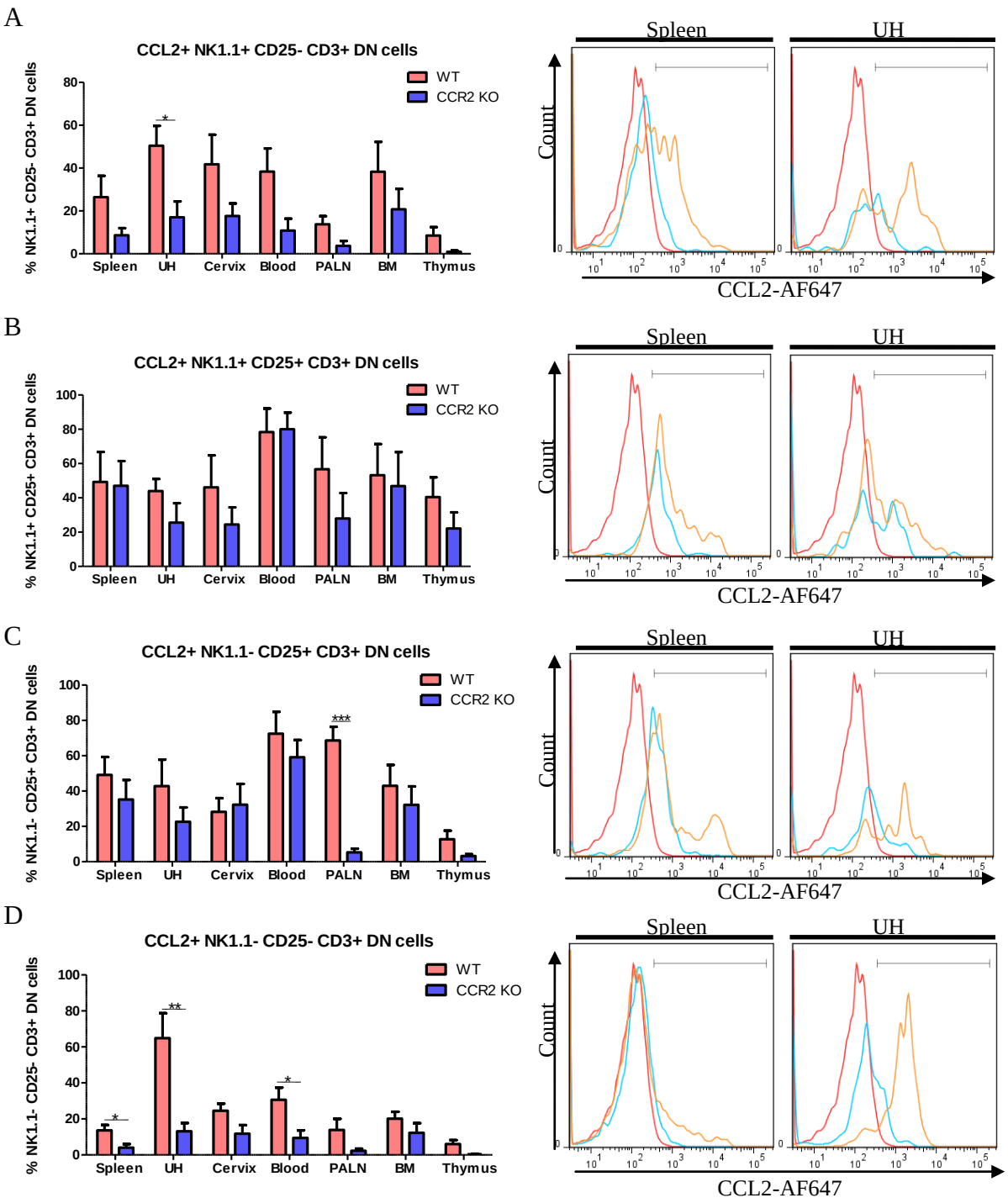

Figure 5.3. *CCR2 is expressed primarily by NK1.1-CD25- cells in the CD3+ DN population (legend opposite).*

Figure 5.4. *Example staining of additional markers on CD3+ DN cells in the uterine horn.* Measurement of CD3+ DN cells in NP WT females and markers on the surface using flow cytometry. Representative images of gating for markers based on FMO controls in the spleen. (A) B220 (B) TCRβ (C) TCRγδ (D) CTLA-4 (E) PD-1 (F) CXCR5.

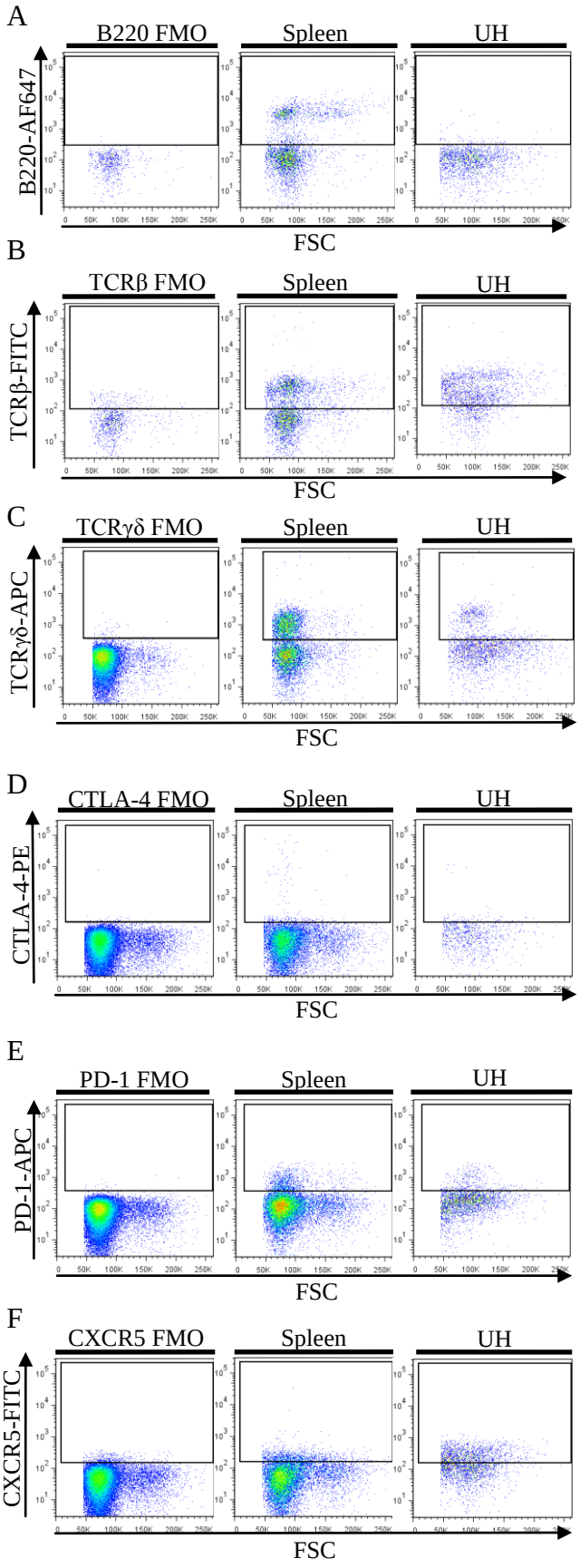

Figure 5.4. *Example staining of additional markers on CD3+ DN cells in the uterine horn (legend opposite).*

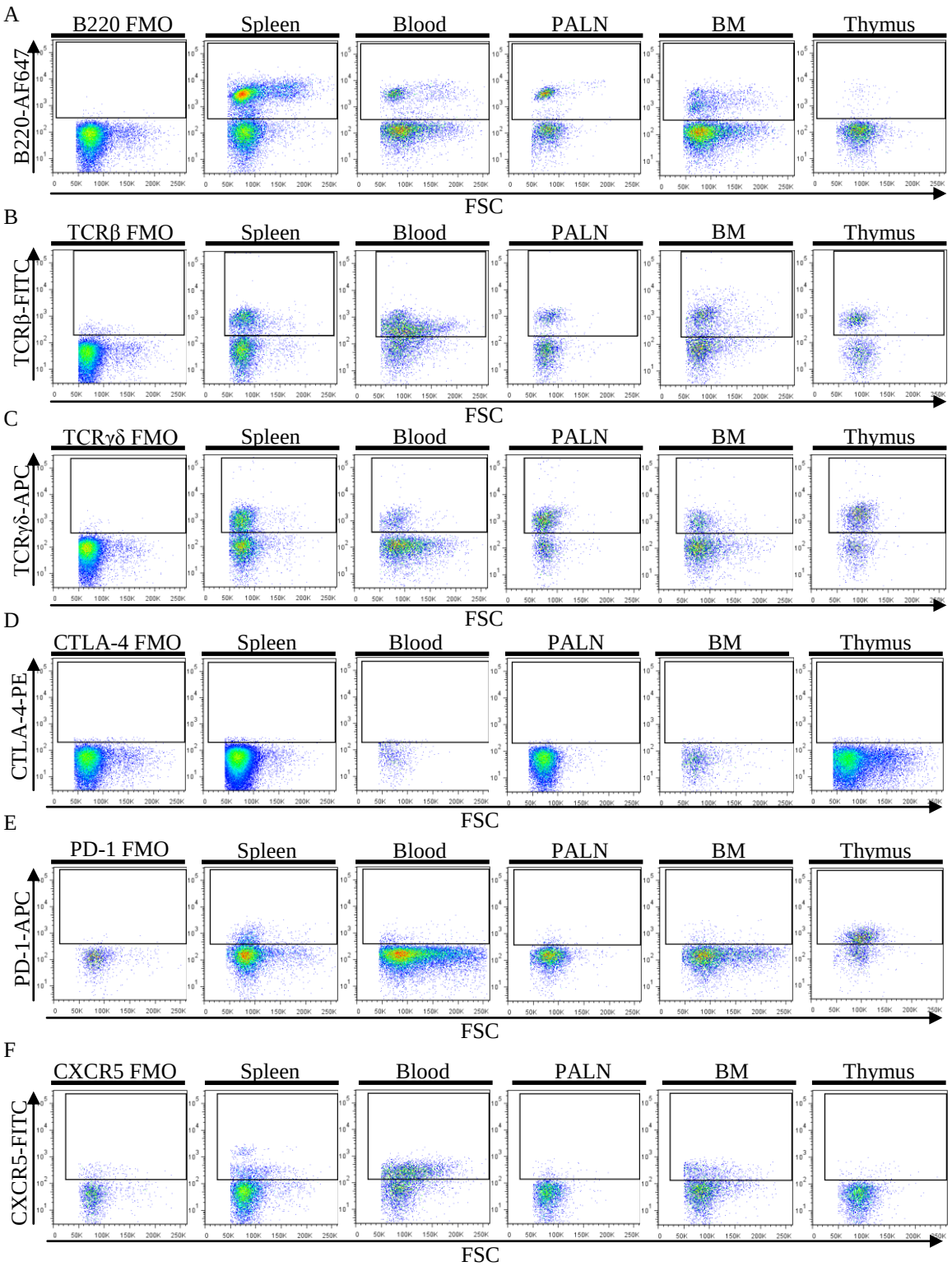

Figure 5.5. *Example staining of additional markers on CD3+ DN cells in peripheral tissues*.

Measurement of CD3+ DN cells and markers on their surface in NP WT females using flow cytometry. Representative images of gating for markers based on FMO controls in the spleen. (A) B220 (B) TCRβ (C) TCRγδ (D) CTLA-4 (E) PD-1 (F) CXCR5.

A

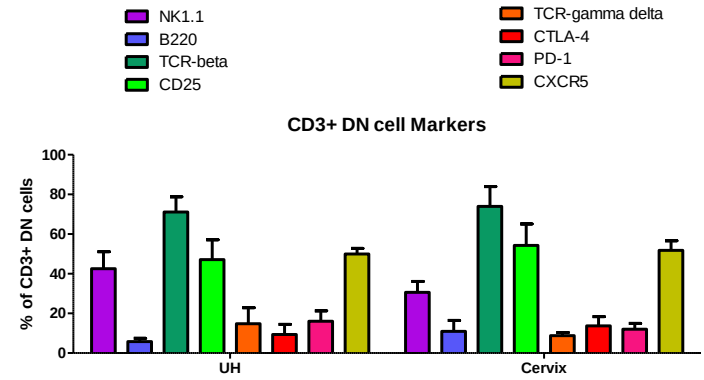

B

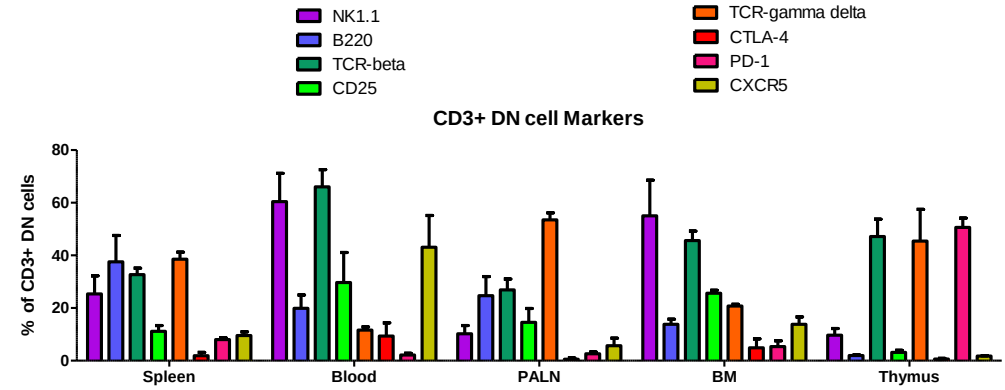

Figure 5.6. *Different patterns of expression of markers on CD3+ DN cells are observed in different tissues*.

Pilot measurement of CD3+ DN cells and markers on their surface in NP WT females using flow cytometry (n=2-6). Gating shown as in fig 5.4 and fig 5.5. (A) Expression of markers in reproductive tissues. (B) Expression of markers in peripheral tissues. Data presented as mean±SEM.

Figure 5.7. *Tests indicated that NKT cells were a major CD3+ DN cell population, particularly in reproductive tissues and blood*.

Pilot measurement of CD3+ DN cells and co-expression of markers on their surface using flow cytometry (n=1-4). Horizontal and vertical gating shown as in fig 5.4 and fig 5.5. (A) Left; Proportion of CD3+ DN cells expressing TCRβ and NK1.1. Right; Representative images of quadrant. (B) Left; Proportion of CD3+ DN cells expressing B220 and NK1.1. Right; Representative images of quadrant. (C) Left; Proportion of CD3+ DN cells expressing TCRβ and TCRγδ. Right; Representative images of quadrant. (D) Left; Proportion of CD3+ DN cells expressing TCRβ and B220. Right; Representative images of quadrant. (E) Left; Proportion of CD3+ DN cells expressing CXCR5 and PD-1. Right; Representative images of quadrant. Results are shown as mean±SEM.

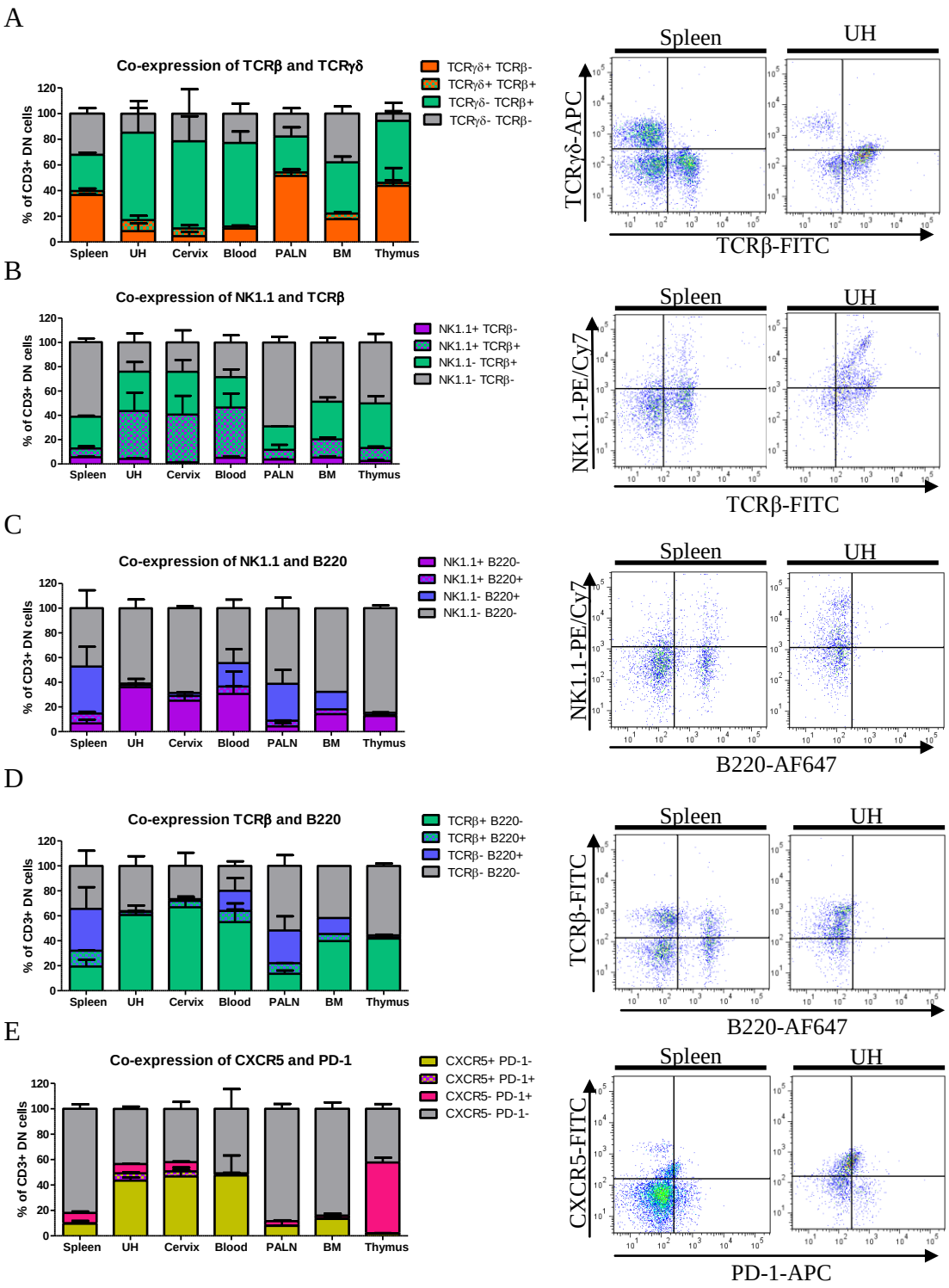

Figure 5.7. *Tests indicated that NKT cells were a major CD3+ DN cell population, particularly in reproductive tissues and blood (legend opposite).*

Figure 5.8. *The composition of CD3+ DN cells appears to change towards a more TCRβ+ NK1.1- phenotype at 1DPP.*

TCRβ and NK1.1 measured in the CD3+ DN cell population from reproductive tissues of NP and 1DPP mice (n=4-8). (A) Plots representing spread of NK1.1 and TCRβ on CD3+ DN cells. (B) Left; TCRβ/NK1.1 quadrant gated populations as a percentage of CD3+ DN cells. Right; TCRβ/NK1.1 quadrant gated CD3+ DN cells calculated to be retrieved from UH. (C) Calculated retrieved cells per g of UH. (D) Left; TCRβ/NK1.1 quadrant gated CD3+ DN cells as a percentage of CD3+ DN cells. Right; TCRβ/NK1.1 quadrant gated CD3+ DN cells calculated to be retrieved from cervix. (E) Calculated retrieved cells per g of cervix. Results presented as mean±SEM, data analysed using Student's t-test, with Welch's correction where appropriate *$p<0.05$ **$p<0.01$. Outliers not excluded.

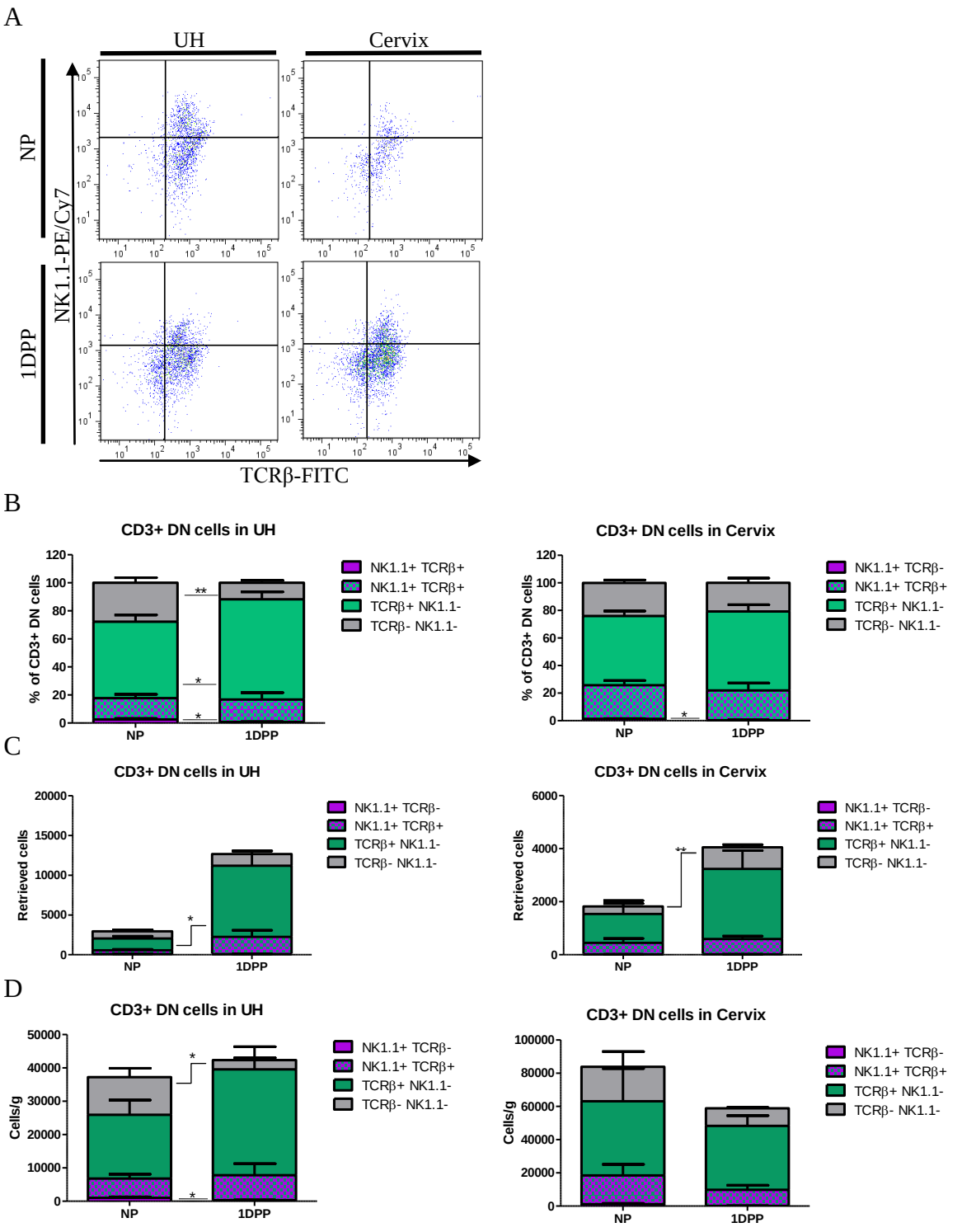

Figure 5.8. *The composition of CD3+ DN cells appears to change towards a more TCRβ+ NK1.1- phenotype at 1DPP (legend overleaf).*

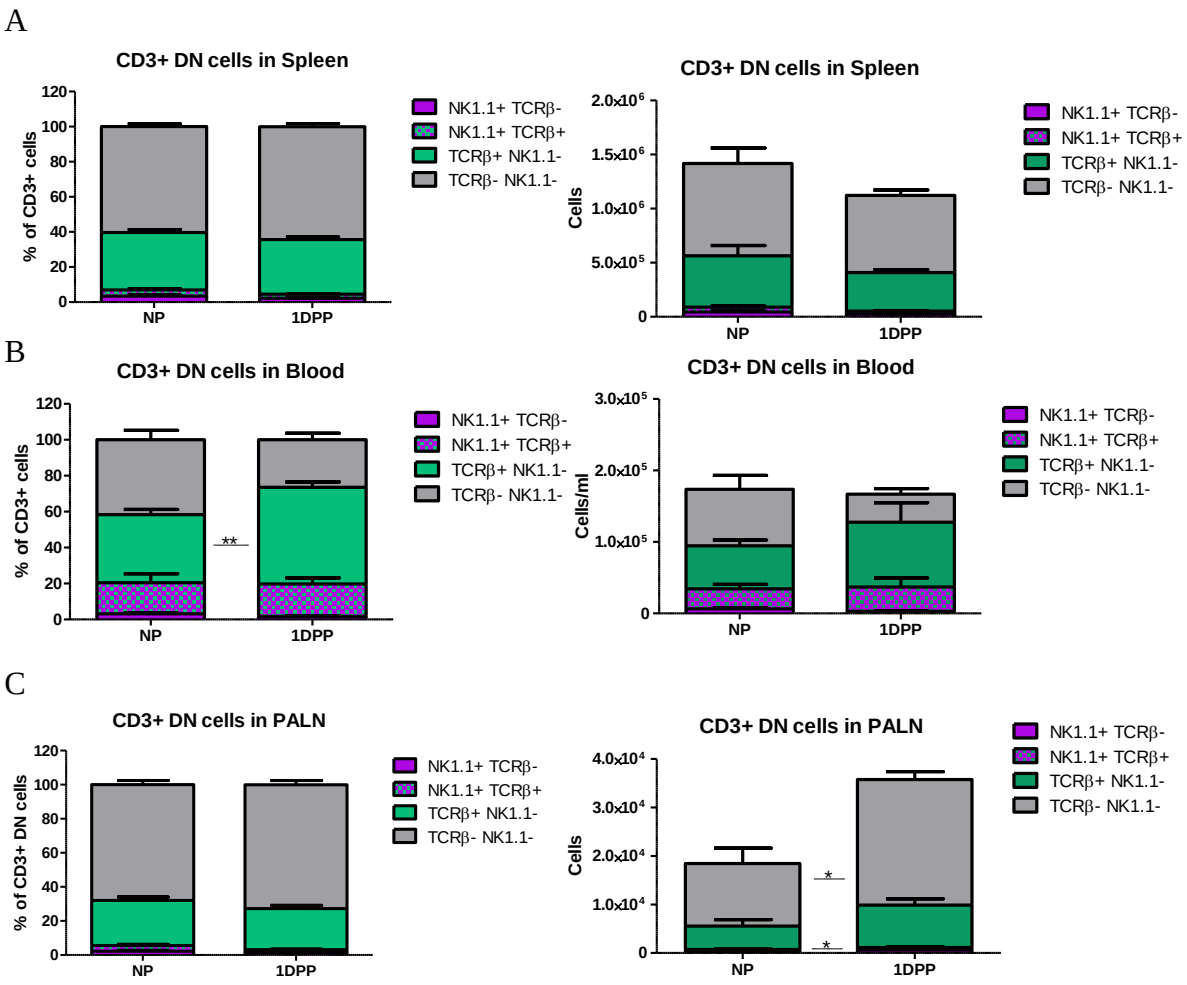

Figure 5.9. *An increase in proportion of TCRβ+NK1.1- CD3+ DN cells was seen at 1DPP in the blood, compared with NP mice.*

TCRβ and NK1.1 measured in the CD3+ DN cell population from peripheral tissues of NP and 1DPP mice (n=4-8). (A) Left; TCRβ/NK1.1 quadrant gated CD3+ DN cells. Right; Numbers of TCRβ/NK1.1 quadrant gated CD3+ DN cells. (B) Left; TCRβ/NK1.1 quadrant gated CD3+ DN cells. Right; Numbers of TCRβ/NK1.1 quadrant gated cells per ml of blood. (C) Left; TCRβ/NK1.1 quadrant gated CD3+ DN cells. Right; Numbers of TCRβ/NK1.1 quadrant gated cells. Results presented as mean±SEM, data analysed using Student's t-test, with Welch's correction where appropriate *$p<0.05$ **$p<0.01$.

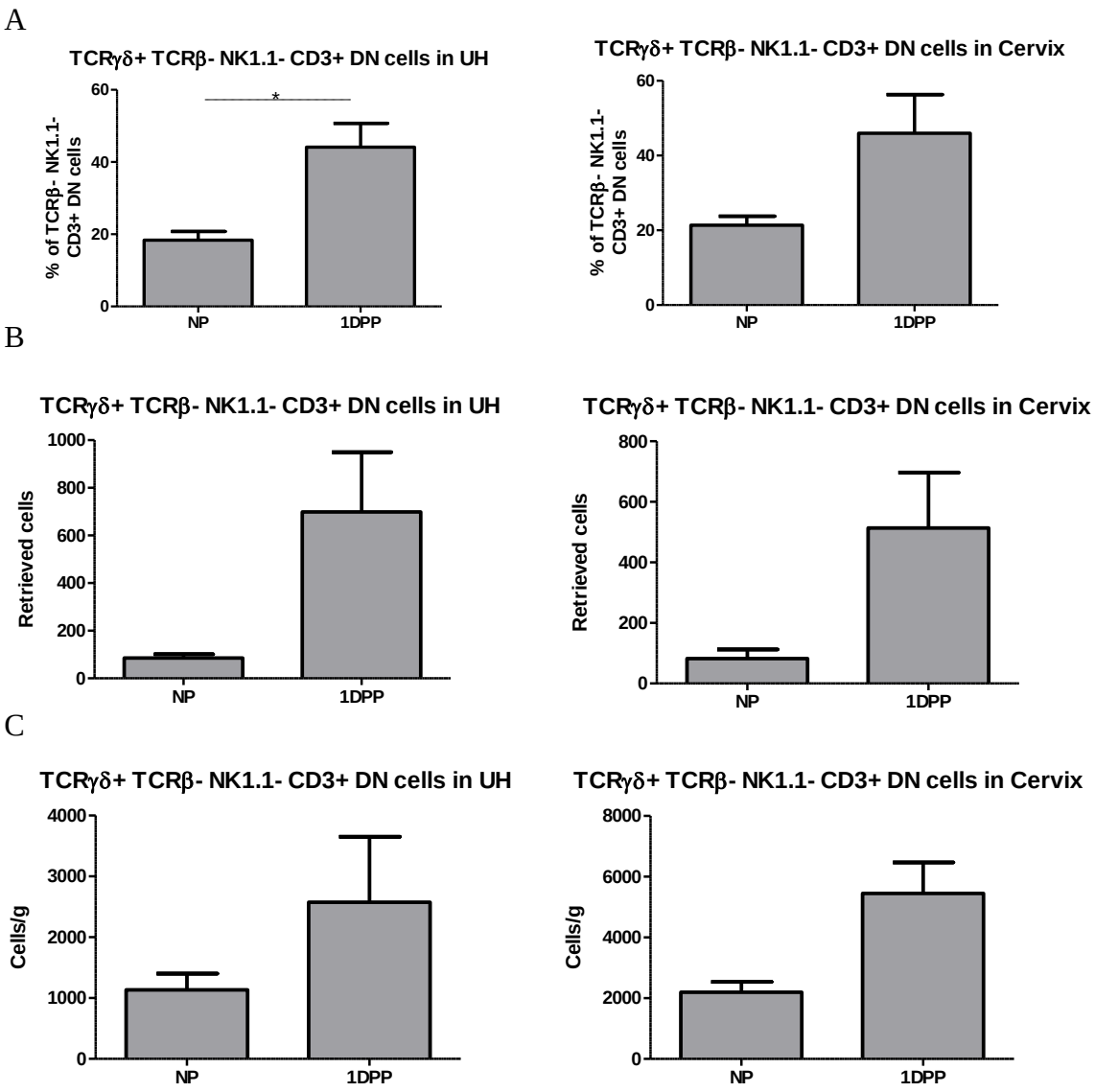

Figure 5.10. *The proportion of TCRβ-NK1.1- CD3+ DN cells expressing TCRγδ increases at 1DPP in the uterine horn.*

TCRγδ expression measured on TCRβ-NK1.1- CD3+ DN cells in UH and cervix (n=3-5) by flow cytometry. (A) Proportion of TCRβ-NK1.1- CD3+ DN cells expressing TCRγδ in UH (left) and cervix (right). (B) TCRγδ+TCRβ-NK1.1- CD3+ DN cells retrieved from UH (left and cervix (right). (C) TCRγδ+TCRβ-NK1.1- CD3+ DN cells per g of UH (left) and cervix (right). Data presented as mean±SEM. Statistical analysis carried out using an unpaired Student's t-test, with Welch's correction for unequal variances where appropriate, *$p<0.05$.

A

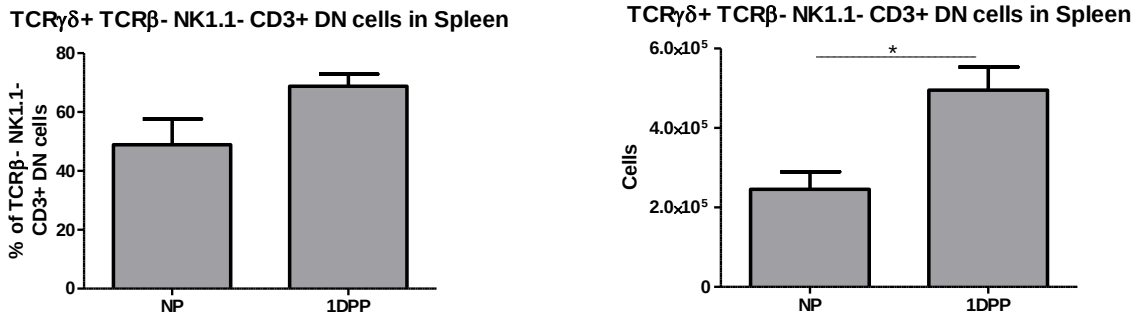

B

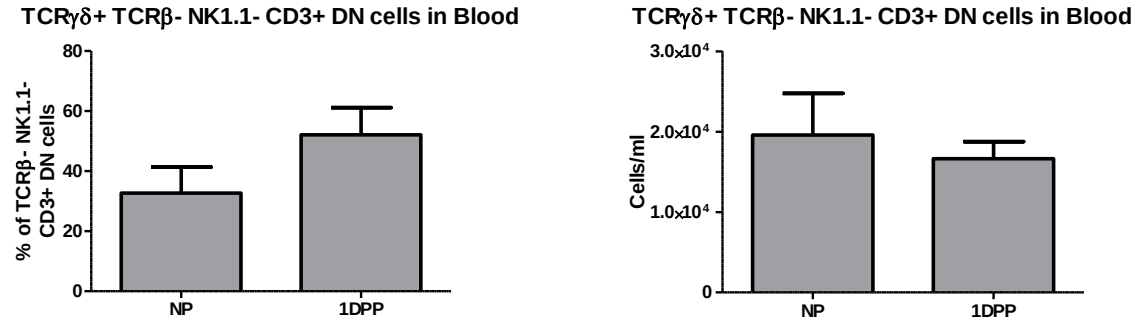

C

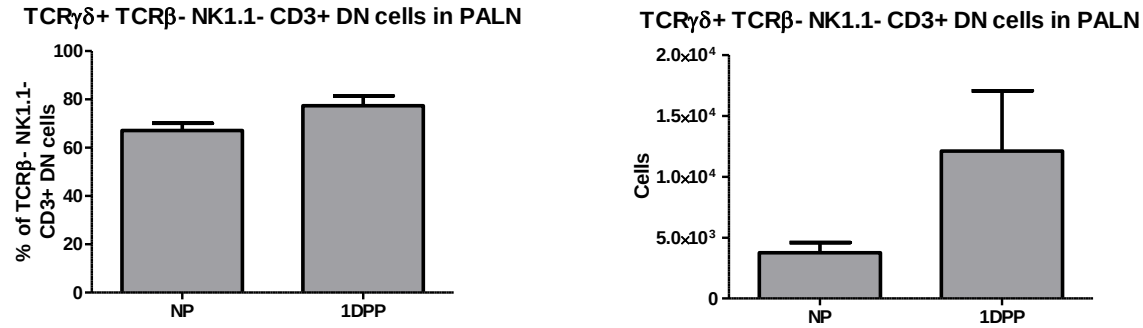

Figure 5.11. *TCRγδ+TCRβ-NK1.1- CD3+ DN cells are more abundant in spleen at 1DPP, compared with NP mice*.

TCRγδ expression measured on TCRβ-NK1.1- CD3+ DN cells in spleen, blood and PALN (n=4-5) by flow cytometry. (A) Left; Proportion of TCRβ-NK1.1- CD3+ DN cells expressing TCRγδ. Right; Number of TCRγδ+TCRβ-NK1.1- CD3+ DN cells in the spleen. (B) Left; Proportion of TCRβ-NK1.1- CD3+ DN cells expressing TCRγδ. Right; Number of TCRγδ+TCRβ-NK1.1- CD3+ DN cells per ml of blood. (C) Left; Proportion of TCRβ-NK1.1- CD3+ DN cells expressing TCRγδ. Right; Number of TCRγδ+TCRβ-NK1.1- CD3+ DN cells in the PALN. Data presented as mean±SEM. Statistical analysis carried out using an unpaired Student's t-test, with Welch's correction for unequal variances where appropriate, *$p<0.05$.

Chapter 6: Hormonal influences on leukocytes in reproductive and peripheral tissues

Introduction

This chapter includes work carried out throughout the project that attempted to address whether hormones can play a role in the control of chemokines and leukocytes in the tissues studied so far in this project. As discussed in chapter 1, female sex hormones have been shown to control chemokine production in various circumstances. As with previous chapters, the chemokine receptor of interest during this chapter was CCR2, and existing data suggest that activation of this receptor might be hormonally regulated. For example, in previous studies, in order to discern the effect of oestrogen on systemic chemokine levels, ovariectomised mice were treated with estradiol, and this led to increased protein levels of the CCR2 ligands, CCL2 and CCL3 (Abu-Taha et al., 2009). In a mouse model of the menstrual cycle, CCR2 mRNA increased following progesterone withdrawal, peaking at 48hrs post-withdrawal, and gene expression of CCL2 and CCL3 both peaked at 24hrs (Menning et al., 2012). In pregnancy, CCL2 expression is present throughout gestation with peaks after mating, at implantation, and during the second half of pregnancy (Wood et al., 1999). Results from our lab indicate that at the end of pregnancy, CCR2 and the chemokines CCL2 and CCL3 are increased during labour compared to gestational day 18 (Menzies et al., 2012). These chemokine changes in different hormonal situations could be similar to the kind seen in the post-partum period, and may give insight into the mechanism driving the changes in leukocyte composition seen in this project. Comparing males and females could also reveal potential roles for sex hormones in the recruitment of leukocytes. I was interested in examining whether male reproductive tissues contained infiltrating leukocyte populations, as very little literature has focused on the role of leukocytes in the male reproductive tract. This led me to question whether leukocytes present in the male reproductive tract were phenotypically similar to those found in females or if the leukocyte composition of reproductive tissues was specific to the sex of the mouse.

Another avenue of investigation was the role of prolactin, a hormone associated with the post-partum period. Lactation can have dramatic effects on the immune system and can induce worsening of autoimmune conditions (Shelly et al., 2012). In both humans and mice circulating prolactin declines after birth and its production is then stimulated by offspring suckling. Therefore in the post-partum period there may be dramatic hormonal differences between mice that lactate and those that do not. Prolactin plays a key role in T cell maturation in the thymus (Gagnerault et al., 1993, Carreno et al., 2005), making examination of these cells in the post-partum period of specific interest. Examining non-

lactating mice also gave me the opportunity to see whether some of the findings regarding CD3+ cells elsewhere in my project only occurred in mice that were lactating and therefore were not as a result of post-partum inflammation *per se*.

The main questions to be addressed in the work described in this chapter were therefore: (i) Are there sex differences in myeloid and CD3+ DN cell populations? (ii) Are CD3+ DN cells also present in male reproductive tissues? and (iii) Does lactation affect CD3+ populations in tissues during the post-partum period?

Results

6.1. *Gating strategy for analysing myeloid subsets using only four colours*.

While optimising flow cytometry techniques for the previous work described in this thesis, only spleen and blood were studied and limited numbers of antibodies were used. Nonetheless, this still enabled the identification of important leukocyte populations and Figure 6.1A shows the gating strategy used for identification of certain myeloid cell populations using four colours. Understandably, this was a simplified version of the gating strategy eventually used when seven colours were employed (as seen in Chapter 3). Firstly, physical extremes were excluded and 7-AAD- live cells were gated. CD11b+ cells were then selected and these were then split between two gates based on their Ly6C/SSC properties. Cells in gate 1 (CD11b+Ly6C^{lo}SSC^{int-hi}) were classified as eosinophils, cells in gate 2 (CD11b+Ly6C^{int}SSC^{int}) are considered to be neutrophils for this section of the project. Gate 3 was selected as an inverted L shaped gate including Ly6C^{int-hi} and SSC^{lo-int} cells that were considered to predominantly be monocytes and macrophages. As macrophages are absent in blood, this gate only described monocytes when blood was analysed. Ly6C^{hi}CCL2-AF647^{hi} cells within this gate are inflammatory monocytes (gate 5), whereas Ly6C^{int}CCL2-AF647^{hi} cells within gate 4 are termed 'other CCL2 monocytes/macrophages'. CCL2^{int} monocytes/macrophages were defined by gate 6 and CCL2^{lo} monocytes/macrophages fall within gate 7.

6.2. *Males have a larger proportion of monocytes and fewer eosinophils in their blood, compared to females*.

In a pilot study to address the question of how hormones might affect myeloid populations in spleen and blood, the simplest course was to analyse age-matched WT females and WT males from our colony to identify potential sex differences for the first three populations shown in Figure 6.1. Consistent with data from Chapter 3 (Figure 3.18), eosinophils made up ~1% of live cells in the spleen, and no sex difference was seen (gate 1, Figure 6.2B, left). In blood, there was a significantly reduced proportion of eosinophils in males, compared to females (gate 1, Figure 6.2B, right). Interestingly, neutrophils were increased as a proportion of live cells in males, compared to females in the spleen but not the blood (gate 2, Figure 6.2C, left). Males also had an elevated total monocyte population in blood which was around double that found in females (gate 3, Figure 6.2D, right). This difference was not immediately obvious from the sample plots in Figure 6.2A, however the variation between individuals meant that finding a plot representative of all the samples was

challenging. This sex discordance was worthy of further investigation, and as shown in Figure 6.1 this population was split into 4 distinct subsets.

6.3. *No monocyte or macrophage subset was specifically affected by sex.*

Gate 3 in Figure 6.1 represents monocytes and macrophages in the spleen but only monocytes in blood. This gate was subdivided by Ly6C and CCL2-AF647 expression. Figure 6.3B refers to other CCL2+ cells, which are $Ly6C^{int}$ and therefore not inflammatory monocytes (gate 4). No sex discordance was observed in this population, although in spleen there was a tendency for males to have a larger population of these cells, compared to females ($p=0.064$). Inflammatory monocytes constituted a large proportion of monocytes/macrophages in both tissues studied, although no significant sex difference in this cell population was seen in spleen or blood (gate 5, Figure 6.3C). Though Figure 6.3A appears to show that inflammatory monocytes had higher CCL2-AF647 fluorescence in females, compared to males, this was not a consistent finding and no significant difference was seen (data not shown). Not all cells in gate 3 were $CCL2^{hi}$ so $CCL2^{int}$ (gate 6, Figure 6.3D) and $CCL2^{lo}$ (gate 7, Figure 6.3E) monocytes/macrophages were considered next, but no sex difference was seen in either population in spleen or blood.

6.4. *CCR2 deletion disrupts myeloid cell populations, particularly in blood.*

One of the major focuses of this work has been the chemokine receptor CCR2, which is required for monocyte emigration from the BM (Serbina and Pamer, 2006). The effect of CCR2 deletion on myeloid cell populations in the spleen and blood was investigated in female mice at 1DPP in Chapter 3 (Figures 3.19 and 3.21). Age-matched male and female mice were compared here (Figure 6.4: note that statistical analyses are contained in the Legend to this Figure). Interestingly, several previously undescribed differences were observed between WT and CCR2 KO mice. First, blood from CCR2 KO mice contained an increased proportion of eosinophils in males, but not females (gate 1, Figure 6.4A-B, right). Second, and surprisingly, neutrophils in the blood were also diminished in both sexes in CCR2 KO mice, compared to WT counterparts (gate 2, Figure 6.4C, right). This was not seen in female mice at 1DPP, and may have been due to the variation between the environmental surroundings between mice used in Chapter 3 and Chapter 6, or a knock-on effect of other in cell populations changing within the tissue. Finally, a large decrease in monocytes and macrophages was seen across both sexes as a consequence of deletion of CCR2 (gate 3, Figure 6.4D), similar to the decreases seen in Figure 3.14 and consistent with previously published findings (Serbina and Pamer, 2006). This is particularly visible

in gate 3 in the plots in Figure 6.4A. These data suggest that CCR2 deletion affects myeloid cells across both sexes, and that eosinophils are only affected by CCR2 deletion in males.

6.5. *Summary 1.*

This section concentrated on addressing whether there were any differences in myeloid cell populations in the blood and spleen of males and females. The main findings were as follows:

- Monocytes in blood are increased as a percentage of live cells in males, compared to females, but CCR2 deletion affects both sexes equally and dramatically reduces the monocyte population.
- The proportion of eosinophils is reduced in the blood of males, compared to females, but this is reversed in CCR2 KO mice.
- Males have a higher percentage of neutrophils in their spleens, compared to female mice, and CCR2 deletion results in a reduction in the number of neutrophils retrieved from the blood of both sexes.

These differences could provide an insight into the sex discordances that are observed in a large range of inflammatory diseases. This will be examined further in the Discussion (Chapter 7). The next section continues the theme of sex differences but studies CD3+ DN cells, the main population examined in Chapter 5.

6.6. *No difference in proportion of CD3+ DN cells in peripheral tissues between males and females.*

As some interesting sex differences were present in the distribution of myeloid cells in blood and spleen, I also wanted to investigate the other main cell type studied in this project, CD3+ DN cells, and enumerate these cells in males and females. NP females were compared with age-matched males for the CD3+ DN cell subsets they had in different tissues. The female data was also shown in Figure 5.9 but were reanalysed for Figure 6.5 to show the overall number of CD3+ DN cells in these tissues. Surprisingly, given the changes seen in these cells in post-partum tissues, the proportion of CD3+ DN cells was constant in the spleen, blood and PALN between males and females (Figure 6.5).

As in Chapter 5, CD3+ DN cells were then split into four subsets; NK1.1+TCRβ-, NK1.1+TCRβ+, TCRβ+NK1.1-, TCRβ-NK1.1- and TCRβ-NK1.1- CD3+ DN cells. In secondary lymphoid tissues no significant differences were seen in the two major CD3+

DN cell subsets between males and females (Figure 6.6A and C). In blood there was a suggestion that NK1.1+TCRβ+ DN cells (i.e. NKT cells) were reduced in males, compared with females, though this was only seen in numbers of cells per ml and not reflected in their percentage (Figure 6.6B).

As shown in Chapter 5, a considerable proportion of TCRβ-NK1.1- CD3+ DN cells in peripheral tissues expressed TCR-γδ. TCR-γδ expression on TCRβ-NK1.1- CD3+ DN cells was examined in males and females. Female data was also presented in Figure 5.11. No difference was seen in the proportion or number of TCRγδ+ cells within this TCRβ-NK1.1- CD3+ DN cell population within spleen, blood and PALN (Figure 6.7).

Collectively, these data show that lymphoid tissues and blood in both males and females are very similar in their CD3+ DN cell profile. Chapters 4 and 5 suggested that the changes in their proportions could be an indicator of a role in post-partum inflammation. Given this supposed reproductive function, the fact that the CD3+ DN cell composition is so similar between males and females was perhaps something of a surprise. To explore this further, reproductive tissues were taken from the same male and female animals and were also analysed for their CD3+ DN cell composition. The purpose of this was to define whether CD3+ DN cells were characteristic of the female reproductive tract, or of reproductive tissues in general.

6.7. *Reproductive tissues are broadly similar in their CD3+ DN cell composition.*

Male reproductive tissues were digested in the same way as in previous chapters for uterine horn and cervix. The male reproductive tissues tested were penis, prostate gland and vas deferens/epididymis. Representative plots of the CD3+ DN cell populations of the tissues are shown in Figure 6.8A. Interestingly, reproductive tissues had similar percentages of CD3+ DN cells, compared to CD3+ cells as a whole and this was generally over 80% (Figure 6.8B). Thus, the population of reproductive tissues by DN CD3+ cells appears to be sex-independent.

The subsets of CD3+ DN cells were then considered, to see if the TCRβ/NK1.1 expression on these cells varied between tissues. Though the other subsets did not fluctuate significantly, TCRβ-NK1.1- CD3+ DN cells did show some changes. The prostate gland had a smaller proportion of TCRβ-NK1.1- cells compared to uterine horn ($p<0.01$), cervix ($p<0.05$) and penis ($p<0.05$, Figure 6.8C, left). When CD3+ DN cell subsets per g were

considered the only significant difference between tissues was for NK1.1+TCRβ+ CD3+ DN cells, which showed a larger number of these cells per g of prostate gland, compared with uterine tissue ($p<0.05$, Figure 6.8C, right).

Finally, TCR-γδ expression was examined on TCRβ-NK1.1- CD3+ DN cells in order to get a measure of potential γδ T cells in male and female reproductive tissues. Uterine horn data and cervix data were also shown in Figure 5.10. Interestingly, prostate gland had the highest percentage of TCRβ-NK1.1- CD3+ DN cells expressing TCR-γδ, over double the level of expression seen in the uterine horn (Figure 6.8D, left). When TCRγδ+ cells per g were considered, the penis contained significantly more TCRγδ+ TCRβ-NK1.1- CD3+ DN cells than were seen in the uterine horn (Figure 6.8D, right).

These results were particularly unexpected, and suggest a role for CD3+ DN cells in reproductive immunology in both sexes, not just females. Very little data exists on T cells in the male reproductive tissues, and this work has catalogued the CD3+ DN cell population within penis, prostate gland and vas deferens/epididymis. Tissues such as the testes have been described as an immune-privileged area (Witkin et al., 1996), and this is thought to help prevent immune responses developing against the sperm produced at the site. It is possible that both male and female reproductive tissues need to balance immune regulation with protection against diseases of the genital tract.

6.8. *Summary 2.*

This section concentrated on CD3+ DN cells in males and females, including separating this population by expression of NK1.1, TCR-β and TCR-γδ. Several tissues were studied, including male and female reproductive tissues. The key results were:

- No sex difference was seen in the overall percentage of CD3+ DN cells in any of the tissues studied.
- Prostate gland was the most distinct reproductive tissue. More cells were retrieved per g of tissue, and the balance of populations was different, with reduced TCRβ-NK1.1- cells.
- There may be a reduced number of NK1.1+TCRβ+ CD3+ DN cells in the blood of males, compared to females.
- TCR-γδ expression on TCRβ-NK1.1- CD3+ DN cells was higher on some male reproductive tissues, compared to uterine horn.

The similarities in CD3+ DN cell populations between the sexes will be explored further in the discussion. The focus of the following section shifts to address the effect of lactation on leukocyte populations at 7DPP. Studying lactation was a way of extending the work on hormonal regulation of leukocytes and inflammation in females as only very subtle differences had been observed in leukocyte abundance between males and females.

6.9. *Circulating prolactin and CCL2 were reduced in non-lactating females*.

Many studies have attempted to link hormonal changes with leukocyte recruitment (De and Wood, 1990, Abu-Taha et al., 2009, Tchernitchin et al., 1974, Wood et al., 2007, Kyaw et al., 1998, Menning et al., 2012, Critchley et al., 1996). As discussed in Chapter 1, the hormone prolactin is associated with the post-partum period. Absence of lactation might be expected to have an effect on the hormonal profile of a post-partum mouse and therefore the cell populations present in the post-partum period. To begin to investigate the role of lactation, prolactin in plasma was measured over the post-partum period and between lactating and non-lactating mice at 7DPP. Plasma from NP and lactating mice was obtained by terminal cardiac puncture from mice sacrificed throughout the project. Mice that were not lactating at 7DPP became available for study when mothers cannibalised their pups, or when pups were removed from mothers. In both cases, mice were not lactating beyond 1DPP.

I had expected that NP serum prolactin levels would be reduced compared to the later post-partum time-points, but this was not the case (Figure 6.9A). Studies in rats have previously shown that NP animals have a lower concentration of circulating prolactin than that observed during the post-partum period (Liu et al., 1992, Hapon et al., 2003). However it must be considered that differences in species, experimental technique and natural variation may account for this difference.

As would be expected, there was a lower concentration of prolactin at 1DPP, compared to the other time-points (Figure 6.9A), as prolactin production has been reported to fall rapidly during the early post-partum period and is stimulated again by the suckling of pups (Glasier and McNeilly, 1990, Glasier et al., 1984). The 7DPP post-partum data was then analysed against plasma from 7DPP mice that had not kept their pups. Circulating prolactin was significantly reduced in non-lactating mice, compared to lactating mice, consistent with the idea that pups stimulate prolactin production. This showed that lactating mice

have a distinct hormonal profile and I wanted to explore whether this was associated with changes in leukocyte distribution.

In the context of the rest of the work and due to the availability of appropriate Luminex plates, I also sought to quantify circulating levels of CCL2 and CCL3 in lactating and non-lactating animals. CCL2 and CCL3 were measured in plasma and CCL2 but not CCL3 was reduced at 7DPP in non-lactating mice, compared to lactating mice (Figure 6.9C-D). When CCL2 was examined over the post-partum period in Chapter 3 there was an increase in circulating CCL2 from 1DPP to 7DPP in WT mice (Figure 3.15). Comparing this with Figure 6.9, this rise was not observed in non-lactating mice (Figure 6.9C). These results provided an incentive to continue to investigate whether lactation had an effect on populations that I had previously shown to express CCR2. Due to the predominance of myeloid cell populations, and their clear CCR2-dependent changes in reproductive tissues, these were investigated first.

6.10. *Lactation had no effect on the expression of genes encoding myeloid cell markers in the reproductive tract at 7DPP*.

Initially expression of genes encoding myeloid cells markers was studied using Taqman in uterine horn and cervix and no effect of lactation was seen in the expression of F4/80, CX3CR1 or CCR2 (Figure 6.10A-C). Granulocyte markers were also measured but lactation had no effect on the gene expression of the eosinophil marker MBP (Figure 6.10D) or the neutrophil marker NGP (Figure 6.10E). On the basis of these data the effect of lactation on myeloid cells was not pursued further. However, elsewhere in the project qRT-PCR was shown to have some disadvantages, so further studies with non-lactating animals using flow cytometry to analyse myeloid cells would be merited, although time constraints meant that this work was not possible.

6.11. *Lactation appeared to decrease the overall proportion of CD3+ cells in the uterine horn at 7DPP.*

The literature describes a role for prolactin in T cell development in the thymus (Carreno et al., 2005, Gagnerault et al., 1993) and therefore it seemed possible that hormonal changes associated with lactation could influence CD3+ cell populations in reproductive tissues and elsewhere. Flow cytometry allowed for greater accuracy in quantifying different cell types, so the effect of lactation at 7DPP on CD3+ cells, including CD3+ DN cells, was examined using this method. 7DPP data used in Chapter 4 were re-analysed alongside

7DPP non-lactating data. Overall, CD3+ cells in uterine horn made up a lower proportion of CD45+ cells in animals lactating at 7DPP compared to those not lactating, although this difference was not seen in the cervix (Figure 6.11A). It appeared that CD8+ T cells represented a higher proportion of CD3+ cells in the reproductive tissues of lactating mice, but this was not significant in uterine horn or cervix (p=0.090, Figure 6.11B). The proportion of CD3+ cells that were CD4+ or CD4+CD25+ was not different between the groups (Figures 6.11C-D). CD3+ DN cells, which were the majority of CD3+ cells in reproductive tissues in both groups, made up an average of ~80-85% of CD3+ cells in non-lactating mice and although these cells appeared to be less abundant in the uterine horn or cervix of lactating mice compared to non-lactating counterparts (p=0.099, Figure 6.11E), no statistically significant differences were detected.

These results indicate that, compared to other cell types, lactation appears to suppress CD3+ cell number in reproductive tissues at 7DPP but that the various cell types within this population were equally affected. However, it is possible that increasing the size of each group could reveal subtle differences. Next, other tissues were explored on the basis of previous results that have indicated that cell populations within peripheral tissues respond differently during the post-partum period, compared to reproductive tissues.

6.12. *Lactation increases the frequency of blood CD3+ cells carrying CD4*.

Spleen, blood and PALN were examined at 7DPP to determine whether lactation had any effect on the cellular composition of CD3+ cell populations. Unlike uterine horn (Figure 6.11), the proportion of CD45+ cells that were CD3+ in spleen, blood and PALN was unaffected by lactation (Figure 6.12A). However, CD8+ T cells made up a higher proportion of CD3+ cells in non-lactating mice in the PALN, compared to lactating mice (Figure 6.12B). More strikingly, lactation was associated with an increase in the frequency of CD4+ T cells in the blood CD3+ cell population (Figure 6.12C). The small population of CD4+CD25+ T cells was unchanged between lactating and non-lactating females (Figure 6.12D).

Compared to lactating females, the CD3+ population in the blood from non-lactating mice appeared to contain a higher percentage of CD3+ DN cells. This was not significant but could be regarded as borderline (p=0.057, Figure 6.12E). CD3+ DN cells in the blood were roughly at this level at 1DPP (Figure 4.3). At 1DPP, the CD4+ T cell proportion in the blood fell as the CD3+ DN cell proportion rose (Figure 4.3), a situation that may be being

prolonged to 7DPP by the absence of lactation. Thus, lactation, and the associated hormonal profile associated with this state, may allow the CD3+ DN content of the blood to fall and the CD4+ T cell population to rise again by 7DPP. This potentially also raises the question of whether these changes in the blood from 1DPP-7DPP relate to completion of post-partum repair of reproductive tissues or are driven by suckling young. However, it should be noted that (i) the study did not conclusively assert that 7DPP non-lactating animals have a raised CD3+ DN cell level, and (ii) studying the proportion of cells of a certain type within the CD3+ population may mask effects of lactation on the absolute number of CD3+ DN cells and other CD3+ cell populations in reproductive tissues and lymphoid organs. Thus, the data were further analysed to determine the total number of cells retrieved from these tissues.

6.13. *Lactation is associated with a reduction in CD3+ DN cells and CD4+CD25+ T cells in the cervix at 7DPP.*

When the total number of retrieved CD3+ cells was calculated, no significant difference between lactating and non-lactating 7DPP females was seen in the uterine horn ($p=0.090$), but far more CD3+ cells were retrieved from the cervix of non-lactating mice at 7DPP (Figure 6.13A). To determine which CD3+ cell subsets might be the source of these changes, individual populations were investigated. In uterine horn and cervix no significant differences between the two groups were seen for CD8+ T cells (Figure 6.13B) and CD4+ T cells (Figure 6.10C). The number of CD4+CD25+ T cells retrieved from the uterine horn did not change significantly between the two groups, but these cells were far more abundant in the cervix of non-lactating mice, compared with those harvested from lactating mice (Figure 6.13D). This was also seen for the CD3+ DN cell subset, with higher numbers were retrieved from the cervix of non-lactating mice (Figure 6.13E). Thus, lactation was associated with a reduction in the number of CD3+ DN cells and CD4+CD25+ T cells that could be retrieved from the cervix.

6.14. *Lactation is associated with a reduction in CD4+ and CD8+ T cells in the spleen.*

The number of cells within the various CD3+ cell populations was also determined in the spleen and PALN of lactating and non-lactating 7DPP mice. Strikingly, in the spleen CD3+ cells were far more abundant in non-lactating females (Figure 6.14A), primarily due to increases in the abundance of CD8+ T cells (Figure 6.14B) and CD4+ T cells (Figure 6.14C). This was not seen in the PALN. CD4+CD25+ T cells and CD3+ DN cells were minor subsets in the spleen and PALN (Figure 6.14D-E). CD3+ DN cells appeared to be

more abundant in the spleen of non-lactating mice, but this failed to reach statistical significance (Figure 6.14E p=0.082). Thus, lactation is associated with a major change in the cellularity of the spleen, and contrary to a previous report (Bustamante et al., 2008), this difference is in favour of non-lactating mice. Previously, spleen weight has been found to be increased in lactating mice (Bustamante et al., 2008). This was found to be due to an increase in the size of the red pulp and an upregulation of genes associated with erythroid cells (Bustamante et al., 2008). This might reflect a reduction spleen resident leukocytes in order to increase the red blood cell compartment, meaning that proportions of CD3+ cells would not change, but cell numbers would decrease in lactating mice.

6.15. *Spleen and blood from non-lactating mice contain a higher percentage of CCL2-AF647+ CD4+ T cells and CD3+ DN cell subsets, compared with lactating females.*

Previously I found that at 1DPP that there was a reduction in CD4+ T cells in the blood, and that this was accompanied by a CCR2-dependent increase in CD3+ DN cells (Figures 4.3 and 4.9). A similar reduction in CD4+ T cells was seen in non-lactating animals at 7DPP (Figure 6.12). Further to this, lactating animals have higher circulating amounts of CCL2 than non-lactating animals (Figure 6.9), which led me to question whether CCR2 was also involved in the CD4+ T cell/CD3+ DN cell dynamic at 7DPP. CCL2-AF647 internalisation by CD3+ cells was investigated in blood and secondary lymphoid organs between lactating and non-lactating animals.

In the spleen, lactation to 7DPP appeared to suppress internalisation of CCL2-AF647 across the board (Figure 6.15B-E). Blood did not exhibit such clear-cut differences. As seen in Figure 6.15A and Figure 6.15C the blood of non-lactating animals had a higher percentage of CD4+ T cells internalising CCL2-AF647 at 7DPP (Figure 6.15C), however when the CD4+CD25+ subset was examined, no change between the groups was seen (p=0.082, Figure 6.15D). CD3+ DN cells also showed a higher percentage of CCL2-AF647+ cells in the blood of mice that had not been lactating (Figure 6.15E).

In reproductive tissues, none of the CD3+ subsets investigated showed significant differences in the proportion of cells internalising CCL2-AF647 (Figure 6.16). The CD4+CD25+ T cell subset showed a tendency towards increased CCL2-AF647 internalisation in non-lactating uterine horn (p=0.069, Figure 6.16D).

It was clear that CCL2-AF647 internalisation is altered depending on lactation status, particularly in spleen and blood. It was possible that either the populations present in the tissues affected CCL2-AF647 internalisation or that altered expression of CCR2 results in a change in the populations present. The increased circulating CCL2 in lactating mice could also result in increased desensitisation of CCR2. Finally, reproductive tissues were tested for their ability to internalise CCL2-AF647 in order to determine whether any lactation dependent difference could be detected. It is clear that several factors interplay in the post-partum period and given the results up to now it is plausible that the distribution of CD3+ populations depends on a mechanism that incorporates lactation and CCL2/CCR2.

6.16. *Summary 3.*

Lactation does appear to affect CD3+ cell populations. 7DPP non-lactating mice were used to examine this difference. Taking the results together it seems that in a few respects such as circulating prolactin, CCL2 and CD4+ T cells/CD3+ DN cell populations in blood, 7DPP non-lactating mice bear some resemblance with 1DPP mice.

- Prolactin and CCL2 in the plasma were significantly reduced in non-lactating mice, compared to lactating animals. 1DPP mice were also shown to have low levels of circulating prolactin.
- Lactating mice have a reduced percentage of CD3+ cells in the uterine horn, compared to non-lactating mice at 7DPP.
- Non-lactating mice showed a reduced percentage of CD4+ cells, matched with a near-significant increase in the proportion of CD3+ DN cells, compared to lactating females.
- Non-lactating mice had an increased number of CD4+ and CD8+ T cells in their spleen, compared to lactating subjects.
- There was an increased number of CCL2-AF647+ CD4+ T cells and CD3+ DN cells in the blood of non-lactating mice.

Although this chapter was unable to show a causal link between levels of hormones and leukocyte populations, it utilised comparisons of males and females and lactating and non-lactating animals to begin to tease out these associations. The effects of lactation in the post-partum period were compelling and indicate a possible avenue for future work. These findings are explored further in the Discussion (Chapter 7).

Figure 6.1. *Gating strategy for analysing myeloid subsets using only four colours.*
Measurement of myeloid subsets in spleen and blood using flow cytometry. (A) Gating strategy for isolation of monocytes, macrophages and neutrophils. First physical extremes were excluded, followed by exclusion of 7-AAD+ cells, cells were then gated as CD11b+. Cells were then classified by their Ly6C/SSC properties. Cells were gated as follows; [1] eosinophils, [2] neutrophils, [3] monocytes/macrophages. Gate [3] was then divided further by its Ly6C/CCL2 properties; [4] other CCL2+ monocytes/macrophages, [5] inflammatory monocytes, [6] $CCL2^{int}$ monocytes/macrophages and [7] $CCL2^{lo}$ monocytes/macrophages. These definitions remained constant for this section.

A

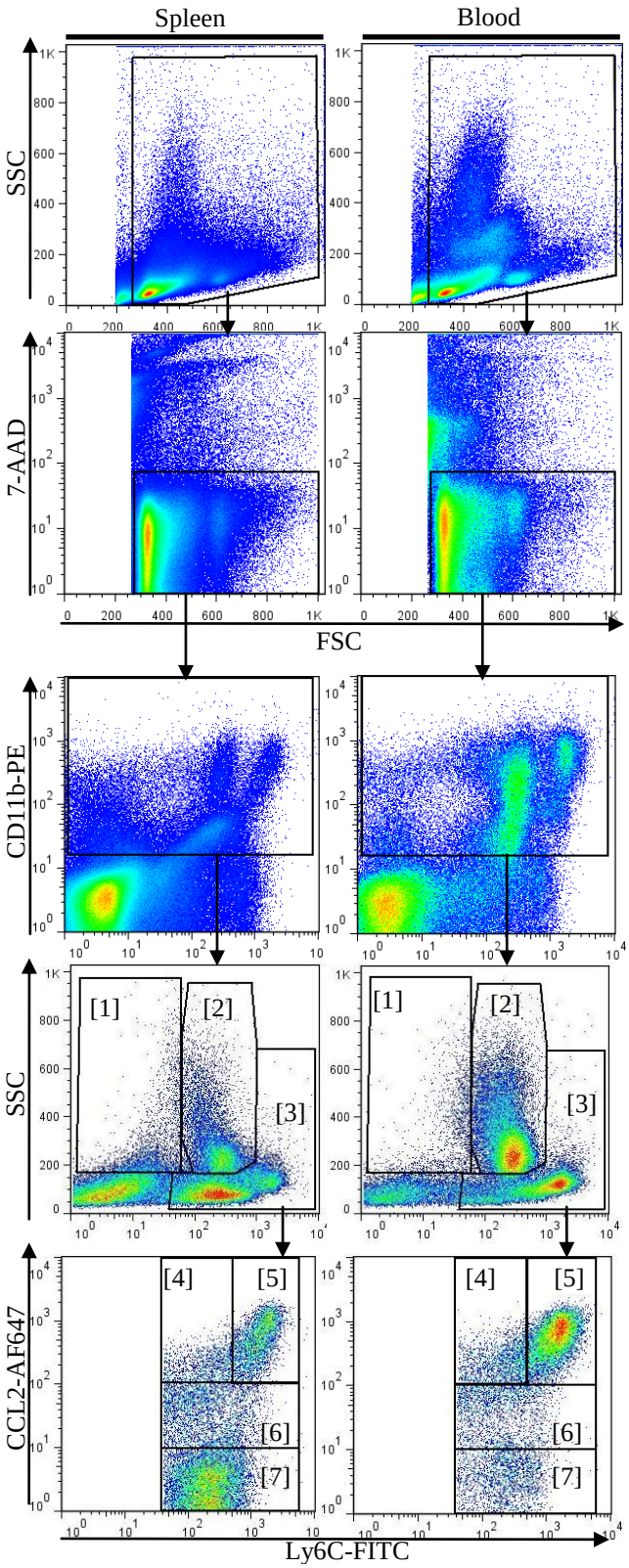

Figure 6.1. *Gating strategy for analysing myeloid subsets using only four colours (legend opposite).*

Figure 6.2. *Males have a larger proportion of monocytes and fewer eosinophils in their blood, compared to females.*

Measurement of monocyte and macrophage subsets in spleen (n=8-9) and blood (n=6) using flow cytometry in males and females. Gating as in fig 6.1. (A) Typical Ly6C/SSC plots from female and male blood and spleen. (B) Proportion of live cells defined as eosinophils in spleen (left) and blood (right). (C) Proportion of live cells defined as neutrophils in spleen (left) and blood (right). (D) Proportion of live cells defined as monocyte and macrophages in spleen (left) and monocytes in blood (right). Data pooled from 3 experiments and presented as mean±SEM. Data analysed by Student's t-test with a Welch's correction, where appropriate, *$p<0.05$ **$p<0.01$.

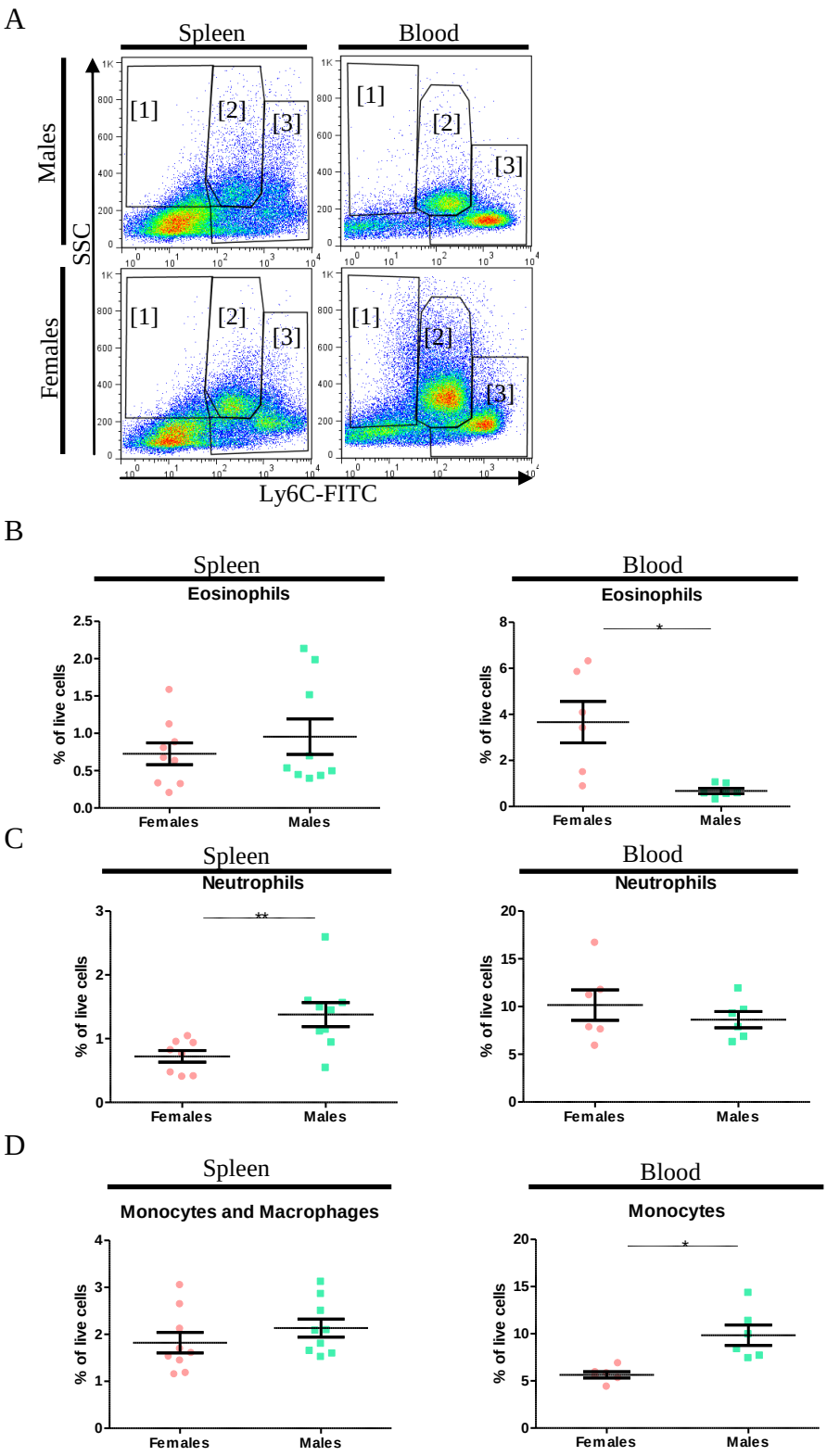

Figure 6.2. *Males have a larger proportion of monocytes and fewer eosinophils in their blood, compared to females (legend opposite).*

Figure 6.3. *No monocyte or macrophage subset was specifically affected by a sex difference.*

Measurement of monocyte and macrophage subsets in spleen (n=6) and blood (n=6) using flow cytometry in males and females. Gating as in fig 6.1. (A) Typical Ly6C/CCL2-AF647 plots from female and male blood and spleen. (B) Proportion of live cells defined as other CCL2+ monocytes and macrophages in spleen (left) and other CCL2+ monocytes in blood (right). (C) Proportion of live cells defined as inflammatory monocytes in spleen (left) and inflammatory monocytes in blood (right). (D) Proportion of live cells defined as $CCL2^{int}$ monocytes and macrophages in spleen (left) and $CCL2^{int}$ monocytes in blood (right). (E) Proportion of live cells defined as $CCL2^{lo}$ monocytes and macrophages in spleen (left) and $CCL2^{lo}$ monocytes in blood (right). Data pooled from 3 experiments and presented as mean±SEM. Data analysed by Student's t-test, not significant.

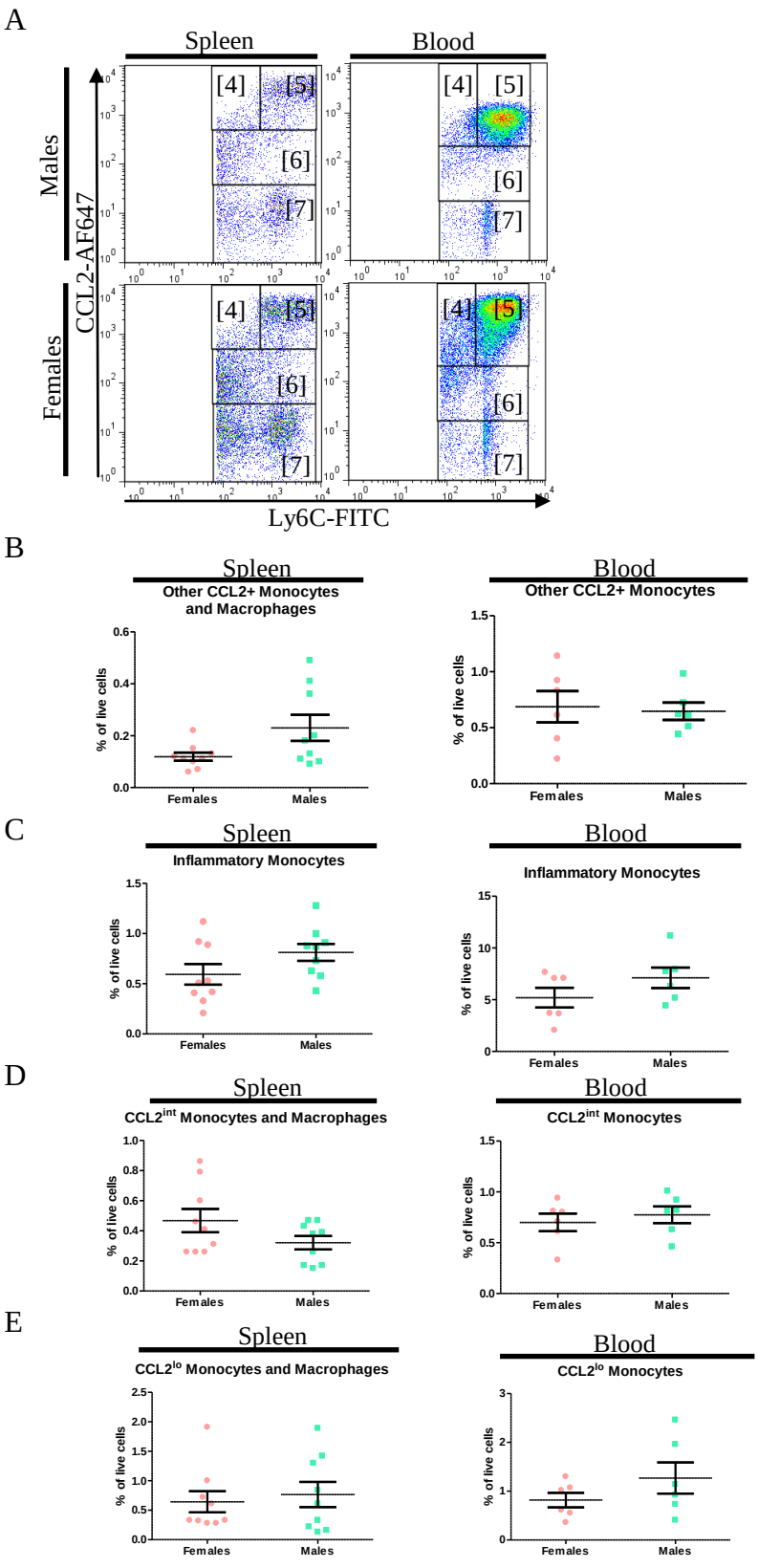

Figure 6.3. *No monocyte or macrophage subset was specifically affected by a sex difference.*

Figure 6.4. *CCR2 deletion disrupts myeloid cell populations, particularly in blood*. Measurement of monocyte and macrophage subsets in WT (n=6-9) and CCR2 KO (n=3) spleen and blood using flow cytometry in males and females. WT data taken from fig 6.2. (A) Typical Ly6C/SSC plots from WTs and CCR2 KOs with female and male blood and spleen. (B) Proportion of live cells defined as eosinophils in spleen (left) and blood (right). (C) Proportion of live cells defined as neutrophils in spleen (left) and blood (right). (D) Proportion of live cells defined as monocyte and macrophages in spleen (left) and monocytes in blood (right). Data presented as mean±SEM. Data analysed by two-way ANOVA. (B) Left; CCR2 effect p=0.43, sex effect p=0.90, interaction p=0.45. Right; **CCR2 effect p=0.021**, sex effect p=0.60, **interaction p=0.0069**. (C) Left; CCR2 effect p=0.91, **sex effect p=0.03**, interaction p=0.97. Right; **CCR2 effect p<0.001**, sex effect p=0.74, interaction p=0.45. (D) Left; **CCR2 effect p<0.001**, sex effect p=0.40, interaction p=0.73. Right; **CCR2 effect p<0.001**, **sex effect p=0.033**, **interaction p=0.0203**.

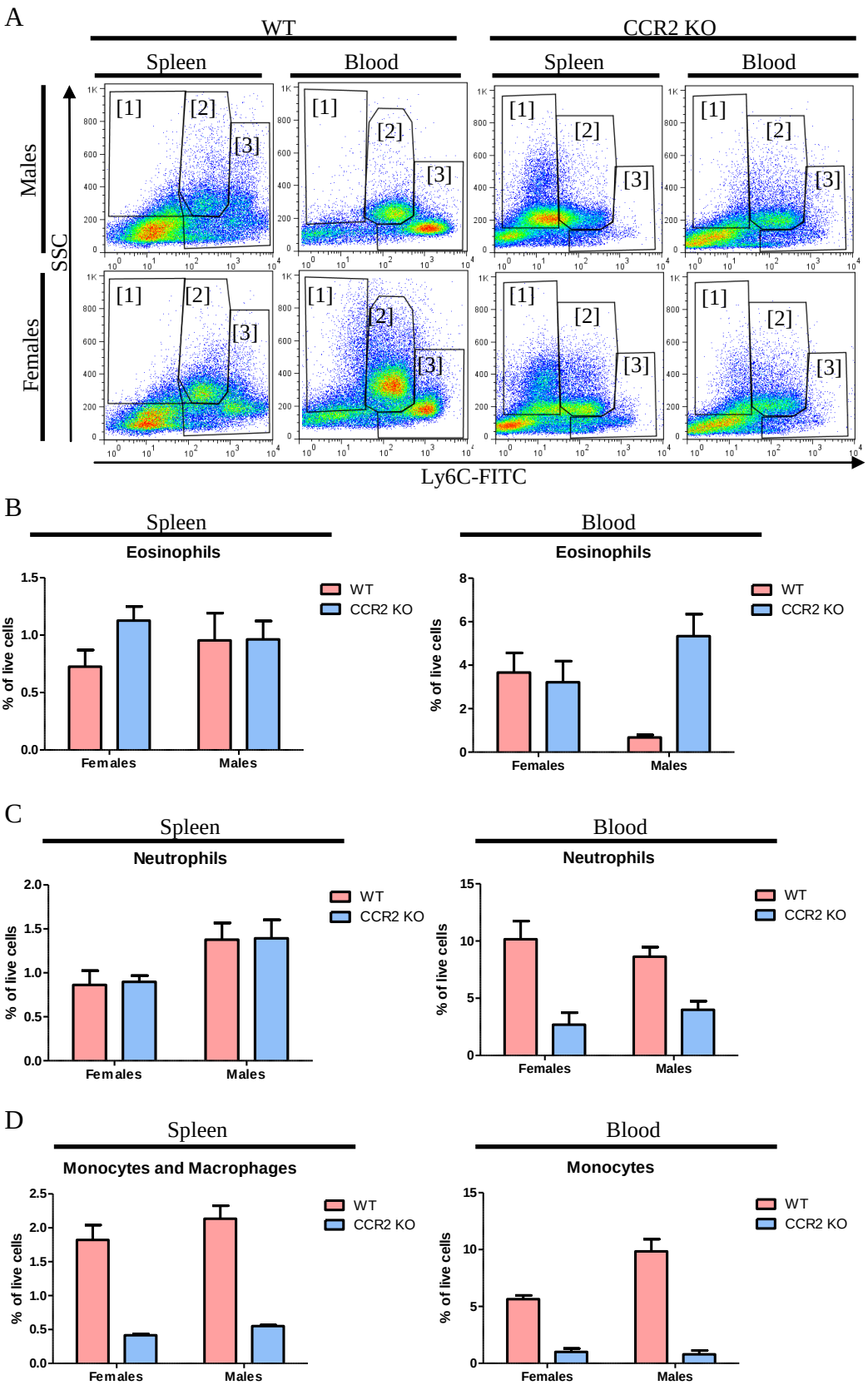

Figure 6.4. *CCR2 deletion disrupts myeloid cell populations, particularly in blood (legend opposite).*

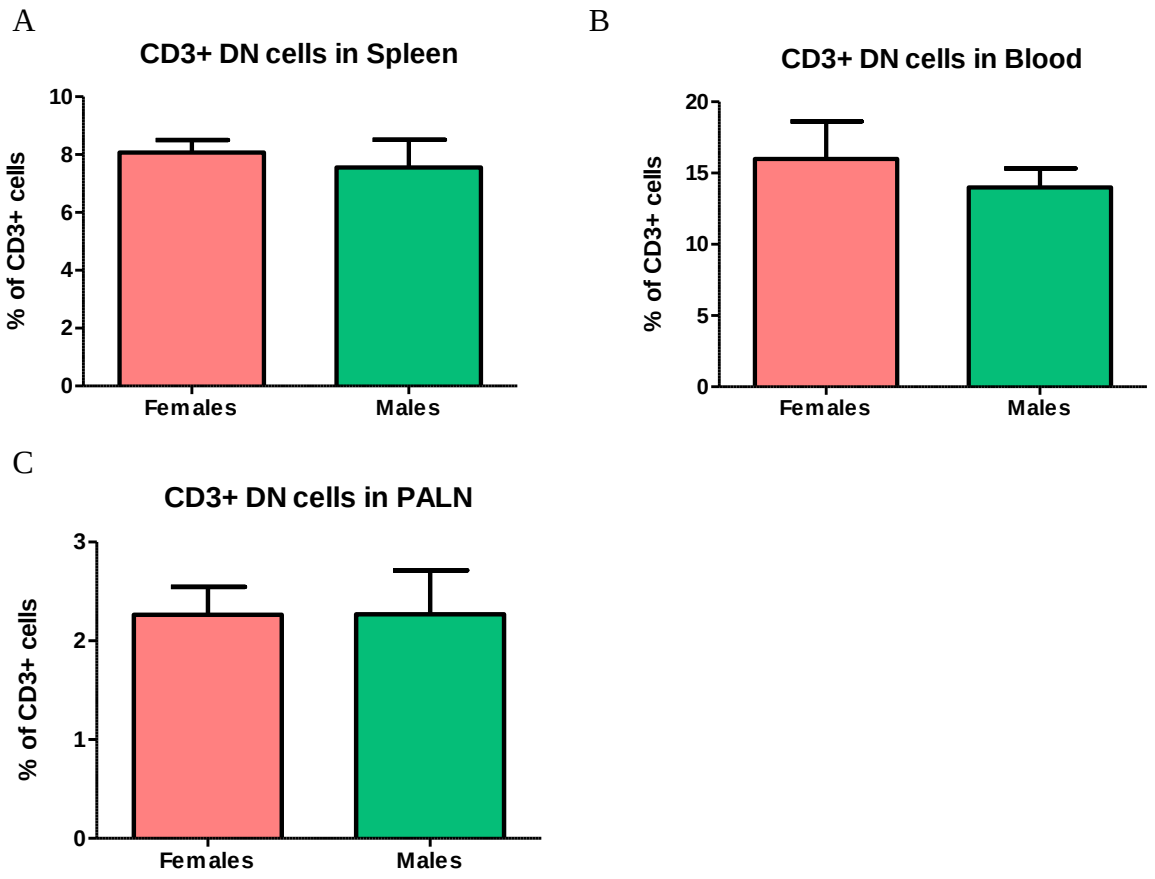

Figure 6.5. *No difference in proportion of CD3+ DN cells in peripheral tissues between males and females.*

CD3+ DN cells from tissues of male and female mice (n=4-8). (A) CD3+ DN cells as a percentage of CD3+ cells in spleen. Female data from fig 5.9 (B) CD3+ DN cells as a percentage of CD3+ cells in blood. (C) CD3+ DN cells as a percentage of CD3+ cells in PALN. Results presented as mean±SEM, data analysed using Student's t-test, not significant.

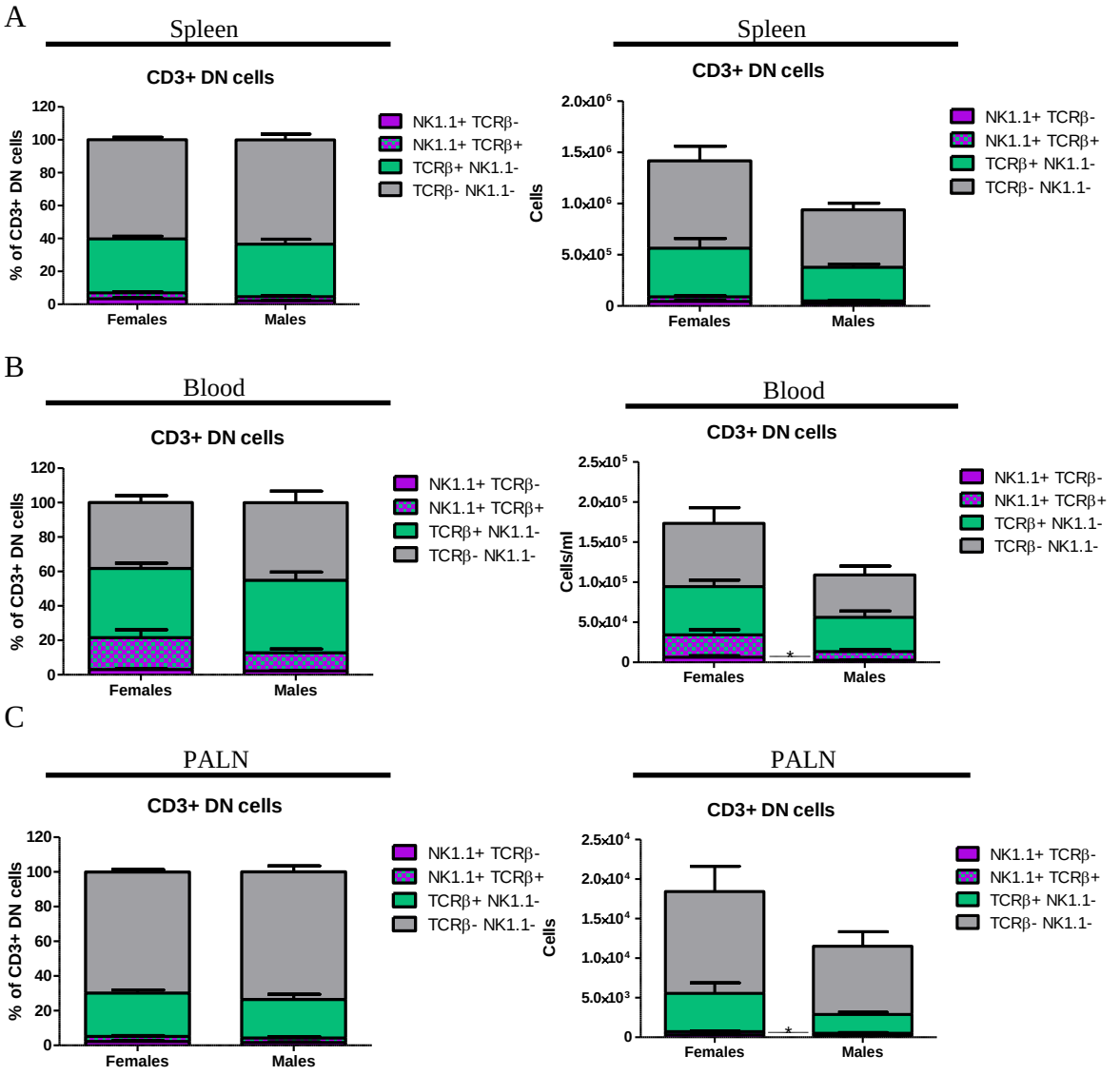

Figure 6.6. *Percentages of CD3+ DN cell subsets are similar between males and females.* TCRβ and NK1.1 measured in the CD3+ DN cell population from tissues of male and NP female mice (n=4-8). Gated as in fig 5.8, female data from fig 5.9. (A) Left; Proportions of TCRβ/NK1.1 gated CD3+ DN cells in spleen. Right; Number of TCRβ/NK1.1 CD3+ DN cells. (B) Left; Proportions of TCRβ/NK1.1 gated CD3+ DN cells. Right; Number of TCRβ/NK1.1 CD3+ DN cells per ml of blood. (C) Left; Proportions of TCRβ/NK1.1 gated CD3+ DN cells. Right; Numbers of TCRβ/NK1.1 CD3+ DN cells in the PALN. Results presented as mean±SEM, data analysed using Student's t-test, with Welch's correction where appropriate *$p<0.05$.

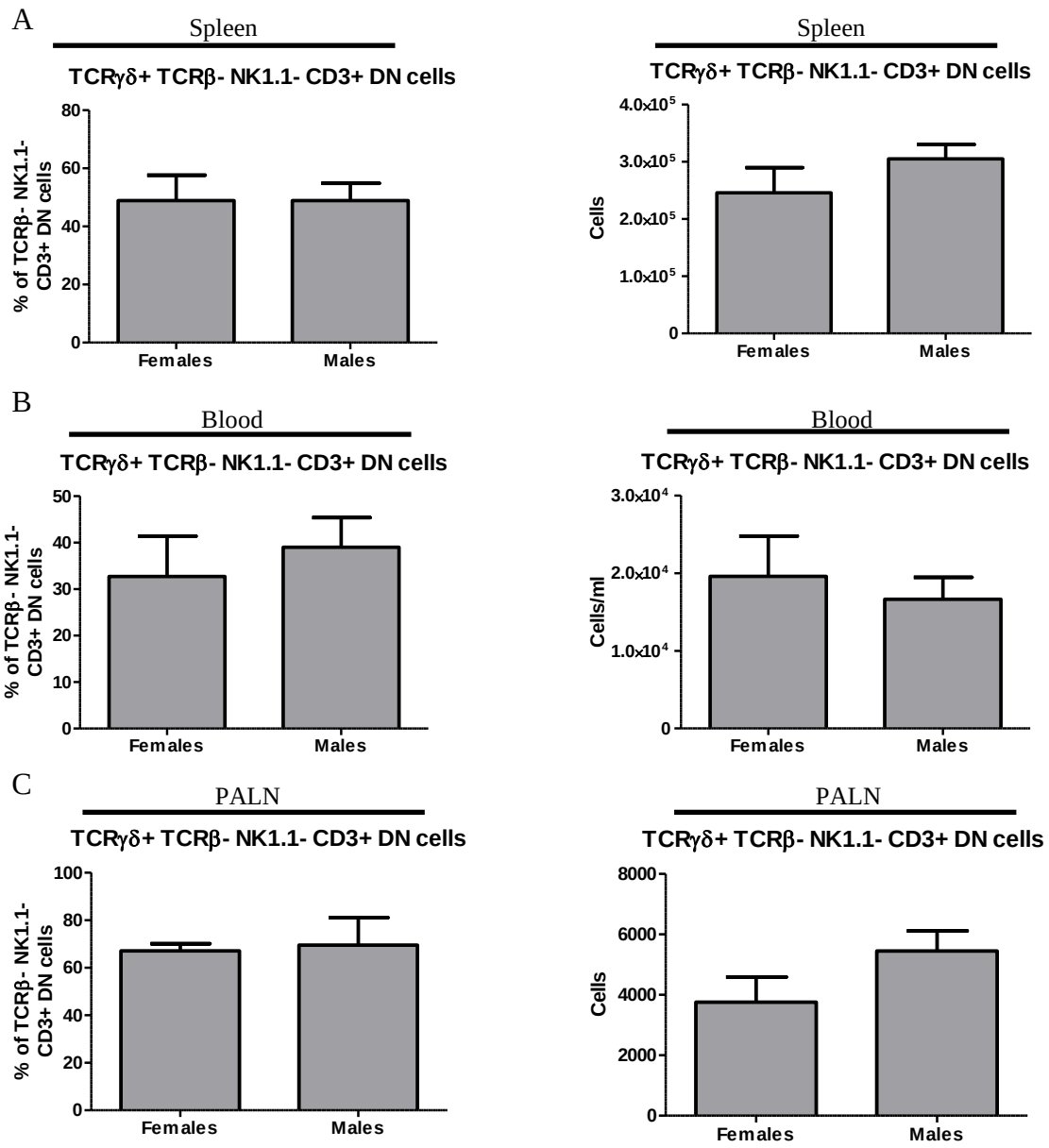

Figure 6.7. *TCRγδ+ expression is constant on CD3+ DN cells in females and males in spleen, blood and PALN.*

TCRγδ expression measured on TCRβ-NK1.1- CD3+ DN cells in tissues in females and males (n=3-6). Female data from fig 5.11. (A) Left; Proportion of TCRβ-NK1.1- CD3+ DN cells expressing TCRγδ in spleen. Right; Number of TCRγδ+TCRβ-NK1.1- CD3+ DN cells. (B) Left; Proportion of TCRβ-NK1.1- CD3+ DN cells expressing TCRγδ. Right; Number of TCRγδ+TCRβ-NK1.1- CD3+ DN cells per ml of blood. (C) Left; Proportion of TCRβ-NK1.1- CD3+ DN cells expressing TCRγδ in PALN. Right; Number of TCRγδ+TCRβ-NK1.1- CD3+ DN cells. Data presented as mean±SEM. Statistical analysis was carried out using a Student's t-test, not significant.

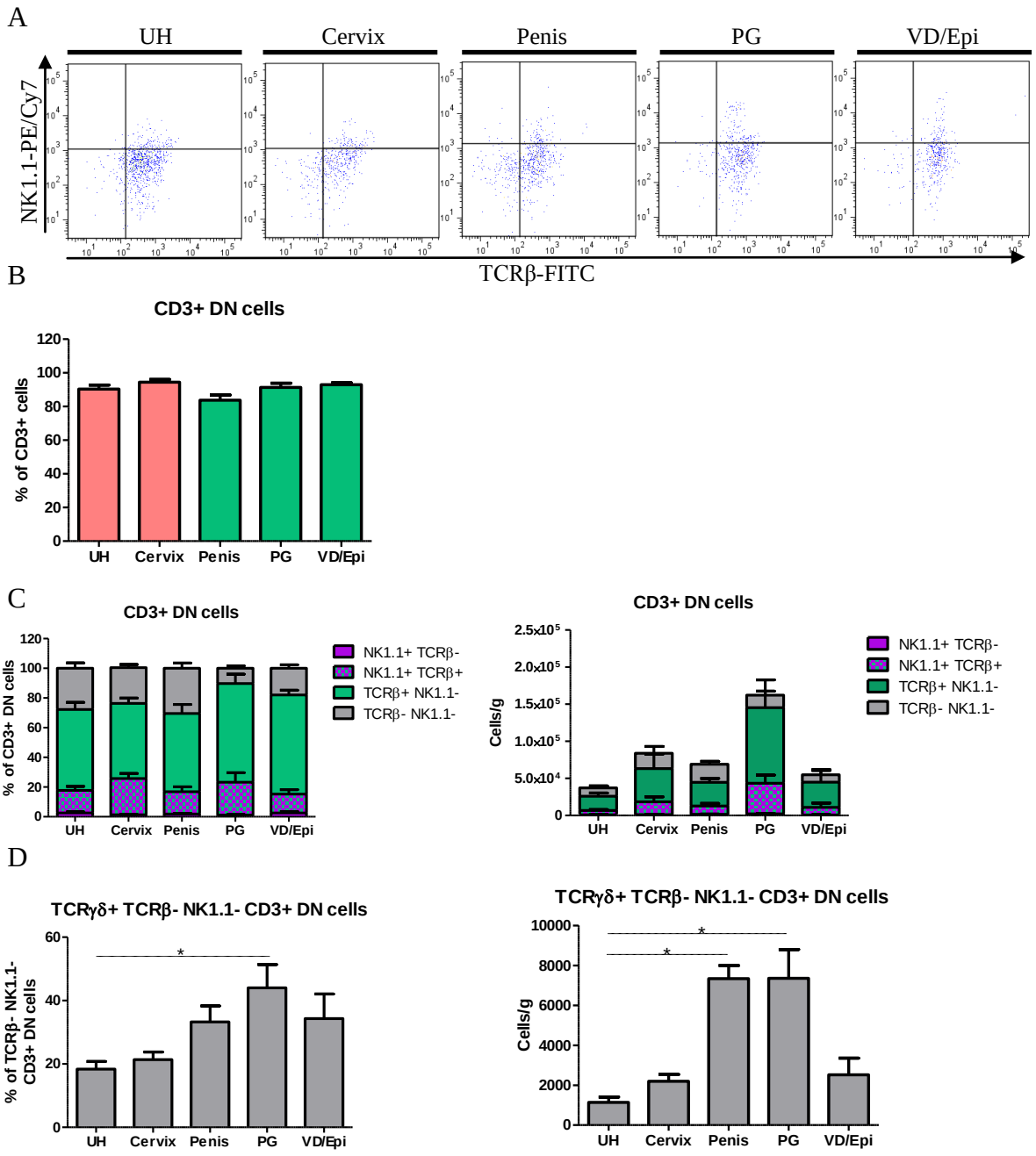

Figure 6.8. *Male reproductive tissues are remarkably similar to female reproductive tissues in their CD3+ DN cell composition*.

Measurement of CD3+ DN cells in UH, cevix, penis, Prostate Gland (PG) and vas deferens and epididymis (VD/Epi). Female data from figs 5.8 and 5.10. (A) Representative plots of TCRβ/NK1.1 CD3+ DN cells in reproductive tissues. (B) CD3+ DN cells as a percentage of CD3+ cells in reproductive tissues. (C) Left; TCRβ/NK1.1 CD3+ DN cells as a percentage of CD3+ cells. Right; TCRβ/NK1.1 CD3+ DN cells per g of tissue. (D) Left; TCRγδ+ CD3+ DN cells as a percentage of CD3+ cells. Right; TCRγδ+ CD3+ DN cells per g of tissue. Data presented as mean±SEM and analysed by Kruskall Wallis test with a Dunn's post-test *p<0.05. Outliers not excluded.

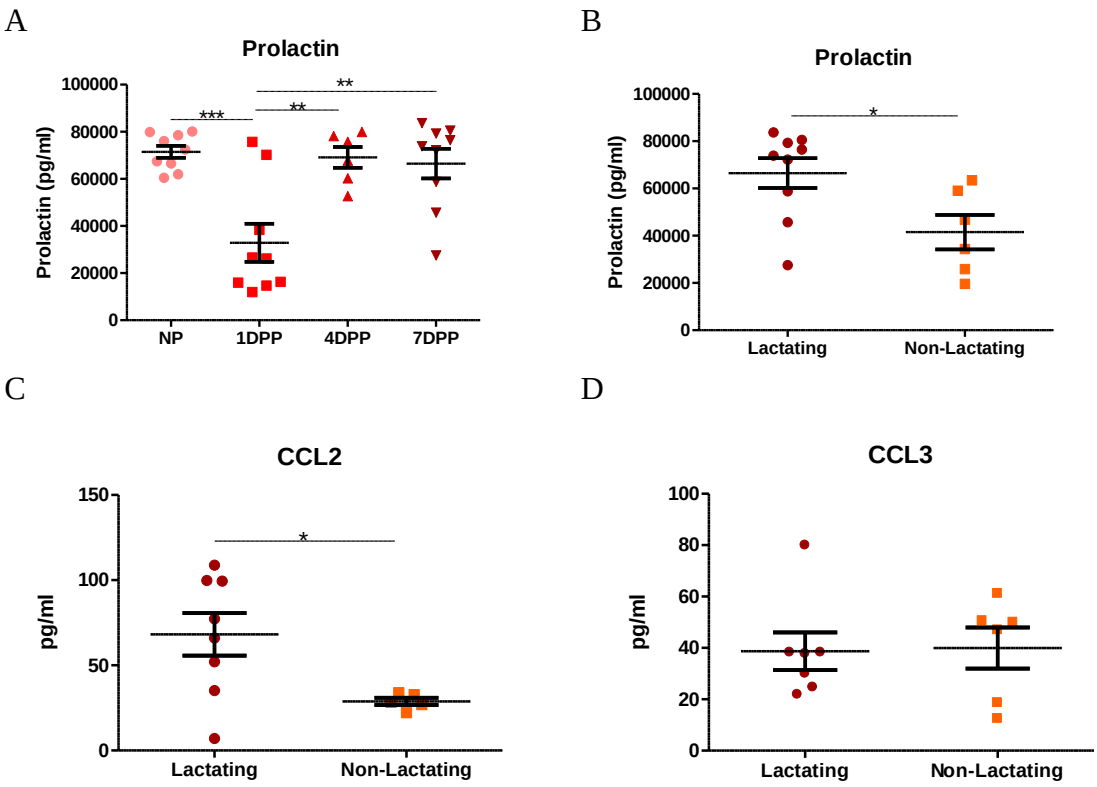

Figure 6.9. *Circulating prolactin and CCL2 are reduced in non-lactating females at 7DPP*. Measurement of prolactin, CCL2 and CCL3 in plasma from mice at different post-partum stages and of different lactation status at 7DPP. (A) Prolactin measured by ELISA. Data analysed by one-way ANOVA with a Tukey post-test. (B) Prolactin measured by ELISA at 7DPP in lactating and non-lactating mice. (C) CCL2 measured by Luminex at 7DPP in lactating and non-lactating mice. (D) CCL3 measured by Luminex at 7DPP in lactating and non-lactating mice. Data presented as mean±SEM. (B)-(D) analysed by Student's t-test, *p<0.05 **p<0.01 ***p<0.001.

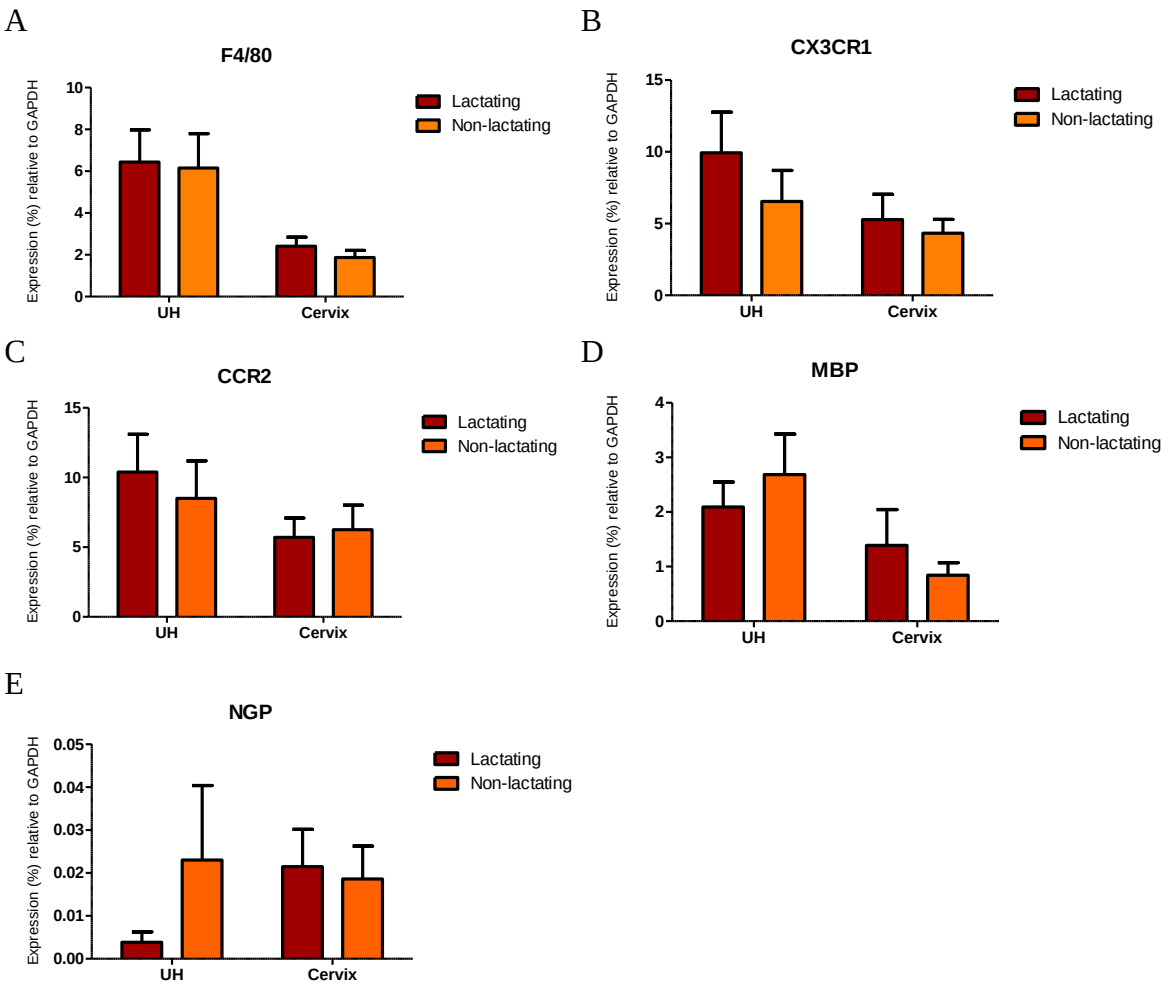

Figure 6.10. *Lactation has no effect on the expression of genes encoding myeloid cell markers in the reproductive tract at 7DPP*.

Gene expression of myeloid cell markers in the reproductive tract in lactating (n=4-5) and non-lactating (n=4-5) mice in the UH and cervix at 7DPP following their first pregnancy. Expression was calculated as $100x2^{\Delta CT}$ where $\Delta CT=CT^{target}-CT^{GAPDH}$ to establish target expression as a percentage of expression of the endogenous control. (A) F4/80 relative to GAPDH. (B) CX3CR1 relative to GAPDH. (C) CCR2 relative to GAPDH. (D) MBP relative to GAPDH. (E) NGP relative to GAPDH. Data presented as mean ± SEM. Statistical analysis was carried out by unpaired Student's t-test with a Welch's correction for unequal variances when appropriate, not significant.

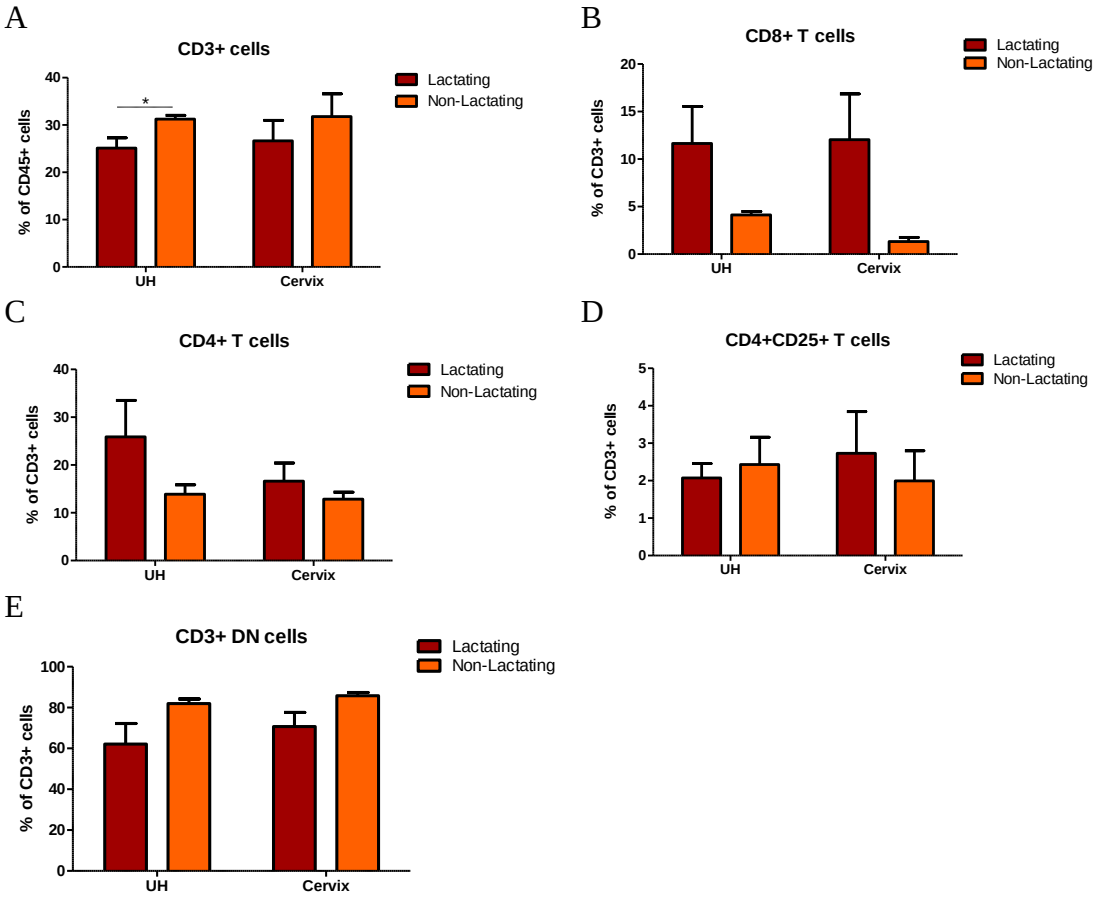

Figure 6.11. *Lactation appeared to decrease the overall proportion of CD3+ cells in the uterine horn at 7DPP*.

CD3+ cell subsets measured by flow cytometry at 7DPP in UH (n=4-5) and cervix (n=4-5). Gates are drawn and 7DPP data from fig 4.2. (A) CD3+ cells as a percentage of CD45+ cells. The proportions of CD3+ cell subsets as a proportion of CD3+ (B) CD8+ T cells (C) CD4+ T cells (D) CD4+CD25+ T cells (E) CD3+ DN cells. Data presented as mean±SEM. Statistical analysis was carried out by Student's t-test, with Welch's correction where appropriate, *$p<0.05$.

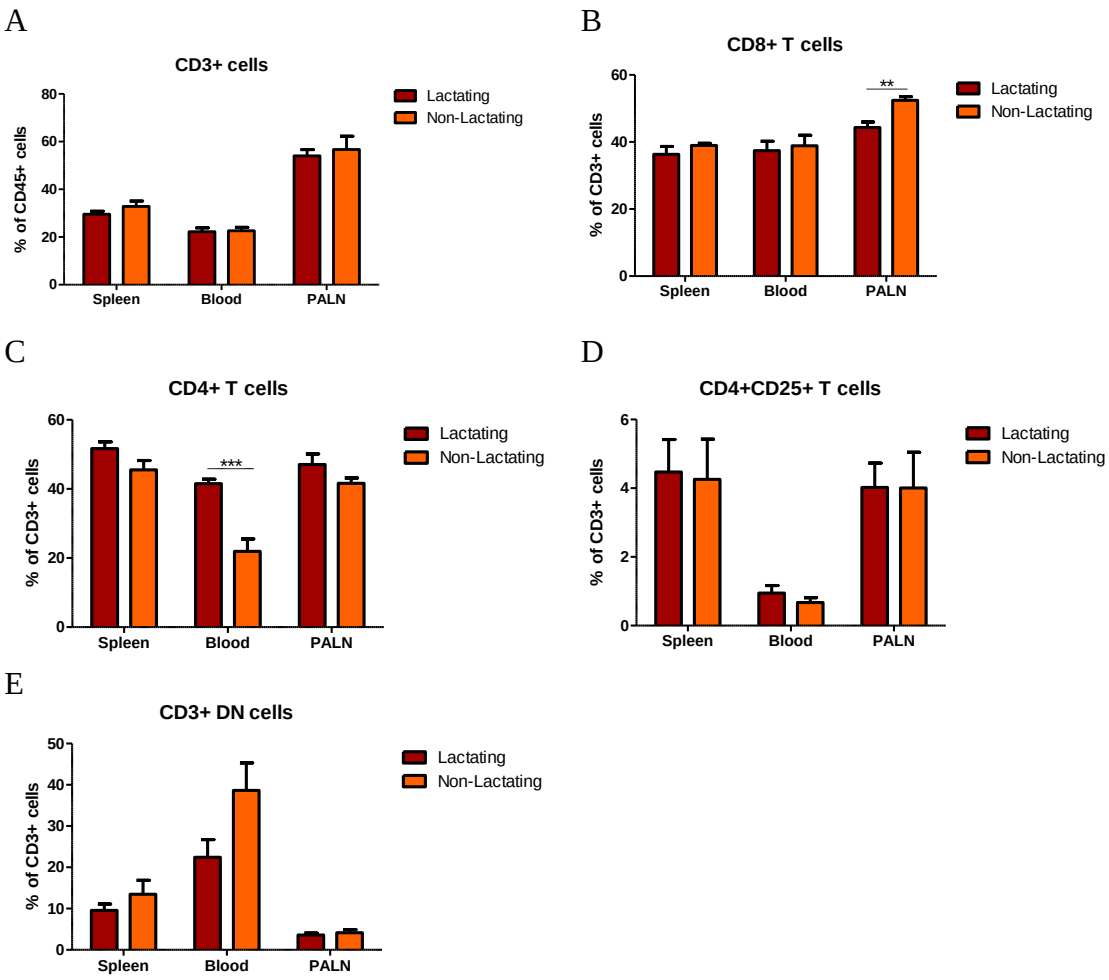

Figure 6.12. *Lactation increases the frequency of blood CD3+ cells carrying CD4.* CD3+ cell subsets measured by flow cytometry at 7DPP in spleen (n=4-8), blood (n=4-8) and PALN (n=4-8). Gates drawn and 7DPP lactating data as in fig 4.3. (A) CD3+ cells as a percentage of CD45+ cells. The proportions of CD3+ cell subsets as a proportion of CD3+ (B) CD8+ T cells (C) CD4+ T cells (D) CD4+CD25+ T cells (E) CD3+ DN cells. Data presented as mean±SEM. Statistical analysis was carried out by Student's t-test, with Welch's correction where appropriate, **p<0.01 ***p<0.001.

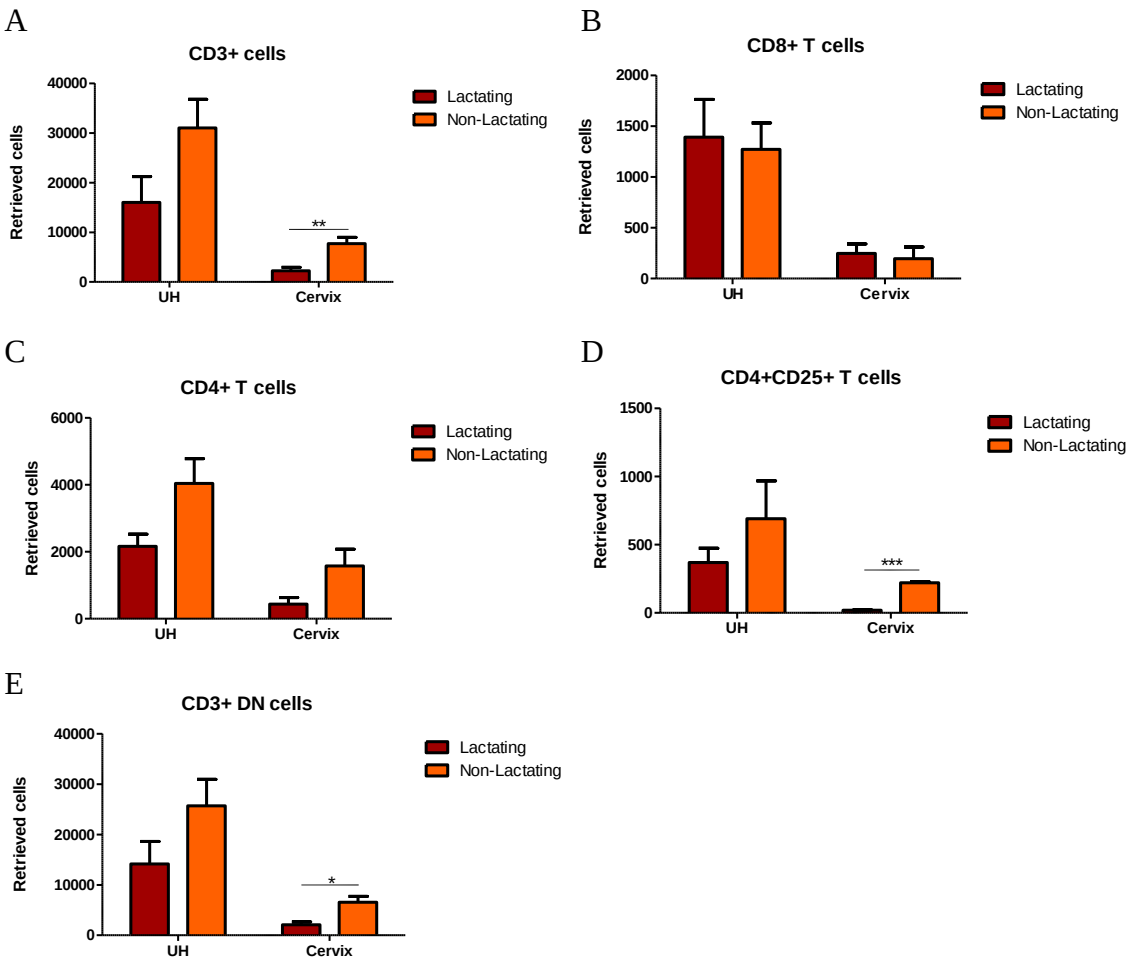

Figure 6.13. *CD3+ DN cells and CD4+ CD25+ T cells are more numerous in the cervix at 7DPP of non-lactating females.*

CD3+ cell subsets measured by flow cytometry at 7DPP in UH (n=3-5) and cervix (n=3-5). Gates drawn and female data from fig 4.2. CD3+ cell subsets retrieved from reproductive tissues (A) CD3+ T cells. (B) CD8+ T cells (C) CD4+ T cells (D) CD4+CD25+ T cells (E) CD3+ DN cells. Data presented as mean±SEM. Statistical analysis was carried out by Student's t-test, *p<0.05 **p<0.01 ***p<0.001.

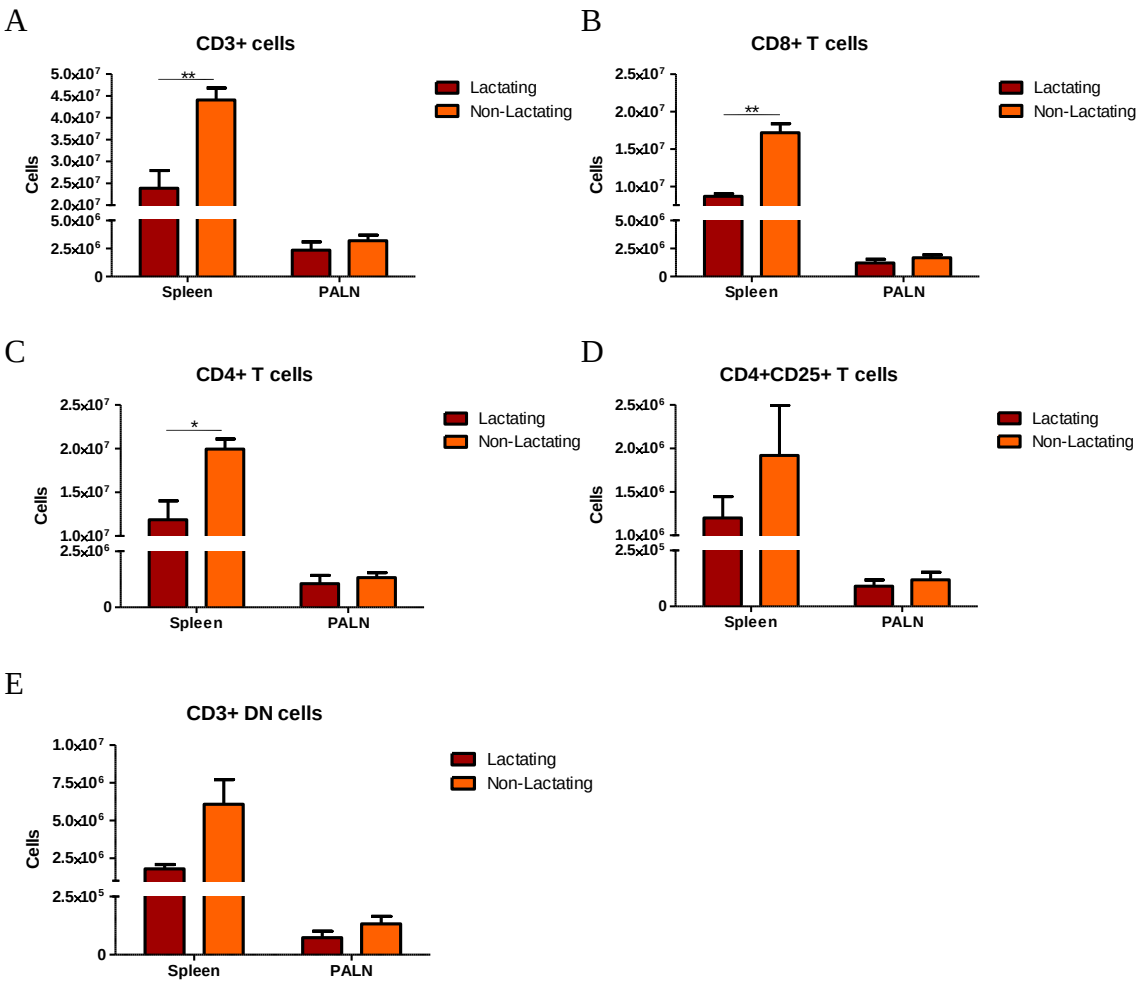

Figure 6.14. *Non-lactating spleens contain more CD4+ and CD8+ T cells at 7DPP*. Measurement of CD3+ cells in the spleen (n=3-4) and PALN (n=4) of lactating and non-lactating females at 7DPP by flow cytometry. Gates are drawn and lactating data as in fig 4.3. Absolute numbers from peripheral tissues (A) CD3+ cells. (B) CD8+ T cells (C) CD4+ T cells (D) CD4+CD25+ T cells (E) CD3+ DN cells. Data presented as mean±SEM. Statistical analysis was carried out by Student's t-test, with a Welch's correction where appropriate *$p<0.05$ **$p<0.01$.

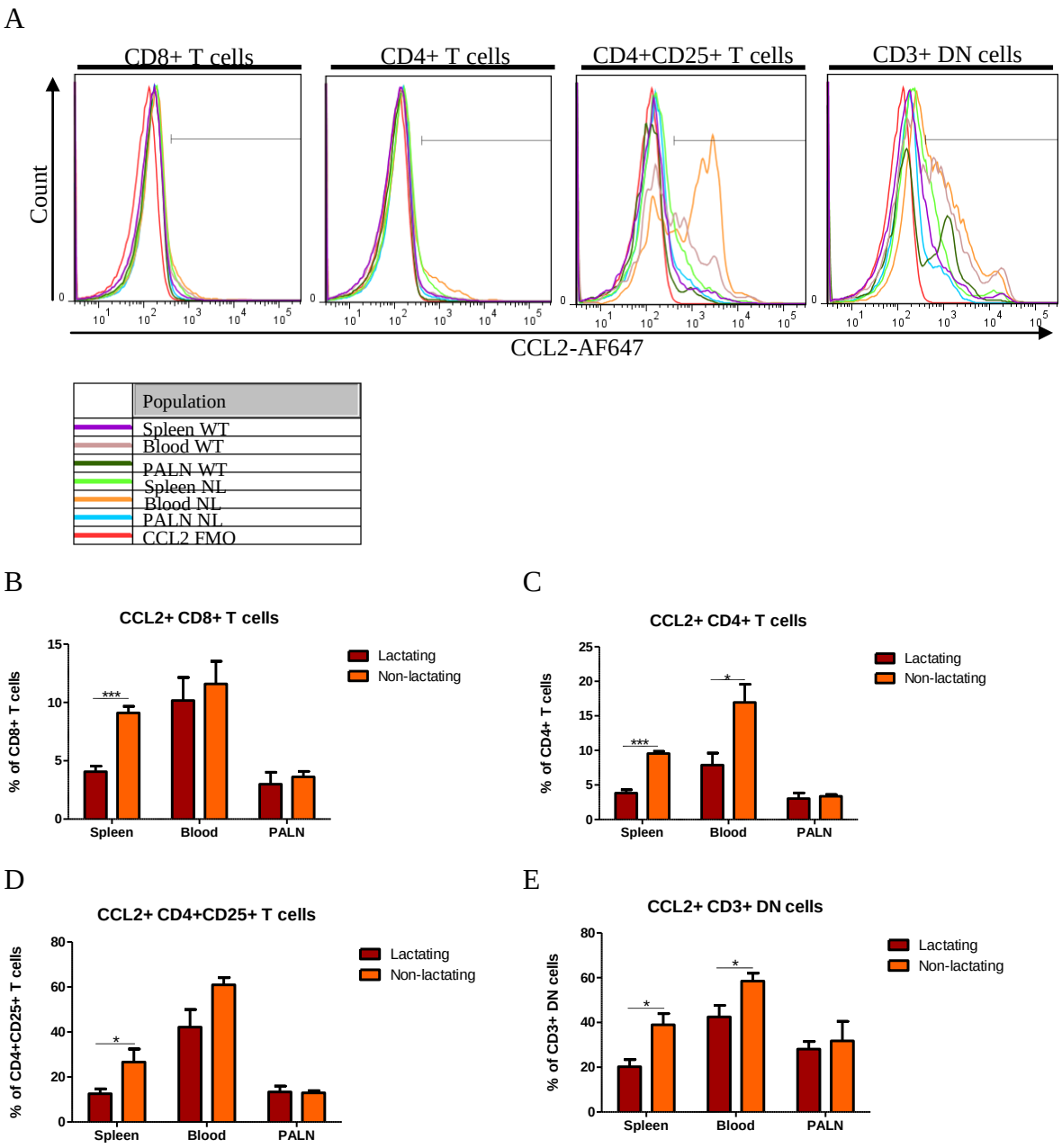

Figure 6.15. *Spleen and blood from non-lactating mice contain a higher percentage of CCL2+ CD4+ T cells and CD3+ DN cell subsets, compared with lactating females.*

Uptake of fluorescent CCL2 by CD3+ cells was measured by flow cytometry in Spleen (n=3-7), blood (n=4-7) and PALN (n=3-8) in 7DPP lactating and non-lactating mice. Cells were incubated with CCL2-AF647 for 65mins. Lactating data as in fig 4.4. (A) Typical histogram of fluorescent CCL2 uptake of CD3+ cell populations in peripheral tissues, with the FMO control for CD45+ T cells in spleen shown in red. Proportion of CCL2+ (B) CD8+ T cells (C) CD4+ T cells (D) CD4+CD25+ T cells (E) CD3+ DN cells. Data presented as mean±SEM. Statistical analysis was carried out by Student's t-test, *p<0.05 **p<0.01 ***p<0.001.

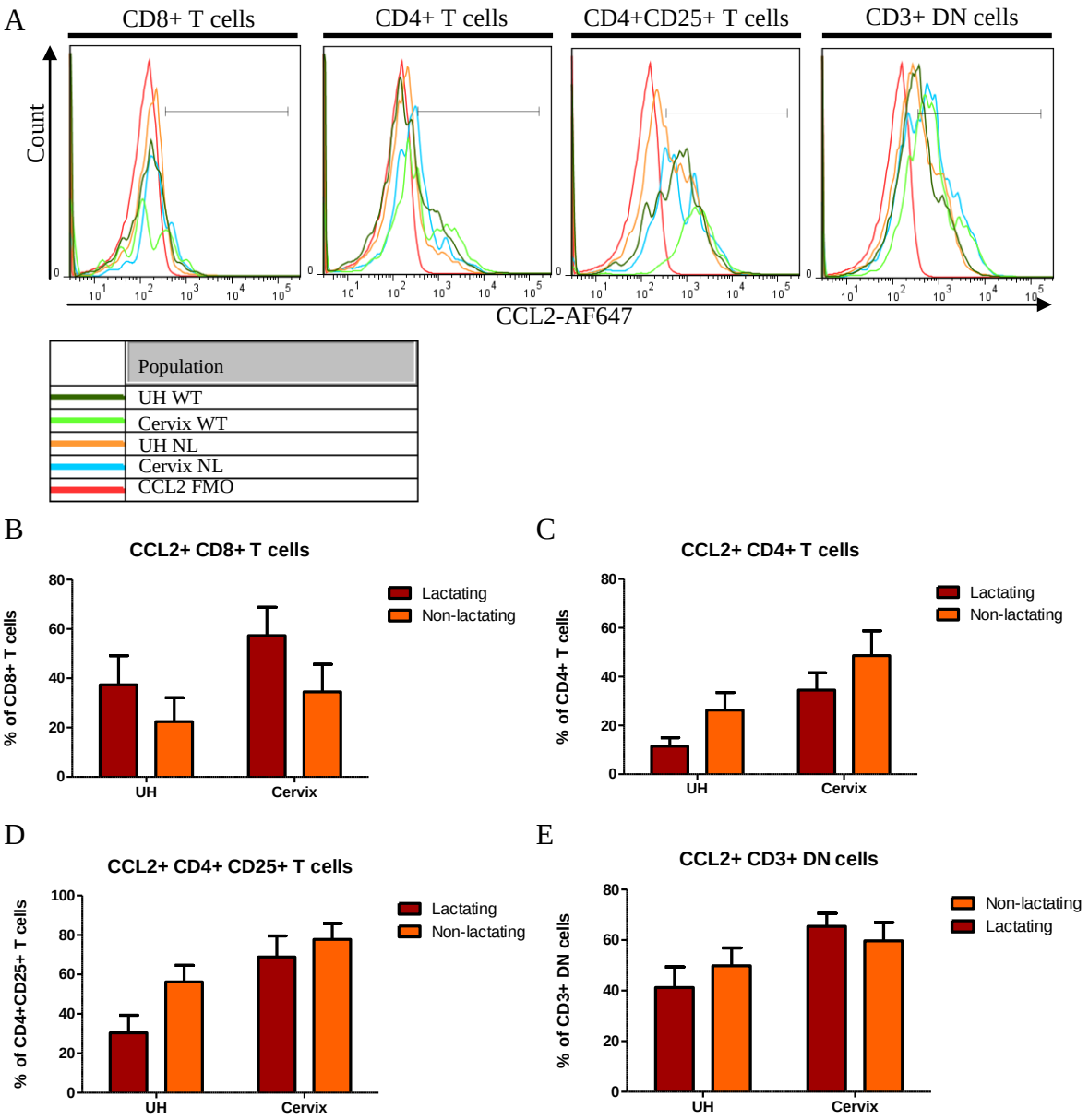

Figure 6.16. *A similar proportion of CD3+ cells from reproductive tissues of lactating and non-lactating females internalised CCL2-AF647 at 7DPP*.

Uptake of fluorescent CCL2 by CD3+ cells was measured by flow cytometry in UH (n=5), cervix (n=4-5) in 7DPP lactating and non-lactating mice. Cells were incubated with CCL2-AF647 for 65mins. Lactating data as in fig 4.6. (A) Typical histogram of fluorescent CCL2 uptake of CD3+ cell populations in reproductive tissues, with the FMO control for CD3+ cells in spleen shown in red. Proportion of CCL2+ (B) CD8+ T cells (C) CD4+ T cells (D) CD4+CD25+ T cells (E) CD3+ DN cells. Data presented as mean±SEM. Statistical analysis was carried out by Student's t-test, not significant.

Chapter 7: Discussion

7.1. Main findings.

Much attention has focussed on the inflammatory infiltrate present in reproductive tissues, particularly during labour (Thomson et al., 1999, Jensen et al., 2012, Gomez-Lopez et al., 2013, Mackler et al., 1999, Timmons et al., 2009, Holt et al., 2011, Gonzalez et al., 2011), but very few studies have examined the leukocyte populations in these tissues during the post-partum period, or assessed whether there are systemic changes in leukocyte distribution or abundance after delivery. My project therefore aimed to catalogue the leukocytes in reproductive and specific peripheral tissues before and after pregnancy. To achieve this, I developed flow cytometry based methods of analysing reproductive tissues, so that surface immunophenotyping could be used to definitively identify and quantify leukocyte subsets in these tissues. Throughout the work, particular emphasis was placed on the role of CCR2 and its chemokine ligands in controlling leukocyte migration into reproductive tissues, primarily because monocytes were one of the principal cell types under investigation and the migration of these cells during homeostasis and inflammation is known to be controlled by CCR2.

The first striking finding of my study was that the 1DPP uterine horn contains large numbers of myeloid cells, and that these cells are not present at 7DPP. These myeloid cells at 1DPP were clearly identified as monocytes, macrophages, neutrophils or eosinophils, and these cells are likely to play key roles in the repair of damaged tissue during the post-partum period. Many of these cells express CCR2, demonstrated by their ability to internalise fluorescent CCL2 in a CCR2-dependent manner, and the 1DPP uterine horn expresses CCR2 ligands. This suggested that CCR2 might be required for the recruitment of leukocytes into the uterine horn at 1DPP, and indeed CCR2 deletion results in a profound reduction in the number of myeloid cells present in the uterine horn. In addition, my studies of NP animals confirmed known phenotypes in CCR2 KO mice relating to monocyte abundance, and identified novel phenotypes affecting eosinophils and neutrophils.

Along with myeloid cells, CD3+ cells are abundant in the 1DPP uterine horn. Most of these cells are CD3+ DN cells lacking CD4 and CD8. They showed lower expression of CCR2 than myeloid cells, and, in stark contrast to myeloid cells, their presence in the 1DPP uterine horn was unaffected by CCR2 deletion. I also found that at 1DPP there was a marked increase in the proportion of CD3+ cells in the blood that were of the CD3+ DN cell phenotype, and unexpectedly that this change was dependent on CCR2. I showed that

the CD3+ DN cells in reproductive tissues could be split into three identifiable populations (NKT cells, TCRαβ+ DN T cells and γδ T cells), and undertook some basic surface immunophenotyping of these cells. Compared to NP animals, DN T cells were increased at 1DPP in uterine horn and blood suggesting that these cells were responding to post-partum inflammation. NKT cells, which were mainly found in reproductive tissues and blood, did not appear to vary between NP and 1DPP mice.

Finally, I brought together work that had been performed throughout the project that was focused on addressing whether sex or lactation were associated with alterations in leukocytes in a range of tissues. I found that monocytes were more abundant in males than females, whereas eosinophils were increased in the blood of females. There were no substantial changes in CD3+ DN cell subsets between the sexes, and interestingly most CD3+ cells in the reproductive tissues of both sexes were CD3+ DN cells. Lactation did appear to affect CD3+ cell subsets, and 7DPP non-lactating mice appeared to have some features in common with 1DPP mice rather than 7DPP lactating animals, along with similar levels of circulating CCL2 and prolactin. There also appeared to be a skew away from CD4+ T cells towards CD3+ DN cells in the blood, perhaps indicating that prolactin participates in the mechanism which returns the CD3+ cell populations back to their NP proportions by 7DPP.

In the following sections I discuss all these findings in more depth, highlight other observations made during my studies and some of the difficulties I encountered, and attempt to put my work in the context of the existing literature. Possible future directions for the work will also be discussed.

7.2. Technical considerations in the analysis of leukocytes in reproductive tissues.

This project used several different techniques to investigate leukocytes and chemokines during the post-partum period and other contexts. At the outset of the project histology and qRT-PCR were used to examine detachment sites in ex-breeders. These techniques had been used extensively in the literature and in our lab, and seemed to be promising ways to investigate my research questions. Though histology produced some interesting images of stages of repair in the post-partum period, it was time-consuming and the concern when viewing histology images is that only a section of tissue is being surveyed and it may not be representative of cellular changes throughout the entire tissue. Histology does provide information about where leukocytes in a tissue are localised, information which is not provided by other techniques such as qRT-PCR or flow cytometry.

qRT-PCR proved to be a particularly disappointing technique. The results I gained, in general, did not conform with what was found in the literature. For example, in Figure 3.2 I identified that expression of leukocyte markers measured by qRT-PCR was not enriched in detachment sites, compared to the rest of the uterine horn and the cervix. The markers tested included F4/80, chosen because the literature had suggested macrophages might accumulate in detachment sites during the post-partum period.

The foremost paper describing the leukocyte populations which might reside in detachment sites was published by (Brandon, 1994). She described their formation and identified cells consistent with macrophage, neutrophil and lymphocyte phenotypes residing in these nodules over a period of 3 months following birth. Contrary to indications from my data, although numbers of F4/80+ cells were lower than earlier post-partum time-points, many F4/80+ macrophages were found to persist specifically in detachment sites (Brandon, 1994). My data were obtained using a different technique, which I think is the most likely explanation for the disparity between my findings and those of Brandon.

Working with ex-breeders made results difficult to interpret due to: (i) the difference in the age of the mice, (ii) the variation in the number of litters per animal and (iii) the variation in the number of weeks post-partum the animals were sacrificed at. The work was then refined by using animals that had only given birth to one litter. I also considered that looking immediately post-partum was more likely to prove fruitful from an inflammatory point of view. To profile cells using markers on a cell by cell basis in reproductive tissues,

a method to examine uterine horn and cervix using flow cytometry was developed. This was challenging and required considerable optimisation, however a successful protocol emerged.

There were several problems encountered when optimising flow cytometry. For example, at the outset I found considerable levels of cell death although I managed to reduce this through experimenting with different digestion protocols (Figure 3.6). Cell death is a problem with flow cytometry protocols in general and it must be remembered that specific subsets may be more prone to cell death during processing than others. Thus, the cells that are finally read by the flow cytometer may not be fully representative of the cells resident in the tissue at time of sacrifice. In reproductive tissues, one of the challenges was being able to accurately count the cells once a single cell suspension was obtained as leukocyte numbers were low and the samples contained more debris from digestion. This was averted by running all the retrieved cells through the flow cytometer, and this was felt to provide a more accurate measurement of the cell populations present in those tissues. As a result, the numbers of leukocytes from reproductive tissues were presented as the number of cells retrieved per tissue. One potential source of variation in the data from reproductive tissue was the digest, which was not standardised to the mass of tissue present. Further to this, the tissues themselves had a range of numbers of detachment sites and the sizes of the tissues varied. As it has been observed that leukocytes cluster around detachment sites (Brandon, 1994), the number of detachment sites would potentially influence the number and proportion of leukocytes retrieved from the uterine horn.

During my optimisation of this technique, I quickly realised that there would not be enough cells to take aliquots of the cells from tissues such as uterine horn for FMO controls and setting gates. Initially, I thought this would be a significant problem. The course of action I decided to take was to use spleen as the standard for setting gates. This had the benefit that all gates would be the same in each tissue so like could be compared with like. For example, a monocyte would be defined the same way in both the spleen and cervix. In reality, it is likely that monocytes in the spleen and cervix would vary in surface phenotype as they will have different functions. For this reason, if I had access to more time, resources and assistance, it may have been preferable to pool tissues from several individuals so gates could be set on a per-tissue basis. Ultimately, defining cells based on the clear staining provided by the spleen was a compromise and though not ideal, it has clearly provided an insight into leukocytes in the reproductive tract. Other parts of the

method were also kept constant in all experiments, for example, cells from all tissues were excluded based on physical characteristics (FSC and SSC), then by 7-AAD before any other antibodies were taken into account, and this was kept consistent between all tissues.

Having worked with these limitations, I decided that surface immunophenotyping was the best technique for profiling leukocytes in tissues. There were several reasons for this decision. First, a large amount of information can be gathered from each mouse in one day of lab-based work. For most of the project seven colours were employed so up to six different surface antigens could be detected as well as providing information about whether cells were live and their size and granularity. Second, in comparison to qRT-PCR, flow cytometry is more accurate as it is measuring markers expressed as protein on the cell surface, not gene expression. Flow cytometry also provides data on a cell by cell basis, not as an overall level of expression. Third, in comparison to histology, all the leukocytes in an entire tissue such as the uterine horn can be profiled, giving a view of the cells present in the tissue as a whole. And fourth, some of the most recent papers relating to my project had employed flow cytometry and I was keen to be able to directly compare my work with theirs by using this technique.

When examining chemokines and prolactin in peripheral blood, I decided to use Luminex and ELISA techniques as these detect protein, and therefore I considered this a more accurate way of measuring these parameters than qRT-PCR, which I had previously used for analysing chemokine expression in the uterine horn.

Immunohistochemistry would have been an incredibly useful tool throughout the project, however time and resources prevented this from being a viable option at this stage in the project. Immunohistochemistry would provide images which would be informative in discerning the location of cells and the production of chemokines during the post-partum period. My data lacked any information on the position of specific cell types and where chemokines were produced, and this would extend the work significantly. Any future work would definitely include immunohistochemistry as one of the key techniques to bring the project forward.

7.3. Myeloid cells are abundant in the post-partum uterine horn.

Chapter 3 focussed on characterising myeloid cells that reside in the reproductive tissues of mice in the post-partum period, and examining the role of CCR2 in regulating myeloid cell abundance in these tissues. There were a far larger number of leukocytes retrieved from the uterine horn at 1DPP, compared to NP and 7DPP animals, and the majority of these leukocytes were CD11b+, indicative of the myeloid lineage. This is consistent with studies from the labouring myometrium, which showed increased populations of macrophages and neutrophils, compared to the non-labouring myometrium at term (Thomson et al., 1999). Cells are likely to continue to be recruited to the uterine horn in the early post-partum period in order to assist with post-partum repair, a process that appears to be resolved by 7DPP. This would be broadly consistent with results from rodents that show that by 7DPP: (i) few apoptotic cells are seen in the uterus (Huang et al., 2012), (ii) a stromal cell derived epithelium has been generated (Huang et al., 2012), (iii) uterine weight may have returned to pre-pregnant levels (Nilsen-Hamilton et al., 2003) and (iv) MMPs expressed in the early post-partum period have fallen (Manase et al., 2006).

7.3.1. *Ly6C^{hi} monocytes and neutrophils may play a crucial role in remodelling of reproductive tissues at 1DPP.*

The 1DPP CD11b+ cell population contained monocytes, macrophages, neutrophils and eosinophils. Monocyte and macrophage subsets were far more abundant at 1DPP, compared to NP or 7DPP, indicating an expansion or recruitment of these cells at this time-point or that they persisted from an influx occurring at labour. Ongoing recruitment seems likely because when monocytes enter tissues they differentiate into cells such as macrophages and dendritic cells, yet I clearly detected cells that resembled blood borne Ly6C^{hi} monocytes in the 1DPP uterine horn. As mentioned in the Introduction, Ly6C^{hi} monocytes are not found in most tissues under resting conditions but migrate in response to an inflammatory stimulus (Sunderkotter et al., 2004, Geissmann et al., 2003). Nonetheless, the monocytes in the 1DPP uterine horn are likely to be more heterogeneous than those circulating in the blood and would probably include cells in the process of differentiation in addition to recently recruited cells. In addition to Ly6C^{hi} monocytes, Ly6C^{lo} monocytes have also been described as being rapidly recruited following tissue damage or infection (Auffray et al., 2007). Similarly, both CX3CR1^{-}CCR2^{+} and CX3CR1^{+}CCR2^{-} monocytes have been shown to be recruited to wounded skin and wound healing macrophages have higher expression of CX3CR1 than CCR2 (Ishida et al., 2008). CX3CR1 KO mice have a more protracted course of skin wound healing, suggesting that recruitment of 'homeostatic'

monocytes is also important for tissue remodelling (Ishida et al., 2008). Both monocyte subsets have also be found to be mobilised following myocardial infarction, although they were recruited to the heart in two phases: 0-3 days following myocardial infarction Ly6C^{hi} monocytes predominate, whereas Ly6C^{lo} monocytes are the main monocyte subset from 5 days onwards (Nahrendorf et al., 2007). These data support the idea that Ly6C^{lo} monocytes can also be recruited to inflamed tissues, such as the 1DPP uterine horn. Neutrophil abundance also increased dramatically at 1DPP in the uterine horn (Figure 3.13). Neutrophils have been reported to be increased in the myometrium during labour (Thomson et al., 1999) and it appears this recruitment continues in the early post-partum period.

The effects of post-partum inflammation are not just local, but rather extend to the BM, the site of leukocyte generation. Though infiltration of Ly6C^{hi} monocytes into inflamed tissues is well described, the increase in the proportion of Ly6C^{hi} cells in the BM during inflammation is less well documented. Presumably, this increase helps replenish monocytes that have been mobilised from the BM to replace those recruited from the blood into the uterine horn, and to prepare more monocytes while resolution is ongoing. Increases in monocyte abundance in the BM have been seen in other scenarios. Ly6C^{hi} monocytes increase in number in the BM 48hrs following hindlimb ischaemia-reperfusion injury (Capoccia et al., 2008), and in a model of burn injury, 8 days after receiving a burn, mice had a significantly higher percentage of Ly6C^{hi} monocytes in their BM, compared to sham-treated animals (Noel et al., 2007). Likewise, intravenous *Listeria monocytogenes* infection also led to increases in BM Ly6C^{hi} monocytes in the days following infection and it was determined that this occurred in a MyD88/TRIF-dependent manner, implicating a role for TLR signalling. However, Ly6C^{hi} monocyte numbers are reduced in the BM 2hrs following intravenous LPS administration, compared to mice treated with saline (O'Dea et al., 2009). This has also been demonstrated 4hrs after an intraperitoneal injection of LPS, compared with control animals (Shi et al., 2011). Thus, it would appear that monocytes are rapidly mobilised from the BM in response to inflammation, and then that these cells are expanded in the BM as the inflammatory response persists. Presumably, this is likely to ensure that sufficient numbers of monocytes are available for the inflamed tissue, with the BM acting as a monocyte reservoir. Interestingly, the spleen has been proposed to serve a similar function, with monocytes mobilised from this tissue in response to myocardial infarction (Swirski et al., 2009). However, there were no changes in monocyte abundance in the spleen when NP and 1DPP mice were analysed.

Neutrophils also increased as a percentage of CD45+ cells in the BM at 1DPP, compared to NP animals, providing further evidence that BM composition is altered at 1DPP in response to post-partum inflammation. Over the post-partum period there was no significant change in eosinophil numbers in the BM, which was surprising as eosinophils in the BM have been shown to be regulated by estradiol (Douin-Echinard et al., 2011) and after pregnancy, systemic oestrogen level falls (Greenstein et al., 2011). Eosinophils were gated as CD45+CD11b+Ly6C^{lo}SSC^{hi}CD115- and were therefore unlikely to be contaminated by CD45+CD11b+SSC^{lo-int}F4/80^{lo}Ly6C^{hi} monocytes, which were the predominant monocyte population in the BM, as they differed so much on Ly6C and SSC especially. Using more selective eosinophil markers would have been desirable and if continuing this section of the project I would aim to confirm these data with a panel of markers specific for granulocyte subsets, such as siglec F for eosinophils and markers such as Ly6G and CXCR2 for identification of neutrophils.

Results in the cervix were difficult to interpret due to the lower number of cells and therefore increased variation inherent in the data. However my results indicated a role for neutrophils and Ly6C^{hi} monocytes in cervical post-partum repair at 1DPP, and this has been suggested previously by others (Timmons et al., 2009, Shynlova et al., 2012). Interestingly, the 7DPP cervix contains more eosinophils than NP cervix, perhaps indicating that they play a longer term role in restoring the tissue.

7.3.2. *CCR2 expression by myeloid cells during the post-partum period.*

Using qRT-PCR I found that CCR2 ligands, most notably CCL2, were most highly expressed by the uterine horn in the early post-partum period and were reduced at 7DPP (Figure 3.4). CCL2 in particular has been reported to be raised during inflammatory periods of the reproductive process in the reproductive tissues, for example, during menstruation (Menning et al., 2012), implantation (Wood et al., 1999), during the second half of pregnancy (Kyaw et al., 1998, Menzies et al., 2012, Wood et al., 1999) and labour (Menzies et al., 2012, Esplin et al., 2005). CCL2 is therefore likely to be one of the chemokines responsible for the major inflammatory infiltrate at 1DPP, bringing monocytes into the damaged uterine horn (Figure 7.1A-B). Though this qRT-PCR data was consistent with the literature, it would be sensible to extend this work by using Luminex to measure CCL2 protein in reproductive tissues, so that these data could be compared with data

obtained from the blood. Immunohistochemisty could also be used to provide information about where chemokines are expressed in the uterine horn.

Ly6C^{hi} monocytes in reproductive and peripheral tissues express CCR2 (Figures 3.11-3.12), implicating CCR2 in migration of monocyte subsets into reproductive tissues at this time-point. Expression of CCR2 was also seen in the resident macrophage population: this was not completely unexpected as inflammatory CCR2+ macrophages have been reported previously (Willenborg et al., 2012). Surprisingly, the other myeloid populations I examined also expressed CCR2. Up to 30% of cells defined as Ly6C^{lo} monocytes expressed CCR2 and some expression was seen on these cells in all tissues studied. Ly6C^{lo} monocytes have usually downregulated their CCR2 expression in the circulation (Geissmann et al., 2003), perhaps a small subset of monocytes sustain their CCR2 expression in response to inflammation. In eosinophils and neutrophils, which are not normally thought to express CCR2, up to 20% were found to show CCR2 activity in some tissues (Figure 3.16 and 3.17). It is possible that CCR2 also mobilises these cell types in response to ligands such as CCL2. It would be interesting to investigate other forms of inflammation to determine whether limited CCR2 activity is also seen in those circumstances.

CCR2 acts to regulate the level of circulating CCL2 but not CCL3 in NP and 1DPP animals, presumably by CCR2-mediated scavenging, although not at 7DPP (Figure 3.22 and 3.23). The role of CCR2 on monocytes as a scavenger of CCR2 has been demonstrated previously (Volpe et al., 2012, Cardona et al., 2008). The scavenging effect can be explained by the fact that when a ligand binds to the receptor it is internalised and degraded, therefore removing the chemokine from environment. It is tempting to hypothesise that at 1DPP the uterine horn is a high CCL2 environment, whereas the blood only has modest levels, creating a gradient which would promote cell recruitment via CCL2 (Figure 7.1B). At 7DPP, the uterine horn is a low CCL2 environment and in the blood CCL2 is raised, disrupting the gradient and perhaps discouraging further leukocyte infiltration to reproductive tissues. It would be interesting to use chemotaxis assays to determine the migratory properties of monocytes at 1DPP and 7DPP.

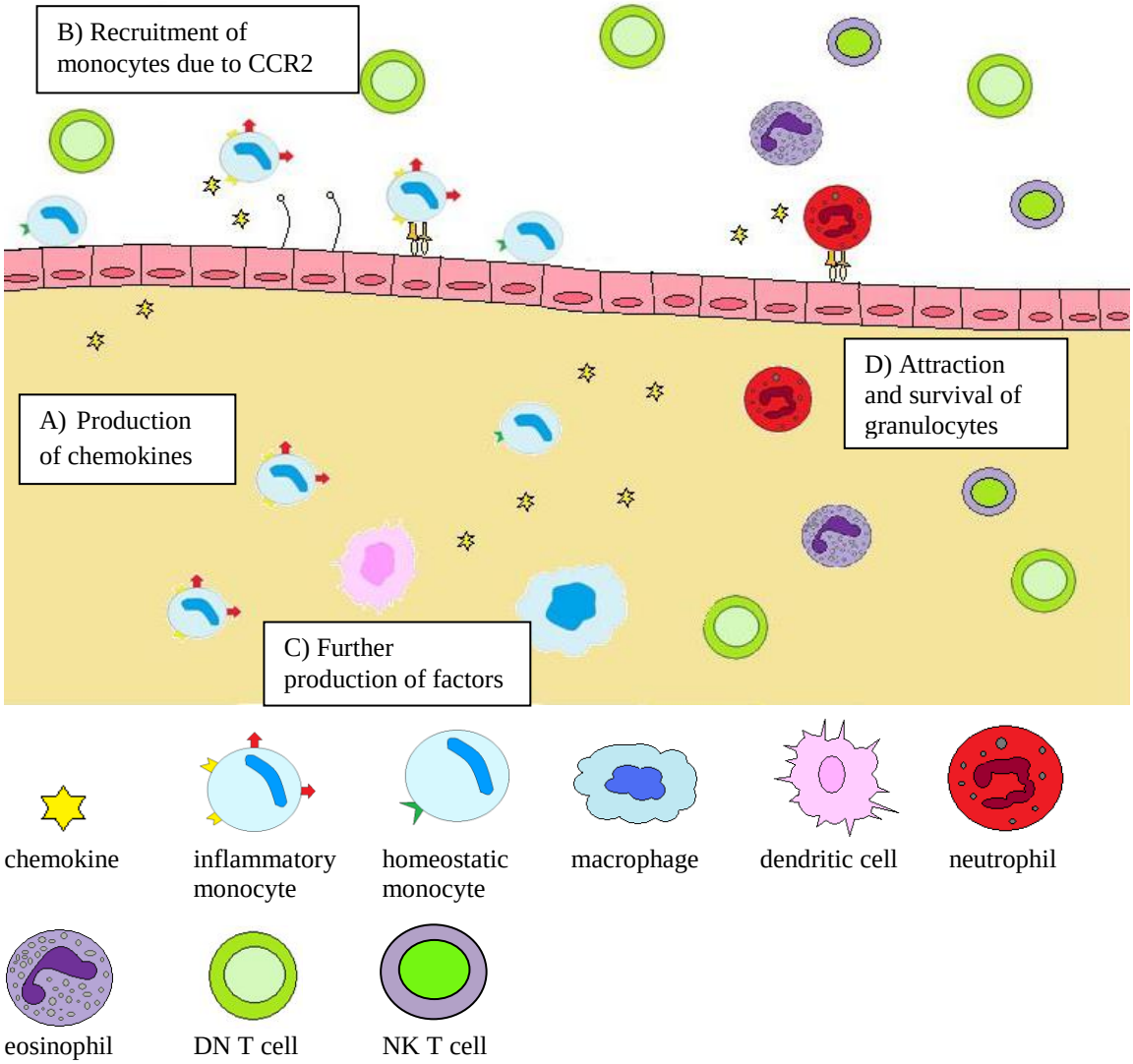

Figure 7.1. *Possible mechanisms at work in mobilising leukocytes from the blood to the uterine horn of the 1DPP WT mouse.*

A) CCR2 binding chemokines such as CCL2 are produced in the uterine horn in response to tissue damage. B) Inflammatory monocytes are recruited to the tissue. Homeostatic monocytes also patrol blood vessels and may also be recruited in response to damage. Monocytes differentiate into macrophages and DCs following entry into tissues. C) These cells in turn produce MMPs, cytokines and other factors which aid the remodelling of the uterine horn. A range of inflammatory chemokines are then produced. DN T cells and NKT cells are also present in the tissue and may contribute to cytokine production. D) Chemokines then attract other cells such as granulocytes, their survival may also be prolonged by other factors.

7.3.3. *Increase in myeloid cells in the uterine horn at 1DPP is CCR2-dependent.*

As CCR2 was abundantly expressed by monocytes in 1DPP uterus and is known to control the migration of these cells, it was perhaps not surprising that at 1DPP all monocyte and macrophage populations were reduced in terms of numbers in CCR2 KO mice in the uterine horn, compared to WT mice (Figure 3.21). The large disparity between the

proportion of Ly6C^{hi} cells in uterine horn at 1DPP in WT and CCR2 KO mice, indicates that CCR2 deletion affects the recruitment of these cells to a greater extent than the other cell types. These cells are reduced in the blood of CCR2 KO mice and so it is logical that as fewer cells are released from the BM, fewer will also migrate from the circulation to reproductive tissues. The lack of macrophages is probably due to this deficiency of monocytes as fewer will mature into macrophages.

Surprisingly there was no increase in monocytes in the BM of CCR2 KO mice as has been reported previously (Kuziel et al., 1997). This may indicate that the rise seen in WT mice at 1DPP brought BM Ly6C^{hi} monocyte levels up to those naturally seen in the CCR2 KO and that this reached the maximum possible for this cell type. CCR2 deletion also resulted in reduced monocytes in the blood and spleen, this was observed in males and NP females (Figure 6.4). This might have been expected as CCR2 controls their release into the blood from the BM and as a result fewer monocytes would accumulate in the reservoir of monocytes which are observed in the spleen (Swirski et al., 2009).

WT reproductive tissues were not larger than those of CCR2 KOs and although the tissues were not weighed, as I was processing the tissues, I did not notice a dramatic difference in the size of the tissue. Moreover, as was shown in Chapter 4, CD3+ cell subsets were not affected in this way by CCR2 deletion. As shown in Figure 3.1, the number of detachment sites does not differ between WT and CCR2 KO animals. If the number of wounds had been different, this could have explained the difference in myeloid cell infiltration between the two genotypes. There was also no difference between the number of sites per number of pups born, which would take into account resorbed pups (data not shown).

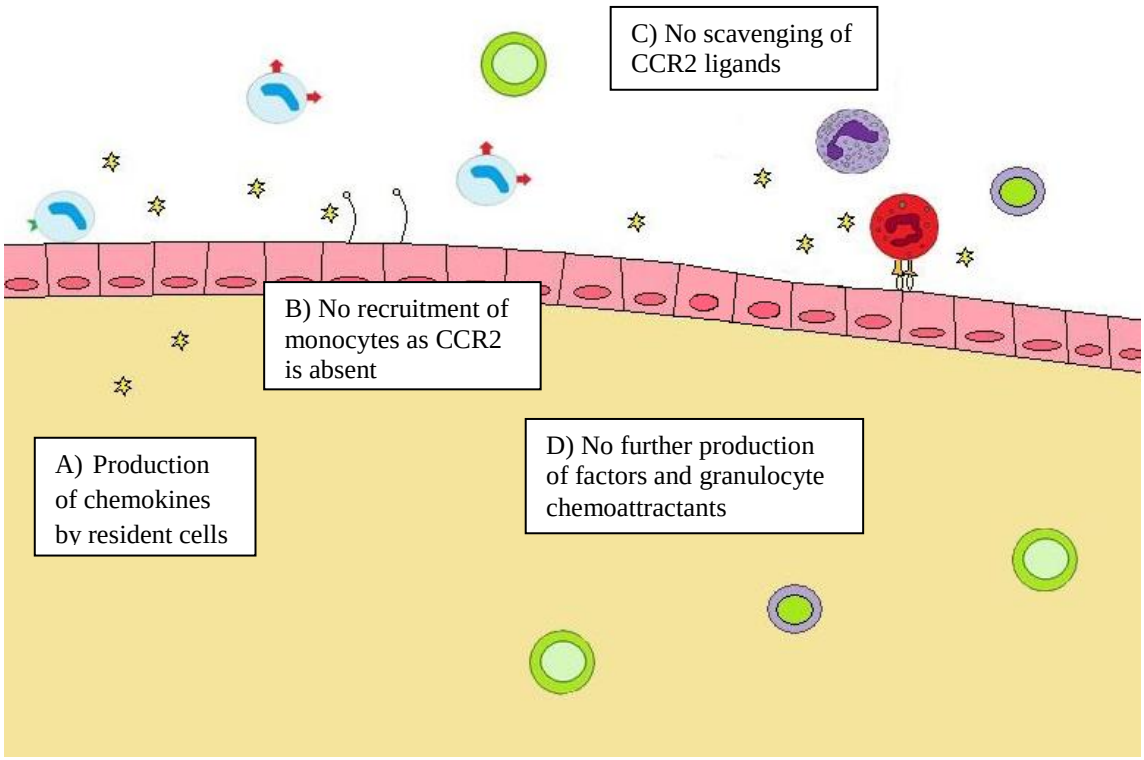

Figure 7.2. *CCR2 deletion could result in protracted wound healing*.

A) CCR2 binding chemokines such as CCL2 are produced in the uterine horn in response to tissue damage. B) Inflammatory monocytes are not recruited to the tissue. Monocytes are only present in low numbers in blood and cannot be recruited by CCR2. DN T cells and NKT cells are also reduced in the blood, though recruitment to the uterus is not affected. C) CCR2 ligands are increased in blood as CCR2 is not present to scavenge the chemokines. This may then have the effect of desensitising other receptors which would normally attract leukocytes to the uterus in the post-partum period. D) Fewer leukocytes, particularly those derived from monocytes are present in the uterine horn so a crucial source of cytokines, chemokines and factors is absent. Key as in Figure 7.1.

As shown in Figure 7.1, monocyte and macrophage cells could produce cytokines and chemokines that would promote the recruitment and survival of other types of cells, particularly through delayed apoptosis (Yang et al., 2012). Therefore a lack of CCR2 could have indirect effects on other cell subsets (Figure 7.2). Though the action of CCR2 on granulocytes and the contribution of uterine monocytes and macrophages to granulocyte recruitment/survival cannot be verified, there may also be a contribution of CCR2 as a scavenger. As seen in my results, at 1DPP CCL2 was increased in CCR2 KOs, compared to WTs. This was not observed for CCL3, but could also be the case for CCL7 and CCL12. As these chemokines bind other receptors, the increase in these ligands could lead to desensitisation of other receptors such as CCR1 and CCR3, which are expressed on granulocytes. This has been described previously, where investigators found that CCR2 deletion resulted in downregulation of CCR1 on CD11b+ cells in the blood (Cardona et al.,

2008). This could be another mechanism result in in a reduced inflammatory infiltrate in the uterine horn at 1DPP in CCR2 KOs (Figure 7.2C-D).

Surprisingly, both granulocyte subsets appeared to be increased in CCR2 KO BM at 1DPP (Figure 3.21), perhaps indicating a role for CCR2 in the release of these cells in a post-partum context. It must also be considered that there may have been some monocyte contamination of the neutrophil population. Many gating steps were taken to minimise this chance and had there been more channels available, more selective neutrophil markers could have been added. The gating steps would suggest that even working within this technical limitation, contaminating monocytes would be a small minority.

Ultimately, this lack of myeloid cell infiltrate in CCR2 KOs may lead to a more protracted course of wound healing, which may be ineffective at reorganising uterine architecture back towards a pre-pregnant state. As shown in Figures 7.1 and 7.2, the release and attraction of monocytes by CCR2 could be a crucial step in the cascade which resolves tissue damage in the WT uterine horn. Monocytes and monocyte derived cells may produce cytokines and factors such as resolvins as well as phagocytosing debris. Non-CCR2 binding chemokines may also be produced by these cells, which bring in granulocytes, particularly neutrophils. In CCR2 KOs, this is absent. This may also be because CCR2 is not available to act as a scavenger and ligands desensitise the receptors used by these cells to position themselves in the uterine horn. As there is a possible association between lack of CCR2 and problems during labour in mice which have had several litters, this suggests that imperfect remodelling results in contractile difficulties. This could be tested using myometrial strips in an organ bath and measuring the contraction of the tissue in response of the tissue to drugs such as oxytocin. Ideally this would include a large breeding programme so that CCR2 KOs and WTs could be tested after several litters, perhaps even have groups after 1 pregnancy, 2 pregnancies, 3 pregnancies and 4 pregnancies to see whether CCR2 KOs decline in their ability to contract in response to agents to a greater extent than WT myometrial strips. This would be an incredibly difficult, time consuming and expensive but would be incredibly interesting and would determine whether CCR2 is a key player in uterine remodelling post-partum.

7.3.4. *Myeloid cell populations are altered between males and females in blood and spleen.*

To get an insight into how leukocyte populations can differ in distinct hormonal environments I began to study sex differences. Many inflammatory diseases exhibit sex differences, and any sex biases in leukocyte populations could contribute to this. The first observation between males and females was that males had a lower proportion of live cells defined as eosinophils, and that this was dependent on the presence of CCR2 (Figure 6.2, Figure 6.4). This contrasts with the literature which describes no sex difference in WT circulating eosinophils at rest (Petkova et al., 2008), however females are more prone to eosinophilia (Antunes et al., 2010). Females have an increased incidence of asthma and this may be a manifestation of increased eosinophil migration (Melgert and Postma, 2009) Ovariectomy has been shown to dramatically reduce lung eosinophilia in models of allergic inflammation, suggesting a role for female sex steroids in promoting eosinophil migration to the lungs (Riffo-Vasquez et al., 2007). When the model of OVA-induced airway hyperresponsiveness was examined in both sexes, females show over 3 times the number of eosinophils in the bronchoalvelar lavage fluid, compared to males, and this is reversed with ovariectomy (Antunes et al., 2010). This perhaps would indicate that the colony mice that I used were subject to some immunological challenge, such as an infection. Unlike mice used for the rest of the chapter, these mice were housed in conventional, not individually ventilated cages, increasing the possibility that the environment could have influenced eosinophil blood counts. This study also found that neutrophils were increased as a proportion of live cells in the spleens of males, compared to females. In the literature, neutrophil numbers in the spleen have been shown to be equal between males and females (Traub et al., 2012). In this section of the project only proportions of cells were measured, therefore this difference could be a knock on effect of changes in the numbers of other cell populations not shown.

In humans, monocytes are more abundant in the blood of males compared to females (Bouman et al., 2004) and my results in mice were consistent with this. Diseases such as coronary artery disease and atherosclerosis are more prevalent in men than pre-menopausal women (Mendelsohn and Karas, 1999, Papakonstantinou et al., 2013). Though many factors are thought to contribute to this process, the key cell type which drives progression of atherosclerosis is the monocyte and the higher proportion of this population in male blood may help to drive development of the disease. In atherosclerosis, low density lipoproteins promote the recruitment of monocytes to plaques and these differentiate into

activated macrophages which can ingest lipids in the lesions (Gautier et al., 2009). Oestrogen has been implicated in reducing monocyte recruitment to lesions by downregulating CCL2 production (Pervin et al., 1998, Frazier-Jessen and Kovacs, 1995, Nilsson, 2007).

7.4. Uterine CD3+ DN cells are a mixed population including three identifiable subsets.

7.4.1. *The majority of CD3+ cells in reproductive tissues are CD3+ DN cells.*

The CCR2-dependent increase in myeloid cells seen in the WT uterus at 1DPP led to the exciting possibility that other cell types such as lymphocytes might also be recruited into the uterus at this time. Chapter 4 aimed to characterise CD3+ cells in the post-partum period in reproductive and peripheral tissues. A similar seven colour flow cytometry protocol was devised to subset CD3+ T cells. Variability between animals and repeats was considerable and therefore caution should be exercised before directly comparing the proportions of populations and cell numbers in Chapter 4 with those shown in Chapter 3. Though an overall view of relative leukocyte populations as a whole can be gained.

One population which was not considered was CD4+CD8+ DP cells, which were observed in peripheral tissues. Initially these were thought to be doublets, where two cells stuck together are measured as one by the flow cytometer, however these were still seen in subsequent experiments when doublets were removed (results not shown). Further work could be done to address the role of this cell population in the post-partum period.

In reproductive tissues CD3+ cells increased considerably at 1DPP and curiously this was mainly due CD3+ DN cells and not CD4+ and CD8+ T cells (Figures 4.1 and 4.2). This was an interesting finding, as CD3+ DN cells are not a common cell type in most other tissues. CD3+ DN cells have been described in the NP female reproductive tract by Johansson and Lycke (Johansson and Lycke, 2003). In this publication, TCR-αβ was expressed by CD3+ DN cells, confirming their status as T cells (Johansson and Lycke, 2003). Interestingly, Johansson and Lycke found that uterine DN T cells did not change in number between NP and early pregnant mice, perhaps indicating that the high number of CD3+ DN cells observed in Figure 4.2 begins to accumulate after this point in the pregnancy, or could even be post-partum specific. A recent study in humans described how CD3+ DN cells varied in the decidua between pre-term birth, term labour and term not in labour samples (Gomez-Lopez et al., 2013). This study suggested that fewer CD3+ DN cells are present at term, than pre-term. The pre-term delivery level was consistent with my data and the findings of Johansson and Lycke, which suggests that the end of pregnancy may be associated with a dip in the CD3+ DN cell population.

DN T cells have been described as displaying a regulatory phenotype in some circumstances (Duncan et al., 2010, Lider et al., 1991, Chen et al., 2003, Chen et al., 2005) and uterine DN T cells were shown to downregulate T cell proliferation in culture (Johansson and Lycke, 2003). DN T cells in the Johansson and Lycke paper were shown to be regulatory in nature and as these cells appear to be similar to DN T cells in this study. This points to a role for these cells in dampening down immune responses at the foetomaternal interface in the final stages of pregnancy or regulating the remodelling in the early post-partum period. Further experimentation as discussed in section 7.6 would help to confirm whether these cells were regulatory T cells.

An interpretation which was seriously considered was whether digestion of the reproductive tissues had caused the CD4 and CD8 coreceptors to be cleaved from the cells, therefore creating false CD3+ DN cells. If this was the case staining would appear as a smear across the plots, however this was not observed in any of the plots and clear CD4+ and CD8+ populations, though small, were still identifiable. Digesting the tissues was a step which was indispensable for liberating the cells from the structures of the cervix and uterine horn. Therefore, the possibility that expression of markers might have been affected by digestion to some extent had to be accepted. The fact that the cells were enclosed in such a dense collagen matrix may have provided protection to the cells. Put another way, liberating cells from a spleen using digestion might be more likely to produce over-digestion than liberating cells from a cervix.

7.4.2. *CD25+ NKT cells are present in uterine horn, cervix and blood.*

When phenotyping these cells I drew on the literature to find potential cell markers to define CD3+ DN cells. By this stage the protocol had been refined further, with a particular focus on NP animals because they were advantageous in terms of time and cost. The main priorities were identifying NKT cells, true DN T cells and γδ T cells, which were all expected to form part of the mixed CD3+ DN cell population described in Chapter 4. The achievements of this chapter should not be underestimated. The simultaneous collection of tissues and challenging protocol allowed for a large number of cells to be profiled and analysed in a structured way. A cell population defined by a lack of markers has been investigated and recognisable cell types identified.

The first population identified were CD25+NK1.1+TCRαβ+ CD3+ DN cells, which were most likely iNKT cells. Interestingly, these cells were generally restricted to reproductive

tissues and blood. They did not change at 1DPP, compared to NP animals in either reproductive tissues or blood, suggesting a homeostatic, rather than inflammatory function for these cells. The literature describes that up to 20% of NKT cells express CCR2 (Thomas et al., 2003), however it seemed that a higher percentage than this internalised CCL2, with up to 80% CCL2-AF647+ CD25+ NKT cells in WT blood (Figure 5.3). Variability was a barrier in confidently asserting the role of CCR2 in CCL2 internalisation by potential NKT cells in the different tissues, expanding the number of subjects studied would be of great value in determining this. These cells were consistent with the Th1-like NKT cell phenotype, which recognise lipid antigens, though in this case the antigen remains unknown. These cells could also contribute to the production of cytokines in the post-partum period. Alternatively, as these cells are present in the NP and 1DPP uterine horn and the male reproductive tract, they may provide a homeostatic role.

7.4.3. *DN T cells are increased in the uterine horn and blood at 1DPP, compared to NP animals.*

Most CD3+ DN cells carry either TCR-αβ or TCR-γδ (Figure 5.7). In the uterine horn, TCRαβ+ DN T cells drives the increase in the number of CD3+ DN cells at 1DPP. The proportion of these cells in the blood was also increased at 1DPP, though when numbers of these cells were measured, results were too variable to be conclusive (Figure 5.9). These results perhaps suggest that these cells do have a function that is induced by post-partum inflammation, such as the regulatory role suggested by Johansson and Lycke (Johansson and Lycke, 2003).

A population of DN T cells was also found in the spleen and PALN. As CD3+ DN cells are in a minority in these tissues and only around 30-40% of these are DN T cells, they are not a particularly numerous subset in these tissues (Figure 5.9). There was a lot of variability between repeats and CD3+ DN cells were defined slightly differently between the Chapter 4 and Chapter 5; therefore a small number of findings could not be replicated. Using larger n numbers would help to address this variability and help to define these subtle differences with greater confidence.

7.4.4. *γδ T cells were identified in low numbers in reproductive tissues but form the majority of NK1.1-TCRβ- CD3+ DN cells in secondary lymphoid organs.*

I hypothesised that the majority of CD3+ DN cells which were not NKT cells or DN T cells would be γδ T cells. TCR-γδ is not generally thought to be expressed on the same

cells as the TCR-αβ complex so the fact that they were not co-expressed was reassuring (Figure 5.7). My results were broadly consistent with the proportion of γδ T cells found in the human decidua during labour (Tilburgs et al., 2009), showing that γδ T cells are not a major cell population in the uterine horn at these time-points. Many more γδ T cells were identified in blood and secondary lymphoid organs.

NK1.1-TCRβ- CD3+ DN cells which were not γδ T cells were also identified. These cells may have been identified as CD3+ due to gating error or alternatively, they may represent other populations which express CD3 but not a TCR. Profiling with further markers might identify these populations, however due to the technical challenge of studying this tiny proportion of cells, it would be more practical to continue investigation of DN T cells and NKT cells in reproductive tissues and blood.

7.4.5. *CD3+ DN cells also populate the male reproductive tract.*

All three main CD3+ DN cell populations; NKT cells, DN T cells and γδ T cells, were also found in males (Figures 6.5-6.7). Males may have a small reduction in the number of NKT cells in their blood, compared to females, though this resulted in no significant change in proportion, consistent with data reporting no sex bias in the proportion of circulating NKT cell subsets has been observed (Snyder-Cappione et al., 2010).

T cells have been described in the male reproductive tract, but the CD3+ DN cell content of these tissues has not been determined (Barratt et al., 1990, Breser et al., 2013). To my surprise I found that reproductive tissues from both females and males contained very similar proportions of NKT cells, DN T cells and γδ T cells (Figure 6.8). Prostate gland contained a higher density of CD3+ DN cells and high numbers of γδ T cells. This might indicate an environment which is more focussed towards tumour defence. Epithelial γδ T cells have been proposed to have a role in immunosurveillance (Witherden and Havran, 2011), and this may be more important in the prostate gland.

7.5. Effects of CCR2 and lactation on CD3+ subsets in the post-partum period.

7.5.1. *CCR2 dependent shift from CD4+ T cells to CD3+ DN cells in the blood at 1DPP.*

From NP to 1DPP one of the main results of note was the shift from CD4+ T cells to CD3+ DN cells as a percentage of CD3+ cells in the blood (Figure 4.9). A large proportion of these blood CD3+ DN cells expressed CCR2 1DPP, as did some CD4+ T cells (Figure 4.5). This ability to bind chemokine may contribute to the reduction in CD4+ cells and a rise of CD3+ DN cells at 1DPP in WT blood that is not seen in CCR2 KOs. The finding that this supposedly rare population is so increased in proportion in the blood at 1DPP in the blood by a CCR2 dependent mechanism was perhaps one of the major findings of this report. Another interesting observation from the blood showed a shift towards an increased proportion of CD4+CD25+ T cells, of which around 30% expressed CCR2. It is tempting to speculate that this could create a more regulatory environment at 1DPP than that seen in NP female blood (Figure 4.9).

The absence of CCR2 appeared to have no effect on the number or proportion of CD4+ T cells, CD8+ T cells, CD3+ DN cells and CD4+CD25+ T cells in reproductive tissues (Figure 4.8), which in the context of the prominent lack of myeloid cells in CCR2 KOs was surprising. Therefore, CCR2 was not seen as important for CD3+ DN cells increasing in number at 1DPP in the uterine horn but was crucial for their presence in the blood. I also discovered in Chapter 5, that the number of cells CD3+ DN cells per ml remains constant so it appears more likely that the number of CD4+ T cells in the blood is reduced, causing the change in proportion of CD3+ DN cells.

7.5.2. *CCR2 activity on CD3+ DN cells is dependent on reproductive status.*

CCR2 expression by CD3+ DN cells in tissues was dependent on whether the mice were NP or 1DPP. This data is complementary with the data in Chapter 3, which indicated an induction of CCR2 on cells which do not normally express it. In NP reproductive tissues CCR2 dependent uptake was demonstrated by CD3+ DN cells, though this was not the case at 1DPP. Blood, which had shown considerable CCR2 expression by this cell population at 1DPP did not in the NP state. These data suggested that the CCR2 dependent shift from CD4+ T cells to CD3+ DN cells in the blood was post-partum specific and that CCR2 based chemokine internalisation was active during the early post-partum period but not in NP animals. Clearly, as with myeloid cells, the activity of CCR2 varies between the NP and the inflammatory environment at 1DPP. It was also apparent that there were

delineations in the findings between different tissues, however the link between reproductive tissues and blood in terms of their CD3+ DN cell content was fascinating. As discussed above in relation to Chapter 3, this may indicate that at 1DPP the uterine horn is a chemokine-rich environment thus causing desensitisation of CCR2 but in NP uterine horn CCR2 based chemokine internalisation can be observed.

It was intriguing to consider how distinct the results for reproductive tissues and peripheral tissues were. Though not analysed any further the possibility that these cells originated from the thymus was seriously considered. CCR2 appeared to perturb DN2 cells and CCL2 uptake specifically by DN1 and DN4 cells (data not shown). CCR2 may indeed play a role in altered DN cell development and it was tempting to speculate that it could also play a role in the release of these cells into the blood. Limited time and resources prevented further investigation in this area.

7.5.3. *Lactation affects CD3+ cell populations in various tissues.*

As well as examining the effects of CCR2 I also examined the influence of lactation on CD3+ cells. My hypothesis was that the differences in the post-partum hormonal profiles would influence leukocyte populations in various tissues. Lactation appears to the play a role in regulating leukocytes in the post-partum period. Non-lactating mice displayed a reduction in the proportion of CD4+ T cells in the blood, matched with a near-significant increase in the proportion of CD3+ DN cells (Figure 6.12). This was incredibly reminiscent of the profile of CD3+ cells in the blood at 1DPP. 1DPP and non-lactating animals also have very similar prolactin and CCL2 levels in their circulation (Figures 3.15 and 6.9). As discussed in Chapter 4, the rise in the proportion of CD3+ DN cells in the blood is CCR2 dependent. Further investigation would be beneficial in determining whether CCR2 is also involved in the change of CD3+ cell populations in lactating animals. CD4+ T cells and CD3+ DN cells from the blood of non-lactating mice internalised more CCL2-AF647 than the equivalent cells in lactating mice, further underlining that the expression of CCR2 might be altered by lactation (Figure 6.15). In the literature, CCL2 production by macrophages has been shown to be dramatically elevated upon *in vitro* treatment of prolactin (Sodhi and Tripathi, 2008). Though no causal connection was observed between levels of circulating prolactin, CCL2 and CD3+ populations, there is clearly much more work to be done in this area. Therefore I believe teasing out the links between lactation, prolactin, CCL2, CCR2, CD4+ T cells and CD3+ DN cells in blood could be fruitful.

7.6. *Future directions.*

Though there are several lines of investigation that I could continue to follow I will briefly outline how I would go about addressing a few. I would begin by further profiling NKT cells in reproductive tissues and blood. I would use more fluorescent channels to measure the expression of markers such as the invariant TCR-α chain Vα14Jα18, I would also want to measure expression of receptors such as NKG2D and NKp46, which are involved in NK mediated killing. Another experiment would involve sorting NKT cells from the uterine horn and blood and culturing the cells so that I could measure cytokines in the supernatant and verify if they are skewed towards a Th1 phenotype and whether this changes between NP and 1DPP animals. I would also like to measure how NP and 1DPP NKT cells respond to αGalCer/CD1 complexes in terms of marker expression and cytokine production and how presence of DN T cells in culture with NKT cells affects this.

As well as assessing the effects of DN T cells on NKT cells I would seek to use adoptive transfer techniques to tease apart the role of CCR2 on CD3+ DN cell populations. I would transfer WT>CCR2 KO, WT>WT, CCR2 KO>CCR2 KO, CCR2 KO>WT and observe whether CCR2 is required on CD3+ cells for the shift from CD4+ T cells to DN T cells at 1DPP.

Finally, I would like to investigate the role of lactation on leukocyte populations. I would begin to do this by administering exogenous prolactin to 1DPP mice whose pups had been removed and measure circulating CCL2, to attempt to find a causal link between prolactin levels and CCL2 in the blood. I would also measure CD3+ cell populations to see whether giving prolactin to non-lactating mice changes their proportions to mimic lactating mice at 7DPP. I would also like to investigate CD3+ populations in CCR2 KO non-lactating mice and compare these to 7DPP CCR2 KO lactating mice. This would help to reveal whether lactation and CCR2 have interacting effects.

7.7. *Conclusions.*

The conclusion of my work is that the majority of cells which are present in the post-partum period are myeloid cells and the accumulation of these cells is CCR2 dependent, and monocytes and neutrophils are disproportionately increased at 1DPP. There were also post-partum effects on CD3+ cells in the blood, at 1DPP there was a CCR2 dependent shift away from CD4+ cells towards CD3+ DN cells, which was probably driven by an increase in DN T cells. Hormones also appear to have some impact on leukocytes, with sex

differences affecting myeloid cells and lactation influencing CD3+ cells. This work has considerably furthered the available literature on leukocytes in post-partum tissues. I have catalogued several cell subsets in various tissues around the body and focussed on the CD3+ DN population which has previously received little attention. This work has shown that the post-partum period is a time of systemic dynamic changes in leukocyte populations, and that CCR2 is a key regulator of some of these populations.

References

ABU-TAHA, M., RIUS, C., HERMENEGILDO, C., NOGUERA, I., CERDA-NICOLAS, J. M., ISSEKUTZ, A. C., JOSE, P. J., CORTIJO, J., MORCILLO, E. J. & SANZ, M. J. 2009. Menopause and ovariectomy cause a low grade of systemic inflammation that may be prevented by chronic treatment with low doses of estrogen or losartan. *J Immunol,* 183**,** 1393-402.

ABUZAKOUK, M., FEIGHERY, C. & O'FARRELLY, C. 1996. Collagenase and Dispase enzymes disrupt lymphocyte surface molecules. *J Immunol Methods,* 194**,** 211-6.

ACHACHE, H. & REVEL, A. 2006. Endometrial receptivity markers, the journey to successful embryo implantation. *Hum Reprod Update,* 12**,** 731-46.

ALLEN, S. J., CROWN, S. E. & HANDEL, T. M. 2007. Chemokine: receptor structure, interactions, and antagonism. *Annu Rev Immunol,* 25**,** 787-820.

ALOISI, A. M., MUSCETTOLA, M. & LUPO, C. 2001. Effects of gonadectomy and pain on interferon-gamma production in splenocytes of male and female rats. *Brain Behav Immun,* 15**,** 266-72.

ALUVIHARE, V. R., KALLIKOURDIS, M. & BETZ, A. G. 2004. Regulatory T cells mediate maternal tolerance to the fetus. *Nat Immunol,* 5**,** 266-71.

ANACKER, J., SEGERER, S. E., HAGEMANN, C., FEIX, S., KAPP, M., BAUSCH, R. & KAMMERER, U. 2011. Human decidua and invasive trophoblasts are rich sources of nearly all human matrix metalloproteinases. *Mol Hum Reprod,* 17**,** 637-52.

ANDERSON, D., POLITCH, J. A. & PUDNEY, J. 2011. HIV infection and immune defense of the penis. *Am J Reprod Immunol,* 65**,** 220-9.

ANSEL, K. M., MCHEYZER-WILLIAMS, L. J., NGO, V. N., MCHEYZER-WILLIAMS, M. G. & CYSTER, J. G. 1999. In vivo-activated CD4 T cells upregulate CXC chemokine receptor 5 and reprogram their response to lymphoid chemokines. *J Exp Med,* 190**,** 1123-34.

ANTUNES, M. A., ABREU, S. C., SILVA, A. L., PARRA-CUENTAS, E. R., AB'SABER, A. M., CAPELOZZI, V. L., FERREIRA, T. P., MARTINS, M. A., SILVA, P. M. & ROCCO, P. R. 2010. Sex-specific lung remodeling and inflammation changes in experimental allergic asthma. *J Appl Physiol,* 109**,** 855-63.

AOKI, K., KAJIURA, S., MATSUMOTO, Y., OGASAWARA, M., OKADA, S., YAGAMI, Y. & GLEICHER, N. 1995. Preconceptional natural-killer-cell activity as a predictor of miscarriage. *Lancet,* 345**,** 1340-2.

ARNON, T. I., HORTON, R. M., GRIGOROVA, I. L. & CYSTER, J. G. 2013. Visualization of splenic marginal zone B-cell shuttling and follicular B-cell egress. *Nature,* 493**,** 684-8.

ASCON, D. B., ASCON, M., SATPUTE, S., LOPEZ-BRIONES, S., RACUSEN, L., COLVIN, R. B., SOLOSKI, M. J. & RABB, H. 2008. Normal mouse kidneys contain activated and CD3+CD4- CD8- double-negative T lymphocytes with a distinct TCR repertoire. *J Leukoc Biol,* 84**,** 1400-9.

AUFFRAY, C., FOGG, D., GARFA, M., ELAIN, G., JOIN-LAMBERT, O., KAYAL, S., SARNACKI, S., CUMANO, A., LAUVAU, G. & GEISSMANN, F. 2007. Monitoring of blood vessels and tissues by a population of monocytes with patrolling behavior. *Science,* 317**,** 666-70.

BAKIR, H. Y., TOMIYAMA-MIYAJI, C., WATANABE, H., NAGURA, T., KAWAMURA, T., SEKIKAWA, H. & ABO, T. 2006. Reasons why DBA/2 mice are resistant to malarial infection: expansion of CD3int B220+ gammadelta T cells with double-negative CD4- CD8- phenotype in the liver. *Immunology,* 117**,** 127-35.

BARRATT, C. L., BOLTON, A. E. & COOKE, I. D. 1990. Functional significance of white blood cells in the male and female reproductive tract. *Hum Reprod,* 5**,** 639-48.

BASTA, P., MAJKA, M., JOZWICKI, W., LUKASZEWSKA, E., KNAFEL, A., GRABIEC, M., STASIENKO, E. & WICHEREK, L. 2010. The frequency of CD25+CD4+ and FOXP3+ regulatory T cells in ectopic endometrium and ectopic decidua. *Reprod Biol Endocrinol,* 8**,** 116.

BAZAN, J. F., BACON, K. B., HARDIMAN, G., WANG, W., SOO, K., ROSSI, D., GREAVES, D. R., ZLOTNIK, A. & SCHALL, T. J. 1997. A new class of membrane-bound chemokine with a CX3C motif. *Nature,* 385**,** 640-4.

BENDELAC, A., SAVAGE, P. B. & TEYTON, L. 2007. The biology of NKT cells. *Annu Rev Immunol,* 25**,** 297-336.

BERAHOVICH, R. D., LAI, N. L., WEI, Z., LANIER, L. L. & SCHALL, T. J. 2006. Evidence for NK cell subsets based on chemokine receptor expression. *J Immunol,* 177**,** 7833-40.

BLEESING, J. J., BROWN, M. R., DALE, J. K., STRAUS, S. E., LENARDO, M. J., PUCK, J. M., ATKINSON, T. P. & FLEISHER, T. A. 2001. TcR-alpha/beta(+) CD4(-)CD8(-) T cells in humans with the autoimmune lymphoproliferative syndrome express a novel CD45 isoform that is analogous to murine B220 and represents a marker of altered O-glycan biosynthesis. *Clin Immunol,* 100**,** 314-24.

BOKSTROM, H., BRANNSTROM, M., ALEXANDERSSON, M. & NORSTROM, A. 1997. Leukocyte subpopulations in the human uterine cervical stroma at early and term pregnancy. *Hum Reprod,* 12**,** 586-90.

BORCHERS, M. T., ANSAY, T., DESALLE, R., DAUGHERTY, B. L., SHEN, H., METZGER, M., LEE, N. A. & LEE, J. J. 2002. In vitro assessment of chemokine receptor-ligand interactions mediating mouse eosinophil migration. *J Leukoc Biol,* 71**,** 1033-41.

BORG, N. A., ELY, L. K., BEDDOE, T., MACDONALD, W. A., REID, H. H., CLEMENTS, C. S., PURCELL, A. W., KJER-NIELSEN, L., MILES, J. J., BURROWS, S. R., MCCLUSKEY, J. & ROSSJOHN, J. 2005. The CDR3 regions of an immunodominant T cell receptor dictate the 'energetic landscape' of peptide-MHC recognition. *Nat Immunol,* 6**,** 171-80.

BOUMAN, A., SCHIPPER, M., HEINEMAN, M. J. & FAAS, M. M. 2004. Gender difference in the non-specific and specific immune response in humans. *Am J Reprod Immunol,* 52**,** 19-26.

BOWEN, J. M., KEYES, P. L., WARREN, J. S. & TOWNSON, D. H. 1996. Prolactin-induced regression of the rat corpus luteum: expression of monocyte chemoattractant protein-1 and invasion of macrophages. *Biol Reprod,* 54**,** 1120-7.

BOYSON, J. E., AKTAN, I., BARKHUFF, D. A. & CHANT, A. 2008. NKT cells at the maternal-fetal interface. *Immunol Invest,* 37**,** 565-82.

BOYSON, J. E., RYBALOV, B., KOOPMAN, L. A., EXLEY, M., BALK, S. P., RACKE, F. K., SCHATZ, F., MASCH, R., WILSON, S. B. & STROMINGER, J. L. 2002. CD1d and invariant NKT cells at the human maternal-fetal interface. *Proc Natl Acad Sci U S A,* 99**,** 13741-6.

BRANDON, J. M. 1990. Decidualization in the post-partum uterus of the mouse. *J Reprod Fertil,* 88**,** 151-8.

BRANDON, J. M. 1994. Distribution of macrophages in the mouse uterus from one day to three months after parturition, as defined by the immunohistochemical localization of the macrophage-restricted antigens F4/80 and macrosialin. *Anat Rec,* 240**,** 233-42.

BRASTED, M., WHITE, C. A., KENNEDY, T. G. & SALAMONSEN, L. A. 2003. Mimicking the events of menstruation in the murine uterus. *Biol Reprod,* 69**,** 1273-80.

BRENNAN, P. J., BRIGL, M. & BRENNER, M. B. 2013. Invariant natural killer T cells: an innate activation scheme linked to diverse effector functions. *Nat Rev Immunol,* 13**,** 101-17.

BRESER, M. L., MOTRICH, R. D., SANCHEZ, L. R., MACKERN-OBERTI, J. P. & RIVERO, V. E. 2013. Expression of CXCR3 on specific T cells is essential for homing to the prostate gland in an experimental model of chronic prostatitis/chronic pelvic pain syndrome. *J Immunol,* 190**,** 3121-33.

BROMLEY, S. K., MEMPEL, T. R. & LUSTER, A. D. 2008. Orchestrating the orchestrators: chemokines in control of T cell traffic. *Nat Immunol,* 9**,** 970-80.

BRUCE, H. M. & EAST, J. 1956. Number and viability of young from pregnancies concurrent with lactation in the mouse. *J Endocrinol,* 14**,** 19-27.

BRUHL, H., CIHAK, J., SCHNEIDER, M. A., PLACHY, J., RUPP, T., WENZEL, I., SHAKARAMI, M., MILZ, S., ELLWART, J. W., STANGASSINGER, M., SCHLONDORFF, D. & MACK, M. 2004. Dual role of CCR2 during initiation and progression of collagen-induced arthritis: evidence for regulatory activity of CCR2+ T cells. *J Immunol,* 172**,** 890-8.

BUGL, S., WIRTHS, S., MULLER, M. R., RADSAK, M. P. & KOPP, H. G. 2012. Current insights into neutrophil homeostasis. *Ann N Y Acad Sci,* 1266**,** 171-8.

BULL, M. M. 1949. Repair of the placental site in the rabbit. *J Obstet Gynaecol Br Emp,* 56**,** 799-818, 3 pl.

BULMER, J. N., WILLIAMS, P. J. & LASH, G. E. 2010. Immune cells in the placental bed. *Int J Dev Biol,* 54**,** 281-94.

BUNTING, M. D., COMERFORD, I., SEACH, N., HAMMETT, M. V., ASQUITH, D. L., KORNER, H., BOYD, R. L., NIBBS, R. J. & MCCOLL, S. R. 2013. CCX-CKR deficiency alters thymic stroma impairing thymocyte development and promoting autoimmunity. *Blood,* 121**,** 118-28.

BURKE, S. D., BARRETTE, V. F., GRAVEL, J., CARTER, A. L., HATTA, K., ZHANG, J., CHEN, Z., LENO-DURAN, E., BIANCO, J., LEONARD, S., MURRANT, C., ADAMS, M. A. & CROY, B. A. 2010. Uterine NK cells, spiral artery modification and the regulation of blood pressure during mouse pregnancy. *Am J Reprod Immunol,* 63**,** 472-81.

BUSTAMANTE, J. J., DAI, G. & SOARES, M. J. 2008. Pregnancy and lactation modulate maternal splenic growth and development of the erythroid lineage in the rat and mouse. *Reprod Fertil Dev,* 20**,** 303-10.

CAMPBELL, J. J., QIN, S., UNUTMAZ, D., SOLER, D., MURPHY, K. E., HODGE, M. R., WU, L. & BUTCHER, E. C. 2001. Unique subpopulations of CD56+ NK and NK-T peripheral blood lymphocytes identified by chemokine receptor expression repertoire. *J Immunol,* 166**,** 6477-82.

CAO, X., CAI, S. F., FEHNIGER, T. A., SONG, J., COLLINS, L. I., PIWNICA-WORMS, D. R. & LEY, T. J. 2007. Granzyme B and perforin are important for regulatory T cell-mediated suppression of tumor clearance. *Immunity,* 27**,** 635-46.

CAPOCCIA, B. J., GREGORY, A. D. & LINK, D. C. 2008. Recruitment of the inflammatory subset of monocytes to sites of ischemia induces angiogenesis in a monocyte chemoattractant protein-1-dependent fashion. *J Leukoc Biol,* 84**,** 760-8.

CARDONA, A. E., SASSE, M. E., LIU, L., CARDONA, S. M., MIZUTANI, M., SAVARIN, C., HU, T. & RANSOHOFF, R. M. 2008. Scavenging roles of chemokine receptors: chemokine receptor deficiency is associated with increased levels of ligand in circulation and tissues. *Blood,* 112**,** 256-63.

CARLSEN, H. S., BAEKKEVOLD, E. S., JOHANSEN, F. E., HARALDSEN, G. & BRANDTZAEG, P. 2002. B cell attracting chemokine 1 (CXCL13) and its receptor CXCR5 are expressed in normal and aberrant gut associated lymphoid tissue. *Gut,* 51**,** 364-71.

CARPENTER, A. C. & BOSSELUT, R. 2010. Decision checkpoints in the thymus. *Nat Immunol,* 11**,** 666-73.

CARR, M. W., ROTH, S. J., LUTHER, E., ROSE, S. S. & SPRINGER, T. A. 1994. Monocyte chemoattractant protein 1 acts as a T-lymphocyte chemoattractant. *Proc Natl Acad Sci U S A,* 91**,** 3652-6.

CARRENO, P. C., SACEDON, R., JIMENEZ, E., VICENTE, A. & ZAPATA, A. G. 2005. Prolactin affects both survival and differentiation of T-cell progenitors. *J Neuroimmunol,* 160**,** 135-45.

CARTER, J., NEWPORT, A., KEELER, K. D. & DRESSER, D. W. 1983. FACS analysis of changes in T and B lymphocyte populations in the blood, spleen and lymph nodes of pregnant mice. *Immunology,* 48**,** 791-7.

CASSANI, B., VILLABLANCA, E. J., QUINTANA, F. J., LOVE, P. E., LACY-HULBERT, A., BLANER, W. S., SPARWASSER, T., SNAPPER, S. B., WEINER, H. L. & MORA, J. R. 2011. Gut-tropic T cells that express integrin alpha4beta7 and CCR9 are required for induction of oral immune tolerance in mice. *Gastroenterology,* 141**,** 2109-18.

CATLEY, M. C., COOTE, J., BARI, M. & TOMLINSON, K. L. 2011. Monoclonal antibodies for the treatment of asthma. *Pharmacol Ther,* 132**,** 333-51.

CHA, J., SUN, X. & DEY, S. K. 2012. Mechanisms of implantation: strategies for successful pregnancy. *Nat Med,* 18**,** 1754-67.

CHAEN, T., KONNO, T., EGASHIRA, M., BAI, R., NOMURA, N., NOMURA, S., HIROTA, Y., SAKURAI, T. & IMAKAWA, K. 2012. Estrogen-dependent uterine secretion of osteopontin activates blastocyst adhesion competence. *PLoS One,* 7**,** e48933.

CHAVEZ-RUEDA, K., HERNANDEZ, J., ZENTENO, E., LEANOS-MIRANDA, A., LEGORRETA-HAQUET, M. V. & BLANCO-FAVELA, F. 2005. Identification of prolactin as a novel immunomodulator on the expression of co-stimulatory molecules and cytokine secretions on T and B human lymphocytes. *Clin Immunol,* 116**,** 182-91.

CHEN, W., FORD, M. S., YOUNG, K. J. & ZHANG, L. 2003. Infusion of in vitro-generated DN T regulatory cells induces permanent cardiac allograft survival in mice. *Transplant Proc,* 35**,** 2479-80.

CHEN, W., ZHOU, D., TORREALBA, J. R., WADDELL, T. K., GRANT, D. & ZHANG, L. 2005. Donor lymphocyte infusion induces long-term donor-specific cardiac xenograft survival through activation of recipient double-negative regulatory T cells. *J Immunol,* 175**,** 3409-16.

CINAMON, G., ZACHARIAH, M. A., LAM, O. M., FOSS, F. W., JR. & CYSTER, J. G. 2008. Follicular shuttling of marginal zone B cells facilitates antigen transport. *Nat Immunol,* 9**,** 54-62.

COLLINS, M. K., TAY, C. S. & ERLEBACHER, A. 2009. Dendritic cell entrapment within the pregnant uterus inhibits immune surveillance of the maternal/fetal interface in mice. *J Clin Invest,* 119**,** 2062-73.

COMERFORD, I., MILASTA, S., MORROW, V., MILLIGAN, G. & NIBBS, R. 2006. The chemokine receptor CCX-CKR mediates effective scavenging of CCL19 in vitro. *Eur J Immunol,* 36**,** 1904-16.

COMERFORD, I. & NIBBS, R. J. 2005. Post-translational control of chemokines: a role for decoy receptors? *Immunol Lett,* 96**,** 163-74.

CONNOR, S. J., PARASKEVOPOULOS, N., NEWMAN, R., CUAN, N., HAMPARTZOUMIAN, T., LLOYD, A. R. & GRIMM, M. C. 2004. CCR2 expressing CD4+ T lymphocytes are preferentially recruited to the ileum in Crohn's disease. *Gut,* 53**,** 1287-94.

COTTON, M. & CLAING, A. 2009. G protein-coupled receptors stimulation and the control of cell migration. *Cell Signal,* 21**,** 1045-53.

CRIPPS, J. G., CELAJ, S., BURDICK, M., STRIETER, R. M. & GORHAM, J. D. 2012. Liver inflammation in a mouse model of Th1 hepatitis despite the absence of invariant NKT cells or the Th1 chemokine receptors CXCR3 and CCR5. *Lab Invest,* 92**,** 1461-71.

CRISPIN, J. C., OUKKA, M., BAYLISS, G., COHEN, R. A., VAN BEEK, C. A., STILLMAN, I. E., KYTTARIS, V. C., JUANG, Y. T. & TSOKOS, G. C. 2008. Expanded double negative T cells in patients with systemic lupus erythematosus produce IL-17 and infiltrate the kidneys. *J Immunol,* 181**,** 8761-6.

CRITCHLEY, H. O., KELLY, R. W., LEA, R. G., DRUDY, T. A., JONES, R. L. & BAIRD, D. T. 1996. Sex steroid regulation of leukocyte traffic in human decidua. *Hum Reprod,* 11**,** 2257-62.

CROY, B. A., HE, H., ESADEG, S., WEI, Q., MCCARTNEY, D., ZHANG, J., BORZYCHOWSKI, A., ASHKAR, A. A., BLACK, G. P., EVANS, S. S., CHANTAKRU, S., VAN DEN HEUVEL, M., PAFFARO, V. A., JR. & YAMADA, A. T. 2003. Uterine natural killer cells: insights into their cellular and molecular biology from mouse modelling. *Reproduction,* 126**,** 149-60.

CUPURDIJA, K., AZZOLA, D., HAINZ, U., GRATCHEV, A., HEITGER, A., TAKIKAWA, O., GOERDT, S., WINTERSTEIGER, R., DOHR, G. & SEDLMAYR, P. 2004. Macrophages of human first trimester decidua express markers associated to alternative activation. *Am J Reprod Immunol,* 51**,** 117-22.

D'ACQUISTO, F. & CROMPTON, T. 2011. CD3+CD4-CD8- (double negative) T cells: saviours or villains of the immune response? *Biochem Pharmacol,* 82**,** 333-40.

DAMBAEVA, S. V., BREBURDA, E. E., DURNING, M., GARTHWAITE, M. A. & GOLOS, T. G. 2009. Characterization of decidual leukocyte populations in cynomolgus and vervet monkeys. *J Reprod Immunol,* 80**,** 57-69.

DE LEON-NAVA, M. A., NAVA, K., SOLDEVILA, G., LOPEZ-GRIEGO, L., CHAVEZ-RIOS, J. R., VARGAS-VILLAVICENCIO, J. A. & MORALES-MONTOR, J. 2009. Immune sexual dimorphism: effect of gonadal steroids on the expression of cytokines, sex steroid receptors, and lymphocyte proliferation. *J Steroid Biochem Mol Biol,* 113**,** 57-64.

DE, M. & WOOD, G. W. 1990. Influence of oestrogen and progesterone on macrophage distribution in the mouse uterus. *J Endocrinol,* 126**,** 417-24.

DE, M. & WOOD, G. W. 1991. Analysis of the number and distribution of macrophages, lymphocytes, and granulocytes in the mouse uterus from implantation through parturition. *J Leukoc Biol,* 50**,** 381-92.

DELGADO, S. R., MCBEY, B. A., YAMASHIRO, S., FUJITA, J., KISO, Y. & CROY, B. A. 1996. Accounting for the peripartum loss of granulated metrial gland cells, a natural killer cell population, from the pregnant mouse uterus. *J Leukoc Biol,* 59**,** 262-9.

DELOIA, J. A., KRASNOW, J. S., BREKOSKY, J., BABAKNIA, A., JULIAN, J. & CARSON, D. D. 1998. Regional specialization of the cell membrane-associated, polymorphic mucin (MUC1) in human uterine epithelia. *Hum Reprod,* 13**,** 2902-9.

DINESH, R. K., HAHN, B. H. & SINGH, R. P. 2010. PD-1, gender, and autoimmunity. *Autoimmun Rev,* 9**,** 583-7.

DOMINGUEZ, F., YANEZ-MO, M., SANCHEZ-MADRID, F. & SIMON, C. 2005. Embryonic implantation and leukocyte transendothelial migration: different processes with similar players? *FASEB J,* 19**,** 1056-60.

DOUIN-ECHINARD, V., CALIPPE, B., BILLON-GALES, A., FONTAINE, C., LENFANT, F., TREMOLLIERES, F., BAYARD, F., GUERY, J. C., ARNAL, J. F. & GOURDY, P. 2011. Estradiol administration controls eosinophilia through estrogen receptor-alpha activation during acute peritoneal inflammation. *J Leukoc Biol,* 90**,** 145-54.

DUNCAN, B., NAZAROV-STOICA, C., SURLS, J., KEHL, M., BONA, C., CASARES, S. & BRUMEANU, T. D. 2010. Double negative (CD3+ 4- 8-) TCR alphabeta splenic cells from young NOD mice provide long-lasting protection against type 1 diabetes. *PLoS One,* 5**,** e11427.

DUNN, C. L., KELLY, R. W. & CRITCHLEY, H. O. 2003. Decidualization of the human endometrial stromal cell: an enigmatic transformation. *Reprod Biomed Online,* 7**,** 151-61.

EBIOSCIENCE Cellular Antigens Guide; Mouse & Human CD & Non-CD Listings.

ELSNER, J., DULKYS, Y., GUPTA, S., ESCHER, S. E., FORSSMANN, W. G., KAPP, A. & FORSSMANN, U. 2005. Differential pattern of CCR1 internalization in human eosinophils: prolonged internalization by CCL5 in contrast to CCL3. *Allergy,* 60**,** 1386-93.

ERLEBACHER, A. 2013. Immunology of the maternal-fetal interface. *Annu Rev Immunol,* 31**,** 387-411.

ESPLIN, M. S., PELTIER, M. R., HAMBLIN, S., SMITH, S., FAUSETT, M. B., DILDY, G. A., BRANCH, D. W., SILVER, R. M. & ADASHI, E. Y. 2005. Monocyte chemotactic protein-1 expression is increased in human gestational tissues during term and preterm labor. *Placenta,* 26**,** 661-71.

FAURIAT, C., LONG, E. O., LJUNGGREN, H. G. & BRYCESON, Y. T. 2010. Regulation of human NK-cell cytokine and chemokine production by target cell recognition. *Blood,* 115**,** 2167-76.

FAZILLEAU, N., MARK, L., MCHEYZER-WILLIAMS, L. J. & MCHEYZER-WILLIAMS, M. G. 2009. Follicular helper T cells: lineage and location. *Immunity,* 30**,** 324-35.

FENG, D., NAGY, J. A., PYNE, K., DVORAK, H. F. & DVORAK, A. M. 1998. Neutrophils emigrate from venules by a transendothelial cell pathway in response to FMLP. *J Exp Med,* 187**,** 903-15.

FERLAZZO, G., TSANG, M. L., MORETTA, L., MELIOLI, G., STEINMAN, R. M. & MUNZ, C. 2002. Human dendritic cells activate resting natural killer (NK) cells and are recognized via the NKp30 receptor by activated NK cells. *J Exp Med,* 195**,** 343-51.

FERNEKORN, U., BUTCHER, E. C., BEHRENDS, J., KARSTEN, C. M., ROBKE, A., SCHULZE, T. J., KIRCHNER, H. & KRUSE, A. 2007. Selectin, platelet plays a critical role in granulocyte access to the pregnant mouse uterus under physiological and pathological conditions. *Biol Reprod,* 76**,** 645-53.

FEST, S., ALDO, P. B., ABRAHAMS, V. M., VISINTIN, I., ALVERO, A., CHEN, R., CHAVEZ, S. L., ROMERO, R. & MOR, G. 2007. Trophoblast-macrophage interactions: a regulatory network for the protection of pregnancy. *Am J Reprod Immunol,* 57**,** 55-66.

FIDEL, P. L., JR., WOLF, N. A. & KUKURUGA, M. A. 1996. T lymphocytes in the murine vaginal mucosa are phenotypically distinct from those in the periphery. *Infect Immun,* 64**,** 3793-9.

FIFE, B. T., HUFFNAGLE, G. B., KUZIEL, W. A. & KARPUS, W. J. 2000. CC chemokine receptor 2 is critical for induction of experimental autoimmune encephalomyelitis. *J Exp Med,* 192**,** 899-905.

FIFE, B. T. & PAUKEN, K. E. 2011. The role of the PD-1 pathway in autoimmunity and peripheral tolerance. *Ann N Y Acad Sci,* 1217**,** 45-59.

FINN, C. A. & POPE, M. 1984. Vascular and cellular changes in the decidualized endometrium of the ovariectomized mouse following cessation of hormone treatment: a possible model for menstruation. *J Endocrinol,* 100**,** 295-300.

FISCHER, K., VOELKL, S., HEYMANN, J., PRZYBYLSKI, G. K., MONDAL, K., LAUMER, M., KUNZ-SCHUGHART, L., SCHMIDT, C. A., ANDREESEN, R. & MACKENSEN, A. 2005. Isolation and characterization of human antigen-specific TCR alpha beta+ CD4(-)CD8- double-negative regulatory T cells. *Blood,* 105**,** 2828-35.

FLYNN, L., BYRNE, B., CARTON, J., KELEHAN, P., O'HERLIHY, C. & O'FARRELLY, C. 2000. Menstrual cycle dependent fluctuations in NK and T-lymphocyte subsets from non-pregnant human endometrium. *Am J Reprod Immunol,* 43**,** 209-17.

FORD, M. S., ZHANG, Z. X., CHEN, W. & ZHANG, L. 2006. Double-negative T regulatory cells can develop outside the thymus and do not mature from CD8+ T cell precursors. *J Immunol,* 177**,** 2803-9.

FORSTER, R., BRAUN, A. & WORBS, T. 2012. Lymph node homing of T cells and dendritic cells via afferent lymphatics. *Trends Immunol,* 33**,** 271-80.

FRAZIER-JESSEN, M. R. & KOVACS, E. J. 1995. Estrogen modulation of JE/monocyte chemoattractant protein-1 mRNA expression in murine macrophages. *J Immunol,* 154**,** 1838-45.

FUKUMA, N., AKIMITSU, N., HAMAMOTO, H., KUSUHARA, H., SUGIYAMA, Y. & SEKIMIZU, K. 2003. A role of the Duffy antigen for the maintenance of plasma chemokine concentrations. *Biochem Biophys Res Commun,* 303**,** 137-9.

GAGNERAULT, M. C., TOURAINE, P., SAVINO, W., KELLY, P. A. & DARDENNE, M. 1993. Expression of prolactin receptors in murine lymphoid cells in normal and autoimmune situations. *J Immunol,* 150**,** 5673-81.

GANGRADE, B. K. & DOMINIC, C. J. 1984. Studies of the male-originating pheromones involved in the Whitten effect and Bruce effect in mice. *Biol Reprod,* 31**,** 89-96.

GAO, J. F., MCINTYRE, M. S., JUVET, S. C., DIAO, J., LI, X., VANAMA, R. B., MAK, T. W., CATTRAL, M. S. & ZHANG, L. 2011. Regulation of antigen-expressing dendritic cells by double negative regulatory T cells. *Eur J Immunol,* 41**,** 2699-708.

GAPIN, L., MATSUDA, J. L., SURH, C. D. & KRONENBERG, M. 2001. NKT cells derive from double-positive thymocytes that are positively selected by CD1d. *Nat Immunol,* 2**,** 971-8.

GARLANDA, C., MAINA, V., MARTINEZ DE LA TORRE, Y., NEBULONI, M. & LOCATI, M. 2008. Inflammatory reaction and implantation: the new entries PTX3 and D6. *Placenta,* 29 Suppl B**,** 129-34.

GAUTIER, E. L., JAKUBZICK, C. & RANDOLPH, G. J. 2009. Regulation of the migration and survival of monocyte subsets by chemokine receptors and its relevance to atherosclerosis. *Arterioscler Thromb Vasc Biol,* 29**,** 1412-8.

GEISSMANN, F., JUNG, S. & LITTMAN, D. R. 2003. Blood monocytes consist of two principal subsets with distinct migratory properties. *Immunity,* 19**,** 71-82.

GLASIER, A. & MCNEILLY, A. S. 1990. Physiology of lactation. *Baillieres Clin Endocrinol Metab,* 4**,** 379-95.

GLASIER, A., MCNEILLY, A. S. & HOWIE, P. W. 1984. The prolactin response to suckling. *Clin Endocrinol (Oxf),* 21**,** 109-16.

GODFREY, D. I., KENNEDY, J., SUDA, T. & ZLOTNIK, A. 1993. A developmental pathway involving four phenotypically and functionally distinct subsets of CD3-CD4-CD8- triple-negative adult mouse thymocytes defined by CD44 and CD25 expression. *J Immunol,* 150**,** 4244-52.

GODFREY, D. I., MACDONALD, H. R., KRONENBERG, M., SMYTH, M. J. & VAN KAER, L. 2004. NKT cells: what's in a name? *Nat Rev Immunol,* 4**,** 231-7.

GOMEZ-LOPEZ, N., VEGA-SANCHEZ, R., CASTILLO-CASTREJON, M., ROMERO, R., CUBEIRO-ARREOLA, K. & VADILLO-ORTEGA, F. 2013. Evidence for a role for the adaptive immune response in human term parturition. *Am J Reprod Immunol,* 69**,** 212-30.

GONZALEZ, J. M., DONG, Z., ROMERO, R. & GIRARDI, G. 2011. Cervical remodeling/ripening at term and preterm delivery: the same mechanism initiated by different mediators and different effector cells. *PLoS One,* 6**,** e26877.

GORDON, S. & TAYLOR, P. R. 2005. Monocyte and macrophage heterogeneity. *Nat Rev Immunol,* 5**,** 953-64.

GOSLING, J., DAIRAGHI, D. J., WANG, Y., HANLEY, M., TALBOT, D., MIAO, Z. & SCHALL, T. J. 2000. Cutting edge: identification of a novel chemokine receptor that binds dendritic cell- and T cell-active chemokines including ELC, SLC, and TECK. *J Immunol,* 164**,** 2851-6.

GRAHAM, C. E. 1966. Cyclic changes in the squamo-columnar junction of the mouse cervix uteri. *Anat Rec,* 155**,** 251-60.

GRAHAM, G. J. 2009. D6 and the atypical chemokine receptor family: novel regulators of immune and inflammatory processes. *Eur J Immunol,* 39**,** 342-51.

GREENSTEIN, B. & WOOD, D. F. 2006. *The endocrine system at a glance,* Malden, Mass., Blackwell Pub.

GREENSTEIN, B., WOOD, D. F. & DAWSON BOOKS. 2011. The endocrine system at a glance. *At a glance series.* 3rd ed. Chichester, West Sussex: Wiley-Blackwell,.

GREER, J. M. & MCCOMBE, P. A. 2011. Role of gender in multiple sclerosis: clinical effects and potential molecular mechanisms. *J Neuroimmunol,* 234**,** 7-18.

GUZZO, A. C., JHEON, J., IMTIAZ, F. & DECATANZARO, D. 2012. Oestradiol transmission from males to females in the context of the Bruce and Vandenbergh effects in mice (Mus musculus). *Reproduction,* 143**,** 539-48.

HABICHT, A., DADA, S., JUREWICZ, M., FIFE, B. T., YAGITA, H., AZUMA, M., SAYEGH, M. H. & GULERIA, I. 2007. A link between PDL1 and T regulatory cells in fetomaternal tolerance. *J Immunol,* 179**,** 5211-9.

HALLER, H., RADILLO, O., RUKAVINA, D., TEDESCO, F., CANDUSSI, G., PETROVIC, O. & RANDIC, L. 1993. An immunohistochemical study of leucocytes in human endometrium, first and third trimester basal decidua. *J Reprod Immunol,* 23**,** 41-9.

HANNA, J., GOLDMAN-WOHL, D., HAMANI, Y., AVRAHAM, I., GREENFIELD, C., NATANSON-YARON, S., PRUS, D., COHEN-DANIEL, L., ARNON, T. I., MANASTER, I., GAZIT, R., YUTKIN, V., BENHARROCH, D., PORGADOR, A., KESHET, E., YAGEL, S. & MANDELBOIM, O. 2006. Decidual NK cells regulate key developmental processes at the human fetal-maternal interface. *Nat Med,* 12**,** 1065-74.

HANSELL, C. A., HURSON, C. E. & NIBBS, R. J. 2011a. DARC and D6: silent partners in chemokine regulation? *Immunol Cell Biol,* 89**,** 197-206.

HANSELL, C. A., SCHIERING, C., KINSTRIE, R., FORD, L., BORDON, Y., MCINNES, I. B., GOODYEAR, C. S. & NIBBS, R. J. 2011b. Universal expression and dual function of the atypical chemokine receptor D6 on innate-like B cells in mice. *Blood,* 117**,** 5413-24.

HAPON, M. B., SIMONCINI, M., VIA, G. & JAHN, G. A. 2003. Effect of hypothyroidism on hormone profiles in virgin, pregnant and lactating rats, and on lactation. *Reproduction,* 126**,** 371-82.

HARTL, D., KRAUSS-ETSCHMANN, S., KOLLER, B., HORDIJK, P. L., KUIJPERS, T. W., HOFFMANN, F., HECTOR, A., EBER, E., MARCOS, V., BITTMANN, I., EICKELBERG, O., GRIESE, M. & ROOS, D. 2008. Infiltrated neutrophils acquire novel chemokine receptor expression and chemokine responsiveness in chronic inflammatory lung diseases. *J Immunol,* 181**,** 8053-67.

HEINZEL, K., BENZ, C. & BLEUL, C. C. 2007. A silent chemokine receptor regulates steady-state leukocyte homing in vivo. *Proc Natl Acad Sci U S A,* 104**,** 8421-6.

HILL, P. D., CHATTERTON, R. T., JR. & ALDAG, J. C. 1999. Serum prolactin in breastfeeding: state of the science. *Biol Res Nurs,* 1**,** 65-75.

HOGER, T. A., TOKUYAMA, M., YONAMINE, K., HAYASHI, K., MASUKO-HONGO, K., KATO, T., KOBATA, T., MIZUSHIMA, Y., NISHIOKA, K. & YAMAMOTO, K. 1996. Time course analysis of alpha+ beta+ T cell clones during normal pregnancy. *Eur J Immunol,* 26**,** 834-8.

HOLT, R., TIMMONS, B. C., AKGUL, Y., AKINS, M. L. & MAHENDROO, M. 2011. The molecular mechanisms of cervical ripening differ between term and preterm birth. *Endocrinology,* 152**,** 1036-46.

HOUSER, B. L., TILBURGS, T., HILL, J., NICOTRA, M. L. & STROMINGER, J. L. 2011. Two unique human decidual macrophage populations. *J Immunol,* 186**,** 2633-42.

HUANG, C. C., ORVIS, G. D., WANG, Y. & BEHRINGER, R. R. 2012. Stromal-to-epithelial transition during postpartum endometrial regeneration. *PLoS One,* 7**,** e44285.

HUANG, M. C., PATEL, K., TAUB, D. D., LONGO, D. L. & GOETZL, E. J. 2010. Human CD4- 8- T cells are a distinctive immunoregulatory subset. *FASEB J,* 24**,** 2558-66.

HULBOY, D. L., RUDOLPH, L. A. & MATRISIAN, L. M. 1997. Matrix metalloproteinases as mediators of reproductive function. *Mol Hum Reprod,* 3**,** 27-45.

IIJIMA, N., MATTEI, L. M. & IWASAKI, A. 2011. Recruited inflammatory monocytes stimulate antiviral Th1 immunity in infected tissue. *Proc Natl Acad Sci U S A,* 108**,** 284-9.

IMAI, T., HIESHIMA, K., HASKELL, C., BABA, M., NAGIRA, M., NISHIMURA, M., KAKIZAKI, M., TAKAGI, S., NOMIYAMA, H., SCHALL, T. J. & YOSHIE, O. 1997. Identification and molecular characterization of fractalkine receptor CX3CR1, which mediates both leukocyte migration and adhesion. *Cell,* 91**,** 521-30.

INFANTINO, S., MOEPPS, B. & THELEN, M. 2006. Expression and regulation of the orphan receptor RDC1 and its putative ligand in human dendritic and B cells. *J Immunol,* 176**,** 2197-207.

ISHIDA, Y., GAO, J. L. & MURPHY, P. M. 2008. Chemokine receptor CX3CR1 mediates skin wound healing by promoting macrophage and fibroblast accumulation and function. *J Immunol,* 180**,** 569-79.

ISLAM, S. A., CHANG, D. S., COLVIN, R. A., BYRNE, M. H., MCCULLY, M. L., MOSER, B., LIRA, S. A., CHARO, I. F. & LUSTER, A. D. 2011. Mouse CCL8, a CCR8 agonist, promotes atopic dermatitis by recruiting IL-5+ T(H)2 cells. *Nat Immunol,* 12**,** 167-77.

ITO, K., KARASAWA, M., KAWANO, T., AKASAKA, T., KOSEKI, H., AKUTSU, Y., KONDO, E., SEKIYA, S., SEKIKAWA, K., HARADA, M., YAMASHITA, M., NAKAYAMA, T. & TANIGUCHI, M. 2000. Involvement of decidual Valpha14 NKT cells in abortion. *Proc Natl Acad Sci U S A,* 97**,** 740-4.

ITOHARA, S., FARR, A. G., LAFAILLE, J. J., BONNEVILLE, M., TAKAGAKI, Y., HAAS, W. & TONEGAWA, S. 1990. Homing of a gamma delta thymocyte subset with homogeneous T-cell receptors to mucosal epithelia. *Nature,* 343**,** 754-7.

IVANISEVIC, M., SEGERER, S., RIEGER, L., KAPP, M., DIETL, J., KAMMERER, U. & FRAMBACH, T. 2010. Antigen-presenting cells in pregnant and non-pregnant human myometrium. *Am J Reprod Immunol,* 64**,** 188-96.

IZIKSON, L., KLEIN, R. S., CHARO, I. F., WEINER, H. L. & LUSTER, A. D. 2000. Resistance to experimental autoimmune encephalomyelitis in mice lacking the CC chemokine receptor (CCR)2. *J Exp Med,* 192**,** 1075-80.

JAMIESON, T., CLARKE, M., STEELE, C. W., SAMUEL, M. S., NEUMANN, J., JUNG, A., HUELS, D., OLSON, M. F., DAS, S., NIBBS, R. J. & SANSOM, O. J. 2012. Inhibition of CXCR2 profoundly suppresses inflammation-driven and spontaneous tumorigenesis. *J Clin Invest,* 122**,** 3127-44.

JAMIESON, T., COOK, D. N., NIBBS, R. J., ROT, A., NIXON, C., MCLEAN, P., ALCAMI, A., LIRA, S. A., WIEKOWSKI, M. & GRAHAM, G. J. 2005. The chemokine receptor D6 limits the inflammatory response in vivo. *Nat Immunol,* 6**,** 403-11.

JENSEN, A. L., COLLINS, J., SHIPMAN, E. P., WIRA, C. R., GUYRE, P. M. & PIOLI, P. A. 2012. A subset of human uterine endometrial macrophages is alternatively activated. *Am J Reprod Immunol,* 68**,** 374-86.

JOHANSSON, M. & LYCKE, N. 2003. A unique population of extrathymically derived alpha beta TCR+CD4-CD8- T cells with regulatory functions dominates the mouse female genital tract. *J Immunol,* 170**,** 1659-66.

JOHNSTON, B., BURNS, A. R., SUEMATSU, M., ISSEKUTZ, T. B., WOODMAN, R. C. & KUBES, P. 1999. Chronic inflammation upregulates chemokine receptors and induces neutrophil migration to monocyte chemoattractant protein-1. *J Clin Invest,* 103**,** 1269-76.

JONES, R. C. 1999. To store or mature spermatozoa? The primary role of the epididymis. *Int J Androl,* 22**,** 57-67.

JONES, R. L., HANNAN, N. J., KAITU'U, T. J., ZHANG, J. & SALAMONSEN, L. A. 2004. Identification of chemokines important for leukocyte recruitment to the human endometrium at the times of embryo implantation and menstruation. *J Clin Endocrinol Metab,* 89**,** 6155-67.

JONES, R. L., KELLY, R. W. & CRITCHLEY, H. O. 1997. Chemokine and cyclooxygenase-2 expression in human endometrium coincides with leukocyte accumulation. *Hum Reprod,* 12**,** 1300-6.

KABAWAT, S. E., MOSTOUFI-ZADEH, M., DRISCOLL, S. G. & BHAN, A. K. 1985. Implantation site in normal pregnancy. A study with monoclonal antibodies. *Am J Pathol,* 118**,** 76-84.

KABELITZ, D. 2011. gammadelta T-cells: cross-talk between innate and adaptive immunity. *Cell Mol Life Sci,* 68**,** 2331-3.

KADENA, T., MATSUZAKI, G., FUJISE, S., KISHIHARA, K., TAKIMOTO, H., SASAKI, M., BEPPU, M., NAKAMURA, S. & NOMOTO, K. 1997. TCR alpha beta+ CD4- CD8- T cells differentiate extrathymically in an lck-independent manner and participate in early response against Listeria monocytogenes infection through interferon-gamma production. *Immunology,* 91**,** 511-9.

KAITU'U-LINO, T. J., MORISON, N. B. & SALAMONSEN, L. A. 2007. Neutrophil depletion retards endometrial repair in a mouse model. *Cell Tissue Res,* 328**,** 197-206.

KAJIWARA, C., KONDO, S., UDA, S., DAI, L., ICHIYANAGI, T., CHIBA, T., ISHIDO, S., KOJI, T. & UDONO, H. 2012. Spermatogenesis arrest caused by conditional deletion of Hsp90alpha in adult mice. *Biol Open,* 1**,** 977-82.

KALLIKOURDIS, M., ANDERSEN, K. G., WELCH, K. A. & BETZ, A. G. 2007. Alloantigen-enhanced accumulation of CCR5+ 'effector' regulatory T cells in the gravid uterus. *Proc Natl Acad Sci U S A,* 104**,** 594-9.

KALLIKOURDIS, M. & BETZ, A. G. 2007. Periodic accumulation of regulatory T cells in the uterus: preparation for the implantation of a semi-allogeneic fetus? *PLoS One,* 2**,** e382.

KAMAT, B. R. & ISAACSON, P. G. 1987. The immunocytochemical distribution of leukocytic subpopulations in human endometrium. *Am J Pathol,* 127**,** 66-73.

KAMMERER, U., EGGERT, A. O., KAPP, M., MCLELLAN, A. D., GEIJTENBEEK, T. B., DIETL, J., VAN KOOYK, Y. & KAMPGEN, E. 2003. Unique appearance of proliferating antigen-presenting cells expressing DC-SIGN (CD209) in the decidua of early human pregnancy. *Am J Pathol,* 162**,** 887-96.

KEIR, M. E., LATCHMAN, Y. E., FREEMAN, G. J. & SHARPE, A. H. 2005. Programmed death-1 (PD-1):PD-ligand 1 interactions inhibit TCR-mediated positive selection of thymocytes. *J Immunol,* 175**,** 7372-9.

KIM, C. H., KUNKEL, E. J., BOISVERT, J., JOHNSTON, B., CAMPBELL, J. J., GENOVESE, M. C., GREENBERG, H. B. & BUTCHER, E. C. 2001. Bonzo/CXCR6 expression defines type 1-polarized T-cell subsets with extralymphoid tissue homing potential. *J Clin Invest,* 107**,** 595-601.

KIM, N. & LUSTER, A. D. 2007. Regulation of immune cells by eicosanoid receptors. *ScientificWorldJournal,* 7**,** 1307-28.

KIMURA 1999. Phenotype Analysis of Peripheral Blood Mononuclear Cells
in Periparturient Dairy Cows. *J Dairy Sci,* 82**,** 315-319.

KINDT, T. J., GOLDSBY, R. A., OSBORNE, B. A. & KUBY, J. 2007. *Kuby Immunology,* New York, N.Y., W.H. Freeman and Co.

KOKUBU, K., HONDO, E., SAKAGUCHI, N., SAGARA, E. & KISO, Y. 2005. Differentiation and elimination of uterine natural killer cells in delayed implantation and parturition mice. *J Reprod Dev,* 51**,** 773-6.

KOYASU, S. 1994. CD3+CD16+NK1.1+B220+ large granular lymphocytes arise from both alpha-beta TCR+CD4-CD8- and gamma-delta TCR+CD4-CD8- cells. *J Exp Med,* 179**,** 1957-72.

KRACKOW, S. 1990. Sex-specific embryonic mortality during concurrent pregnancy and lactation in house mice. *J Exp Zool,* 256**,** 106-12.

KURIHARA, T., WARR, G., LOY, J. & BRAVO, R. 1997. Defects in macrophage recruitment and host defense in mice lacking the CCR2 chemokine receptor. *J Exp Med,* 186**,** 1757-62.

KUZIEL, W. A., MORGAN, S. J., DAWSON, T. C., GRIFFIN, S., SMITHIES, O., LEY, K. & MAEDA, N. 1997. Severe reduction in leukocyte adhesion and monocyte extravasation in mice deficient in CC chemokine receptor 2. *Proc Natl Acad Sci U S A,* 94**,** 12053-8.

KYAW, Y., HASEGAWA, G., TAKATSUKA, H., SHIMADA-HIRATSUKA, M., UMEZU, H., ARAKAWA, M. & NAITO, M. 1998. Expression of macrophage colony-stimulating factor, scavenger receptors, and macrophage proliferation in the pregnant mouse uterus. *Arch Histol Cytol,* 61**,** 383-93.

LASH, G. E., ROBSON, S. C. & BULMER, J. N. 2010. Review: Functional role of uterine natural killer (uNK) cells in human early pregnancy decidua. *Placenta,* 31 Suppl**,** S87-92.

LASKARIN, G., KAMMERER, U., RUKAVINA, D., THOMSON, A. W., FERNANDEZ, N. & BLOIS, S. M. 2007. Antigen-presenting cells and materno-fetal tolerance: an emerging role for dendritic cells. *Am J Reprod Immunol,* 58**,** 255-67.

LAVERS, A. E., SWANLUND, D. J., HUNTER, B. A., TRAN, M. L., PRYOR, J. L. & ROBERTS, K. P. 2006. Acute effect of vasectomy on the function of the rat epididymal epithelium and vas deferens. *J Androl,* 27**,** 826-36.

LE GALL, S. M., LEGRAND, J., BENBIJJA, M., SAFYA, H., BENIHOUD, K., KANELLOPOULOS, J. M. & BOBE, P. 2012. Loss of P2X7 Receptor Plasma Membrane Expression and Function in Pathogenic B220(+) Double-Negative T Lymphocytes of Autoimmune MRL/lpr Mice. *PLoS One,* 7**,** e52161.

LEE, B. O., JONES, J. E., PETERS, C. J., WHITACRE, D., FRELIN, L., HUGHES, J., KIM, W. K. & MILICH, D. R. 2011a. Identification of a unique double-negative regulatory T-cell population. *Immunology,* 134**,** 434-47.

LEE, B. P., CHEN, W., SHI, H., DER, S. D., FORSTER, R. & ZHANG, L. 2006. CXCR5/CXCL13 interaction is important for double-negative regulatory T cell homing to cardiac allografts. *J Immunol,* 176**,** 5276-83.

LEE, B. P., MANSFIELD, E., HSIEH, S. C., HERNANDEZ-BOUSSARD, T., CHEN, W., THOMSON, C. W., FORD, M. S., BOSINGER, S. E., DER, S., ZHANG, Z. X., ZHANG, M., KELVIN, D. J., SARWAL, M. M. & ZHANG, L. 2005. Expression profiling of murine double-negative regulatory T cells suggest mechanisms for prolonged cardiac allograft survival. *J Immunol,* 174**,** 4535-44.

LEE, S. K., KIM, J. Y., HUR, S. E., KIM, C. J., NA, B. J., LEE, M., GILMAN-SACHS, A. & KWAK-KIM, J. 2011b. An imbalance in interleukin-17-producing T and Foxp3(+) regulatory T cells in women with idiopathic recurrent pregnancy loss. *Hum Reprod,* 26**,** 2964-71.

LEE, S. K., KIM, J. Y., LEE, M., GILMAN-SACHS, A. & KWAK-KIM, J. 2012. Th17 and regulatory T cells in women with recurrent pregnancy loss. *Am J Reprod Immunol,* 67**,** 311-8.

LENGI, A. J., PHILLIPS, R. A., KARPUZOGLU, E. & AHMED, S. A. 2007. Estrogen selectively regulates chemokines in murine splenocytes. *J Leukoc Biol,* 81**,** 1065-74.

LEVITSKY, H. I., GOLUMBEK, P. T. & PARDOLL, D. M. 1991. The fate of CD4-8- T cell receptor-alpha beta+ thymocytes. *J Immunol,* 146**,** 1113-7.

LI, L. P., FANG, Y. C., DONG, G. F., LIN, Y. & SAITO, S. 2012. Depletion of invariant NKT cells reduces inflammation-induced preterm delivery in mice. *J Immunol,* 188**,** 4681-9.

LIDER, O., MILLER, A., MIRON, S., HERSHKOVIZ, R., WEINER, H. L., ZHANG, X. M. & HEBER-KATZ, E. 1991. Nonencephalitogenic CD4-CD8- V alpha 2V beta 8.2+ anti-myelin basic protein rat T lymphocytes inhibit disease induction. *J Immunol,* 147**,** 1208-13.

LING, E., SHUBINSKY, G. & PRESS, J. 2007. Increased proportion of CD3+CD4-CD8-double-negative T cells in peripheral blood of children with Behcet's disease. *Autoimmun Rev,* 6**,** 237-40.

LINOS, A., WORTHINGTON, J. W., O'FALLON, W. M. & KURLAND, L. T. 1980. The epidemiology of rheumatoid arthritis in Rochester, Minnesota: a study of incidence, prevalence, and mortality. *Am J Epidemiol,* 111**,** 87-98.

LIU, Y., HYDE, J. F. & VORE, M. 1992. Prolactin regulates maternal bile secretory function post partum. *J Pharmacol Exp Ther,* 261**,** 560-6.

LLOYD, C. M. & RANKIN, S. M. 2003. Chemokines in allergic airway disease. *Curr Opin Pharmacol,* 3**,** 443-8.

LOKE, Y. W., KING, A. & BURROWS, T. D. 1995. Decidua in human implantation. *Hum Reprod,* 10 Suppl 2**,** 14-21.

LUPPI, P., HALUSZCZAK, C., BETTERS, D., RICHARD, C. A., TRUCCO, M. & DELOIA, J. A. 2002a. Monocytes are progressively activated in the circulation of pregnant women. *J Leukoc Biol,* 72**,** 874-84.

LUPPI, P., HALUSZCZAK, C., TRUCCO, M. & DELOIA, J. A. 2002b. Normal pregnancy is associated with peripheral leukocyte activation. *Am J Reprod Immunol,* 47**,** 72-81.

LUSTER, A. D. 1998. Chemokines--chemotactic cytokines that mediate inflammation. *N Engl J Med,* 338**,** 436-45.

MACKENZIE, J. R., MATTES, J., DENT, L. A. & FOSTER, P. S. 2001. Eosinophils promote allergic disease of the lung by regulating CD4(+) Th2 lymphocyte function. *J Immunol,* 167**,** 3146-55.

MACKLER, A. M., GREEN, L. M., MCMILLAN, P. J. & YELLON, S. M. 2000. Distribution and activation of uterine mononuclear phagocytes in peripartum endometrium and myometrium of the mouse. *Biol Reprod,* 62**,** 1193-200.

MACKLER, A. M., IEZZA, G., AKIN, M. R., MCMILLAN, P. & YELLON, S. M. 1999. Macrophage trafficking in the uterus and cervix precedes parturition in the mouse. *Biol Reprod,* 61**,** 879-83.

MADIGAN, J., FREEMAN, D. J., MENZIES, F., FORROW, S., NELSON, S. M., YOUNG, A., SHARKEY, A., MOFFETT, A., GRAHAM, G. J., GREER, I. A., ROT, A. & NIBBS, R. J. 2010. Chemokine scavenger D6 is expressed by trophoblasts and aids the survival of mouse embryos transferred into allogeneic recipients. *J Immunol,* 184**,** 3202-12.

MALASSINE, A., FRENDO, J. L. & EVAIN-BRION, D. 2003. A comparison of placental development and endocrine functions between the human and mouse model. *Hum Reprod Update,* 9**,** 531-9.

MANASE, K., ENDO, T., CHIDA, M., NAGASAWA, K., HONNMA, H., YAMAZAKI, K., KITAJIMA, Y., GOTO, T., KANAYA, M., HAYASHI, T., MITAKA, T. & SAITO, T. 2006. Coordinated elevation of membrane type 1-matrix metalloproteinase and matrix metalloproteinase-2 expression in rat uterus during postpartum involution. *Reprod Biol Endocrinol,* 4**,** 32.

MANTOVANI, A., BISWAS, S. K., GALDIERO, M. R., SICA, A. & LOCATI, M. 2013. Macrophage plasticity and polarization in tissue repair and remodelling. *J Pathol,* 229**,** 176-85.

MARTIN, C., BURDON, P. C., BRIDGER, G., GUTIERREZ-RAMOS, J. C., WILLIAMS, T. J. & RANKIN, S. M. 2003. Chemokines acting via CXCR2 and CXCR4 control the release of neutrophils from the bone marrow and their return following senescence. *Immunity,* 19**,** 583-93.

MARTINEZ-GARCIA, E. A., SANCHEZ-HERNANDEZ, P. E., CHAVEZ-ROBLES, B., NUNEZ-ATAHUALPA, L., MARTIN-MARQUEZ, B. T., ARANA-ARGAEZ, V. E., GARCIA-IGLESIAS, T., GONZALEZ-LOPEZ, L., GAMEZ-NAVA, J. I., PETRI, M. H., VELAZQUEZ-RODRIGUEZ, J., SALAZAR-PARAMO, M., DAVALOS-RODRIGUEZ, I. P., DANERI-NAVARRO, A. & VAZQUEZ-DEL MERCADO, M. 2011. The distribution of CD56(dim) CD16+ and CD56(bright) CD16- cells are associated with prolactin levels during pregnancy and menstrual cycle in healthy women. *Am J Reprod Immunol,* 65**,** 433-7.

MARTINEZ DE LA TORRE, Y., BURACCHI, C., BORRONI, E. M., DUPOR, J., BONECCHI, R., NEBULONI, M., PASQUALINI, F., DONI, A., LAURI, E., AGOSTINIS, C., BULLA, R., COOK, D. N., HARIBABU, B., MERONI, P., RUKAVINA, D., VAGO, L., TEDESCO, F., VECCHI, A., LIRA, S. A., LOCATI, M. & MANTOVANI, A. 2007. Protection against inflammation- and autoantibody-caused fetal loss by the chemokine decoy receptor D6. *Proc Natl Acad Sci U S A,* 104**,** 2319-24.

MASUDA, T., OHTEKI, T., ABO, T., SEKI, S., NOSE, S., NAGURA, H. & KUMAGAI, K. 1991. Expansion of the population of double negative CD4-8- T alpha beta-cells in the liver is a common feature of autoimmune mice. *J Immunol,* 147**,** 2907-12.

MATLOUBIAN, M., DAVID, A., ENGEL, S., RYAN, J. E. & CYSTER, J. G. 2000. A transmembrane CXC chemokine is a ligand for HIV-coreceptor Bonzo. *Nat Immunol,* 1**,** 298-304.

MCQUIBBAN, G. A., GONG, J. H., WONG, J. P., WALLACE, J. L., CLARK-LEWIS, I. & OVERALL, C. M. 2002. Matrix metalloproteinase processing of monocyte chemoattractant proteins generates CC chemokine receptor antagonists with anti-inflammatory properties in vivo. *Blood,* 100**,** 1160-7.

MELGERT, B. N., ORISS, T. B., QI, Z., DIXON-MCCARTHY, B., GEERLINGS, M., HYLKEMA, M. N. & RAY, A. 2010. Macrophages: regulators of sex differences in asthma? *Am J Respir Cell Mol Biol,* 42**,** 595-603.

MELGERT, B. N. & POSTMA, D. S. 2009. All men are created equal?: new leads in explaining sex differences in adult asthma. *Proc Am Thorac Soc,* 6**,** 724-7.

MELGERT, B. N., SPAANS, F., BORGHUIS, T., KLOK, P. A., GROEN, B., BOLT, A., DE VOS, P., VAN PAMPUS, M. G., WONG, T. Y., VAN GOOR, H., BAKKER, W. W. & FAAS, M. M. 2012. Pregnancy and preeclampsia affect monocyte subsets in humans and rats. *PLoS One,* 7**,** e45229.

MENDELSOHN, M. E. & KARAS, R. H. 1999. The protective effects of estrogen on the cardiovascular system. *N Engl J Med,* 340**,** 1801-11.

MENNING, A., WALTER, A., RUDOLPH, M., GASHAW, I., FRITZEMEIER, K. H. & ROESE, L. 2012. Granulocytes and vascularization regulate uterine bleeding and tissue remodeling in a mouse menstruation model. *PLoS One,* 7**,** e41800.

MENZIES, F. 2010. *RE: Personal communication.*

MENZIES, F. M., KHAN, A. H., HIGGINS, C. A., NELSON, S. M. & NIBBS, R. J. 2012. The chemokine receptor CCR2 is not required for successful initiation of labor in mice. *Biol Reprod,* 86**,** 118.

MIAO, Z., LUKER, K. E., SUMMERS, B. C., BERAHOVICH, R., BHOJANI, M. S., REHEMTULLA, A., KLEER, C. G., ESSNER, J. J., NASEVICIUS, A., LUKER, G. D., HOWARD, M. C. & SCHALL, T. J. 2007. CXCR7 (RDC1) promotes breast and lung tumor growth in vivo and is expressed on tumor-associated vasculature. *Proc Natl Acad Sci U S A,* 104**,** 15735-40.

MITCHELL, B. F. & TAGGART, M. J. 2009. Are animal models relevant to key aspects of human parturition? *Am J Physiol Regul Integr Comp Physiol,* 297**,** R525-45.

MIXTER, P. F., RUSSELL, J. Q., MORRISSETTE, G. J., CHARLAND, C., ALEMAN-HOEY, D. & BUDD, R. C. 1999. A model for the origin of TCR-alphabeta+ CD4-CD8- B220+ cells based on high affinity TCR signals. *J Immunol,* 162**,** 5747-56.

MJOSBERG, J., BERG, G., JENMALM, M. C. & ERNERUDH, J. 2010. FOXP3+ regulatory T cells and T helper 1, T helper 2, and T helper 17 cells in human early pregnancy decidua. *Biol Reprod,* 82**,** 698-705.

MOLD, J. E., MICHAELSSON, J., BURT, T. D., MUENCH, M. O., BECKERMAN, K. P., BUSCH, M. P., LEE, T. H., NIXON, D. F. & MCCUNE, J. M. 2008. Maternal alloantigens promote the development of tolerogenic fetal regulatory T cells in utero. *Science,* 322**,** 1562-5.

MONK, P. N., SCOLA, A. M., MADALA, P. & FAIRLIE, D. P. 2007. Function, structure and therapeutic potential of complement C5a receptors. *Br J Pharmacol,* 152**,** 429-48.

MOSCHOVAKIS, G. L. & FORSTER, R. 2012. Multifaceted activities of CCR7 regulate T-cell homeostasis in health and disease. *Eur J Immunol,* 42**,** 1949-55.

MUPPIDI, J. R., ARNON, T. I., BRONEVETSKY, Y., VEERAPEN, N., TANAKA, M., BESRA, G. S. & CYSTER, J. G. 2011. Cannabinoid receptor 2 positions and retains marginal zone B cells within the splenic marginal zone. *J Exp Med,* 208**,** 1941-8.

MURRAY, P. J. & WYNN, T. A. 2011. Protective and pathogenic functions of macrophage subsets. *Nat Rev Immunol,* 11**,** 723-37.

NAGAMATSU, T. & SCHUST, D. J. 2010. The contribution of macrophages to normal and pathological pregnancies. *Am J Reprod Immunol,* 63**,** 460-71.

NAHRENDORF, M., SWIRSKI, F. K., AIKAWA, E., STANGENBERG, L., WURDINGER, T., FIGUEIREDO, J. L., LIBBY, P., WEISSLEDER, R. & PITTET, M. J. 2007. The healing myocardium sequentially mobilizes two monocyte subsets with divergent and complementary functions. *J Exp Med,* 204**,** 3037-47.

NANSEN, A., MARKER, O., BARTHOLDY, C. & THOMSEN, A. R. 2000. CCR2+ and CCR5+ CD8+ T cells increase during viral infection and migrate to sites of infection. *Eur J Immunol,* 30**,** 1797-806.

NASHAN, D., COOPER, T. G., KNUTH, U. A., SCHUBEUS, P., SORG, C. & NIESCHLAG, E. 1990. Presence and distribution of leucocyte subsets in the murine epididymis after vasectomy. *Int J Androl,* 13**,** 39-49.

NASHAN, D., MALORNY, U., SORG, C., COOPER, T. & NIESCHLAG, E. 1989. Immuno-competent cells in the murine epididymis. *Int J Androl,* 12**,** 85-94.

NATHAN, C. 2006. Neutrophils and immunity: challenges and opportunities. *Nat Rev Immunol,* 6**,** 173-82.

NERQUAYE-TETTEH, J. O. & CLARKE, J. R. 1990. Avoidance of used endometrial sites by blastocysts of the bank vole, Clethrionomys glareolus. *J Reprod Fertil,* 89**,** 729-34.

NEWPORT, A. & CARTER, J. 1983. Changes in T and B lymphocyte populations in the lymph nodes draining the uterus in pregnant mice. *J Reprod Fertil,* 67**,** 433-40.

NIBBS, R. J., GILCHRIST, D. S., KING, V., FERRA, A., FORROW, S., HUNTER, K. D. & GRAHAM, G. J. 2007. The atypical chemokine receptor D6 suppresses the development of chemically induced skin tumors. *J Clin Invest,* 117**,** 1884-92.

NIJKAMP, F. P., PARNHAM, M. J. & SPRINGERLINK (ONLINE SERVICE) 2011. Principles of Immunopharmacology 3rd revised and extended edition. Basel: Birkhäuser Basel.

NILSEN-HAMILTON, M., LIU, Q., RYON, J., BENDICKSON, L., LEPONT, P. & CHANG, Q. 2003. Tissue involution and the acute phase response. *Ann N Y Acad Sci,* 995**,** 94-108.

NILSSON, B. O. 2007. Modulation of the inflammatory response by estrogens with focus on the endothelium and its interactions with leukocytes. *Inflamm Res,* 56**,** 269-73.

NOEL, J. G., OSTERBURG, A., WANG, Q., GUO, X., BYRUM, D., SCHWEMBERGER, S., GOETZMAN, H., CALDWELL, C. C. & OGLE, C. K. 2007. Thermal injury elevates the inflammatory monocyte subpopulation in multiple compartments. *Shock,* 28**,** 684-93.

O'DEA, K. P., WILSON, M. R., DOKPESI, J. O., WAKABAYASHI, K., TATTON, L., VAN ROOIJEN, N. & TAKATA, M. 2009. Mobilization and margination of bone marrow Gr-1high monocytes during subclinical endotoxemia predisposes the lungs toward acute injury. *J Immunol,* 182**,** 1155-66.

ORFANOU, D. C., VERVERIDIS, H. N., POURLIS, A., FRAGKOU, I. A., KOKOLI, A. N., BOSCOS, C. M., TAITZOGLOU, I. A., TZORA, A., NEROU, C. M., ATHANASIOU, L. & FTHENAKIS, G. C. 2009. Post-partum involution of the canine uterus - gross anatomical and histological features. *Reprod Domest Anim,* 44 Suppl 2**,** 152-5.

ORSINI, M. W. 1957. The vascular knot of the hamster uterus: The placental arterial supply and its changes during gestation and postpartum involution. *Journal of Morphology,* 100**,** 565-599.

ORTOLANI, C., FORTI, E., RADIN, E., CIBIN, R. & COSSARIZZA, A. 1993. Cytofluorimetric identification of two populations of double positive (CD4+,CD8+) T lymphocytes in human peripheral blood. *Biochem Biophys Res Commun,* 191**,** 601-9.

OSMAN, I., YOUNG, A., LEDINGHAM, M. A., THOMSON, A. J., JORDAN, F., GREER, I. A. & NORMAN, J. E. 2003. Leukocyte density and pro-inflammatory cytokine expression in human fetal membranes, decidua, cervix and myometrium before and during labour at term. *Mol Hum Reprod,* 9**,** 41-5.

PANDIYAN, P., ZHENG, L., ISHIHARA, S., REED, J. & LENARDO, M. J. 2007. CD4+CD25+Foxp3+ regulatory T cells induce cytokine deprivation-mediated apoptosis of effector CD4+ T cells. *Nat Immunol,* 8**,** 1353-62.

PAPAKONSTANTINOU, N. A., STAMOU, M. I., BAIKOUSSIS, N. G., GOUDEVENOS, J. & APOSTOLAKIS, E. 2013. Sex differentiation with regard to coronary artery disease. *J Cardiol*.

PAREL, Y. & CHIZZOLINI, C. 2004. CD4+ CD8+ double positive (DP) T cells in health and disease. *Autoimmun Rev,* 3**,** 215-20.

PAUST, S., GILL, H. S., WANG, B. Z., FLYNN, M. P., MOSEMAN, E. A., SENMAN, B., SZCZEPANIK, M., TELENTI, A., ASKENASE, P. W., COMPANS, R. W. & VON ANDRIAN, U. H. 2010. Critical role for the chemokine receptor CXCR6 in NK cell-mediated antigen-specific memory of haptens and viruses. *Nat Immunol,* 11**,** 1127-35.

PERVIN, S., SINGH, R., ROSENFELD, M. E., NAVAB, M., CHAUDHURI, G. & NATHAN, L. 1998. Estradiol suppresses MCP-1 expression In vivo : implications for atherosclerosis. *Arterioscler Thromb Vasc Biol,* 18**,** 1575-82.

PETERSON, R. A. 2012. Regulatory T-cells: diverse phenotypes integral to immune homeostasis and suppression. *Toxicol Pathol,* 40**,** 186-204.

PETKOVA, S. B., YUAN, R., TSAIH, S. W., SCHOTT, W., ROOPENIAN, D. C. & PAIGEN, B. 2008. Genetic influence on immune phenotype revealed strain-specific variations in peripheral blood lineages. *Physiol Genomics,* 34**,** 304-14.

PETRI, M. 2002. Epidemiology of systemic lupus erythematosus. *Best Pract Res Clin Rheumatol,* 16**,** 847-58.

PIEPER, K., GRIMBACHER, B. & EIBEL, H. 2013. B-cell biology and development. *J Allergy Clin Immunol,* 131**,** 959-71.

PITETTI, J. L., CALVEL, P., ZIMMERMANN, C., CONNE, B., PAPAIOANNOU, M. D., AUBRY, F., CEDERROTH, C., URNER, F., FUMEL, B., CRAUSAZ, M., DOCQUIER, M., HERRERA, P. L., PRALONG, F., GERMOND, M., GUILLOU, F., JEGOU, B. & NEF, S. 2013. An essential role for insulin and IGF1 receptors in regulating Sertoli cells proliferation, testis size and FSH action in mice. *Mol Endocrinol*.

POROPATICH, C., ROJAS, M. & SILVERBERG, S. G. 1987. Polymorphonuclear leukocytes in the endometrium during the normal menstrual cycle. *Int J Gynecol Pathol,* 6**,** 230-4.

PROUDFOOT, A. E., HANDEL, T. M., JOHNSON, Z., LAU, E. K., LIWANG, P., CLARK-LEWIS, I., BORLAT, F., WELLS, T. N. & KOSCO-VILBOIS, M. H. 2003. Glycosaminoglycan binding and oligomerization are essential for the in vivo activity of certain chemokines. *Proc Natl Acad Sci U S A,* 100**,** 1885-90.

PRUENSTER, M., MUDDE, L., BOMBOSI, P., DIMITROVA, S., ZSAK, M., MIDDLETON, J., RICHMOND, A., GRAHAM, G. J., SEGERER, S., NIBBS, R. J. & ROT, A. 2009. The Duffy antigen receptor for chemokines transports chemokines and supports their promigratory activity. *Nat Immunol,* 10**,** 101-8.

QIU, C. L., ZHAO, H., YANG, G. B., LIU, Q. & SHAO, Y. 2008. Flow cytometric characterization of T lymphocyte subsets in the peripheral blood of Chinese rhesus

macaques: normal range, age- and sex-related differences. *Vet Immunol Immunopathol,* 124**,** 313-21.
RABIN, R. L., PARK, M. K., LIAO, F., SWOFFORD, R., STEPHANY, D. & FARBER, J. M. 1999. Chemokine receptor responses on T cells are achieved through regulation of both receptor expression and signaling. *J Immunol,* 162**,** 3840-50.
RAMAGOPALAN, S. V., BYRNES, J. K., ORTON, S. M., DYMENT, D. A., GUIMOND, C., YEE, I. M., EBERS, G. C. & SADOVNICK, A. D. 2010. Sex ratio of multiple sclerosis and clinical phenotype. *Eur J Neurol,* 17**,** 634-7.
RAMATHAL, C. Y., BAGCHI, I. C., TAYLOR, R. N. & BAGCHI, M. K. 2010. Endometrial decidualization: of mice and men. *Semin Reprod Med,* 28**,** 17-26.
RATKAY, L. G., WEINBERG, J. & WATERFIELD, J. D. 2000. The effect of lactation in the post-partum arthritis of MRL-lpr/fasmice. *Rheumatology (Oxford),* 39**,** 646-51.
RAULET, D. H. 2003. Roles of the NKG2D immunoreceptor and its ligands. *Nat Rev Immunol,* 3**,** 781-90.
REICHEL, C. A., KHANDOGA, A., ANDERS, H. J., SCHLONDORFF, D., LUCKOW, B. & KROMBACH, F. 2006. Chemokine receptors Ccr1, Ccr2, and Ccr5 mediate neutrophil migration to postischemic tissue. *J Leukoc Biol,* 79**,** 114-22.
REINHARDT, C. & MELMS, A. 2000. Normalization of elevated CD4-/CD8- (double-negative) T cells after thymectomy parallels clinical remission in myasthenia gravis associated with thymic hyperplasia but not thymoma. *Ann Neurol,* 48**,** 603-8.
RIBEIRO-GOMES, F. L., PETERS, N. C., DEBRABANT, A. & SACKS, D. L. 2012. Efficient capture of infected neutrophils by dendritic cells in the skin inhibits the early anti-leishmania response. *PLoS Pathog,* 8**,** e1002536.
RIEGER, L., HOFMEISTER, V., PROBE, C., DIETL, J., WEISS, E. H., STECK, T. & KAMMERER, U. 2002. Th1- and Th2-like cytokine production by first trimester decidual large granular lymphocytes is influenced by HLA-G and HLA-E. *Mol Hum Reprod,* 8**,** 255-61.
RIFFO-VASQUEZ, Y., LIGEIRO DE OLIVEIRA, A. P., PAGE, C. P., SPINA, D. & TAVARES-DE-LIMA, W. 2007. Role of sex hormones in allergic inflammation in mice. *Clin Exp Allergy,* 37**,** 459-70.
ROBERTSON, S. A., GUERIN, L. R., BROMFIELD, J. J., BRANSON, K. M., AHLSTROM, A. C. & CARE, A. S. 2009. Seminal fluid drives expansion of the CD4+CD25+ T regulatory cell pool and induces tolerance to paternal alloantigens in mice. *Biol Reprod,* 80**,** 1036-45.
ROCA, H., VARSOS, Z. S., SUD, S., CRAIG, M. J., YING, C. & PIENTA, K. J. 2009. CCL2 and interleukin-6 promote survival of human CD11b+ peripheral blood mononuclear cells and induce M2-type macrophage polarization. *J Biol Chem,* 284**,** 34342-54.
ROMANO, M., CACCIATORE, A., GIORDANO, R. & LA ROSA, B. 2010. Postpartum period: three distinct but continuous phases. *J Prenat Med,* 4**,** 22-5.
ROSE, S., MISHARIN, A. & PERLMAN, H. 2012. A novel Ly6C/Ly6G-based strategy to analyze the mouse splenic myeloid compartment. *Cytometry A,* 81**,** 343-50.
ROSENBERG, H. F., DYER, K. D. & FOSTER, P. S. 2013. Eosinophils: changing perspectives in health and disease. *Nat Rev Immunol,* 13**,** 9-22.
ROSSANT, J. & CROSS, J. C. 2001. Placental development: lessons from mouse mutants. *Nat Rev Genet,* 2**,** 538-48.
ROT, A. & VON ANDRIAN, U. H. 2004. Chemokines in innate and adaptive host defense: basic chemokinese grammar for immune cells. *Annu Rev Immunol,* 22**,** 891-928.
SAGE, P. T., FRANCISCO, L. M., CARMAN, C. V. & SHARPE, A. H. 2012. The receptor PD-1 controls follicular regulatory T cells in the lymph nodes and blood. *Nat Immunol*.

SAKAGUCHI, S., MIYARA, M., COSTANTINO, C. M. & HAFLER, D. A. 2010. FOXP3+ regulatory T cells in the human immune system. *Nat Rev Immunol,* 10**,** 490-500.

SALAMONSEN, L. A. 1998. Current concepts of the mechanisms of menstruation: a normal process of tissue destruction. *Trends Endocrinol Metab,* 9**,** 305-9.

SALAMONSEN, L. A., BUTT, A. R., HAMMOND, F. R., GARCIA, S. & ZHANG, J. 1997. Production of endometrial matrix metalloproteinases, but not their tissue inhibitors, is modulated by progesterone withdrawal in an in vitro model for menstruation. *J Clin Endocrinol Metab,* 82**,** 1409-15.

SALAMONSEN, L. A. & WOOLLEY, D. E. 1999. Menstruation: induction by matrix metalloproteinases and inflammatory cells. *J Reprod Immunol,* 44**,** 1-27.

SALLUSTO, F., SCHAERLI, P., LOETSCHER, P., SCHANIEL, C., LENIG, D., MACKAY, C. R., QIN, S. & LANZAVECCHIA, A. 1998. Rapid and coordinated switch in chemokine receptor expression during dendritic cell maturation. *Eur J Immunol,* 28**,** 2760-9.

SANCHEZ-MARTIN, L., SANCHEZ-MATEOS, P. & CABANAS, C. 2013. CXCR7 impact on CXCL12 biology and disease. *Trends Mol Med,* 19**,** 12-22.

SANDERSON, J. P., BRENNAN, P. J., MANSOUR, S., MATULIS, G., PATEL, O., LISSIN, N., GODFREY, D. I., KAWAHARA, K., ZAHRINGER, U., ROSSJOHN, J., BRENNER, M. B. & GADOLA, S. D. 2013. CD1d protein structure determines species-selective antigenicity of isoglobotrihexosylceramide (iGb3) to invariant NKT cells. *Eur J Immunol,* 43**,** 815-25.

SASAKI, Y., SAKAI, M., MIYAZAKI, S., HIGUMA, S., SHIOZAKI, A. & SAITO, S. 2004. Decidual and peripheral blood CD4+CD25+ regulatory T cells in early pregnancy subjects and spontaneous abortion cases. *Mol Hum Reprod,* 10**,** 347-53.

SCHMETTERER, K. G., NEUNKIRCHNER, A. & PICKL, W. F. 2012. Naturally occurring regulatory T cells: markers, mechanisms, and manipulation. *FASEB J,* 26**,** 2253-76.

SCHULZ, C., GOMEZ PERDIGUERO, E., CHORRO, L., SZABO-ROGERS, H., CAGNARD, N., KIERDORF, K., PRINZ, M., WU, B., JACOBSEN, S. E., POLLARD, J. W., FRAMPTON, J., LIU, K. J. & GEISSMANN, F. 2012. A lineage of myeloid cells independent of Myb and hematopoietic stem cells. *Science,* 336**,** 86-90.

SCOTLAND, R. S., STABLES, M. J., MADALLI, S., WATSON, P. & GILROY, D. W. 2011. Sex differences in resident immune cell phenotype underlie more efficient acute inflammatory responses in female mice. *Blood,* 118**,** 5918-27.

SELVATICI, R., FALZARANO, S., MOLLICA, A. & SPISANI, S. 2006. Signal transduction pathways triggered by selective formylpeptide analogues in human neutrophils. *Eur J Pharmacol,* 534**,** 1-11.

SERBINA, N. V. & PAMER, E. G. 2006. Monocyte emigration from bone marrow during bacterial infection requires signals mediated by chemokine receptor CCR2. *Nat Immunol,* 7**,** 311-7.

SHELLY, S., BOAZ, M. & ORBACH, H. 2012. Prolactin and autoimmunity. *Autoimmun Rev,* 11**,** A465-70.

SHERIDAN, B. S. & LEFRANCOIS, L. 2011. Regional and mucosal memory T cells. *Nat Immunol,* 12**,** 485-91.

SHI, C., JIA, T., MENDEZ-FERRER, S., HOHL, T. M., SERBINA, N. V., LIPUMA, L., LEINER, I., LI, M. O., FRENETTE, P. S. & PAMER, E. G. 2011. Bone marrow mesenchymal stem and progenitor cells induce monocyte emigration in response to circulating toll-like receptor ligands. *Immunity,* 34**,** 590-601.

SHIMIZU, K. & HOKANO, M. 1988. Removal of collagen bundles in murine uterus during postpartum involution. *Anat Rec,* 220**,** 138-42.

SHIRAISHI, K., TAKIHARA, H. & MATSUYAMA, H. 2010. Elevated scrotal temperature, but not varicocele grade, reflects testicular oxidative stress-mediated apoptosis. *World J Urol,* 28**,** 359-64.

SHYNLOVA, O., KWONG, R. & LYE, S. J. 2010. Mechanical stretch regulates hypertrophic phenotype of the myometrium during pregnancy. *Reproduction,* 139**,** 247-53.

SHYNLOVA, O., NEDD-RODERIQUE, T., LI, Y., DOROGIN, A. & LYE, S. J. 2012. Myometrial immune cells contribute to term parturition, preterm labour and post-partum involution in mice. *J Cell Mol Med*.

SHYNLOVA, O., TSUI, P., DOROGIN, A. & LYE, S. J. 2008. Monocyte chemoattractant protein-1 (CCL-2) integrates mechanical and endocrine signals that mediate term and preterm labor. *J Immunol,* 181**,** 1470-9.

SLIGHT, S. R., RANGEL-MORENO, J., GOPAL, R., LIN, Y., FALLERT JUNECKO, B. A., MEHRA, S., SELMAN, M., BECERRIL-VILLANUEVA, E., BAQUERA-HEREDIA, J., PAVON, L., KAUSHAL, D., REINHART, T. A., RANDALL, T. D. & KHADER, S. A. 2013. CXCR5+ T helper cells mediate protective immunity against tuberculosis. *J Clin Invest*.

SMITH, M. L., OLSON, T. S. & LEY, K. 2004. CXCR2- and E-selectin-induced neutrophil arrest during inflammation in vivo. *J Exp Med,* 200**,** 935-9.

SNYDER-CAPPIONE, J. E., TINCATI, C., ECCLES-JAMES, I. G., CAPPIONE, A. J., NDHLOVU, L. C., KOTH, L. L. & NIXON, D. F. 2010. A comprehensive ex vivo functional analysis of human NKT cells reveals production of MIP1-alpha and MIP1-beta, a lack of IL-17, and a Th1-bias in males. *PLoS One,* 5**,** e15412.

SODHI, A. & TRIPATHI, A. 2008. Prolactin and growth hormone induce differential cytokine and chemokine profile in murine peritoneal macrophages in vitro: involvement of p-38 MAP kinase, STAT3 and NF-kappaB. *Cytokine,* 41**,** 162-73.

SOEHNLEIN, O. & LINDBOM, L. 2010. Phagocyte partnership during the onset and resolution of inflammation. *Nat Rev Immunol,* 10**,** 427-39.

SOUTO, F. O., ALVES-FILHO, J. C., TURATO, W. M., AUXILIADORA-MARTINS, M., BASILE-FILHO, A. & CUNHA, F. Q. 2011. Essential role of CCR2 in neutrophil tissue infiltration and multiple organ dysfunction in sepsis. *Am J Respir Crit Care Med,* 183**,** 234-42.

STEEVELS, T. A. & MEYAARD, L. 2011. Immune inhibitory receptors: essential regulators of phagocyte function. *Eur J Immunol,* 41**,** 575-87.

STEWART, I. J. & MITCHELL, B. S. 1992. Macrophages and other endocytic cells in the mouse uterus during the second half of pregnancy and into the postpartum period. *J Anat,* 181 (Pt 1)**,** 119-26.

STRAUSS, L., BERGMANN, C. & WHITESIDE, T. L. 2009. Human circulating CD4+CD25highFoxp3+ regulatory T cells kill autologous CD8+ but not CD4+ responder cells by Fas-mediated apoptosis. *J Immunol,* 182**,** 1469-80.

SUMMERS, C., RANKIN, S. M., CONDLIFFE, A. M., SINGH, N., PETERS, A. M. & CHILVERS, E. R. 2010. Neutrophil kinetics in health and disease. *Trends Immunol,* 31**,** 318-24.

SUNDERKOTTER, C., NIKOLIC, T., DILLON, M. J., VAN ROOIJEN, N., STEHLING, M., DREVETS, D. A. & LEENEN, P. J. 2004. Subpopulations of mouse blood monocytes differ in maturation stage and inflammatory response. *J Immunol,* 172**,** 4410-7.

SUSANTO, O., TRAPANI, J. A. & BRASACCHIO, D. 2012. Controversies in granzyme biology. *Tissue Antigens,* 80**,** 477-87.

SUTTON, C. E., MIELKE, L. A. & MILLS, K. H. 2012. IL-17-producing gammadelta T cells and innate lymphoid cells. *Eur J Immunol,* 42**,** 2221-31.

SVENSSON, J., JENMALM, M. C., MATUSSEK, A., GEFFERS, R., BERG, G. & ERNERUDH, J. 2011. Macrophages at the fetal-maternal interface express markers of alternative activation and are induced by M-CSF and IL-10. *J Immunol,* 187**,** 3671-82.

SWIRSKI, F. K., NAHRENDORF, M., ETZRODT, M., WILDGRUBER, M., CORTEZ-RETAMOZO, V., PANIZZI, P., FIGUEIREDO, J. L., KOHLER, R. H., CHUDNOVSKIY, A., WATERMAN, P., AIKAWA, E., MEMPEL, T. R., LIBBY, P., WEISSLEDER, R. & PITTET, M. J. 2009. Identification of splenic reservoir monocytes and their deployment to inflammatory sites. *Science,* 325**,** 612-6.

TAKEUCHI, Y., TANAKA, T., HAMAMURA, K., SUGIMOTO, T., MIYASAKA, M., YAGITA, H. & OKUMURA, K. 1992. Expression and role of interleukin-2 receptor beta chain on CD4-CD8- T cell receptor alpha beta+ cells [corrected]. *Eur J Immunol,* 22**,** 2929-35.

TCHERNITCHIN, A., ROORIJCK, J., TCHERNITCHIN, X., VANDENHENDE, J. & GALAND, F. 1974. Dramatic early increase in uterine eosinophils after oestrogen administration. *Nature,* 248**,** 142-3.

TERWEY, T. H., KIM, T. D., KOCHMAN, A. A., HUBBARD, V. M., LU, S., ZAKRZEWSKI, J. L., RAMIREZ-MONTAGUT, T., ENG, J. M., MURIGLAN, S. J., HELLER, G., MURPHY, G. F., LIU, C., BUDAK-ALPDOGAN, T., ALPDOGAN, O. & VAN DEN BRINK, M. R. 2005. CCR2 is required for CD8-induced graft-versus-host disease. *Blood,* 106**,** 3322-30.

THIRUCHELVAM, U., DRANSFIELD, I., SAUNDERS, P. T. & CRITCHLEY, H. O. 2013. The importance of the macrophage within the human endometrium. *J Leukoc Biol,* 93**,** 217-25.

THOMAS, S. Y., HOU, R., BOYSON, J. E., MEANS, T. K., HESS, C., OLSON, D. P., STROMINGER, J. L., BRENNER, M. B., GUMPERZ, J. E., WILSON, S. B. & LUSTER, A. D. 2003. CD1d-restricted NKT cells express a chemokine receptor profile indicative of Th1-type inflammatory homing cells. *J Immunol,* 171**,** 2571-80.

THOMSON, A. J., TELFER, J. F., YOUNG, A., CAMPBELL, S., STEWART, C. J., CAMERON, I. T., GREER, I. A. & NORMAN, J. E. 1999. Leukocytes infiltrate the myometrium during human parturition: further evidence that labour is an inflammatory process. *Hum Reprod,* 14**,** 229-36.

TILBURGS, T., ROELEN, D. L., VAN DER MAST, B. J., DE GROOT-SWINGS, G. M., KLEIJBURG, C., SCHERJON, S. A. & CLAAS, F. H. 2008. Evidence for a selective migration of fetus-specific CD4+CD25bright regulatory T cells from the peripheral blood to the decidua in human pregnancy. *J Immunol,* 180**,** 5737-45.

TILBURGS, T., VAN DER MAST, B. J., NAGTZAAM, N. M., ROELEN, D. L., SCHERJON, S. A. & CLAAS, F. H. 2009. Expression of NK cell receptors on decidual T cells in human pregnancy. *J Reprod Immunol,* 80**,** 22-32.

TIMMONS, B. C., FAIRHURST, A. M. & MAHENDROO, M. S. 2009. Temporal changes in myeloid cells in the cervix during pregnancy and parturition. *J Immunol,* 182**,** 2700-7.

TIMMONS, B. C. & MAHENDROO, M. S. 2006. Timing of neutrophil activation and expression of proinflammatory markers do not support a role for neutrophils in cervical ripening in the mouse. *Biol Reprod,* 74**,** 236-45.

TOPHAM, N. J. & HEWITT, E. W. 2009. Natural killer cell cytotoxicity: how do they pull the trigger? *Immunology,* 128**,** 7-15.

TOWNSON, J. R. & NIBBS, R. J. 2002. Characterization of mouse CCX-CKR, a receptor for the lymphocyte-attracting chemokines TECK/mCCL25, SLC/mCCL21 and MIP-3beta/mCCL19: comparison to human CCX-CKR. *Eur J Immunol,* 32**,** 1230-41.

TRAUB, S., DEMARIA, O., CHASSON, L., SERRA, F., DESNUES, B. & ALEXOPOULOU, L. 2012. Sex bias in susceptibility to MCMV infection: implication of TLR9. *PLoS One,* 7**,** e45171.

TRIPATHI, V., VERMA, R., DINDA, A., MALHOTRA, N., KAUR, J. & LUTHRA, K. 2009. Differential expression of RDC1/CXCR7 in the human placenta. *J Clin Immunol,* 29**,** 379-86.

TSOU, C. L., HASKELL, C. A. & CHARO, I. F. 2001. Tumor necrosis factor-alpha-converting enzyme mediates the inducible cleavage of fractalkine. *J Biol Chem,* 276**,** 44622-6.

TURKA, L. A., FLETCHER, M. C., CRAIGHEAD, N., THOMPSON, C. B. & JUNE, C. H. 1992. Defective signal transduction by the CD2 molecule in immature T-cell receptor/CD3- thymocytes. *Proc Natl Acad Sci U S A,* 89**,** 8706-10.

UTTING, O., TEH, S. J. & TEH, H. S. 2000. A population of in vivo anergized T cells with a lower activation threshold for the induction of CD25 exhibit differential requirements in mobilization of intracellular calcium and mitogen-activated protein kinase activation. *J Immunol,* 164**,** 2881-9.

VAN DER HEIJDEN, O. W., ESSERS, Y. P., WIJNANDS, E., MEY, J. G., PEETERS, L. L. & VAN EYS, G. J. 2009. Postpartum reversal of the pregnancy-induced uterine artery remodeling in young, aging, and eNOS-deficient mice. *Reprod Sci,* 16**,** 642-9.

VAN VOLLENHOVEN, R. F. 2009. Sex differences in rheumatoid arthritis: more than meets the eye. *BMC Med,* 7**,** 12.

VANTOUROUT, P. & HAYDAY, A. 2013. Six-of-the-best: unique contributions of gammadelta T cells to immunology. *Nat Rev Immunol,* 13**,** 88-100.

VARGAS, C. L., POURSINE-LAURENT, J., YANG, L. & YOKOYAMA, W. M. 2011. Development of thymic NK cells from double negative 1 thymocyte precursors. *Blood,* 118**,** 3570-8.

VOELKL, S., GARY, R. & MACKENSEN, A. 2011. Characterization of the immunoregulatory function of human TCR-alphabeta+ CD4- CD8- double-negative T cells. *Eur J Immunol,* 41**,** 739-48.

VOLPE, S., CAMERONI, E., MOEPPS, B., THELEN, S., APUZZO, T. & THELEN, M. 2012. CCR2 acts as scavenger for CCL2 during monocyte chemotaxis. *PLoS One,* 7**,** e37208.

WATARAI, H., SEKINE-KONDO, E., SHIGEURA, T., MOTOMURA, Y., YASUDA, T., SATOH, R., YOSHIDA, H., KUBO, M., KAWAMOTO, H., KOSEKI, H. & TANIGUCHI, M. 2012. Development and function of invariant natural killer T cells producing T(h)2- and T(h)17-cytokines. *PLoS Biol,* 10**,** e1001255.

WECKERLE, C. E. & NIEWOLD, T. B. 2011. The unexplained female predominance of systemic lupus erythematosus: clues from genetic and cytokine studies. *Clin Rev Allergy Immunol,* 40**,** 42-9.

WEI, J., YEE, C., RAMANATHAN, P., BENDALL, L. J. & WILLIAMSON, P. 2011. Variation in immunophenotype of lactating mice. *J Reprod Immunol,* 89**,** 178-84.

WILLENBORG, S., LUCAS, T., VAN LOO, G., KNIPPER, J. A., KRIEG, T., HAASE, I., BRACHVOGEL, B., HAMMERSCHMIDT, M., NAGY, A., FERRARA, N., PASPARAKIS, M. & EMING, S. A. 2012. CCR2 recruits an inflammatory macrophage subpopulation critical for angiogenesis in tissue repair. *Blood,* 120**,** 613-25.

WILLIAMS, P. J., SEARLE, R. F., ROBSON, S. C., INNES, B. A. & BULMER, J. N. 2009. Decidual leucocyte populations in early to late gestation normal human pregnancy. *J Reprod Immunol,* 82**,** 24-31.

WINKLER, M., FISCHER, D. C., RUCK, P., MARX, T., KAISERLING, E., OBERPICHLER, A., TSCHESCHE, H. & RATH, W. 1999. Parturition at term:

parallel increases in interleukin-8 and proteinase concentrations and neutrophil count in the lower uterine segment. *Hum Reprod,* 14**,** 1096-100.

WITHERDEN, D. A. & HAVRAN, W. L. 2011. Molecular aspects of epithelial gammadelta T cell regulation. *Trends Immunol,* 32**,** 265-71.

WITKIN, S. S., JEREMIAS, J., BONGIOVANNI, A. M. & MUNOZ, M. G. 1996. Immune regulation in the male genital tract. *Infect Dis Obstet Gynecol,* 4**,** 131-5.

WOOD, G. A., FATA, J. E., WATSON, K. L. & KHOKHA, R. 2007. Circulating hormones and estrous stage predict cellular and stromal remodeling in murine uterus. *Reproduction,* 133**,** 1035-44.

WOOD, G. W., HAUSMANN, E. H. & KANAKARAJ, K. 1999. Expression and regulation of chemokine genes in the mouse uterus during pregnancy. *Cytokine,* 11**,** 1038-45.

WU, M. T. & HWANG, S. T. 2002. CXCR5-transduced bone marrow-derived dendritic cells traffic to B cell zones of lymph nodes and modify antigen-specific immune responses. *J Immunol,* 168**,** 5096-102.

YANG, E. J., CHOI, E., KO, J., KIM, D. H., LEE, J. S. & KIM, I. S. 2012. Differential effect of CCL2 on constitutive neutrophil apoptosis between normal and asthmatic subjects. *J Cell Physiol,* 227**,** 2567-77.

YELLON, S. M., BURNS, A. E., SEE, J. L., LECHUGA, T. J. & KIRBY, M. A. 2009a. Progesterone withdrawal promotes remodeling processes in the nonpregnant mouse cervix. *Biol Reprod,* 81**,** 1-6.

YELLON, S. M., EBNER, C. A. & ELOVITZ, M. A. 2009b. Medroxyprogesterone acetate modulates remodeling, immune cell census, and nerve fibers in the cervix of a mouse model for inflammation-induced preterm birth. *Reprod Sci,* 16**,** 257-64.

ZENCLUSSEN, A. C., GERLOF, K., ZENCLUSSEN, M. L., SOLLWEDEL, A., BERTOJA, A. Z., RITTER, T., KOTSCH, K., LEBER, J. & VOLK, H. D. 2005. Abnormal T-cell reactivity against paternal antigens in spontaneous abortion: adoptive transfer of pregnancy-induced CD4+CD25+ T regulatory cells prevents fetal rejection in a murine abortion model. *Am J Pathol,* 166**,** 811-22.

ZENCLUSSEN, M. L., THUERE, C., AHMAD, N., WAFULA, P. O., FEST, S., TELES, A., LEBER, A., CASALIS, P. A., BECHMANN, I., PRILLER, J., VOLK, H. D. & ZENCLUSSEN, A. C. 2010. The persistence of paternal antigens in the maternal body is involved in regulatory T-cell expansion and fetal-maternal tolerance in murine pregnancy. *Am J Reprod Immunol,* 63**,** 200-8.

ZHANG, H. H., SONG, K., RABIN, R. L., HILL, B. J., PERFETTO, S. P., ROEDERER, M., DOUEK, D. C., SIEGEL, R. M. & FARBER, J. M. 2010. CCR2 identifies a stable population of human effector memory CD4+ T cells equipped for rapid recall response. *J Immunol,* 185**,** 6646-63.

ZHANG, Z. X., MA, Y., WANG, H., ARP, J., JIANG, J., HUANG, X., HE, K. M., GARCIA, B., MADRENAS, J. & ZHONG, R. 2006. Double-negative T cells, activated by xenoantigen, lyse autologous B and T cells using a perforin/granzyme-dependent, Fas-Fas ligand-independent pathway. *J Immunol,* 177**,** 6920-9.

ZHANG, Z. X., YANG, L., YOUNG, K. J., DUTEMPLE, B. & ZHANG, L. 2000. Identification of a previously unknown antigen-specific regulatory T cell and its mechanism of suppression. *Nat Med,* 6**,** 782-9.

ZHAO, J. X., ZENG, Y. Y. & LIU, Y. 2007. Fetal alloantigen is responsible for the expansion of the CD4(+)CD25(+) regulatory T cell pool during pregnancy. *J Reprod Immunol,* 75**,** 71-81.